

THE π -H ELIX IN FMN-DEPENDENT REDUCTASES PROMOTES OLIGOMERIC CHANGES TO COORDINATE THE MECHANISMS OF THE ALKANESULFONATE MONOOXYGENASE SYSTEMS

By

Chioma Helen Aloh

July, 2023

Director of Dissertation: Holly Ellis, PhD

Major Department: Biochemistry and Molecular Biology

ABSTRACT

Bacteria two-component flavin-dependent systems are upregulated for sulfur acquisition under sulfur limiting conditions. Two-component flavin-dependent systems are comprised of a reductase (SsuE/MsuE) that catalyzes the reduction of flavin, and the monooxygenase (SsuD/MsuD) catalyzes the desulfonation of organosulfur compounds for sulfur acquisition. The unique reactions catalyzed by these systems are enabled by a diverse range of structural features: π -helix, oligomeric changes, and protein-protein interactions. However, it is not clear how these structural features work synergistically to catalyze flavin reduction, transfer, and desulfonation. In this study, we take a holistic view of these structural features by investigating how they are coordinated for overall catalysis.

SsuE and MsuE belong to the NADPH:FMN reductase family and they share 30% amino acid identity. Results from several studies revealed that SsuE exists in different oligomeric states depending on the technique utilized. However, the precise oligomeric state of the reductases and how it functions in flavin reduction and transfer have not been explored. The oligomeric state of SsuE and MsuE were determined in the presence and absence of substrates. SsuE exists as a tetramer but shifts to a tetramer-dimer

equilibrium in the presence of NADPH or FMN. Interestingly, MsuE exists as a dimer in the apo form and with NADPH present. However, MsuE shifts from a dimer to a tetramer in the presence of flavin. These results reveal that the oligomeric state of SsuE and MsuE is altered in the presence of substrates. Transfer of reduced flavin from SsuE to SsuD was observed to occur through protein-protein interactions. Experiments were performed to determine if the oligomeric changes of SsuE are coordinated with the formation of protein-protein interactions with SsuD. In the presence of FMN, the proposed SsuE-SsuD complex was formed and the dimeric form of SsuE was the predominant form. The dimer interface of SsuE will expose protein interaction sites required for the efficient transfer of reduced flavin. The dimer-dimer interface of SsuE houses the π -helix which has been proposed to be responsible for flavin transfer. The π -helix is a distinct secondary structure which is characterized by an insertional residue into an α -helix that differentiates canonical flavoproteins from two-component FMN reductases. Results from previous studies revealed that the insertional residue is not solely responsible for the structural differences between these reductases. The insertional residue in SsuE is the Tyr128 and a Tyr126 was found in a similar position in a canonical flavoprotein, chromate reductase (ChrR). Clearly, additional structural adaptations may be responsible for the structural divergence between these reductases. Variants of ChrR (Q132P, Q127D, Q132P/127D ChrR) were generated from the conserved residues on the π -helical region of two-component FMN reductases. There was no measurable oxidase activity nor desulfonation activity with SsuD for any of the ChrR variants. Interestingly, wild-type and Q132P ChrR were capable of transferring electrons to ferricyanide in ferricyanide assays. However, Q127D and Q132P/127D ChrR had no measurable ferricyanide activity. Further studies

would need to be performed to evaluate the structural differences between these reductases. The unique π -helix of FMN reductases clearly bridges the functionality of the oligomeric changes of SsuE that are linked to protein-protein interactions critical for reduced flavin transfer.

THE π -HELIX IN FMN-DEPENDENT REDUCTASES PROMOTES OLIGOMERIC
CHANGES TO COORDINATE THE MECHANISMS OF THE ALKANESULFONATE
MONOOXYGENASE SYSTEMS

A Dissertation

Presented to the Faculty of the Department of Biochemistry and Molecular Biology

East Carolina University

In Partial Fulfillment of the Requirements for the Degree

Doctor of Philosophy in Biochemistry and Molecular Biology

By

Chioma Helen Aloh

July, 2023

Director of Dissertation: Holly Ellis, PhD

Thesis Committee Members:

John Cavanagh, PhD

Tonya Zeczycki, PhD

Anne Spuches, PhD

© Chioma Helen Aloh, 2023

ACKNOWLEDGEMENTS

When I started this program, I had no idea that five years would fly by so fast. I have had a rewarding journey, but this would not have been possible without the help that was rendered to me along the way. My sincere gratitude to Prof. Holly Ellis for the opportunity to work in her laboratory and for her unwavering support throughout my graduate studies here at ECU, Brody School of Medicine. I want to thank my committee members: Dr. John Cavanagh, Dr. Tonya Zeczycki, and Dr. Anne Spuches for always being available and ensuring I stayed on track during my graduate studies and for providing expertise on different scientific questions. I deeply appreciate my former and current lab mates: Dr. Katie Tombrello, Dr. Richard Hagen, Dr. Shruti Somai, Chukwuemeka Steve Adindu and Eric Eaton for their constant support and understanding through the years. I also want to thank the Department of Biochemistry and Molecular Biology at ECU for the opportunity to further my academic career and the National Science Foundation for funding my project. I am the last of three siblings and my two older siblings, Sophia Aloh and Walter Aloh have carried me through the years and looked out for me and I want to thank them for it. I want to thank my uncle and aunt, Mr., and Mrs. Nwigwe for being the first people to stake their sweat so that I could go to the university. I want to thank my close friends, extended family, the mothers of my three friends and my neighbors from the first house I lived in for guiding, providing, and correcting me when needed. This dissertation is dedicated to my mum, Mrs. Comfort Aloh, who passed away in September 2003, for the light she left that has helped me.

TABLE OF CONTENTS

LIST OF TABLES.....	x
LIST OF FIGURES.....	xi
LIST OF SCHEMES.....	xiv
LIST OF SYMBOLS/ABBREVIATIONS.....	xv
CHAPTER 1: LITERATURE REVIEW.....	1
1.1 Sulfur metabolism in Bacteria.....	1
1.1.1 Role and Availability of Sulfur.....	1
1.1.2 Sulfur Assimilation in Bacteria.....	3
1.1.3 Sulfur Trafficking and Incorporation into Biomolecules.....	5
1.1.4 Organosulfur Sources utilized during Sulfur Starvation Conditions.....	9
1.1.5 Regulation of the <i>ssi</i> Operons.....	14
1.2 Flavin and Flavoproteins.....	16
1.2.1 Flavin.....	16
1.2.2 Spectral Properties of Flavin.....	19
1.2.3 Flavoproteins.....	22
1.2.3.1 Flavin Reductases.....	23
1.2.3.2 Flavin Monooxygenases.....	24
1.3 Two-Component Flavin-Dependent Systems.....	26

1.3.1	General Overview of Two-Component Flavin-Dependent Systems.....	26
1.3.2	Kinetic Mechanisms utilized by Two-Component Monooxygenase Systems...	30
1.3.2.1	FMN Reductases of Two-Component Monooxygenase Systems.....	30
1.3.2.2	Structural Features utilized by FMN Reductases.....	35
1.3.2.3	FMNH ₂ -Dependent Monooxygenases of Two-Component Monooxygenase Systems.....	39
1.3.2.4	Structural Features of FMNH ₂ -Dependent Monooxygenases.....	41
1.3.2.5	Mechanism of Reduced Flavin Transfer in Two-Component Flavin- Dependent Systems.....	45
1.4	Structural Features utilized by Two-Component Flavin-Dependent Systems.....	49
1.4.1	Presence of π -Helices in Proteins.....	49
1.4.2	Structural Properties of the π -Helix.....	51
1.4.3	Preferences for Certain Amino Acids in π -Helices.....	52
1.4.4	Evolutionary Advantage of π -Helix in Proteins.....	54
1.5	Protein Oligomerization.....	60
1.5.1	Characteristics of Oligomeric Proteins.....	61
1.5.2	Different Roles of Oligomerization in Protein Metabolism.....	62
1.5.3	Mechanisms for Regulating Oligomerization of Proteins.....	64

1.5.4	Oligomerization exhibited by Two-Component Systems.....	66
1.6	Protein-Protein Interactions.....	67
1.6.1	Interface Parameters Involved in Determining Protein-Protein Interactions....	69
1.6.1.1	Hot Spots at Protein Interfaces.....	69
1.6.1.2	Residue Interface Propensity.....	70
1.6.1.3	Accessible Surface Area (ASA).....	70
1.6.1.4	Secondary Structure Preferences.....	71
1.6.1.5	Surface Complementarity.....	72
1.6.1.6	Conformational Change.....	72
1.6.1.7	Binding Affinity.....	73
1.6.2	Role of Protein-Protein Interaction in Enzyme Metabolism.....	73
1.7	Summary.....	75
CHAPTER 2.....		80
2	The Substrate-induced Oligomeric Changes of Two-Component FMN Reductases Involved in Sulfur Metabolism.....	80
2.1	Introduction.....	80
2.2	Experimental Procedures.....	83
2.2.1	Materials.....	83
2.2.2	Non-Denaturing Polyacrylamide Gel Electrophoresis.....	83

2.2.3	Spectrofluorimetric Titrations.....	84
2.2.4	Thermal Melt Circular Dichroism Spectroscopy.....	85
2.2.5	Sedimentation Velocity Analytical Ultracentrifugation.....	86
2.2.6	Differential H/D-X Experiments.....	87
2.3	Results.....	90
2.3.1	Substrate Affinity and Stability.....	90
2.3.2	Oligomeric State of SsuE and MsuE.....	92
2.3.3	Thermal Stability of SsuE and MsuE.....	95
2.3.4	H/D-Exchange Mass Spectrometry.....	97
2.4	Discussion.....	103
CHAPTER 3.....		109
3	The Role of Oligomeric Changes of SsuE in Protein-Protein Interactions in the Alkanesulfonate Monooxygenase System.....	109
3.1	Introduction.....	109
3.2	Materials and Methods.....	112
3.2.1	Materials.....	112
3.2.2	Fluorimetric Titrations of SsuE and SsuD.....	112
3.2.3	Analytical Ultracentrifugation of SsuE and SsuD.....	113
3.3	Results.....	114

3.3.1	Binding of SsuD to FMN-bound SsuE.....	114
3.3.2	Oligomeric State of SsuE-SsuD Complex Following Protein-Protein Interactions.....	116
3.4	Discussion.....	120
CHAPTER 4.....		124
4	Transformation of a Canonical Flavoprotein to a Flavin-Free NADPH-FMN Reductase Through Mutations of the α -Helix.....	124
4.1	Introduction.....	124
4.2	Materials and Methods.....	124
4.2.1	Materials.....	127
4.2.2	Construction of ChrR Variants.....	128
4.2.3	Circular Dichroism Spectroscopy of Wild-Type and Variants of ChrR.....	129
4.2.4	Kinetic Properties of Wild-Type and Variants of ChrR.....	129
4.2.5	Deflavination of Wild-Type and Q132P ChrR.....	130
4.2.6	Fluorimetric Titrations of Wild-Type and Variants of ChrR.....	131
4.2.7	Native PAGE of wild-type ChrR and its variants.....	131
4.2.8	Proteolytic Susceptibility of Wild-Type and Q127D ChrR.....	132
4.2.9	Flavin-Loading of Wild-Type and Variants of ChrR.....	132
4.3	Results.....	133

4.3.1	Site-Directed Mutagenesis and Purification of Wild-Type and Variants of ChrR.....	133
4.3.2	Steady-State Kinetic Properties of Wild-Type and Variants of ChrR.....	135
4.3.3	Substrate Binding Studies of Wild-Type and Variants of ChrR.....	138
4.3.4	Native PAGE Electrophoresis and Proteolytic Susceptibility of Wild-Type and Variants of ChrR.....	139
4.4	Discussion.....	140
CHAPTER 5.....		148
5	Conclusion.....	148
References.....		155
Appendices.....		177

LIST OF TABLES

Table 2.1: Substrate binding affinity of SsuE and MsuE.....	92
Table 2.2: Results from AUC analysis of SsuE and MsuE.....	95
Table 2.3: Thermal stability of SsuE and MsuE.....	97
Table 3.1: Results from AUC analysis of SsuD at different concentrations.....	117
Table 3.2: Results from AUC analysis of SsuE-SsuD.....	118
Table 3.3: Results from AUC analysis of SsuE(FMN)-SsuD.....	120
Table 4.1: Steady-state kinetic parameters for wild-type and variants of ChrR measuring ferricyanide activity.....	137
Table 4.2: Amount of flavin bound after flavin loading of ChrR and variants.....	137
Table 4.3: Steady-state kinetic parameters for wild-type and variants of ChrR measuring ferricyanide activity after flavin loading.....	137

LIST OF FIGURES

Figure 1.1: Sulfur assimilation pathway and biosynthesis of cysteine in bacteria.....	4
Figure 1.2: Persulfides can act as both electrophiles and nucleophiles in sulfur trafficking.....	6
Figure 1.3: Cysteine desulfurases catalyze the formation of persulfides from free cysteine.....	7
Figure 1.4: Biosynthesis of sulfur-containing cofactors involving the three sulfur acceptors (ThiI, IscU, and TusA) in <i>E. coli</i>	8
Figure 1.5: The <i>tau</i> and <i>ssu</i> operons induced during sulfur limiting conditions.....	10
Figure 1.6: Desulfonation of taurine (2-aminoethanesulfonate) by TauD to sulfite and aminoacetaldehyde.....	
Figure 1.7: Desulfonation of alkanesulfonates by SsuE and SsuD of the alkanesulfonate two-component FMN-dependent system.....	12
Figure 1.8: Uptake and desulfonation of alkanesulfonates and taurine in <i>E. coli</i>	13
Figure 1.9: Proposed model for the mechanism of sulfur assimilation by CysB and Cbl in <i>E. coli</i>	15
Figure 1.10: The isoalloxazine ring of flavin.....	17
Figure 1.11: Structures of naturally occurring flavin molecules.....	18
Figure 1.12: Distinct spectral properties of flavin that correspond to different oxidation states.....	20
Figure 1.13: Flavin can exist in nine physiological redox and ionic states.....	21
Figure 1.14: Activation of dioxygen by reduced flavin.....	26
Figure 1.15: Reactions catalyzed by different Two-component flavin-dependent monooxygenase systems.....	29
Figure 1.16: Desulfonation of dimethyl sulfide (DMS) in the <i>Pseudomonas</i> sp.....	30
Figure 1.17: Structures of reduced pyridine nucleotides and the isoalloxazine ring of flavin.....	31
Figure 1.18: Flavin reductases utilize either ping-pong or ordered sequential mechanism for the binding and release of flavin and the pyridine nucleotide.....	32
Figure 1.19: The flavodoxin fold of NADPH-FMN reductases of two-component flavin monooxygenase.....	35
Figure 1.20: SsuE tetramer showing the dimer of dimers.....	36

Figure 1.21: The three-dimensional structure of the active site of SsuE showing residues that position FMN.....	37
Figure 1.22: The flavin-N5-oxide intermediate.....	40
Figure 1.23: The TIM-barrel fold in SsuD is comprised of eight alternating α -helices and β -strands arranged in sequence.....	41
Figure 1.24: The active site residues in the monooxygenase, SsuD.....	44
Figure 1.25: Different mechanisms of reduced flavin transfer in two-component monooxygenase systems.....	47
Figure 1.26: Protein-protein interactions between SsuE and SsuD were identified through HDX-MS.....	48
Figure 1.27: The top-view of the π -helix and 3_{10} -helix.....	50
Figure 1.28: The hydrogen bonding pattern and top view of the α -helix and π -helix....	50
Figure 1.29: Hydrogen bonding pattern in helical structures in proteins.....	52
Figure 1.30: The π -helix in Soybean lipoxygenase increases with substrate binding...	54
Figure 1.31: Interactions involving the insertional residue, Tyr118 in the π -helix across the tetramer interface of SsuE.....	58
Figure 1.32: Different roles of oligomerization in enzyme activity.....	63
Figure 1.33: Two-dimensional schematic of the morpheein model in an equilibrium of morpheein forms.....	65
Figure 2.1: Fluorescent titrations of SsuE and MsuE with FMN and NADPH.....	91
Figure 2.2: Nondenaturing polyacrylamide gel of SsuE and MsuE.....	93
Figure 2.3: Sedimentation distribution plots of SsuE and MsuE.....	94
Figure 2.4: Thermal denaturation CD of SsuE and MsuE.....	97
Figure 2.5: Differential H/D-X analysis of SsuE and SsuE/FMN.....	100
Figure 2.6: Differential H/D-X analysis of MsuE and MsuE/FMN.....	102
Figure 2.7: Model for SsuE and MsuE oligomeric changes.....	108
Figure 3.1: Protein-protein interactions with SsuE and SsuD.....	111
Figure 3.2: Binding affinity of FMN-bound SsuE to SsuD.....	115
Figure 3.3: Sedimentation distribution plot of SsuD.....	116
Figure 3.4: Sedimentation distribution plot for SsuE-SsuD complex.....	118

Figure 3.5: Sedimentation distribution plot for SsuE-SsuD complex without and with flavin.....	119
Figure 3.6: Proposed model for the formation of the protein-complex between SsuE-SsuD complex.....	123
Figure 4.1: Tetramer of ChrR and SsuE.....	127
Figure 4.2: Structure based sequence analysis of the α 4-helix of the NADPH:FMN reductases.....	134
Figure 4.3: The far-UV circular dichroism spectra of wild-type and variants of ChrR.	135
Figure 4.4: Steady-state kinetic plots of wild-type and Q132P ChrR with ferricyanide.	136
Figure 4.5: Fluorescent titrations of wild-type and Q127D ChrR with FMN.....	138
Figure 4.6: Native-PAGE analysis of wild-type and variants of ChrR.....	139
Figure 4.7: Proteolytic susceptibility of wild-type and Q127D ChrR.....	140
Figure 4.8: Comparison of the α -helix of the canonical flavoprotein, ChrR from <i>E. coli</i> to the π -helix in two-component FMN reductase, SsuE from <i>E. coli</i>	143
Figure 4.9: Hydrogen bonding interactions of ChrR and SsuE.....	145
Figure 5.1: Coordination of the structural features of the alkanesulfonate monooxygenase system for catalysis.....	154

LIST OF SCHEMES

Scheme 1.1: Formation of charge-transfer complex in FMN reduction by SsuE.....	34
Scheme 1.2: The insertional Tyr residue in flavin reductases of two-component monooxygenase systems.....	56
Scheme 2.1: Reactions catalyzed by the alkanesulfonate monooxygenase enzymes..	81

LIST OF SYMBOLS/ABBREVIATIONS

ATP	Adenosine Triphosphate.....	3
DNA	Deoxyribonucleic Acid.....	16
FAD	Flavin Adenine Dinucleotide.....	17
FMN	Flavin Mononucleotide.....	14
NADH	Nicotinamide Adenine Dinucleotide.....	11
NADPH	Nicotinamide Adenine Dinucleotide Phosphate.....	3
PAGE	Polyacrylamide Gel Electrophoresis.....	83
PDB	Protein Data Bank.....	37
PMSF	Phenylmethylsulfonylfluoride.....	132
RF	Radio Frequency.....	89
RNA	Ribonucleic Acid.....	5
SCOP	Structural Classification of Proteins.....	24
SDS	Sodium Dodecyl Sulfate.....	83
TCA	Tricarboxylic Acid.....	9
TPCK	Tosyl Phenylalanyl Chloromethyl Ketone.....	132
tRNA	Transfer RNA.....	7

CHAPTER ONE

LITERATURE REVIEW

1.1 Sulfur Metabolism in Bacteria

1.1.1 Role and Availability of Sulfur

Sulfur is the sixth most abundant element on the earth surpassed by oxygen, iron, magnesium, silicon and nickel.¹ However, the biomass of sulfur by weight is less than 1%. Sulfur is ubiquitous, and it exists in different forms such as sulfate minerals with gypsum (CaSO_4), in crystal rocks, or as sulfide minerals in the earth's mantle as pyrite (FeS_2).²⁻⁴ Also, it is present as dimethyl sulfide in the ocean, and as a trace gas in the atmosphere.¹ The main reserve of sulfur occurs in the form of inorganic sulfate in the ocean. The global sulfur cycle is formed from the steady exchange of sulfur atoms from volatile sulfur gases as sulfur dioxide and hydrogen sulfide which are released into the atmosphere.¹ These gases are emitted from different sources including artificial human activities, volcanic eruptions, and biological tissue decomposition.^{3,5}

Next to calcium and phosphorus, sulfur is the most abundant element found in the body.^{6,7} The principal proteinogenic sulfur amino acids include methionine and cysteine and they are incorporated into proteins.⁸ The other primary amino acids are comprised of carbon, hydrogen, oxygen, and nitrogen atoms only.⁹ In mammals, methionine is an essential amino acid acquired by dietary intake while cysteine is nonessential and can be synthesized from methionine. Methionine from the diet can provide all the required sulfur for the body excluding vitamins, thiamin, and biotin. However, in microorganisms, cysteine and homocysteine are the precursors of methionine. Methionine and its derivative, N-formyl methionine initiates amino acid synthesis in eukaryotes and

prokaryotes, respectively. Most of these methionine residues are removed after initiation, which suggests that their role lies in the initiation of translation but not in protein structure.¹⁰ Methionine is one of the most hydrophobic amino acids often present in globular proteins and it is present in the protein hydrophobic interior. In membrane-spanning proteins, methionine can interact with the phospholipid bilayer.⁹ Cysteine plays an important role in protein structure. Its unique ability to form inter and intrachain disulfide bonds with other cysteine atoms is pertinent for the stability of the protein backbone.

Sulfur is an important constituent of tissue proteins and sulfur containing amino acids influence protein metabolism.¹¹ Due to the redox properties of sulfur, it is a constituent of antioxidants such as glutathione which ensures that cellular integrity is not compromised by participating in the removal of radicals, toxic agents, and reactive oxygen species.¹² Cysteine and methionine are precursors for the synthesis of several non-proteinogenic amino acids (taurine), vitamins and cofactors (thiamine, Coenzyme A, Coenzyme M, S-adenosylmethionine, biotin, lipoic acid), electron carriers (iron-sulfur (Fe-S) clusters), sulfate in adenosine-5'-phosphosulfate and phosphoadenosine-5'-phosphosulfate and other sulfur containing biomolecules.^{7,13–16}

Sulfur is present in different stable compounds where it can have either positive or negative oxidation states and these compounds are a part of the global sulfur cycle.^{3,17,18} Sulfur isotope data from different Archean and preanthropogenic rock samples suggest that sulfur derived metabolism dates back several billion years.^{19–23} Natural and anthropogenic contributions of sulfate make up most of the sulfur available in the atmosphere. The assimilation of sulfur for the synthesis of sulfur containing biomolecules is made possible through the utilization of inorganic and organic sulfur sources in the

environment. Readily available forms of inorganic sulfur are predominantly sulfate and sulfide.³ Sulfide functions as a signaling molecule in mammals and as a defense mechanism against oxidative stress in bacteria.^{24–26} When sulfide levels are high, it is oxidized to sulfate and thiosulfate in heterotrophic bacteria as a means of detoxification.^{27–29} The different inorganic states of sulfur have been well investigated, however the organic forms of sulfur, its metabolism and mechanisms of regulation have not been fully explored.³⁰

1.1.2 Sulfur Assimilation in Bacteria

Sulfur metabolism requires significant energy in the form of ATP. The first step in sulfur assimilation is the entrance of sulfate into the cell through a sulfate permease before subsequent activation and reduction steps that are energy consuming.³¹ The intracellular space where reduced sulfur resides has an electric potential that is highly negative (-70 mV). Also, due to the presence of oxygen in the intracellular space, cell compartmentalization is required for the maintenance of a low oxidation reduction potential.³⁰

Inorganic sulfate (SO_4^{2-}) is transported into the cell and activated with ATP by an ATP sulfurylase (1) to generate adenosine phosphosulfate (APS) and pyrophosphate.³² APS is further transformed to 3'-phosphoadenosine phosphosulfate (PAPS) by phosphorylation at the 3'-OH position (2). This reaction is catalyzed by APS kinase which requires a second ATP molecule (**Fig. 1.1**).³⁰ PAPS is reduced by PAPS reductase (3) to yield sulfite (SO_3^{2-}) and adenosine 3'-5' diphosphate (PAP) as a by-product.^{3,30} Lastly, sulfite ion is reduced by a NADPH-sulfite reductase (4) to sulfhydryl ion (bisulfide), HS^- .^{33,34} The biosynthesis of cysteine and other sulfur biomolecules is initiated from the

reaction of bisulfide, HS^- with an organic substrate, O-acetylserine (5).³⁵ The metabolism of sulfur in bacteria is generally similar with that of plants except for a few differences. Plants can use only inorganic sulfate for the acquisition of sulfur; however, many bacteria can utilize alternative sulfur sources including sulfonates (RSO_3^-) and sulfate esters (ROSO_3^-).³⁶

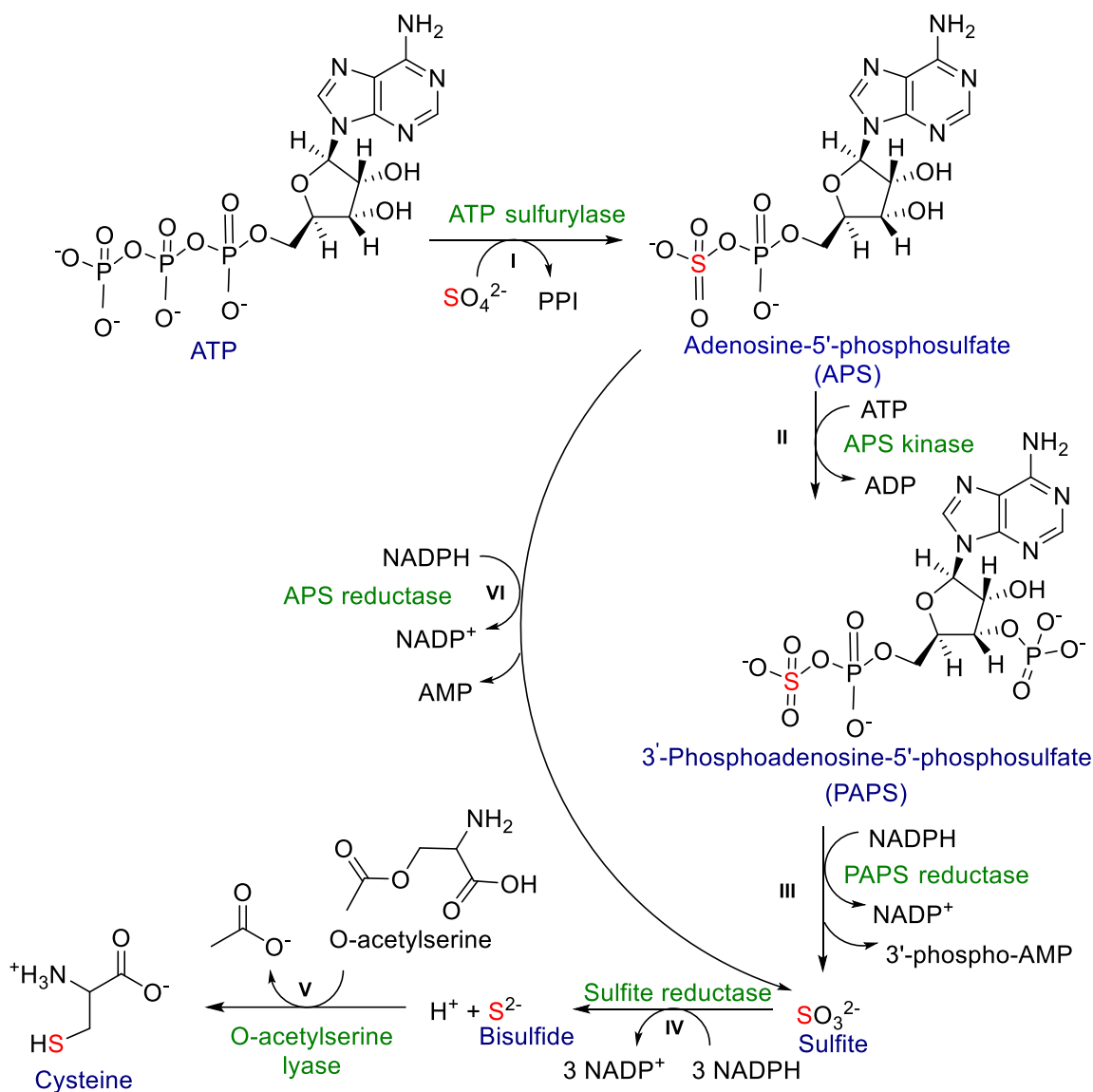


Figure 1.1: Sulfur assimilation pathway and biosynthesis of cysteine in bacteria. (Adapted from^{30,34,35}).

Plants, bacteria, and algae can reduce APS directly to sulfite bypassing the PAPS step. This reduction is catalyzed by APS reductase (APR) (6); however, fungi and certain enteric bacteria such as *Escherichia coli* and *Salmonella typhimurium* utilize the second phosphorylation step catalyzed by PAPS reductase.³⁷ These reductases catalyze the first committed step in the biosynthesis of cysteine and are present in several human pathogens. APR plays a crucial role in the regulation of sulfate assimilation and reduction in plants and its activity is directly linked to the survival of the persistent stage of infection of *Mycobacterium tuberculosis*.^{34,38–41} An increase in the concentration of APS serves as a positive effector for the upregulation of sulfur assimilation enzymes^{42,43} Also, an excess of reduced sulfur inhibits the uptake and assimilation of sulfate and O-acetylserine or its isomer, N-acetylserine, serves as a positive regulator for the biosynthesis of sulfur.^{44,45}

1.1.3 Sulfur Trafficking and Incorporation into Biomolecules

The chemistry of essential sulfur containing molecules such as cofactors, vitamins, and RNA thio-nucleosides has been well studied. However, the biosynthetic process by which sulfur is incorporated into these biomolecules has just begun to be fully explored. This is because persulfides were only recently discovered and they are unstable which makes them difficult to be investigated.⁴⁶ Bisulfide, generated from the reduction of inorganic sulfate was the likely source of sulfur for the biosynthesis of cysteine at low micromolar concentrations.³³ However, bisulfide is toxic, and recent reports show that cells can utilize persulfides as a safer medium for the delivery of sulfur.³³ Persulfides can be formed *in vivo* by two mechanisms. The first mechanism occurs between bisulfide and cysteine disulfides (RSSR) or sulfenic acids (RSOH). The second mechanism requires the action of enzymes such as cysteine desulfurases and 3-mercaptopyruvate sulfur

transferases on nonactivated sulfur compounds.⁴⁷ The sulfur atoms in persulfide have three dissimilar oxidation states which makes them capable of acting as both electrophiles and nucleophiles (**Fig. 1.2**).³³ Due to its oxidation state, sulfane sulfur (S^0) acts as an electrophile which is susceptible to attack by nucleophiles. Different reactions can be observed in the presence of nucleophiles including an attack on either of the inner (sulfenyl) (**Fig. 1.2A**) or outer (sulfhydryl) sulfur atoms (**Fig. 1.2B**), deprotonation of the alpha-carbon and deprotonation of the sulfhydryl group.^{48–50} Less nucleophilic reagents (hydroxide and sulfite) attack the inner sulfur atom while stronger nucleophiles (cyanide and thiolate) attack both sulfur atoms.^{33,46} The more reduced forms of persulfides, persulfide (S^{1-}) or sulfide (HS^-) are more nucleophilic when compared to thiols.^{50,51} Increased nucleophilicity arises as a result of the alpha effect where the terminal sulfur of the persulfide group acts as a nucleophile leading to the formation of a disulfide bond ($R-S-S-R$) (**Fig. 1.2C**).^{48,52}

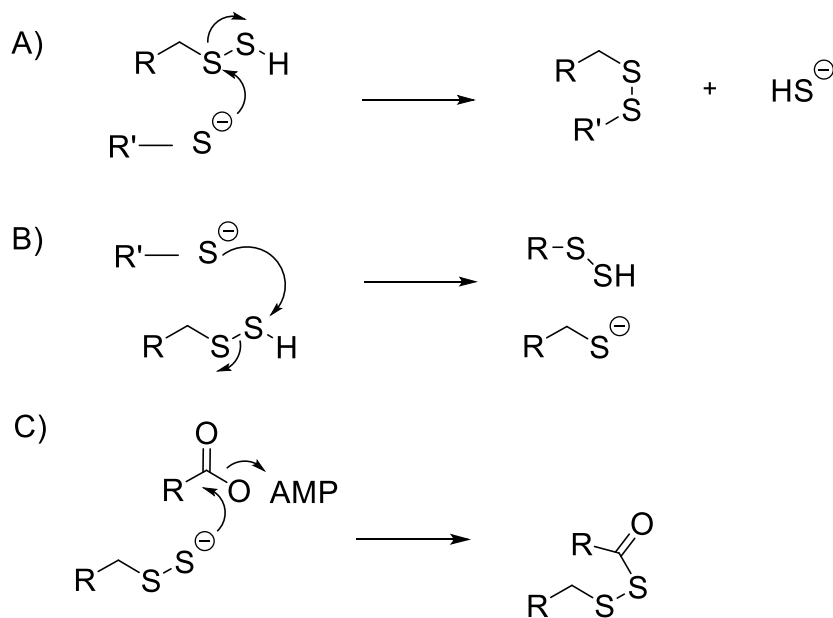


Figure 1.2: Persulfides can act as both electrophiles and nucleophiles in sulfur trafficking. a) The inner sulfur or b) the outer sulfur can act as an electrophile and c) the terminal sulfur can function as a nucleophile. (Adapted from³³).

Cysteine is essential for the synthesis of different biomolecules. Persulfides in proteins are formed by a family of enzymes called cysteine desulfurases. These enzymes utilize the cofactor pyridoxal 5'-phosphate to catalyze the conversion of L-cysteine to alanine and sulfane sulfur through the formation of an enzyme bound persulfide intermediate (**Fig. 1.3**).^{53–56} The persulfide formed is subsequently infused into the pathways responsible for the synthesis of sulfur containing biomolecules.

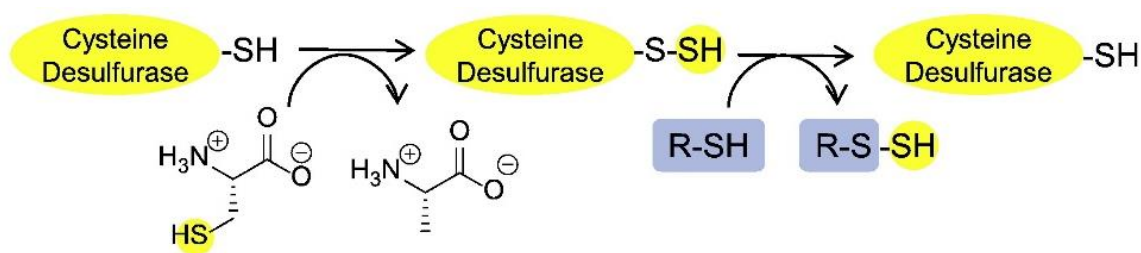


Figure 1.3: Cysteine desulfurases catalyze the formation of persulfides from free cysteine.⁵⁶ Copyright © 2014 Elsevier B. V.

The first cysteine desulfurase that was characterized was NifS from *Azobacter vinlandii*, which catalyzes the transfer of sulfur for the synthesis of iron-sulfur clusters in nitrogenase enzymes.^{57,58} However, *E. coli* has three cysteine desulfurases that are homologous to NifS: IscS, CsdA (also known as CSD), SufS (also known as CsdB) and many pathways rely on these enzymes for sulfur provision.^{59,60} IscS is involved in the biosynthesis of thiamin, thio-nucleosides, molybdopterin and iron-sulfur cluster assembly (**Fig. 1.4**). IscS also supplies sulfur for tRNA modification pathways.⁶¹ CsdA can function in either iron-sulfur cluster assembly or may traffic sulfur for the biosynthesis of molybdopterin. SufS presumably generates and repairs iron-sulfur cluster assembly when IscS-dependent systems are inactive due to oxidative stress or iron paucity.^{33,62}

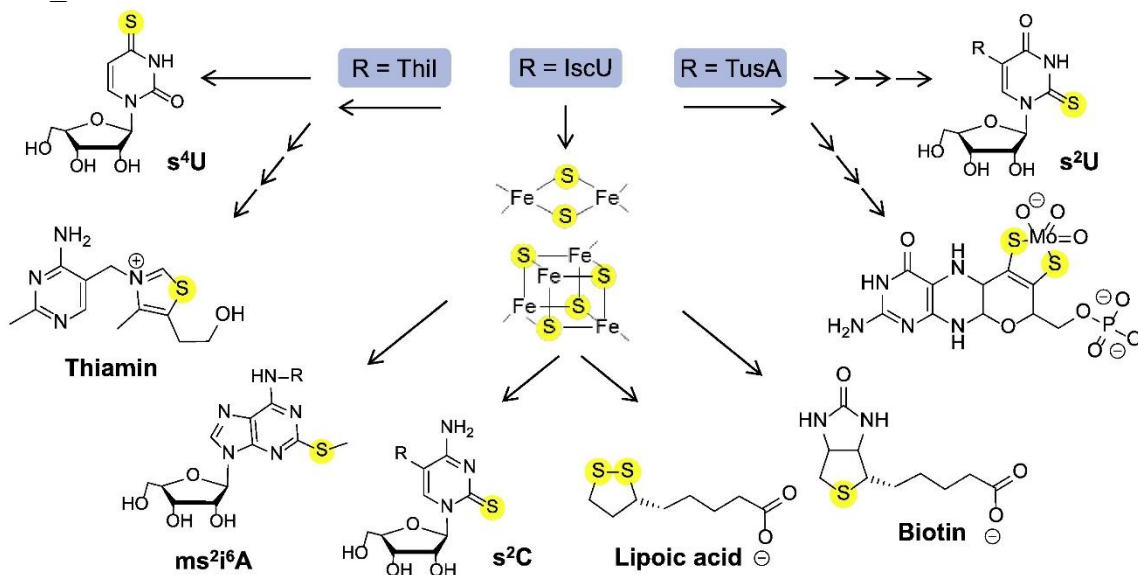


Figure 1.4: Biosynthesis of sulfur-containing cofactors involving the three sulfur acceptors (Thil, IscU, and TusA) in *E. coli*.⁵⁶ Copyright © 2014 Elsevier B.V.

Another enzyme system that plays a role as the acceptor of the terminal sulfur of the persulfide group is the Rhodanese homology domain proteins. The active site cysteine of rhodanese attacks the terminal sulfur of thiosulfates to form an enzyme persulfide and sulfite.⁶³ The terminal sulfur on the enzyme persulfide is acted upon by a cyanide to generate thiocyanate and the active site cysteine is regenerated for another cycle of sulfur transfer. Many organisms such as archaea, bacteria and eukaryotes contain the rhodanese domain proteins, signifying their utility in sulfur transfer.⁶³ Rhodanese also functions as a persulfide carrier in the biosynthesis of 4-thiouridine in tRNA and molybdopterin.³³

Sulfur containing biomolecules plays diverse functional roles in cells. Molybdopterin combined with the molybdate cofactor is essential in the overall catalysis of enzymes

such as sulfite oxidase, aldehyde oxidase and xanthine dehydrogenase.⁶⁴ These enzymes catalyze the transfer of oxygen to or from a biological molecule.⁶⁵ The sulfur atom of molybdopterin acts as a ligand to coordinate the binding of the molybdenum cofactor for catalysis to occur.^{66–68} Biotin is an essential cofactor crucial for the metabolism of amino acids, biosynthesis of fatty acids, and in replenishing intermediates of the TCA cycle. The final step catalyzed by biotin synthase in the synthesis of biotin is the incorporation of a sulfur atom into dethiobiotin to generate biotin.⁶⁹ Biotin is present in different carboxylase enzymes where it aids in the transfer of carbon dioxide between metabolites. Several thio-modified transfer RNAs (tRNA) such as 4-thiouridine are crucial for accuracy during translation.⁷⁰ Some tRNA modifications act as biochemical sensors for environmental stress.⁷¹ The functions of the thio-nucleosides may be dependent on where the modified group is located on the tRNA.⁵⁶ Modifications present at the T-loop and D-loop of tRNA function in maintaining structural stability and serve as recognition centers for tRNA-modifying enzymes.⁵⁷

1.1.4 Organosulfur Sources utilized during Sulfur Starvation Conditions

Bacteria utilize sulfur from diverse sources for their growth and survival. Sulfur can be assimilated from a broad range of sources such as inorganic sulfate, thiosulfate, sulfite and sulfide.^{72,73} The preferred sulfur source is cysteine and inorganic sulfate. In the laboratory, bacteria are grown in media that contains sulfate and amino acid sulfur obtained from cell hydrolysates or in an excess of inorganic sulfate.⁷⁴ The percentage availability of inorganic sulfate in the environment is often low, so bacteria utilize organosulfonates as an alternative sulfur source for sulfur acquisition. Organosulfonates are naturally occurring compounds often found in large portions (>95%) in organic matter

in soil and marine sediments.^{75–77} Some examples of these compounds include sulfate esters, sulfonates, organosulfides, and sulfamates.^{36,72,78} Many of the organically bound sulfur compounds not only serve as sulfur sources for bacteria but also as sources for carbon and energy.^{74,79}

During sulfur limiting conditions, certain enzymes under the sulfate starvation response are expressed for the utilization of organosulfur compounds.⁸⁰ These proteins are termed sulfate starvation-induced proteins (SSI) and when expressed they comprise proteins utilized for the acquisition of sulfur and proteins involved in organosulfonate uptake into the cells.^{78,81} SSI proteins were first identified in *E. coli*, where they were upregulated in the presence of sulfonate sulfur as the sulfur source in place of inorganic sulfate.⁸² SSI proteins expressed in *E. coli* include *tauABCD* and *ssuEADCB* genes (**Fig. 1.5**).⁸³ These proteins utilize linear aliphatic sulfonates and taurine as sulfur sources which are desulfonated when sulfate is limiting and are repressed in the presence of sulfate.^{84,85}

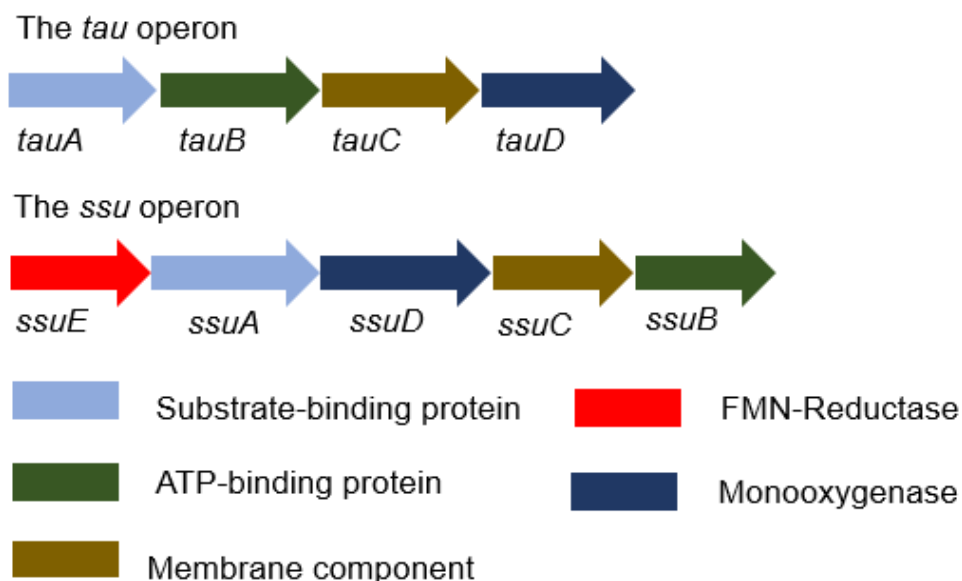


Figure 1.5: The *tau* and *ssu* operons induced during sulfur limiting conditions in *E. coli* (Adapted from⁸⁵).

TauD of the *tau* operon represents an α -ketoglutarate (α -KG)-dependent dioxygenase that desulfonates the substrate, taurine (2-aminoethane sulfonate) to 2-aminoacetaldehyde and sulfite.⁸⁶ This reaction is dependent on the presence of molecular oxygen, iron (II), and α -ketoglutarate (**Fig. 1.6**).^{36,85} The entire reaction leads to the formation of sulfite and succinate showing that the desulfonation of taurine and decarboxylation of α -ketoglutarate are indeed coupled. The dioxygenase, TauD utilizes, albeit poorly, other substrates such as butanesulfonate, pentanesulfonate, and 3-(N-morpholino) propanesulfonic acid) buffer (MOPS).⁸⁷

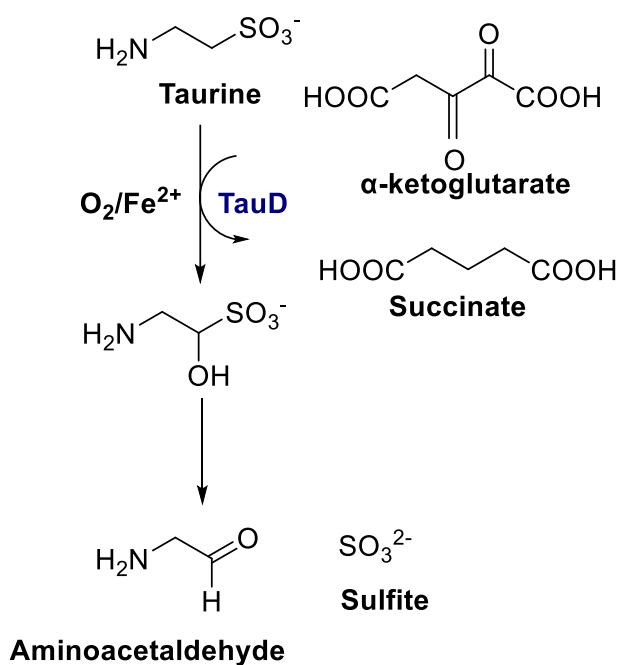


Figure 1.6: Desulfonation of taurine (2-aminoethanesulfonate) by TauD to sulfite and aminoacetaldehyde. (Adapted from³⁶).

The *ssu* operon encodes genes that enable bacteria to utilize alkanesulfonates when sulfur is limiting. SsuE expressed from the *ssu* operon is a flavin reductase that catalyzes the reduction of flavin by NAD(P)H and transfers reduced flavin to the monooxygenase partner, SsuD. The flavin-dependent monooxygenase, SsuD relies on

reduced flavin transferred from SsuE to catalyze the desulfonation of a range of substrates to the corresponding aldehyde and sulfite (**Fig. 1.7**).⁸⁸ The substrate range includes linear aliphatic sulfonates (ethanesulfonate to tetradecanesulfonate), substituted ethane-sulfonic acids, and sulfonated buffers.⁸³ However, SsuD does not catalyze the desulfonation of such substrates as methanesulfonate, sulfonates, taurine and cysteate. The monooxygenase, SsuD, is found in a broad range of bacteria species. Often, the reductase, SsuE is located on the same operon as an SsuD homologue.⁸⁹ However, in *Corynebacterium glutamicum*, and *Burkholderia cenocepacia* the reductase is absent on an operon that encodes SsuD.^{90–92} In such cases, SsuD may utilize reduced flavin supplied by a non-specific reductase. This phenomenon has been observed in Nitrilotriacetate monooxygenase from *Chelobacter heintzii*, where its specific reductase, NmoB was replaced by a reductase from *Photobacterium fischeri*.⁸⁵

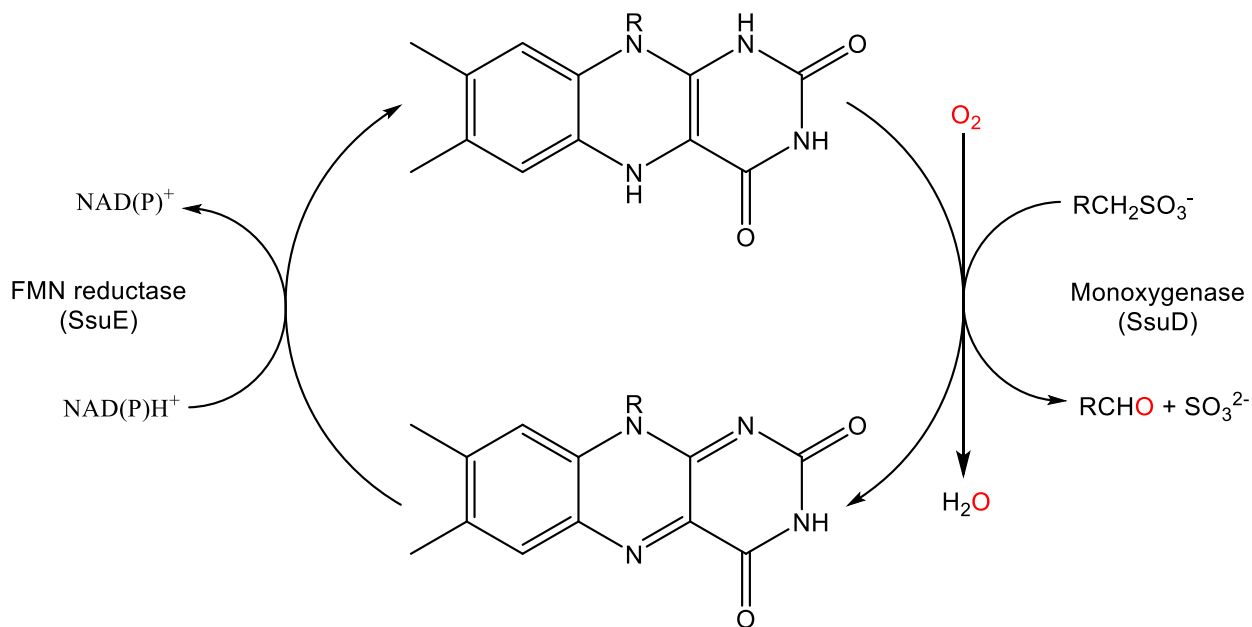


Figure 1.7: Desulfonation of alkanesulfonates by SsuE and SsuD of the alkanesulfonate two-component FMN-dependent system. (Adapted from⁸⁸).

The *tauABC* and *ssuABC* genes code for ATP-binding cassette (ABC-type) transporters involved in the uptake of taurine and alkanesulfonates into the cell.^{87,93,94} TauA and SsuA have been observed to act as periplasmic sulfonate binding proteins. TauB and SsuB as well as TauC and SsuC could function as ATP binding proteins and permease proteins, respectively (**Fig. 1.8**).^{76,85} The transportation of taurine into the cell is only mediated by the TauABC transporter proteins and longer-chain alkanesulfonates by the SsuABC system. It was observed that the TauABC and SsuABC transporter proteins are not exchangeable.⁸⁵ In certain instances, some substrates such as butanesulfonate and 3-aminopropanesulfonate served as substrates for both systems and were translocated by either transporter proteins.⁸³

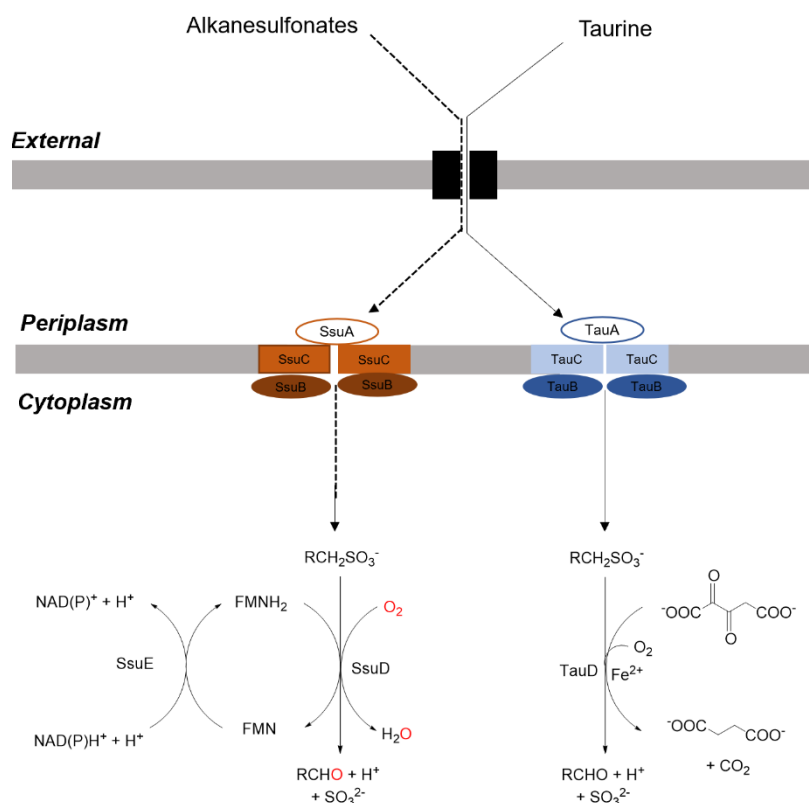


Figure 1.8: Uptake and desulfonation of alkanesulfonates and taurine in *E. coli*. Alkanesulfonates and taurine are transported into the cell via SsuABC and TauABC transport system. (Adapted from⁸⁵).

Certain genes are upregulated under the sulfur starvation response which enables other organisms utilize additional organosulfur sources under sulfur limiting conditions. *Pseudomonas putida* utilizes arylsulfonates, dimethyl sulfide (DMS), dimethyl sulfonate (DMSO₂), and methanesulfonate as an alternative sulfur source and the *ssuEADCBF* gene was essential for the desulfonation of these substrates.^{74,78,80,95,96} Also, arylsulfatase activity was observed in *Pseudomonas aeruginosa* after growth with a diverse range of sulfate esters and with alternative sulfur sources such as taurine, cysteine sulfonate, cysteine sulfinic acid and cysteic acid.^{96,97} The *ssu*, *tau*, and *msu* operon are utilized by *Pseudomonas* sp. for sulfur acquisition from these organosulfonates.⁹⁸

The *msu* operon encodes the *msuEDC* gene product responsible for the desulfonation of methanesulfinic acid, a product of the oxidation of dimethylsulfide.⁹⁹ The *msuEDC* operon encodes MsuE, the NADPH-dependent FMN reductase that supplies reduced flavin to two different monooxygenases, MsuD and MsuC.^{31,100} MsuC and MsuD are FMN-dependent monooxygenases that catalyze the oxidation of methanesulfinic acid and methanesulfonate respectively. The product from the oxidation of MsuC, methanesulfonate is converted to sulfite by MsuD.

1.1.5 Regulation of *ssi* Operons

The assimilation of sulfur from organosulfur compounds when inorganic sulfate is limiting is under the influence of sulfur starvation proteins (SSI).⁸¹ The synthesis of these proteins is repressed in the presence of sulfate and cysteine but upregulated in the absence of sulfate or in the presence of organosulfonates. Regulation of the sulfur

starvation proteins, *ssuEADCB* and *tauABCD* in *E. coli* is performed by the CysB protein. The CysB protein is a transcriptional regulatory protein of the LysR family.⁷² CysB is a global regulator of sulfur assimilation for both inorganic and organic sulfur sources. It binds upstream of the -35 region of several promoters of cysteine biosynthesis.^{101–103} CysB is in turn positively regulated by the binding of a coinducer, N-acetylserine or O-acetylserine, however it is downregulated in the presence of antiinducers, thiosulfate or sulfide (Fig. 1.9).^{72,102,104} The *cys* regulon not only encodes the genes for the synthesis of cysteine but also the genes utilized for the uptake and desulfonation of organosulfonates.⁷²

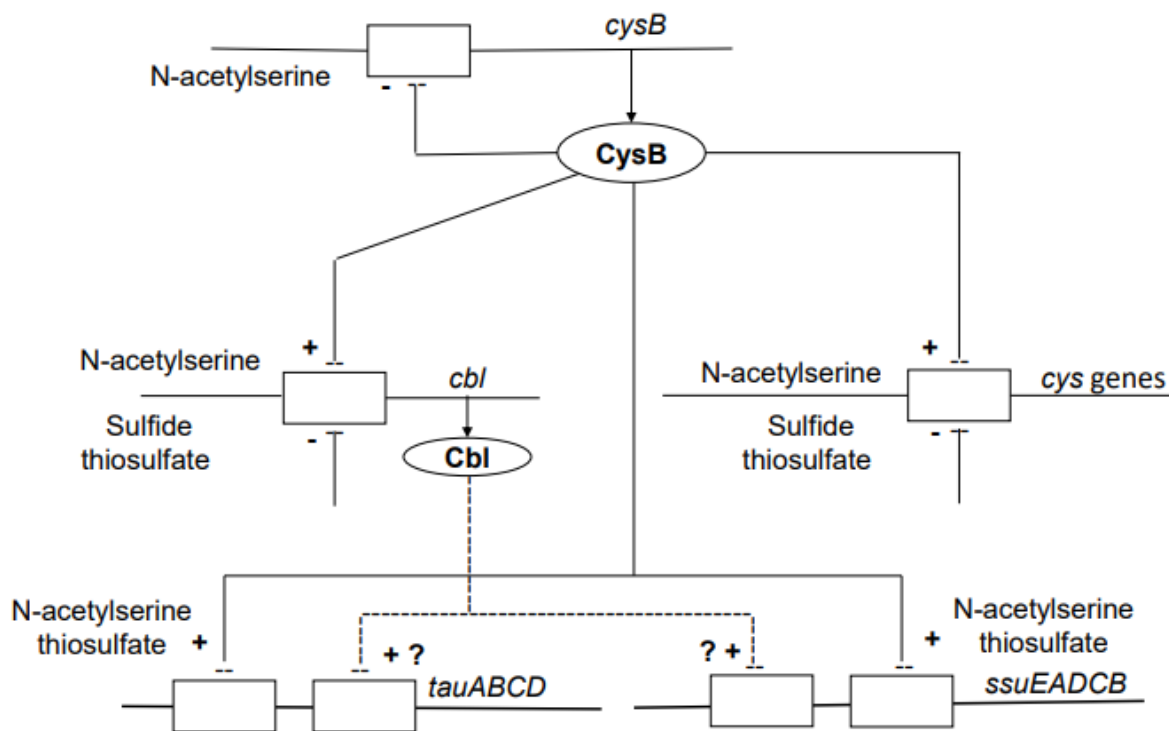


Figure 1.9: Proposed model for the mechanism of sulfur assimilation by CysB and Cbl in *E. coli*. (Adapted from⁸⁵).

The synthesis of the periplasmic proteins, SsuA and TauA is a costly process and has a second level of regulation involving a specific LysR regulator. Cbl is a “CysB-like” protein present in *E. coli* that regulates the synthesis of the *tau* and *ssu* operon. The expression of the *cbl* gene is regulated by CysB which is an extra level of regulation by the cell. Under sulfate starvation conditions, Cbl binds upstream of the -35 region of the *ssu* promoter and CysB and Cbl have been shown to both interact with the *tau* operon promoter region.^{72,105} However, when sulfate is in excess, an intermediate in the sulfate assimilation pathway, adenosine-5'-phosphosulfate (APS) serves as corepressor of Cbl.^{43,81} It also inhibits Cbl DNA binding leading to the absence of *ssu* and *tau* operon expression.⁷⁸

SSI protein expression in pseudomonads is different from *E. coli*. CysB has been shown to be vital for sulfur assimilation in *Pseudomonas* sp.; however, there is no equivalent *cbl* gene in *P. aeruginosa* and *P. putida*.^{106,107} Several specific regulators have been reported through extensive research performed on pseudomonads.^{108–110} However, it is still unknown how they regulate sulfur starvation conditions and control the expression of the genes required for sulfur assimilation from organosulfonates.^{106,107}

1.2 Flavin and Flavoproteins

1.2.1 Flavin

Many proteins utilize a flavin cofactor to catalyze diverse biological processes.¹¹¹ The compound, flavin (7,8-dimethylisoalloxazine) was first identified by Wynter Blyth as a yellow pigment that was isolated from cow's milk, which he termed lactochrome (**Fig. 1.10**).^{87,111} Subsequent research efforts by different groups isolated a yellow compound with bright green fluorescence which was later found to be a component of the vitamin B

complex. The structure of this compound was determined by Richard Kuhn and other prominent scientists to be riboflavin.^{112,113} The name derives from its constituents, the ribityl side chain and the yellow color stems from the conjugated ring system. Other structures which were later identified had slight modifications of the riboflavin parent compound.¹¹⁴ These structures include natural occurring flavins; flavin mononucleotide (FMN) and flavin adenine dinucleotide (FAD), which are the forms of riboflavin that enable different enzymes to carry out diverse functions.¹¹⁵ Flavin cofactors may be either covalently bound or act as co-substrates to a wide variety of enzymes where they play different roles in the catalytic process.

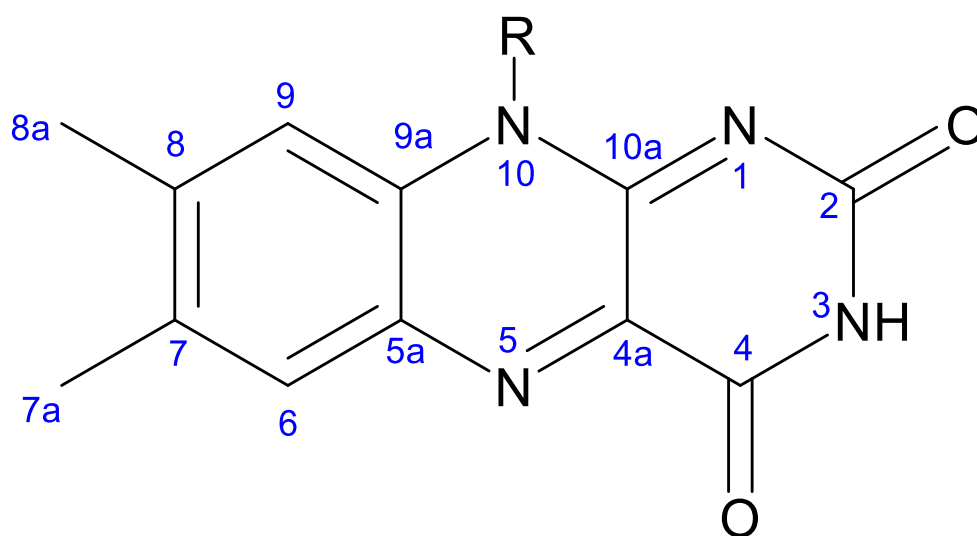


Figure 1.10: The isoalloxazine ring of flavin.

Naturally occurring flavins such as lumiflavin, riboflavin, FMN and FAD contain the tricyclic isoalloxazine ring, which is the business-end of the flavin molecule; however, the difference in the structures lies in the R-groups (**Fig. 1.11**).¹¹⁶ Due to this adaptability, they are found as cofactors or substrates in different enzymes such as dehydrogenases, oxygenases, oxidases, oxidoreductases, and electron transfer proteins.^{117,118} Flavins have been implicated in a variety of processes, their versatility range from two-electron transfers in enzymes such as the dehydrogenases to participating in one-electron transfer processes with their different free radical states.¹¹¹ Due to these unique properties, they are an important component of multi-redox enzymes such as nitric oxide synthase, cytochrome P450 systems, succinate dehydrogenase and xanthine oxidase.¹¹²

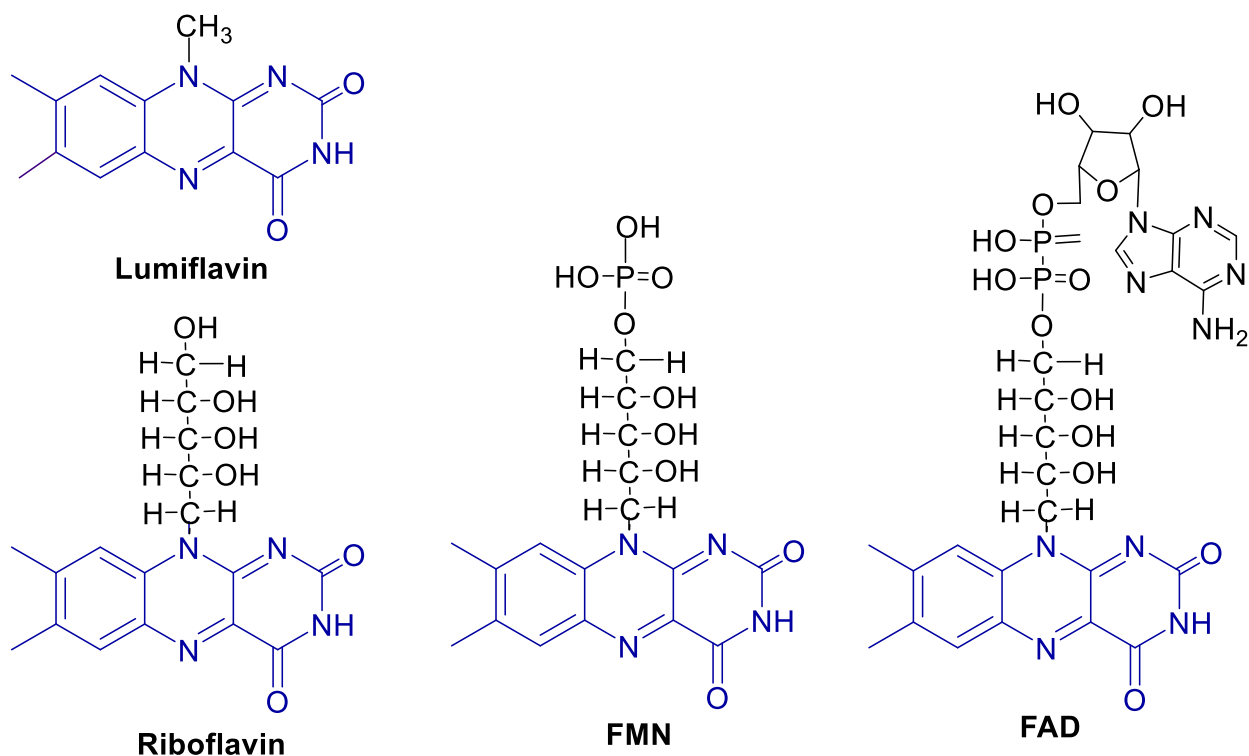


Figure 1.11: Structures of naturally occurring flavin molecules.

1.2.2 Spectral Properties of Flavins

Riboflavin is produced by all green plants and many microorganisms. It is a water-soluble vitamin which is vital for the growth and survival of humans and animals. However, riboflavin cannot be synthesized by humans but can be acquired from different dietary sources, most notably vegetables and milk.^{119,120} Initial synthesis of riboflavin begins with the opening of the imidazole ring of guanosine triphosphate (GTP) and culminates in the formation of the isoalloxazine ring from another precursor, ribulose 5-phosphate.^{121,122} Riboflavin is also the precursor of all biologically active flavins such as FMN and FAD. The conversion of riboflavin to FMN is catalyzed by flavokinase or riboflavin kinase and this reaction is an adenosine triphosphate (ATP)-dependent reaction.^{120,123,124} The biosynthesis of FAD from FMN is catalyzed by FAD synthetase which is also dependent on ATP.

These coenzymes were proposed to participate in different redox processes through the transfer of one or two electrons.¹²⁵ Flavin transfer reactions are made possible through the formation of three oxidation states: oxidized or quinone state, one-electron reduced (semiquinone) and two-electron reduced (fully reduced) states (**Fig. 1.12**).^{126,127} These three oxidation states have characteristic absorbance spectra and different ionic states that makes them distinguishable from each other. The different absorption spectra of flavin are due to the different redox forms and protonation levels. There are about nine forms in free solution, six of which are physiologically feasible due to their pK_a values.¹¹⁵ These properties are dependent on the enzyme environment and provide useful information about the environment where the flavin is located.

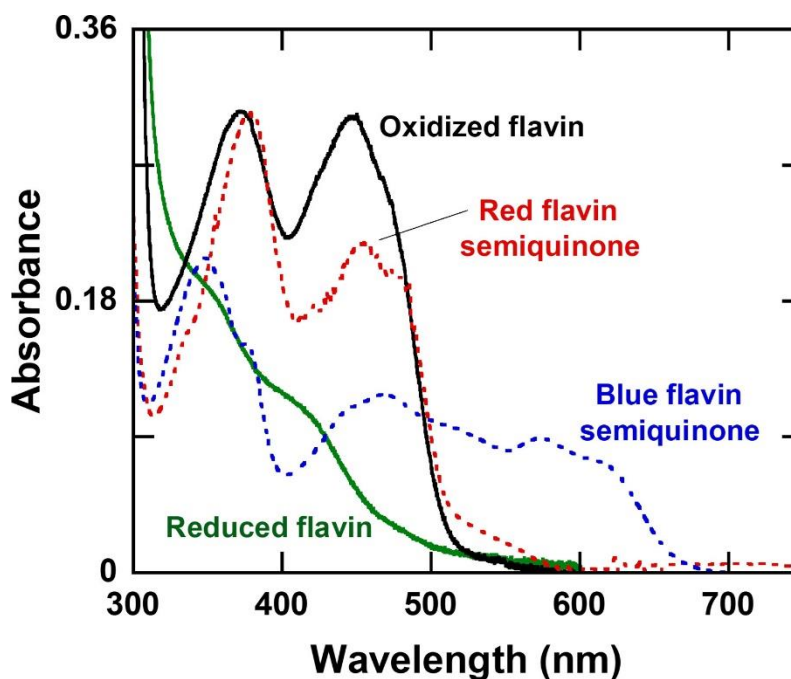


Figure 1.12: Distinct spectral properties of flavin that correspond to different oxidation states. Copyright © 2020 Elsevier Inc. All Rights Reserved.

Oxidized flavin is yellow in color because of the isoalloxazine chromophore, which is visible at approximately 450 nm. The absorption spectrum of oxidized flavin is impacted by the ionization states with pK_a of approximately 0 and 10 and protonation at N1 and deprotonation N3-H respectively (**Fig. 1.13**).^{115,125} However, these pK_a values are not attainable physiologically. Also, oxidized flavin is prone to nucleophilic attack, specifically at the C(4a) and N(5) position.¹²⁶ At neutral pH, and when not bound to protein, semiquinone flavin is formed from an equimolar amount of oxidized flavin and reduced flavin.¹²⁶ This reaction is in an equilibrium and shifts in favor of the semiquinone species when protein is bound.

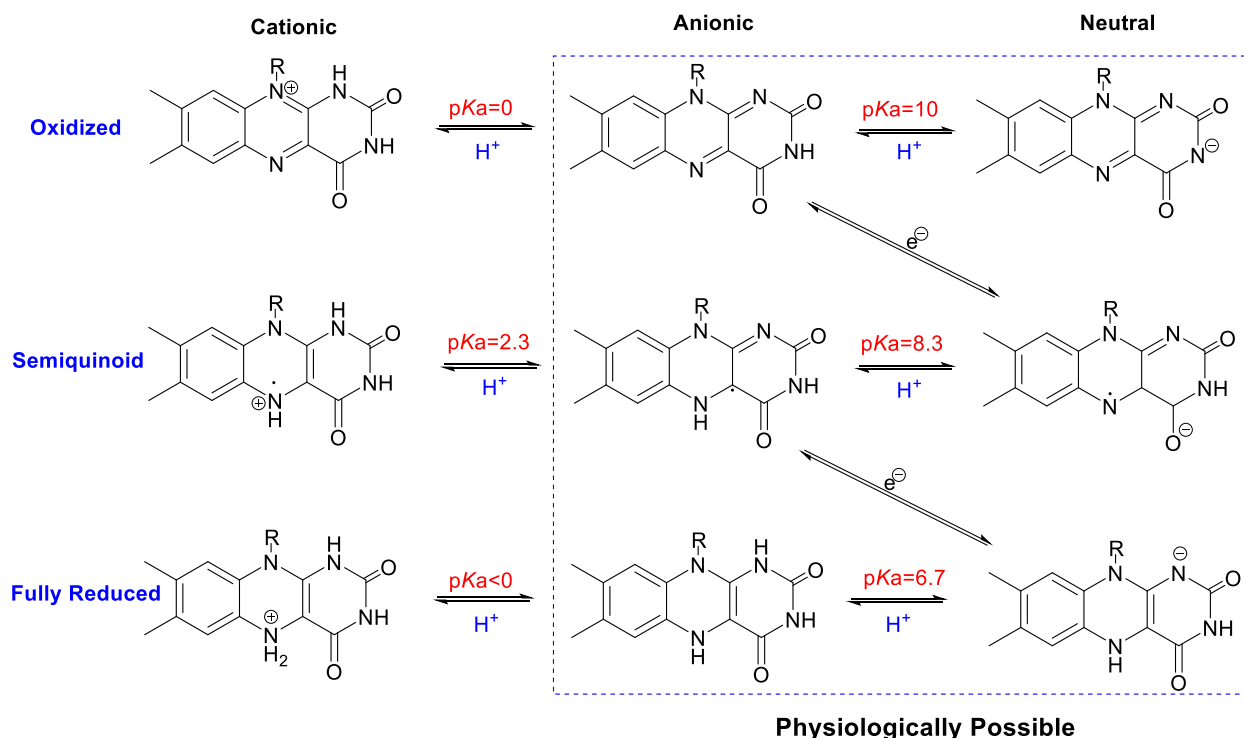


Figure 1.13: Flavin can exist in nine physiological redox and ionic states. (Adapted from¹¹⁵).

Reduction of oxidized flavin by the addition of one electron produces the semiquinone or monoprotonated form.¹¹⁸ Flavin exists as an amphoteric molecule with three different redox states: neutral, anionic and cation species. The neutral semiquinone has a characteristic blue color and a broad absorbance at 600 nm, with a spectra maximum at 615 nm and another at 580 nm. The cationic and anionic semiquinone has a red color with pK_a values of 2.3 and 8.3 respectively and their spectral properties are different.¹²⁸ The cationic semiquinone is formed at extremely low pH values. The neutral and anionic flavosemiquinone are the more biologically active species that are found in flavoproteins.

Flavin reduction generated by the addition of two electrons or two single-electrons to the semiquinone form yields hydroquinone or 1,5-dihydroflavin (fully reduced flavin).

This reduced form is colorless in a dilute solution due to the absence of any prominent electronic transitions in the visible region. However, at high concentrations, the fully reduced flavin shows a deep reddish color due to a low absorption intensity around the 500 nm region. Reduced flavin has one biologically relevant ionization state with a pK_a of approximately 6.5 and the deprotonation occurring at the N(1)-H position.¹²⁹ Several studies have revealed that reduced flavin is a flexible molecule with bending occurring along the N(5)-N(10) axis and its nucleophilicity and reactivity is dependent on the degree of bending.¹²⁹

Flavins also form charge-transfer complexes with various compounds which are observed in biochemical systems. Charge transfer complexes are electronic states that do not belong to any of the three redox states. In these molecular complexes, oxidized flavin acts as the acceptor while the reduced species is the donor.¹²⁶ These complexes have distinguishable weak absorption spectra between 500 and 800 nm. The distinct redox, ionic, and electronic states add to the complexity of flavin and can be regulated in different enzymes providing rich insights into the interaction between the cofactor and the enzyme.¹²⁸

1.2.3 Flavoproteins

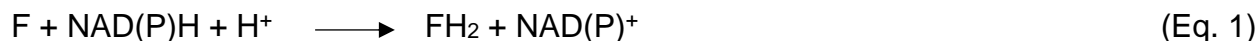
Flavoproteins are proteins that utilize flavin as a cofactor or co-substrate for catalysis. Due to their versatility and the various reactions that they catalyze they have been implicated in many important physiological processes required for the sustenance of living organisms.¹¹⁹ Flavoproteins are grouped based on the number of electrons involved in the reaction, the substrates utilized for catalysis, their structural motif, and the physical and chemical properties of the enzymes.¹¹⁵ Classification of flavoproteins is

difficult because of the diversity in the types of reactions they catalyze and their different biological functions.¹³⁰ However, it has been shown that enzymes that catalyze similar reactions may have common properties unique to that class.

Flavoproteins participate in many essential reactions through one and two-electron transfers.^{111,116,131} Canonical flavoproteins catalyze these reactions with flavin tightly or covalently bound while flavin-free proteins require a continuous supply of flavin.^{116,132} Flavoproteins are generally categorized as oxidases, dehydrogenases, reductases, and monooxygenases.^{133–135} These enzymes catalyze a broad range of biological processes including DNA repair, photochemistry, energy metabolism, protein folding, detoxification, chromatin remodeling etc.¹³⁶ Flavin oxidases utilize molecular oxygen for substrate oxidation and produces hydrogen peroxide in two-half reactions. In the reductive-half reaction, the organic substrate is oxidized yielding fully reduced flavin. Oxidized flavin is regenerated by dioxygen in the oxidative half-reaction.¹¹¹ Examples of flavin oxidases include glucose, D-amino acid and monoamine oxidases.^{137–139} Flavin dehydrogenases utilize organic coenzymes such as quinones or NAD⁺ or pyrroloquinoline quinone as electron acceptors but do not use dioxygen.¹⁴⁰ Some examples of flavin dehydrogenases include acyl-CoA, alcohol, and succinate dehydrogenases. The next two sections will focus on the properties and function of flavin reductases and monooxygenases.

1.2.3.1 Flavin Reductases

Flavin reductases (FR) or NAD(P)H-flavin oxidoreductases refer to enzymes that catalyze the reduction of flavin mononucleotide (FMN) and/or flavin adenine dinucleotide (FAD) utilizing reducing equivalents from NAD(P)H to generate reduced flavin using this equation (Eq. 1):



The reduced flavin (FH₂) produced from this reaction is essential for different biological functions such as release of iron from ferrisiderophores, activation of ribonucleotide reductase and chorismate synthase, oxygen activation, bacteria bioluminescence, and reduction of methemoglobin.^{141–143} Many flavin reductases are bacterial enzymes, however some are from mammalian sources. These flavin reductases are usually small in size and belong to the flavodoxin-like superfamily. The flavin reductases which have been identified in the flavodoxin superfamily belong to four major groups according to the SCOP database: quinone reductases, flavodoxin-related proteins, WrbA-like proteins, and NAD(P)H:FMN reductases.⁸⁹ In the NADPH:FMN reductase family, canonical flavoproteins have flavin bound and they catalyze the reduction of a variety of substrates such as quinones, azo dyes, cyanide, and chromate. Two-component reductases belong to the NADPH:FMN reductase enzyme family and these reductases are flavin-free proteins and function in providing reduced flavin as a substrate to monofunctional flavin-dependent monooxygenases. The monooxygenases only catalyze oxidation half-reactions and would require reduced flavin from an external source.¹⁴⁴

1.2.3.2 Flavin Monooxygenases

Reduced flavoenzymes react with dioxygen. Typically, fully reduced flavin remains at the enzyme active site throughout the catalytic cycle preventing flavin from non-enzymatic reactions with oxygen. However, uncontrolled oxygen reductions often leads to the generation of reactive oxygen species which are toxic and react nonspecifically with many cellular compounds.^{111,134,145} Non-enzymatic reactions of reduced flavin with

oxygen leads to wasteful consumption of energy from continuous utilization of physiological energy sources such as NADH or NADPH, which donate electrons for flavin reduction.¹⁴⁶ Therefore, oxygen-utilizing enzymes need to be tightly controlled to prevent the formation of unwanted reactive oxygen species.

Flavin monooxygenases depend on flavin reductases for the reduction of oxidized flavin. Flavin monooxygenases utilize molecular oxygen (O_2) to oxygenate an organic compound and the reaction relies on reduced flavin to donate electrons to O_2 for activation (1) (**Fig. 1.14**). The initial reaction for flavin-dependent monooxygenases is the activation of dioxygen by reduced flavin to generate reactive intermediates peroxyflavin (FI-OO \cdot) or hydroperoxyflavin (FI-OOH). First, a caged radical pair of neutral flavin radical and superoxide (II) is formed from the reduction of dioxygen by one-electron from reduced flavin (2).¹²⁵ The caged radical pair thus formed has several routes. The radical pair is unstable and can collapse into a nucleophile, C4a peroxyflavin (4) and on protonation generate the electrophilic form, hydroperoxyflavin (5).¹¹¹ The hydroperoxyflavin formed can eliminate hydrogen peroxide to generate oxidized flavin (6). Both intermediates can insert one oxygen atom into a substrate and the other oxygen atom in dioxygen is converted to water.¹¹¹ The hydroperoxyflavin species are generally involved in hydroxylation reactions while the peroxyflavin form functions in the cleavage of the carbon-carbon or carbon-sulfur bonds next to the carbonyl group of the sulfonated substrate. Lastly, the radical pair can dissociate into its components, flavin radical and superoxide as side reactions (3). The superoxide generated can react with peroxide to produce hydroxyl radicals.

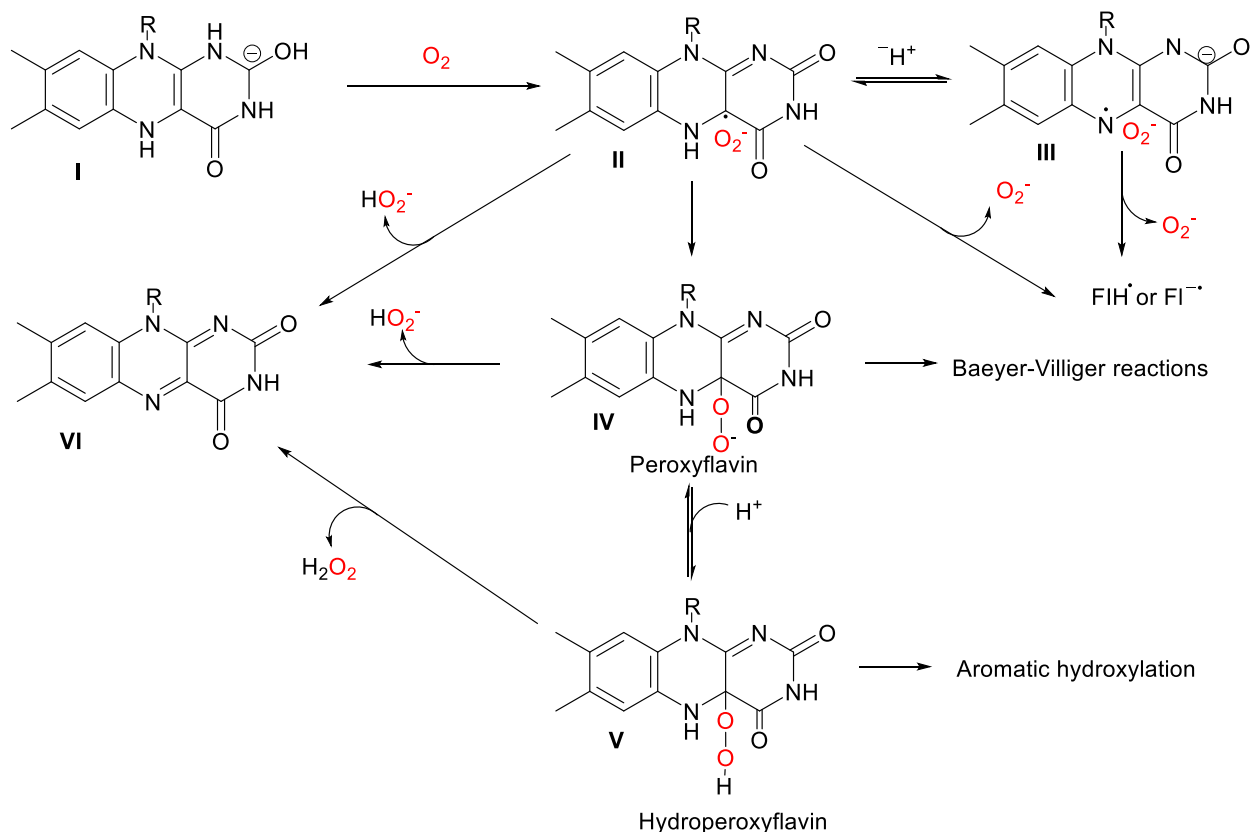


Figure 1.14: Activation of dioxygen by reduced flavin (Adapted from¹¹¹).

1.3 Two-Component Flavin-Dependent Systems

1.3.1 General Overview of Two-Component Flavin-Dependent Systems

Two-component flavin-dependent systems are comprised of a flavin reductase and monooxygenase. The reductase and monooxygenase genes of the two-component flavin-dependent systems are usually expressed together on the same operon. The flavin reductase catalyzes the reduction of flavin, while the monooxygenase catalyzes the cleavage of the oxygen-oxygen bond of dioxygen and inserts one oxygen atom into a substrate and reduces the other oxygen to water.¹⁴⁷ The mechanism of catalysis of the monooxygenase proceeds through the activation of oxygen to form a C4a-(hydro) peroxyflavin intermediate which can act as a nucleophile or electrophile depending on the

nature of the reaction.¹⁴⁷ The flavin reductase catalyzes the reductive half-reaction, while the partner monooxygenase catalyzes the oxidative half reaction. Most canonical flavoproteins catalyze both the reductive and oxidative half-reactions without needing a separate flavin reductase.

Several two-component flavin-dependent systems have been characterized. All two-component systems have been identified in bacteria and they utilize flavin as a substrate. They are involved in bioluminescence, the biosynthesis of antibiotics, the oxidation of long-chain alkanes, the desulfonation of sulfonated compounds and the oxidation of environmental aromatic and polycyclic compounds for utilization as sources of carbon.¹⁴⁷ The first two-component flavin-dependent system that was identified and investigated thoroughly was bacterial luciferase (**Fig. 1.15**).^{148,149} Bacterial luciferase utilizes reduced flavin, a long chain aliphatic aldehyde and dioxygen to generate carboxylic acid with the emission of blue-green light.^{145,150} Bioluminescent proteins have been used to study various biological functions such as protein-protein interactions, identification of transcription factors, investigation of the functional state of proteins in the cell and as bioreporters.^{151–153}

Some two-component flavin-dependent systems degrade chelating agents nitrilotriacetate (NTA) and ethylenediaminetetraacetic acid (EDTA) and the products are utilized as sources for energy.¹⁴⁷ Nitrilotriacetate monooxygenase system (NTA-MO) catalyzes the oxidation of nitrilotriacetate to iminodiacetate and glyoxylate. NTA monooxygenase utilizes reduced flavin from its partner reductase, component B.^{154,155} The EDTA monooxygenase EmoA degrades EDTA to ethylenediaminetriacetate (ED3A) and glyoxylate and further breaks down ED3A to ethylenediaminediacetate. This system

is also capable of degrading NTA and diethylenetriaminepentaacetate (DPTA). EmoB, the flavin reductase in the EDTA monooxygenase system supplies reduced flavin to EmoA monooxygenase.^{147,156,157} Other FMN-dependent systems are associated with the biosynthesis of antibiotics. The Actinorhodin VA monooxygenase system identified in *Streptomyces coelicolor* catalyzes the hydroxylation of kalafungin to form actinorhodin.^{158,159} The other system involved in the biosynthesis of the polyunsaturated cyclic peptolide, pristinamycin IIA is SnaA (PIIA synthase). This reaction involves an oxidation reaction and not the oxygenation reaction typically observed in monooxygenases.^{160,161}

Other two-component systems involved in the acquisition of sulfur have been investigated. Sulfur acquisition from dibenzothiophene (DBT) involves two separate FMN-dependent monooxygenase systems. The first two steps are catalyzed by the DszC FMN-dependent monooxygenase systems that convert DBT to DBT sulfone. A second FMN-dependent monooxygenase, DszA converts DBT sulfone to 2-hydroxyphenyl-2-sulfinite.^{162–164} This system was the first system identified to utilize a single flavin reductase to supply reduced flavin to two separate FMN-dependent monooxygenases, DszC and DszA.^{165,166}

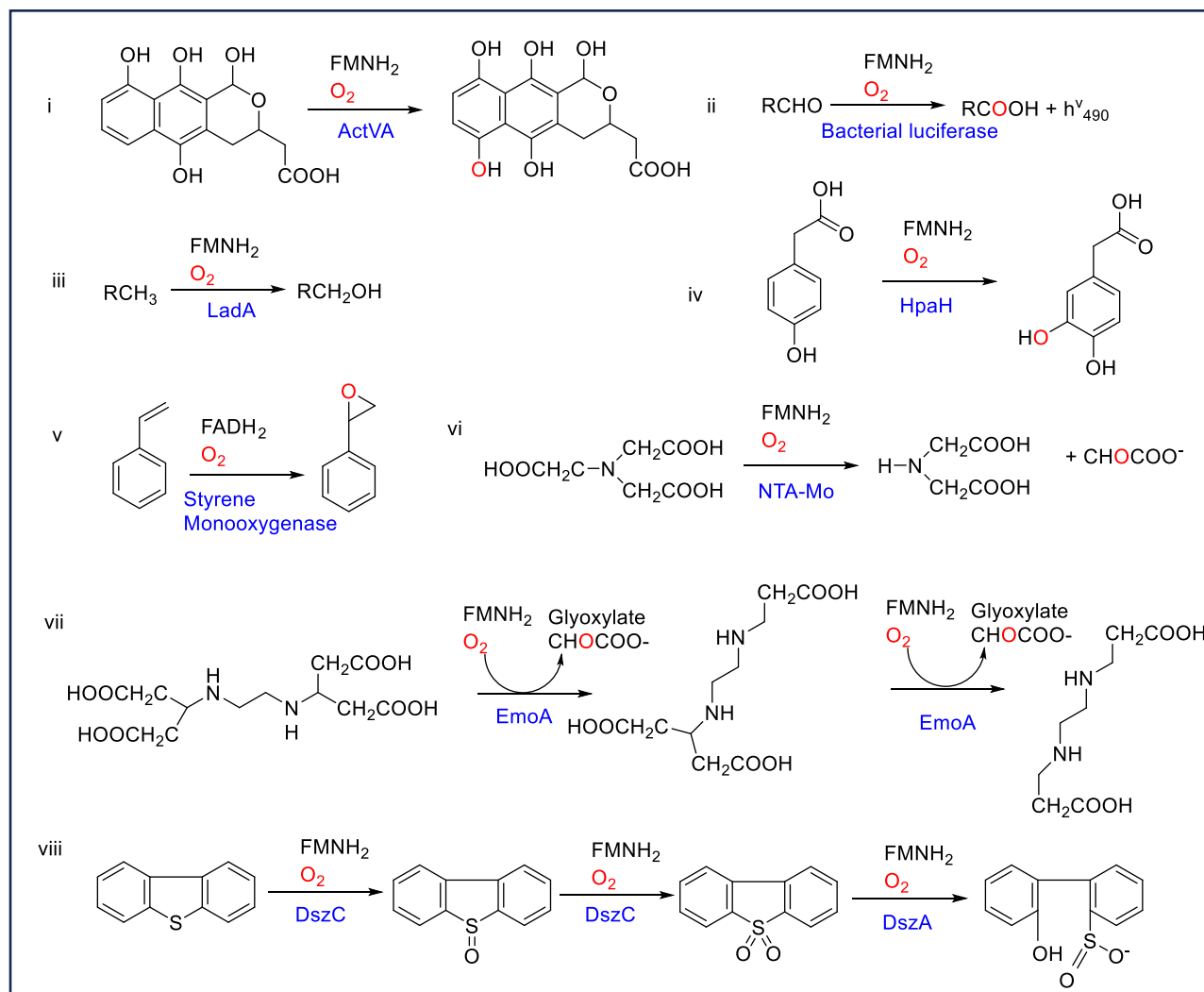


Figure 1.15: Reactions catalyzed by different two-component flavin-dependent monooxygenase systems (Adapted from¹⁴⁷).

The alkanesulfonate monooxygenase system SsuE, an FMN reductase and the SsuD monooxygenase are utilized for the cleavage of the C-S bond of diverse alkanesulfonates to generate sulfite and aldehyde during sulfur limiting conditions. Several two-component FMN-dependent systems were identified in *Pseudomonas* sp. that are utilized for the acquisition of sulfur. *P. aeruginosa* and *P. putida* can utilize a broad range of sulfonated substrates. In addition to acquiring sulfur from alkanesulfonates, these organisms utilize dimethylsulfone (DMSO), an oxidation product

of dimethylsulfide (DMS) when sulfur is limiting in the environment (2) (**Fig. 1.16**).¹⁰⁰ Reduced flavin is supplied by SfnF in *P. putida*, a flavin reductase to the monooxygenase partner, SfnG for the conversion of dimethylsulfone to methanesulfite and formaldehyde (3). A comparable SfnF homolog has not been identified in *P. aeruginosa*. Methanesulfinate is converted to methanesulfonate (MSA) by the methanesulfinate monooxygenase system which comprises the flavin reductase, MsuE and its partner monooxygenase, MsuC (4).¹⁰⁰ The desulfonation of methanesulfonate is catalyzed by MsuE, which transfers reduced flavin to the monooxygenase, MsuD to produce sulfite and aldehyde (5). The methanesulfinate and methanesulfonate monooxygenase systems utilize separate FMNH₂-dependent monooxygenases, MsuC and MsuD but a single FMN reductase, MsuE.^{31,167}

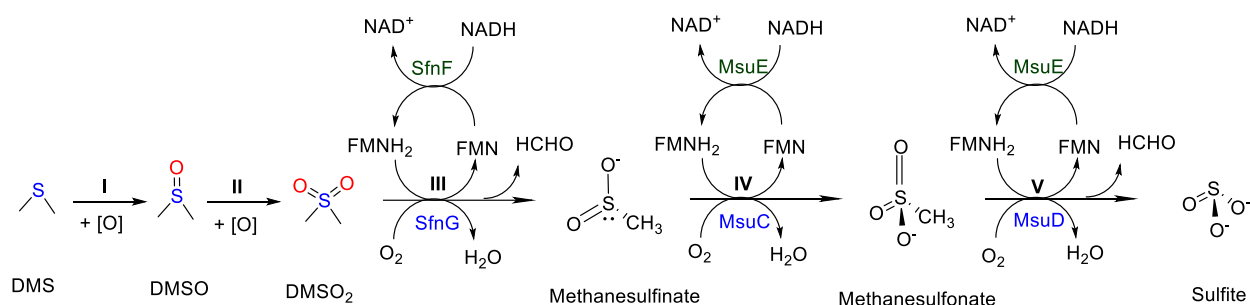


Figure 1.16: Desulfonation of dimethyl sulfide (DMS) in *Pseudomonas* sp. (Adapted from^{31,167}).

1.3.2 Kinetic Mechanisms utilized by Two-Component Monooxygenase Systems

1.3.2.1 FMN Reductases of Alkanesulfonate Monooxygenase Systems

Flavin reductases of two-component systems catalyze the reduction of flavin by utilizing electrons from pyridine nucleotides, NAD(P)H. Most of the reductase enzymes are smaller than their partner monooxygenase. The reductases typically show a preference for either NADPH or NADH, while some reductases utilize both similarly.¹⁴⁴

They are also specific for either FMN and/or FAD, and this specificity extends to the monooxygenases (**Fig. 1.17**).^{94,147}

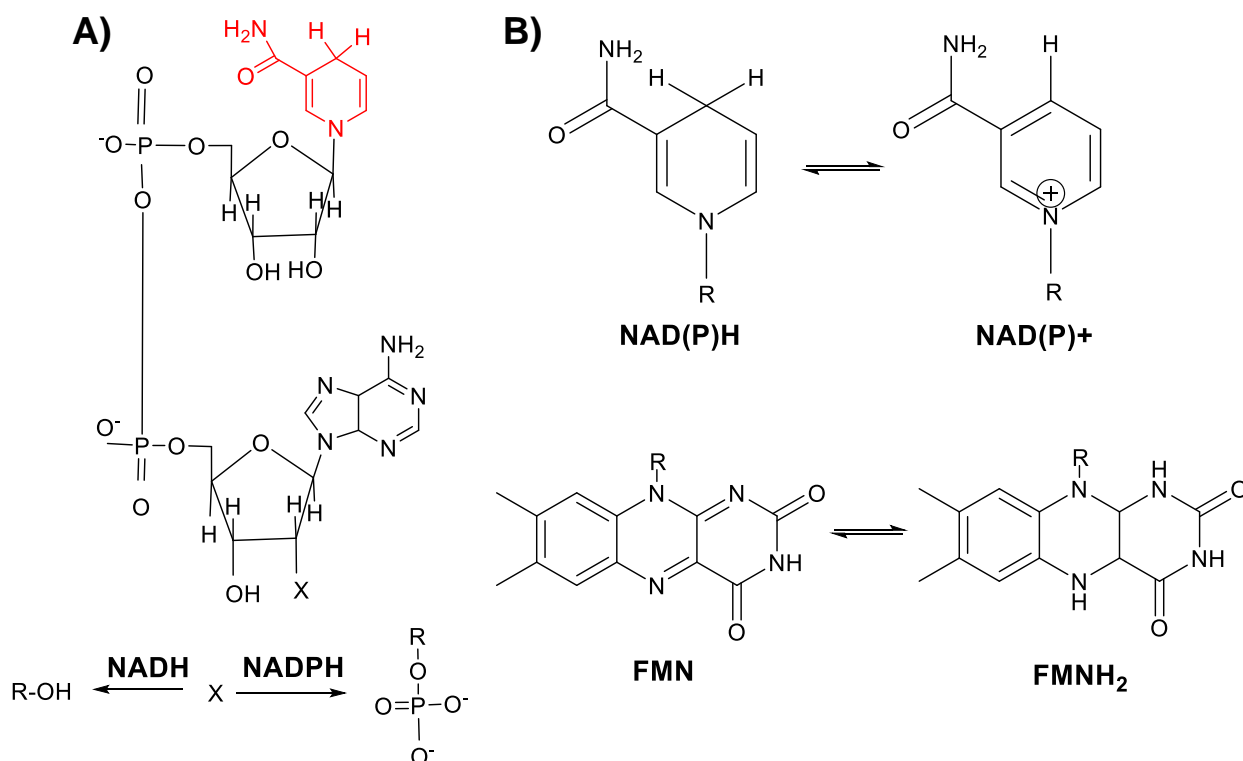


Figure 1.17: Structures of reduced pyridine nucleotides and the isoalloxazine ring of flavin a) Structure of pyridine nucleotides NADH or NADPH. The letter (X) represents the difference between the two molecules. b) Reduction of NAD(P)H to NAD(P)⁺ and FMN to FMNH₂.

Different kinetic mechanisms have been observed for the binding and release of reduced flavin and the pyridine nucleotide. These mechanisms are dependent on whether the reductase contains flavin as a tightly bound cofactor or if it is utilized as a substrate. Flavin reductases with tightly bound flavin utilize a ping-pong mechanism for flavin reduction. For the ping-pong mechanism, the bound flavin is reduced by the pyridine nucleotide (**Fig. 1.18A**). This is accompanied by the release of the pyridine nucleotide, followed by the binding of a second flavin which is reduced by the bound flavin.^{147,168,169}

The kinetic mechanism for flavin binding and release for the flavin reductase, EmoB is a ping pong mechanism. The crystal structure of EmoB was solved with two FMN molecules stacked with similar conformations. The deeply inserted FMN molecule was the cofactor while the other FMN molecule located at the surface acts as the substrate which is reduced by NADH. Conversely, the reductases which utilize reduced flavin as a substrate follow an ordered sequential mechanism where either flavin or the pyridine nucleotide binds first, and a ternary complex is formed (**Fig. 1.18B**). The formation of the ternary complex is a prerequisite for the reduction of flavin in the ordered sequential mechanism. Following the reduction of flavin, either the oxidized NADP^+ or reduced flavin is released first followed by the other product.^{158,169}

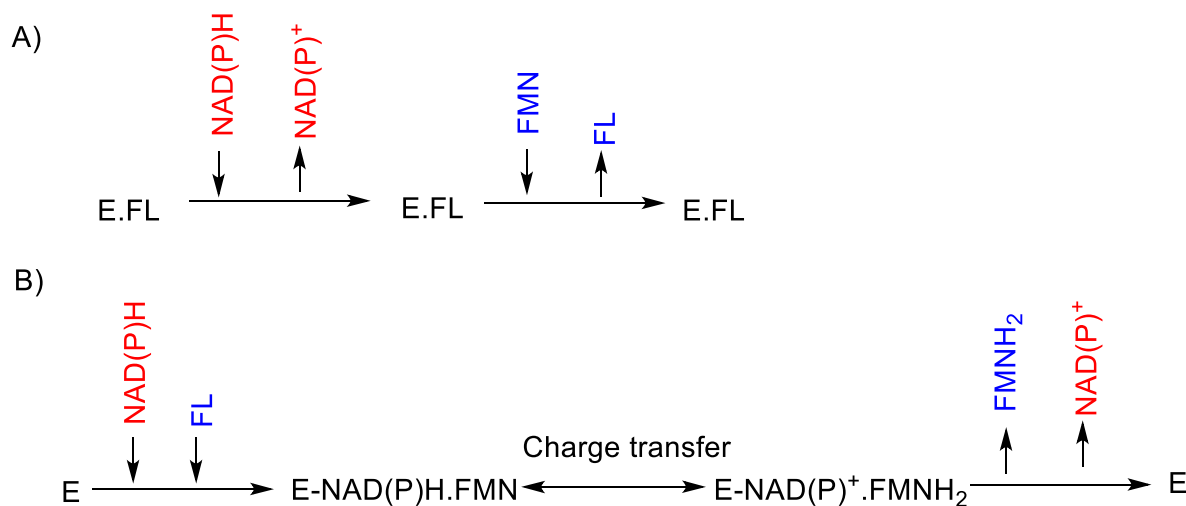
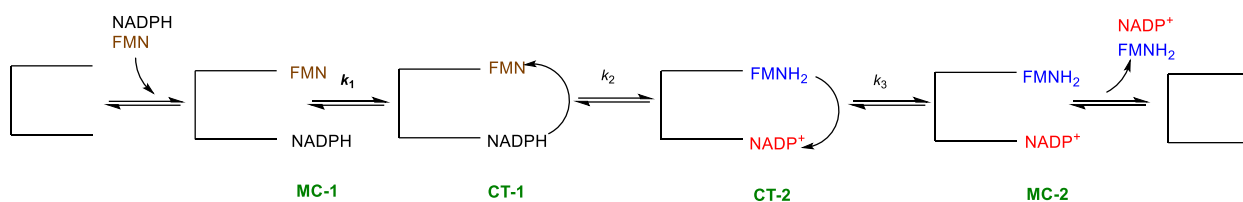


Figure 1.18: Flavin reductases utilize either ping-pong or ordered sequential mechanism for the binding and release of flavin and the pyridine nucleotide. a) Flavin reductases with flavin bound follow a ping-pong kinetic mechanism. b) Flavin reductases which utilize flavin as substrate follow an ordered sequential kinetic mechanism. FL represents the flavin substrate. (Adapted from¹⁴⁷).

In the two-component alkanesulfonate monooxygenase system, the flavin reductase, SsuE was purified without flavin bound and oxidized flavin is utilized as a

substrate. Although SsuE was able to reduce other substrates such as riboflavin and FAD, the enzyme had a higher affinity for FMN. Also, SsuE showed equal preference for NADH and NADPH for the supply of reducing equivalents.^{94,147} A higher binding affinity of about 1000-fold was observed with oxidized flavin as compared to the reduced form indicating that SsuE preferred oxidized flavin.^{170,171} The binding and release of oxidized flavin followed an ordered sequential mechanism, with NADPH binding first, followed by oxidized FMN to form the ternary complex. With the formation of the ternary complex, charge transfer intermediates are formed which generates reduced FMN, then the products dissociate sequentially with NADP⁺ release.¹⁷⁰

Single wavelength measurements at 450 and 550 nm identified three steps involved in flavin reduction following formation of the ternary complex.¹⁷² Flavin reductases that utilize flavin as a substrate generally form charge-transfer complexes in the reductive-half reactions.^{173,174} The initial step is a fast phase involving the formation of a charge-transfer complex between NADPH and FMN (CT-1) with a rate constant (k_1) of 241 s⁻¹. The next step is the hydride transfer step with the formation of the charge-transfer complex between oxidized NADP⁺ and reduced flavin (CT-2) with a rate constant (k_2) of 11 s⁻¹ (**Scheme 1.1**). The last phase is the decay of the charge transfer complex to generate MC-2 with a rate constant (k_3) of 19 s⁻¹, or this may represent the release of products from CT-2. The rate limiting step for flavin reduction in SsuE was the hydride transfer step as evidenced from isotope studies.¹⁷² Hydride transfer was inhibited at increased flavin concentrations and flavin inhibition has been reported for other flavin reductases. Due to the tight binding of FMN to SsuE, the increased concentration of FMN might result in FMN occupying the active site of SsuE, occluding the binding of NADPH.¹⁷²



Scheme 1.1 Formation of charge-transfer complex in FMN reduction by SsuE. (Adapted from¹⁷²).

The kinetic mechanism for the binding and release of flavin was observed to follow a sequential ordered mechanism. SsuE catalyzes the transfer of reduced flavin to SsuD for the desulfonation of alkanesulfonates to yield sulfite. The steady state kinetic parameters of SsuE showed no change in NADPH oxidase assays when SsuD was present. Interestingly, the kinetic parameters of SsuE changed in the presence of SsuD and the octanesulfonate substrate, following a rapid equilibrium-ordered kinetic mechanism. In the rapid equilibrium ordered kinetic mechanism, the NADPH substrate and the NADP⁺ product are in equilibrium with the free enzyme.¹⁷⁰ This implies that the rate of the reaction is not dependent on the concentration of NADPH and the equilibrium favors the formation of the ternary complex. The dissociation constant (K_d) of SsuE was comparable to the K_m of SsuE in single enzyme assays, which suggests that the K_m represents the K_d value. In the presence of SsuD and octanesulfonate, the K_m increased 10-fold implying a decrease in FMN binding. The decrease in flavin binding in the presence of SsuD ensures that upon reduction of flavin, it is transferred from SsuE to SsuD. The observed change in the kinetic mechanism from a sequential ordered to rapid equilibrium ordered favors the formation of the ternary complex and facilitates reduced flavin transfer. This would lead to the desulfonation of the alkanesulfonates and prevent oxidation of reduced flavin which would generate oxygen radicals.¹⁷⁰

1.3.2.2 Structural Features utilized by FMN Reductases

NADPH-FMN reductases are members of the flavodoxin-superfamily based on a flavodoxin fold. The flavodoxin fold is an α/β protein fold which consists of two α -helical layers that sandwiches five-stranded parallel β -sheets (**Fig. 1.19**). Flavin reductases have a characteristic conserved flavodoxin motif (T/S)XRXXSX(T/S) located in the loop for the binding of flavin.^{175,176} The conserved motif in EmoB is located on loop SPSRNSTT from residues 11 to 18 and the flavodoxin motif for SsuE is located on SPRFPSRS from residues 8 to 15.¹⁷⁷

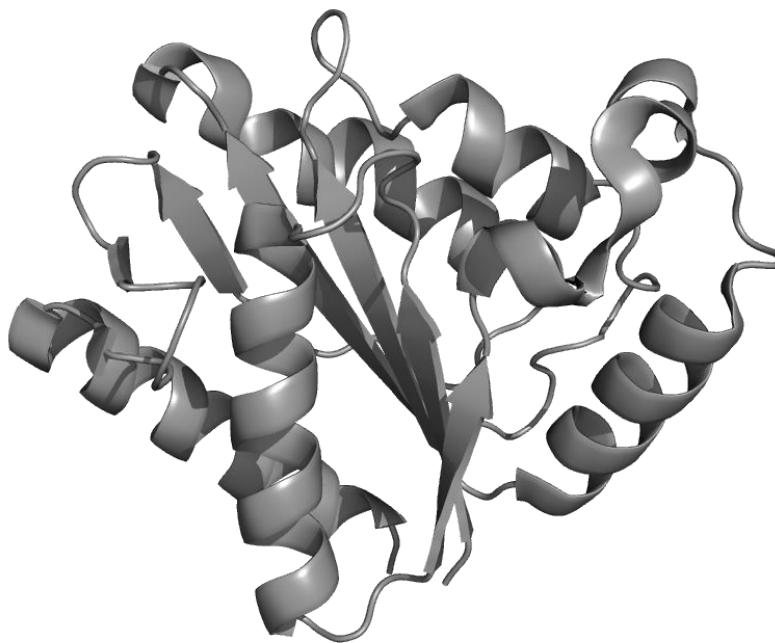


Figure 1.19: The flavodoxin fold of NADPH:FMN reductases of two-component flavin monooxygenase systems.

The crystal structure of SsuE was determined in three different states: apo-SsuE, FMN-bound SsuE and FMNH₂-bound SsuE. The three-dimensional structure was solved utilizing molecular replacement of the crystal structure of EmoB, which shares about 37%

sequence identity with SsuE. In the three structures solved, four chains in the asymmetric unit form a tetramer with 222 symmetry. The four chains constitute chains A and B and chains C and D which are pairs that form two different types of half-tetramers (dimer of dimers) (**Fig. 1.20**).⁸⁹

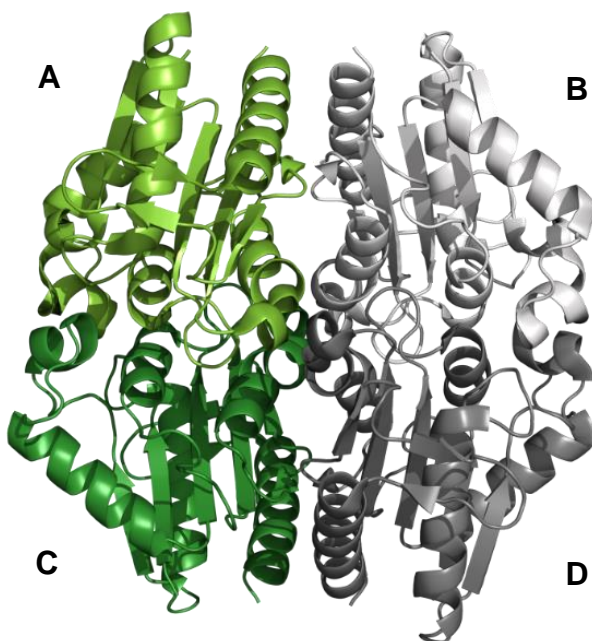


Figure 1.20: SsuE tetramer showing the dimer of dimers.

The crystal structure of the FMN-bound form of SsuE shows one FMN molecule occupying the same site as other flavoprotein reductases and a second FMN molecule in chains A-C that is less ordered compared to the first FMN molecule. SsuE has the characteristic flavodoxin fold with five central β -strands arranged in a $\beta 2$ - $\beta 1$ - $\beta 3$ - $\beta 4$ - $\beta 5$ sandwiched by α -helices, with two helices ($\alpha 2A$ and $\alpha 2B$) located between $\beta 1$ and $\beta 2$.

The phosphate group of the well-ordered FMN forms interactions with residues Ser 8, Ser 13, Ser 15 and Arg 10 residues of SsuE (**Fig. 1.21**).⁸⁹

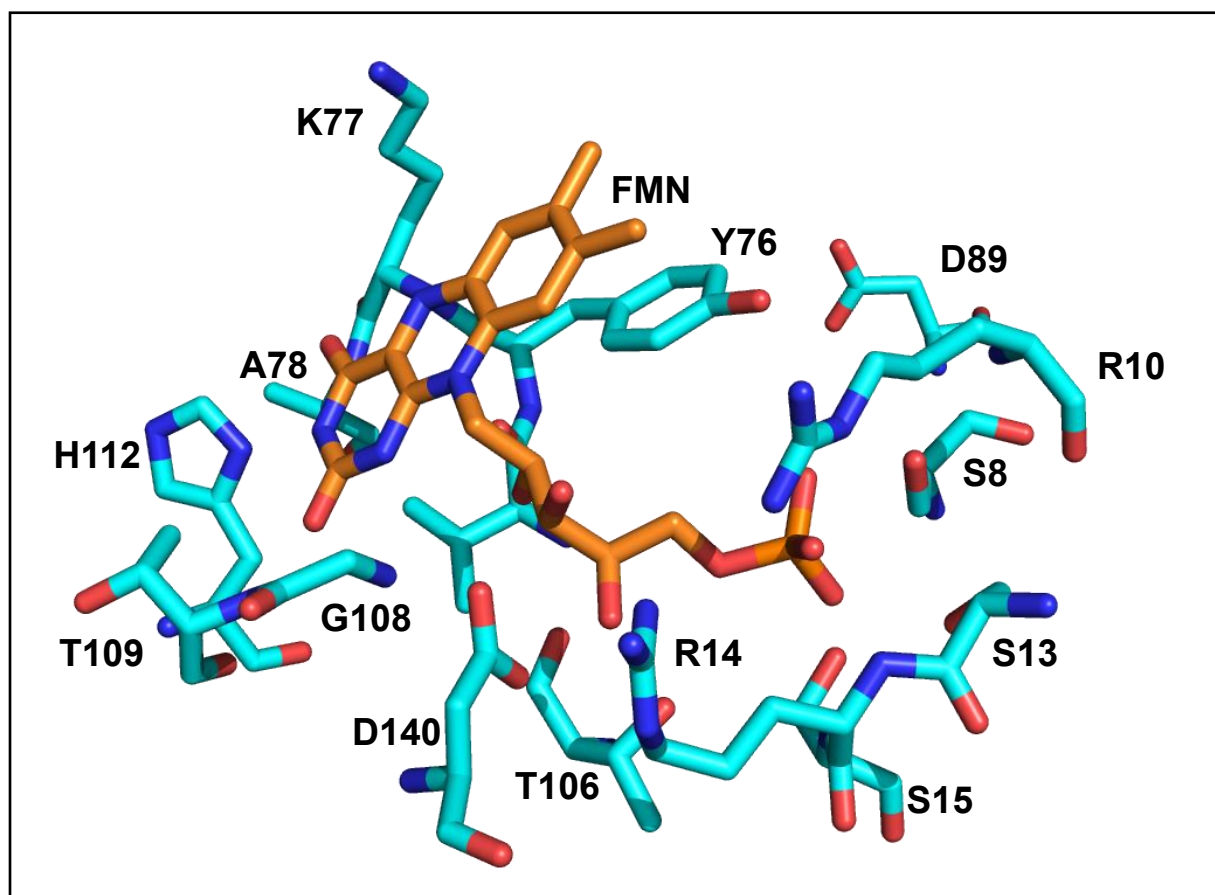


Figure 1.21: The three-dimensional structure of the active site of SsuE showing residues that position FMN. The amino acid residues Ser 8, 13, 15 and Arg 10 interact with the phosphate group of FMN in the active site. PDB:4PTY.

The three-dimensional structure of FMNH₂-bound SsuE was achieved by treating FMN-soaked crystals with dithionite to generate the reduced form. In this structure, one flavin molecule was bound to chains A, C and B but no FMNH₂ was bound to chain B. Also, the electron density of the crystal with FMNH₂ was weaker implying that there was either low occupancy or less rigidity. The absence of FMNH₂ in chain B was proposed to

be caused by the stabilization of the “out” conformation of Arg 10 which in the FMN-bound SsuE crystal structure shifts to the “in” conformation.⁸⁹ Results from previous binding studies show that SsuE had a 1000-fold higher binding affinity for oxidized flavin compared to the reduced form (FMNH₂). Less affinity for the reduced flavin exhibited by SsuE might imply that when oxidized flavin is reduced it is readily transferred to SsuD.

From previous studies, SsuE was shown to exist as a dimer, however it existed as a tetramer in the three-dimensional structure.^{89,94} The three-dimensional structure of FMN-bound SsuE was generated by soaking SsuE crystals in a large excess of FMN.⁸⁹ Therefore, the oligomeric state of the SsuE/FMN complex stems from the crystal lattice of apo SsuE and does not represent its true oligomeric state upon FMN binding. Also, in the crystal structure of SsuE with flavin bound, there were two FMN molecules bound to some monomers.⁸⁹ Previous studies established that SsuE binds to flavin in an equimolar fashion, one monomer of SsuE binds one molecule of FMN. This observation with the FMN-bound SsuE might be due to the excess of flavin utilized to obtain the crystal of FMN-bound SsuE.

In addition to the flavodoxin fold that was observed in the three-dimensional structure of SsuE, a distinct π -helix is present in the conserved $\alpha 4$ helix found in canonical flavoproteins. The π -helix is characterized by an insertional amino acid, and in the amino acid sequence alignment with other flavin reductases, the insertional residue for SsuE is Tyr118.⁸⁹ The π -helix is only found in FMN reductases under the same sub-branch as SsuE, and it is conserved among them. It is proposed that the π -helix differentiates the canonical flavoproteins from two-component flavin reductases.

1.3.2.3 FMNH₂-Dependent Monooxygenases of Two-Component Monooxygenase Systems

Two-component FMNH₂-dependent monooxygenases catalyze the oxidation of a diverse range of substrates. In the alkanesulfonate monooxygenase system, SsuD catalyzes the oxygenolytic cleavage of the carbon-sulfur bond of alkanesulfonates to generate sulfite and the corresponding aldehyde when sulfur is limiting in the environment. The desulfonation reaction was proposed to proceed through the formation of a C4a-(hydro)peroxyflavin intermediate generated by the reaction of dioxygen and reduced flavin supplied by SsuE. However, there has been no spectra evidence for the C4a-peroxyflavin intermediate for the SsuD enzyme.

For the longest time, flavoprotein monooxygenases were proposed to catalyze oxygenation reactions with a transient C4a-peroxyflavin intermediate. The proposed reaction intermediate could either be C4a-hydroperoxyflavin (FI-OOH) or a C4a-peroxyflavin (FI-OO-) intermediate. These intermediates are utilized for aromatic hydroxylation or Baeyer-Villiger oxidation reactions. Recently, the oxygenation reaction has been proposed to occur through an unprecedented flavin oxygenating species proposed as the flavin N5-oxide intermediate (FI_{N5O}) (**Fig. 1.22**). This intermediate has been overlooked in past years because of the limitation often encountered with protein crystallography where X-ray radiation causes artificial reduction of flavins and other redox groups. Also, dithiothreitol (DTT) which is often utilized for protein purification and storage reduces the N5-oxide making it undetectable in UV-vis spectroscopy. The formation of the flavin N5-oxide as an intermediate has been observed in EncM, which catalyzes the key step in the biosynthesis of the unusual polyketide antibiotic, enterocin.^{166,178} Also, the

flavin N5-oxide can be generated as the final product, and has been shown in different two component monooxygenase enzymes such as DszA and RutA.^{165,179,180} DszA is involved in dibenzothiophene sulfone oxidation to a sulfinic acid and RutA catalyzes the oxidative amide cleavage of uracil to 3-ureidoacrylic acid. A RutA like O₂ reactivity motif critical for N5-oxygenation was found in a monooxygenase, YxeK. The monooxygenase, YxeK present in *Bacillus subtilis* catalyzes the oxidative cleavage of the C-S bond of N-acetyl-S-(2-succino) cysteine to generate oxaloacetate and N-acetylserine. YxeK is a critical enzyme in a pathway that detoxifies and exploits S-(2-succino)-adducts for utilization as sulfur sources. S-(2-succino)-adducts are formed spontaneously from the reaction of cysteine and citric acid cycle intermediate fumarate. The proposed C-S bond cleavage catalyzed by YxeK may depend on flavin N5-peroxide (Fl_{N5OO}) rather than the flavin N5-oxide adduct (Fl_{N5O}).¹⁸¹ Based on what has been observed with similar two-component monooxygenases like SsuD, we propose that the enzyme catalyzes the desulfonation of organosulfonates utilizing the flavin N5-oxide intermediate.^{182,183}

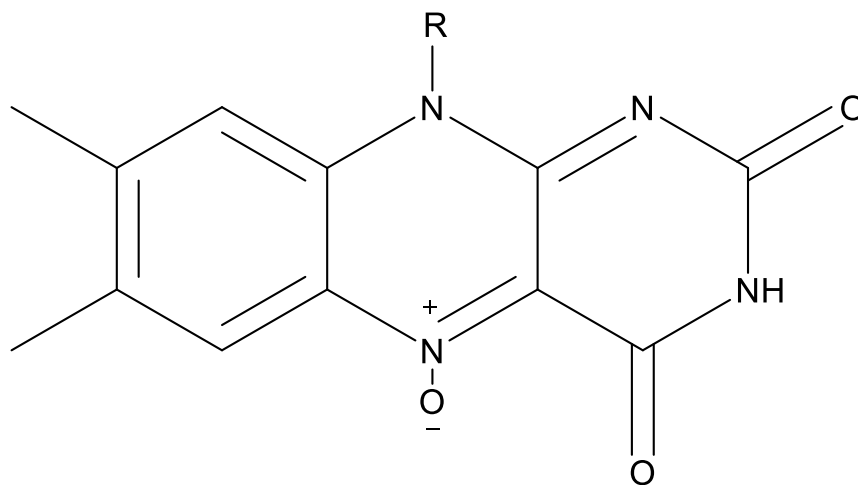


Figure 1.22: The flavin-N5-oxide intermediate.

1.3.2.4 Structural Features of FMNH₂-Dependent Monooxygenases

The monooxygenase, SsuD shares similar structural properties with other flavin-dependent monooxygenases, LadA and bacterial luciferase. They all belong to the bacterial luciferase structural family. The monooxygenases in this family form a triosephosphate isomerase (TIM)-barrel fold which consists of eight alternating α -helices and β -strands arranged in sequence, with the parallel β -strands surrounded by an α -helical shell (**Fig. 1.23**). Proteins with the TIM-barrel fold have their active sites located at the C-terminal end of the β -barrel.^{184–187} Although SsuD belongs to the bacterial luciferase family, there is some deviation from the classical TIM-barrel structure with the presence of several insertion regions. One insertion region prominent in SsuD contains a loop that was mostly unresolved in the three-dimensional structure implying conformational mobility in this region. This disordered loop is conserved in all SsuD homologs and is located close to the active site of SsuD.^{188,189} The disordered loop has been proposed to cover the active site following the binding of substrates and may be responsible for the conformational changes observed in kinetic studies.^{190,191}

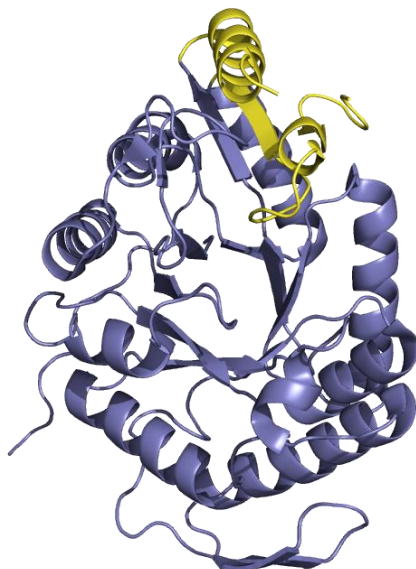


Figure 1.23: The TIM-barrel fold in SsuD is comprised of eight alternating α -helices and β -strands arranged in sequence. The unresolved loop structure is highlighted in brown.

Loop closure over the active site protects substrates and intermediates from bulk solvent during catalysis. The flexible loops contribute to the architecture of the active site and aids substrate binding during catalysis in TIM-barrel proteins. The functional role of the flexible loops was investigated by studying the variants of conserved residues in the loop region. The Arg297 residue located on the insertion sequence near the disordered loop region is present in SsuD from different bacterial organisms. The role of this residue was investigated utilizing several approaches. The variants, R297A and R297C SsuD had no measurable activity in desulfonation assays; however, the activity of R297K SsuD showed an approximate 30-fold decrease in catalytic activity compared to wild-type SsuD.¹⁹² Also, partial deletion variants of the loop region were able to bind reduced flavin with comparable binding affinities as the wild-type enzyme. However, the reduced flavin environment in the active site of the deletion variants of the loop region was similar to the reduced flavin environment in the absence of SsuD. This indicates that the loop aids in maintaining the structural integrity of the enzyme active site.

Conformational changes caused by the binding of substrates have been reported for wild-type SsuD from previous kinetic studies. These changes could be because closure of the loop may facilitate conformational changes exhibited by SsuD which is consistent with what is observed in other TIM-barrel proteins.^{190,191,193} The variants, R297K and R297A SsuD were investigated for their role in substrate binding and/or loop closure. These variants were more prone to tryptic digestion compared to wild-type SsuD in the presence of FMNH₂ only or FMNH₂ and octanesulfonate. This suggests that Arg297 located on the mobile loop plays a key role in stabilizing the conformational change instigated by the binding of reduced flavin.¹⁹²

The loop region was observed to be highly active and flexible in molecular simulation experiments when both octanesulfonate (OCS) and the C4a-peroxyflavin intermediate (FMN^{•••••}) were bound to SsuD.¹⁹⁴ Additionally, three mobile loop conformations caused by substrate-induced conformational changes were observed by accelerated molecular dynamics (aMD) in SsuD. These distinct loop forms include: “open,” “closed” and “semi-closed” conformations. The open conformation was observed when SsuD was substrate-free while the closed conformation was the dominant form when SsuD was bound solely with reduced flavin (FMNH₂). In the closed conformation, the mobile loop closes over the binding pocket of SsuD preventing unproductive oxidation of FMNH₂ in the absence of OCS. The semi-closed conformation was observed with the addition of OCS to the active site of SsuD with FMNH₂ already bound. This conformation may be important for the entrance of dioxygen into the binding pocket, or it better positions the substrates for oxygenolytic cleavage. A semi-closed or closed conformation was the tentative conformation observed with OCS and FMN^{•••••} bound. This observation implies that the putative oxygenating intermediate may be the N5-peroxyflavin intermediate which has been observed in several two-component monooxygenases that share similar structural features with SsuD.¹⁹⁵

Several conserved amino acid residues were located at the active site of SsuD, and similar residues were present in *V. harveyi* luciferase LuxAB, which shares about 15% amino acid identity with SsuD.^{88,196} This implies that though these enzymes are structural homologs with low sequence identity, they may fold similarly and utilize similar residues that are vital for catalysis. Conserved active site amino acid residues utilized for flavin binding in LuxAB were similarly arranged in SsuD.¹⁸⁶ Several conserved active site

residues were observed in SsuD (Cys54, His11, His333, Tyr331, His228 and Arg226) and variants of these residues were generated to investigate their importance in enzyme catalysis (**Fig. 1.24**). The Cys54 residue is the only cysteine in SsuD, and it is hypothesized to play a role in stabilizing the proposed C4a-(hydro)peroxyflavin

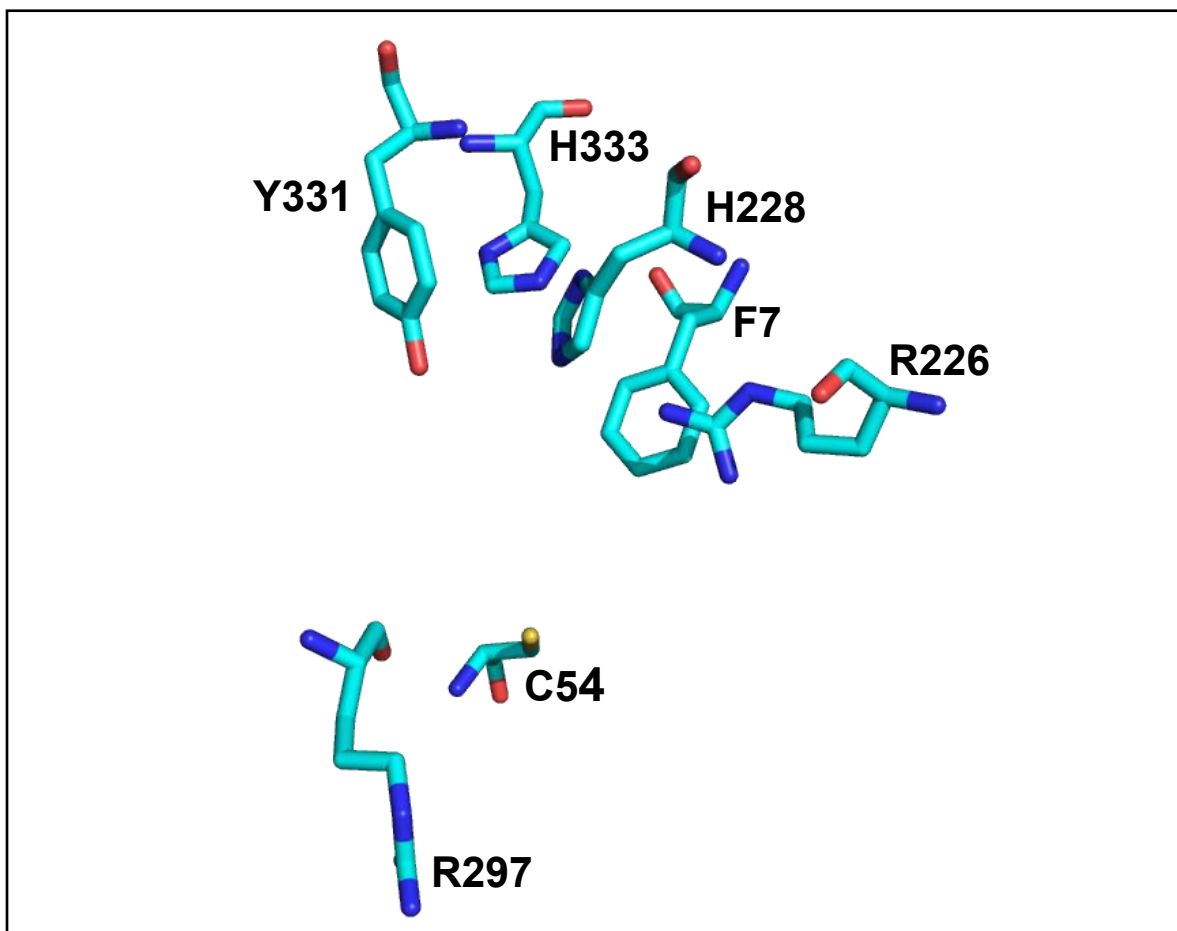


Figure 1.24: The active site residues in the monooxygenase, SsuD. PDB:1M41.

intermediate.^{171,197} A conserved residue, His44 in bacterial luciferase was observed to function as a catalytic base in the bioluminescence reaction.^{147,198} A similar histidine residue, His228 was shown in SsuD and substitution to an alanine reduced the catalytic efficiency by half. However, the His11 and His333 SsuD variants showed comparable activity with wild-type SsuD. These results suggested that the histidine residue was not

responsible for the abstraction of a proton and another active site residue, Arg226, was proposed to perform this function. The variant R226A and R226K SsuD did not show any measurable activity. However, kinetic isotope effects show Arg226 playing a dual role in facilitating the activation of oxygen by stabilizing the C4a-(hydro)peroxyflavin intermediate and in the protonation of FMNO⁻ intermediate which causes conformational changes that leads to product release.¹⁹⁹

1.3.2.5 Mechanism of Reduced Flavin Transfer in Two-Component Flavin-Dependent Systems

The reduction and transfer of reduced flavin from the FMN reductase to the monooxygenase partner is a critical step for the desulfonation reaction to occur. Reduced flavin is labile and prone to oxidation when exposed to dioxygen causing the production of reaction oxygen species such as hydrogen peroxide and superoxide anion radicals. Investigations into the mechanism of the safe hand-off of reduced flavin in these systems are critical as it prevents non-enzymatic oxidation of reduced flavin.²⁰⁰ Several mechanisms of reduced flavin transfer have been observed including free diffusion, channeling, or both (**Fig. 1.25**).²⁰¹

In the free diffusion mechanism, reduced flavin diffuses through bulk solvent from the flavin reductase to the monooxygenase without forming protein-protein interactions. In *E. coli*, the transfer of FADH₂ from NADP(H)-flavin oxidoreductase (HpaC) and 4-hydroxyphenylacetate 3-monooxygenase (HpaB) was through free diffusion (**Fig. 1.25A**).²⁰² In size-exclusion chromatography, HpaC and HpaB eluted differently, if a complex was formed the proteins would have eluted earlier from the column compared to the individual proteins. Also, the apparent $K_{m,FAD}$ value of HpaC in coupled assays with

HpaB did not change in single reductase assays with HpaC alone.²⁰³ This implied that the mode of reduced flavin transfer was through diffusion and no protein-protein complexes were formed. In the actinorhodin monooxygenase system in *Streptomyces coelicolor*, reduced flavin transfer from the ActVB flavin reductase to the ActVA-ORF5 monooxygenase occurred through diffusion as observed from affinity chromatography. Following diffusion from ActVB to ActVA, reduced flavin reacts with oxygen forming the reactive intermediate which hydroxylates the substrate and regenerates oxidized flavin.¹⁵⁹

Initial investigations into the method of flavin transfer in the EDTA two-component system proposed that reduced flavin diffuses from the flavin reductase, EmoB to the monooxygenase, EmoA.¹⁷⁷ However, reports from recent studies have identified protein-protein interactions as the medium for reduced flavin transfer following several investigations utilizing isothermal calorimetry, molecular docking, and kinetic assays (**Fig. 1.25B**). From diffusion experiments, reduced flavin was transferred from EmoB to EmoA when separated by a membrane. However, the rate of glyoxylate production from EmoA was slow compared to when EmoB and EmoA were in physical contact.²⁰⁴ This suggests a channeling mechanism that utilizes specific protein-protein interaction sites and the proximity of both proteins.²⁰⁵

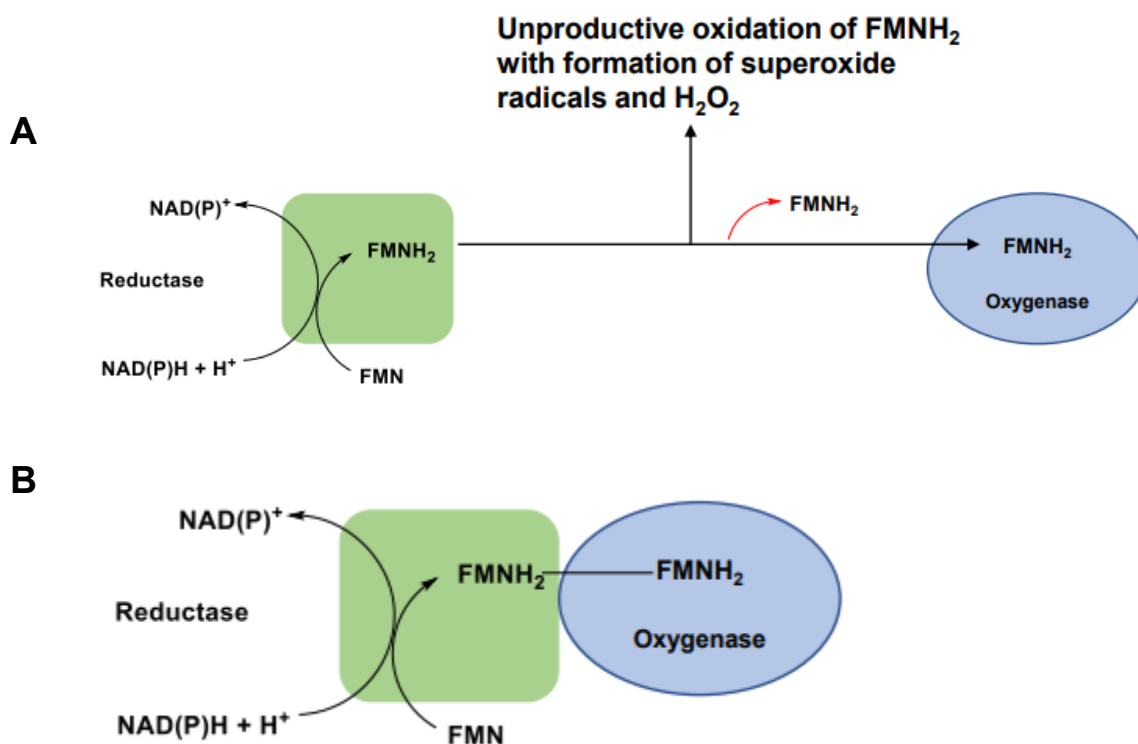


Figure 1.25: Different mechanisms of reduced flavin transfer in two-component monooxygenase systems. a) Transfer of reduced flavin by free diffusion. b) Direct transfer of reduced flavin by protein-protein interaction (channeling mechanism).

Free diffusion and channeling mechanisms have been reported as the medium for reduced flavin transfer in the styrene monooxygenase system in *P. putida*. Styrene monooxygenase is comprised of a reductase, SmoB and the styrene epoxidase, SmoA, responsible for FAD-dependent epoxidation of styrene to styrene epoxide.²⁰⁶ In the styrene monooxygenase system, flavin dynamics plays a crucial role in reduced flavin transfer. A transient flavin-transfer complex is formed whereby the AMP portion of FAD is attached to SmoA and the isoalloxazine ring is associated with SmoB. This transient complex enables the efficient transfer of flavin with the release of the isoalloxazine ring

of FAD and transfer to the oxygenation site of SmoA, hence preventing unwanted interaction of reduced FAD with molecular oxygen in solution.²⁰⁷

Due to the instability of reduced flavin and its intermediate, several two-component flavin-dependent systems utilize protein-protein interactions to protect reduced flavin from oxidation in bulk solvent.¹⁴⁶ Hydrogen-deuterium exchange mass spectrometry was utilized to identify protein-protein interaction sites utilized for flavin transfer in the alkanesulfonate monooxygenase system (**Fig. 1.26**). Protein-protein interaction sites identified for SsuE were located on two distinct α -helical regions (78-89 and 119-125), which also contains the π -helix. Interaction regions on SsuD are conserved and were identified on an α -helix (251-261) and on an α -helix and a loop region (285-295).²⁰⁸

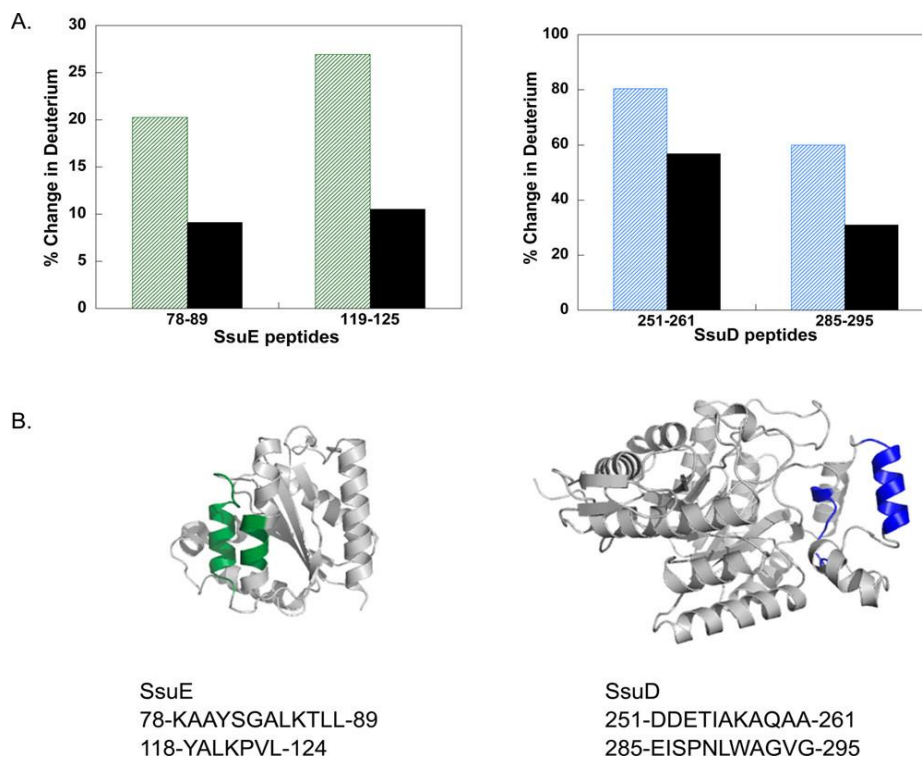


Figure 1.26: Protein-protein interaction sites between SsuE and SsuD were identified through HDX-MS. (Adapted from²⁰⁸). Copyright © 2015 American Chemical Society.

The protected sites on SsuD are present at the active site opening connected by the loop. This implies that the interaction sites of both SsuE and SsuD would bring the active sites into proximity of each other for the transfer of reduced flavin. Positive and negatively charged residues which may be involved in the formation of salt bridges were observed at SsuE and SsuD protein-protein interaction sites. Electrostatic residues in SsuE include Lys77, Lys86 and Lys121 and residues in SsuD involved in binding with SsuE include Asp251, Asp252, Glu253 and Lys257.²⁰⁸ Several variants of SsuD (DDE(251/252/253)AAA) and Δ D251-A261) were generated to investigate the functional role of these binding regions. The triple alanine variant showed a four-fold decrease in enzyme activity in desulfonation assays compared to wild-type SsuD, however the deletion variant, Δ D251-A261 SsuD showed no measurable activity. The variants had a similar binding affinity for reduced flavin as wild-type SsuD. However, the deletion variant was not able to bind SsuE implying that there was a disruption of the protein-protein interaction region of this variant.²⁰⁸ Two-component systems utilize several distinct structural features for the acquisition of sulfur, and they are efficiently coordinated for overall catalysis.

1.4 Structural Features utilized by Two-Component Flavin-Dependent Systems

1.4.1 Presence of π -Helices in Proteins

There are different secondary structures required for protein stability and folding. The most common secondary structures found in proteins are the α -helices and β -sheets. They are both shaped by periodic hydrogen bonding between the backbone carbonyl oxygen and the amide hydrogen. Helical structures found in proteins are characterized by these hydrogen bonding patterns: α -helix ($i \rightarrow i + 4$), 3_{10} -helix ($i \rightarrow i + 3$), π -helix ($i \rightarrow i +$

5) (**Fig. 1.27 and Fig 1.28**). The α -helices are the most abundant helices occurring in about 31% of total protein secondary structure while 3_{10} -helices makes up about 4%.²⁰⁹

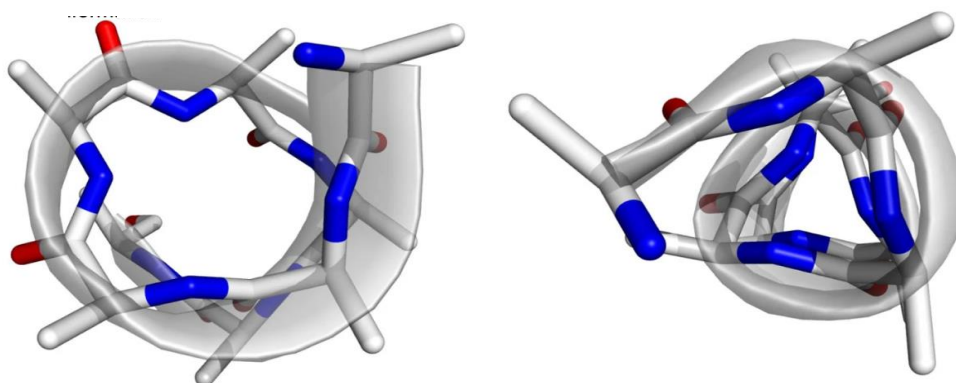


Figure 1.27: The top view of π -helix (left) and 3_{10} -helix (right). Copyright © 2016, Rights Managed by Nature Publishing Group.

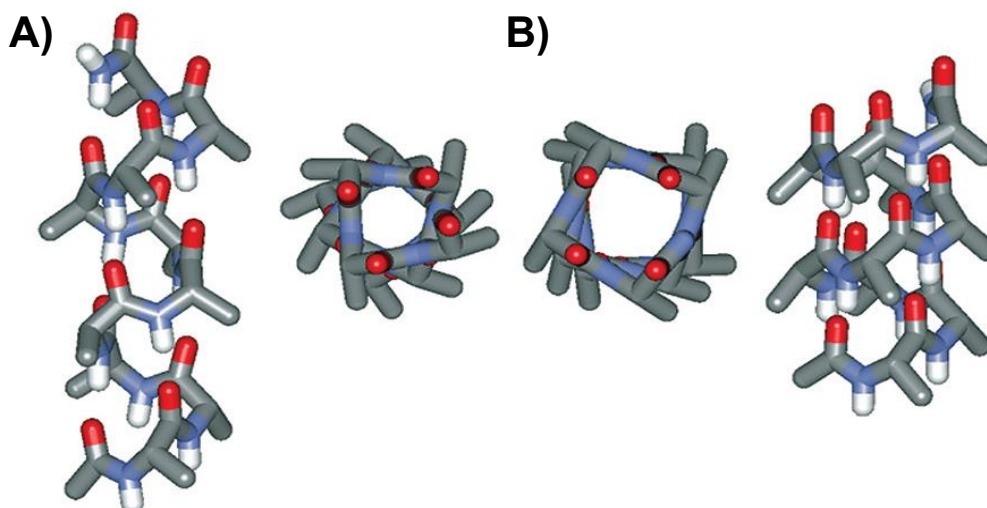


Figure 1.28: The hydrogen bonding patterns and top view of the a) α -helix and b) π -helix. Copyright © 2008, American Chemical Society.

1.4.2 Structural Properties of the π -Helix

Formerly, π -helices were not identified in proteins, and they were later reported to be rarely found in protein structures. However, recent studies show that they are often present but misannotated as an α -helix.^{210,211} π -helices have now been identified in approximately 15% of known proteins and may arise from the insertion of a single amino acid into an existing α -helix. The hydrogen bonding pattern in the π -helix is five residues apart as compared to 3.6 residues for the α -helix. The π -helices are not found as extended forms in proteins but as short π -helical segments. The majority of natural occurring π -helices comprise 7 residue segments with 2-type- π -bonds.²¹² Recent studies have grouped the π -helices with other helical structures such as π -bulges, α -aneurisms, α -bulges and looping out, all of which exhibit similar features. The π -helices were observed to be present and conserved within members of protein superfamilies.²¹³

The presumed rarity of the π -helices has been linked to its instability due to its structural properties: (1) the dihedral angles, ϕ (-76°) and ψ (-41°) of the π -helix are unfavorable. On the Ramachandran plot, they lie at the very edge of the favorable minimum energy region; (2) formation of the π -helix is entropically costly because five residues need to be aligned to allow the ($i \rightarrow i + 5$) hydrogen bonding (**Fig. 1.29**).^{214,215} Also, the diameter of the π -helix is wider than that of the α -helix by 1 Å; (3) main chain atoms can no longer form van der Waals contacts due to the larger radius, leading to the formation of a hole too small to be filled by a water molecule.^{214,216} However, results from previous studies have shown that π -helices are formed during protein evolution and other reports have revealed a transition from an α -helix to a π -helix in molecular simulations

which suggests that the π -helices may not be as unstable as was originally thought.^{215,217–}

219

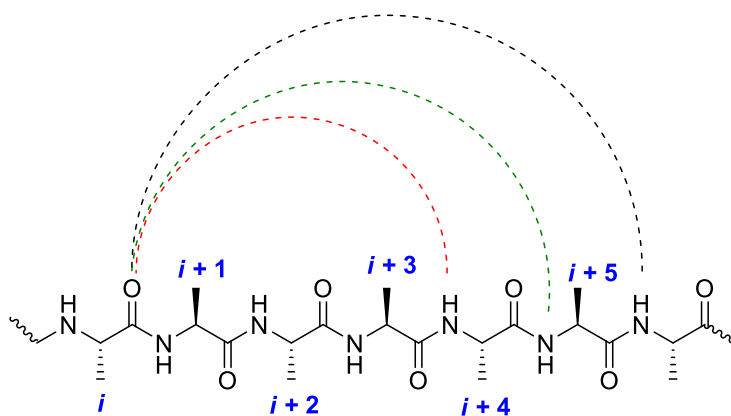


Figure 1.29: Hydrogen bonding pattern in helical structures in proteins. (Adapted from²²⁰).

1.4.3 Preferences for Certain Amino Acids in π -Helices

Secondary structures inherent in proteins have different amino acid preferences in certain positions that function in stabilizing protein structure. π -helices show a preference for aromatic and large aliphatic amino acids such as Trp, Tyr, Ile, Leu, Asn and His. However, it disfavors small amino acids such as Ala, Gly and Pro. The π -helices also have specific positions where these amino acids are located. Large amino acids such as Trp, Tyr, Ile, Phe, Met and Leu, would most likely be found at the beginning and the end of the helix.²¹² This preference for bulky and hydrophobic residues may be due to the stabilization afforded by van der Waals interactions between the side chains of these residues. Also, the middle position of π -helices was observed to prefer polar residues such as Thr, Ser, Glu and Asn residues, with Asn being the most preferred at this position.²¹²

Positions before and after the π -helix show no clear statistical preference for any specific residues except for the first position (+1) where Pro residues are preferred.

Previous reports have shown that the occurrence of the Pro residue leads to disruption of at least two adjacent hydrogen bonds due to its cyclic pyrrolidine side chain.²²⁰ With the π -helices, the Pro residue at the first position would form hydrogen bonds with a residue at the π 3 position in a seven-residue π -helix.^{213,221} It has been hypothesized that the presence of the proline residue aids in the formation of a β turn.²²² However, the proline residue has been frequently located where the π -helix converts back to an α -helix.²²³ This may imply that the Pro residue at this position serves to terminate the π -helix.

While the π -helix was considered to be rare and unstable, closer investigation into this unique secondary structure suggests otherwise. Several factors were observed to contribute to the stability of the π -helices depending on its specific conformation and amino acid content. Steric repulsion was previously shown to be a destabilizing factor due to the close distance of the side chains of the π -helix.²²⁴ However, results from recent studies report extensive interactions between side chains through van der Waals contacts, a small number of electrostatic interactions and aromatic ring stacking. This observation aligns with the preference for aromatic and bulky amino acids in the π -helix. Also, the alignment of helical residues in the π -helix causes the alignment of main chain components involved in hydrogen bonds, leading to shorter and stronger bonds compared to α - and 3_{10} -helices. Lastly, entropic effects contribute to the stability of proteins with π -helices occupying less volume and surface area compared to the α -helix.^{212,225} This implies that solvent entropic effects are more favorable for the π -helix and may make up for the entropic cost required to align four residues for a single turn in the π -helix.²¹²

1.4.4 Evolutionary Advantage of π -Helix in Proteins

The π -helices have been associated with the evolutionary gain of function and new and improved roles in different proteins. π -helix structures are located at the enzyme active site and participate directly in catalysis. The π -helix in soybean lipoxygenase is highly dynamic and its flexibility plays a role in the recognition of the fatty acid substrate (**Fig. 1.30**).²²⁶ The π -helix forms a portion of the active site in fumarase C and allows a direct connection between the activator site and the active site through several hydrogen

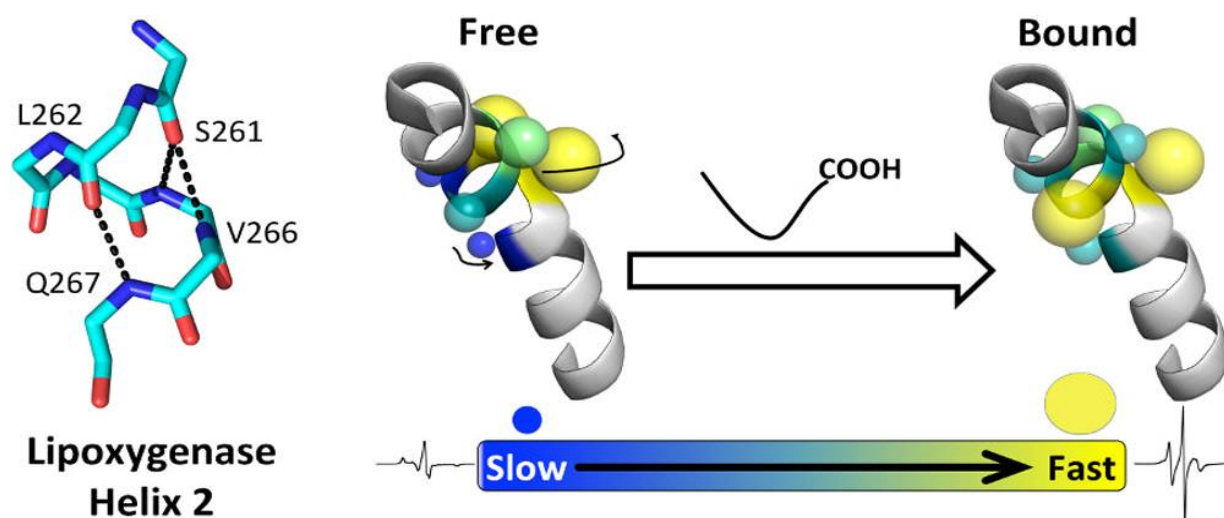


Figure 1.30: The flexibility of the π -helix in Soybean lipoxygenase increases with substrate binding. Copyright © 2014 American Chemical Society. Further permission requests should be directed to ACS.

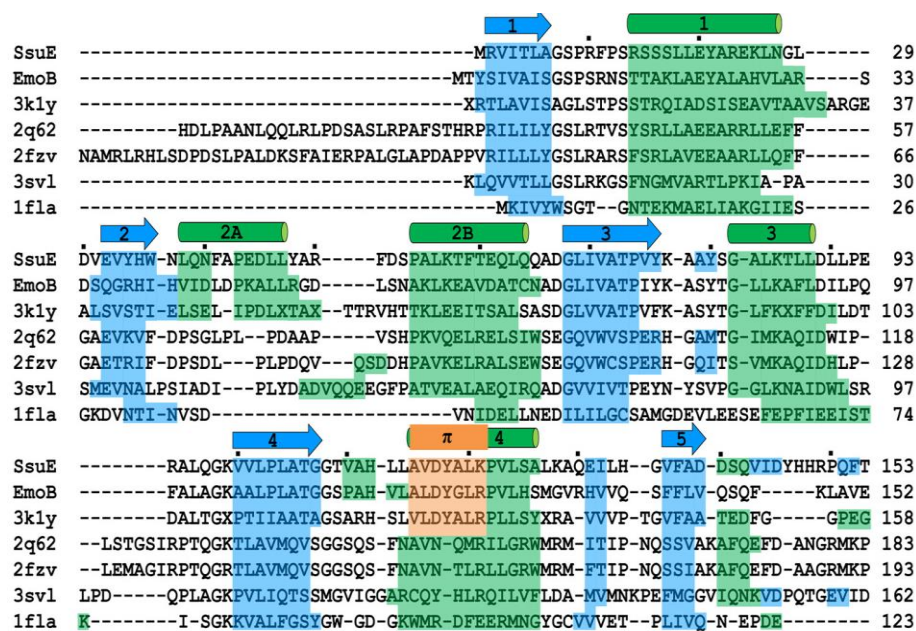
bonds.²¹¹ In most of these enzymes, the π -helix is conserved within the protein superfamily. In acetylcholine esterase, an enzyme that belongs to a subgroup of the α/β hydroxylase superfamily, a unique conversion from an α -helix to a π -helix causes a change in the shape of the active site. This change allows a new chain segment of the enzyme to supply the glutamate of the Glu-His-Ser catalytic triad. In mercuric ion reductase, an insertional residue responsible for the change from an α -helix to a π -helix, positions a key Tyr residue involved in metal binding into the mercury binding site.²¹³ An α -helix to π -helix conversion in UDP-glucose dependent glycosyl transferases, positions

a Trp residue at the pyridoxal phosphate binding site.²²⁷ The switch from an α -helix to π -helix correlates well with the transition from the dependence on UDP-glucose to pyridoxal phosphate in the phosphorylase branch of the enzyme superfamily.^{213,228}

Oftentimes, the π -helix may not be directly linked to the active site of the enzyme; however, it plays a role in structural versatility that promotes protein function. Formerly, it was reported that the active site π -helix of the hydroxylase component of soluble methane monooxygenase (MMOH), a member of the bacterial multicomponent monooxygenase (BMM), stretches out upon binding of a product analog, 6-bromohexan-1-ol.^{206,229} Thorough inspection of the active site shows that there no stretches but with the binding of the product analog, one of two overlapping π -helices (π D) is shifted six residues towards the C-terminal direction in a peristaltic-like manner. The two overlapping π -helices (π B and π D) then form one long π -helix. The peristaltic shifts of the π -helix cause an expansion of the buried active site of the enzyme in preparation for substrate binding. Such movements have been proposed to be utilized as a tenable activation mechanism for BMM by their regulatory subunits. Also, the shift in π D was observed to be synchronized to a shift in an adjacent π -helix (π E), common to all BMMs. This shift transfers the impact of the binding of the regulatory subunit to the active site, showing how a π -helix can indirectly influence catalysis. This peristaltic shift was observed in the active site π -helix of toluene-4-monooxygenase hydroxylase.²³⁰

The π -helix in FMN reductases is located at the tetrameric interface of the protein. The FMN reductases belong to the NADPH:FMN dependent family based on the flavodoxin fold present in these enzymes. This family of enzymes have partner monooxygenases which require reduced flavin from the FMN reductases for catalysis.

Canonical flavoproteins that belong to the flavodoxin-like superfamily do not depend on a partner monooxygenase for catalysis and do not possess the π -helix. Other enzymes which are FMN reductases and possess the π -helix include EmoB from *Mesorhizobium* sp. BNC1, an uncharacterized oxidoreductase from *Corynebacterium diptheriae*, MsuE from *P. aeruginosa* and SfnF from *P. putida* (**Scheme 1.2**).^{89,177,231}



Scheme 1.2: The insertional Tyr residue in flavin reductases of two-component monooxygenase systems. Copyright (2014) American Chemical Society.

The π -helix in SsuE is characterized by an insertion of Tyr into an α 4-helix in the subgroup of the NADPH:FMN reductase family. The insertional residues in the π -helices of MsuE and SfnF are His126 and His128 respectively.^{89,231} The π -helix has been proposed to provide a gain of function and given its location at the tetrameric interface of FMN reductases, it may impart a unique functional role to these group of enzymes.

Several variants of SsuE were generated to investigate the functional and structural role of the π -helix. The Tyr118A variant converted the flavin-free SsuE into a

flavin-bound form.²³² Flavin bound to Y118A SsuE was confirmed through mass spectrometric analysis, where the mass of FMN observed after extraction from Y118A SsuE was consistent with the molecular weight for FMN. Bound flavin in Y118A SsuE was reduced by NADPH in anaerobic titrations. The Y118A SsuE variant was unable to support NADPH oxidase activity but there was measurable activity in ferricyanide assays. This unusual observation was due to the slow reactivity of Y118A SsuE with oxygen in NADPH oxidase assays.²³² In addition, there was no measurable production of sulfite in desulfonation reactions with SsuD because reduced flavin was not effectively transferred from Y118A to SsuD for desulfonation to occur.

Critical hydrogen bonding interactions across the tetramer interface involving Tyr118 of the π -helix and FMN may preserve crucial contacts responsible for reduced flavin transfer. Also, Tyr118 forms π -stacking interactions with Tyr118 residues of each monomer across the tetramer interface (**Fig. 1.31**). Other variants of Tyr118 were generated by taking into consideration the aromaticity afforded by tyrosine (Y118F SsuE) and the hydroxyl group of Tyr118 which participates in hydrogen bonding across the tetramer interface (Y118S SsuE).²³³ Additionally, a deletion variant, Δ Y118 SsuE was generated to remove the reported insertional residue that forms the π -helix. The Y118S variant was purified flavin-bound, like the Y118A SsuE variant but the Y118F and Δ Y118 SsuE variants were purified flavin free. In NADPH-oxidase assays, there was no measurable oxidase activity for the Y118S and Δ Y118 SsuE variants; however, Y118F SsuE showed sustained NADPH oxidase activity.²³³ The binding affinity of the variants for FMN were comparable to that of wild-type SsuE. Interestingly, though Δ Y118 SsuE had no activity in NADPH-oxidase assays, when flavin was added, it was able to transfer

electrons to ferricyanide in ferricyanide assays. The Y118S and Δ Y118 SsuE variants could not support desulfonation activity which is consistent with what was observed in NADPH-oxidase assays.

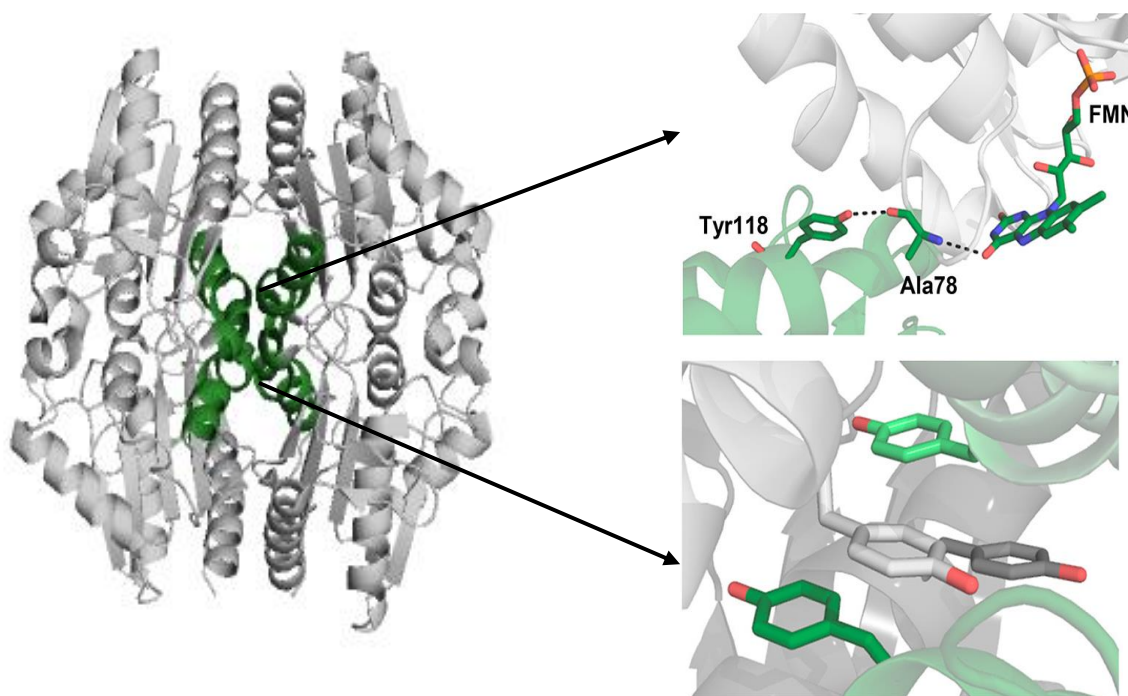


Figure 1.31: Interactions involving the insertional residue, Tyr118 in the π -helix across the tetramer interface of SsuE. Copyright © 2018, American Chemical Society.

Crystal structures of Y118A without and with FMN and Δ Y118 were generated to determine the alterations to the structure of the variants.²³¹ All the SsuE variants were crystallized as dimers. Interestingly, the substitution of Tyr118 to Ala converted the π -helix to an α -helix. The Δ Y118 SsuE variant could not support the helical hydrogen bonding pattern for residues 115-119, which resulted in a random coil for these residues. Irregular helical turns in the wild-type SsuE create an alternating pattern of hydrophobic residues which pack with the opposite homodimer. In contrast, the Y118A SsuE structure showed helical turns with equal diameters that disrupts the hydrophobic packing pattern

and other residues take up new positions in the tetramer interface creating steric clashes that makes it impossible to form a stable tetramer.²³¹ However, Δ Y118 SsuE is primarily a tetramer because the less rigid broken helix allows for arrangement to regenerate the tetramerization interface.²³¹

The SsuE and MsuE insertional residues are aromatic and may be key in the tetramerization interactions mediated by aromatic π -stacking. Further investigations were performed to evaluate the effect of the aromatic insertional residues to determine if interchanging these residues would generate chimeric proteins (Y118H SsuE and H126Y MsuE) which had unchanged kinetic activity.²³¹ The H126Y MsuE variant showed similar kinetic parameters as wild-type MsuE in NADPH-oxidase assays which suggests that the substitution did not affect the ability of the enzyme to reduce FMN. However, the Y118H SsuE variant showed no measurable activity, which implies that reduced flavin was not released and reoxidized similar to the Y118A SsuE variants. In coupled assays, the H126Y MsuE/MsuD pair showed comparable activity to the wild-type MsuE/MsuD enzyme. However, the Y118H SsuE/SsuD showed no measurable desulfonation activity.²³¹ The same experiments were performed with the opposite monooxygenase partners (H126Y MsuE/SsuD and Y118H SsuE/MsuD) to determine if the release of reduced flavin from the reductases, SsuE and MsuE could be triggered through interactions with their monooxygenase partner. The results obtained from desulfonation assay with H126Y MsuE were comparable regardless of what monooxygenase was included. However, Y118H SsuE variant was unable to support the transfer of reduced flavin to either monooxygenase (SsuD/MsuD) which shows that the tyrosine to histidine substitution did not possess similar functional properties for catalysis as H126Y MsuE.²³¹

These findings show the critical role the π -helix plays in two-component FMN reductases which makes them different from canonical flavoproteins. The π -helix would not be selected if it did not confer a gain-of-function for the FMN reductases. Canonical flavoproteins do not require a partner monooxygenase for the reactions they catalyze, and they do not have the π -helix. A series of hydrogen bonding patterns between Tyr118 of SsuE and the isoalloxazine ring of FMN may serve as a medium for communication between the oligomerization interface and FMN binding. The location of the π -helix at the tetramer interface may trigger the oligomeric changes required for flavin reduction and transfer to SsuD for the desulfonation of organosulfonates.

1.5 Protein Oligomerization

Protein oligomerization is a phenomenon whereby proteins form supramolecular structures that can self-associate to form oligomers ranging from monomers to higher-order oligomers. Oligomers are composed of multiple subunits which may either form homooligomers that have identical subunits, or heterooligomers that are comprised of different subunits. Dimers and tetramers constitute the vast majority of oligomers with increased number of subunits and odd number oligomers are less prevalent. However, most proteins are homo-oligomers. The formation of oligomers is made possible by covalent interactions between subunits or by noncovalent interactions such as hydrogen bonds, hydrophobic, and electrostatic interactions.²³⁴

Formerly, proteins were thought to exist primarily in only one stable oligomeric state hence the possibility that they perform their respective functions in this proposed state.^{235,236} However, recent studies have shown that about 30-50% of proteins self-associate to form oligomers that can exist in different oligomeric states and have different

functions that serve distinct purposes.^{236,237} Oligomerization impacts proteins with different structural and functional advantages such as improved stability, increased complexity, and new opportunities for regulation of enzyme activity.^{238,239}

1.5.1 Characteristics of Oligomeric Proteins

Homooligomers can be organized in an isologous state which involves association of subunits between the same surface of two monomers related by two-fold symmetry. Additionally, oligomerization can occur in a heterologous manner using different interfaces.^{239–241} However, heterooligomers are organized only *via* heterologous associations because their assembly involves different subunits.^{240,242} Oligomeric complexes are further classified as obligate and non-obligate, permanent and transient, and strong and weak.^{243,244} Obligate complexes comprise proteins that are not stable when isolated and depend on cooperative folding between the subunits. However, non-obligate complexes form proteins that can fold on their own, are independently stable, and take part in transient or permanent protein interactions.²⁴⁵ Transients interactions are further divided into strong or weak interactions.²⁴⁵

The concentration and dissociation constant of the protein primarily determines its oligomeric state where one state dominates over the other.²⁴⁶ Interactions between the subunits of the proteins may vary in strength and lifetime and can be quantified by measuring the dissociation constant. Many proteins form stable oligomers that do not undergo oligomeric changes to perform their specific functions. These proteins have protein-protein dissociation constants in the nanomolar range. Other proteins with K_d values in the millimolar or micromolar range have a weak tendency to associate with changes in oligomerization often caused by certain environmental factors. Some proteins

are dynamic, undergoing readily reversible transient changes in the presence of substrates and/or other proteins.^{244,247}

1.5.2 Different Roles of Oligomerization in Protein Metabolism

Oligomerization is a widespread phenomenon and there are advantages a protein obtains from its quaternary structure. Many oligomeric proteins do not carry out their activities in one oligomeric state, they undergo changes in their oligomeric states and the role of oligomerization in protein structure and function has only recently been explored (**Fig. 1.32**).²³⁶ Oligomerization favors the efficient use of genetic material by the synthesis of small subunits to form a large protein, rather than utilizing one large gene for protein synthesis.

Oligomerization enhances the complexity of proteins which promotes diverse functions. Different oligomers of the same enzyme can have different functions by the introduction of a new active site between subunit interfaces.²⁴⁸ Estimates show that about one-sixth of oligomeric proteins have active sites present at intersubunit interfaces. Also, oligomerization is dependent on enzyme concentration, an increase above the threshold of an active oligomeric state may lead to activation. However, a decrease in concentration may lead to deactivation and dissociation. Post-translational modification or ligand binding can also influence oligomerization to either activate or deactivate enzyme activity.

Large oligomers are more advantageous because of increased intramolecular interactions. The entropic cost of the rigid conformation of larger proteins is over-compensated by the enthalpic contribution of several weak interactions.²⁴⁸ The formation of large oligomers from multiple identical monomers is an economical process and may

serve as a general means of enhancing stability against denaturation and degradation. Many weak interactions between inter-subunit interfaces affords less exposure to water, proteases, and denaturants, which promotes the stability of oligomeric enzymes.²⁴⁸ Another advantage of oligomerization for enzymes occurs when subunits perform different roles that depend on one another.²⁴⁸ The enzyme, tryptophan synthase, is a heterotetramer comprised of two α and two β subunits. The product of the α subunit, indole, is siphoned off through a hydrophobic tunnel from the α to the β active site, hence protecting indole from diffusion. The cooperation between the two subunits enhances the catalytic efficiency in forming the final product, tryptophan.^{249–251}

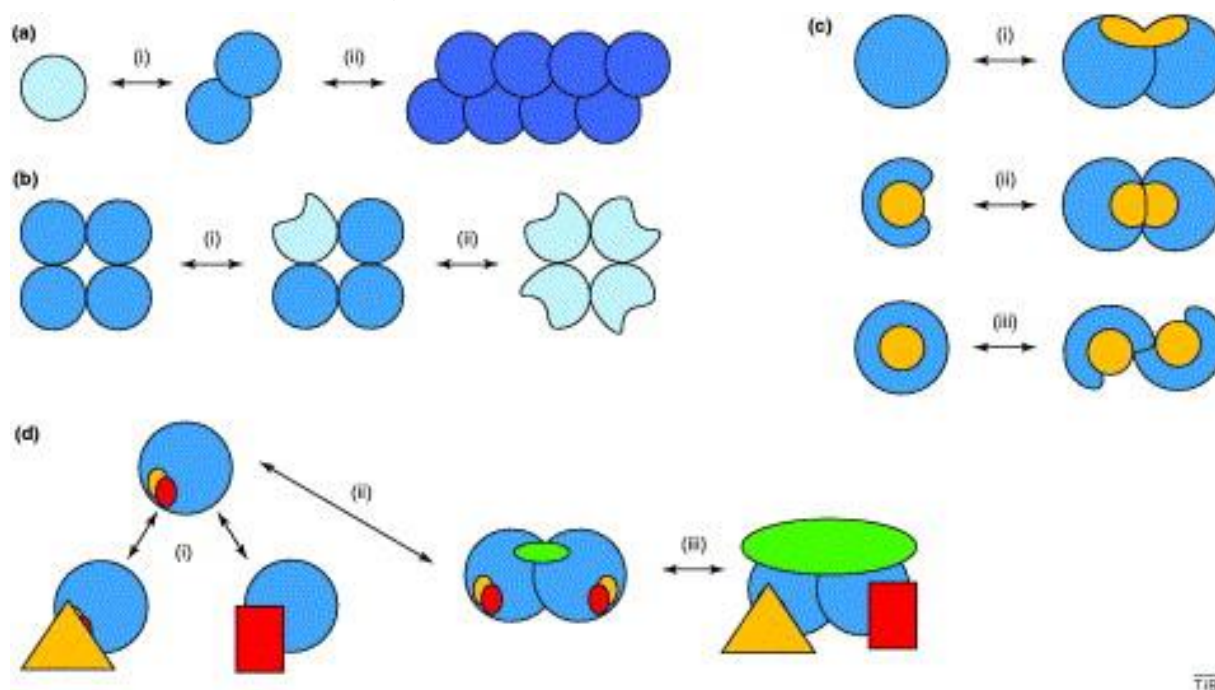


Figure 1.32: Different roles of oligomerization in enzyme activity. Oligomerization can a) increase enzyme activity and stability, b) trigger cooperativity and affect enzyme regulation through allostery, c) reveal or conceal new active sites at enzyme interfaces, d) create new binding sites which serves as a mechanism for enzyme regulation. Copyright © 2004 Elsevier Ltd.

Due to the location of new active sites at subunit interfaces, oligomeric proteins have developed different mechanisms for regulation of enzyme activity.²⁴⁹ The increase

or decrease in enzyme concentration above a certain concentration can act as a mechanism for modulating enzyme activity. Also, the generation of new inter-subunit interfaces can produce non-substrate binding sites promoting allosteric regulation or substrate binding sites and alter the structure of other subunits leading to cooperativity.

1.5.3 Mechanisms for Regulating Oligomerization of Proteins

Oligomeric enzymes can be regulated through several mechanisms. Firstly, the binding of small molecules (inhibitors) to the protein interface can block oligomerization.²⁵² These inhibitors do not stabilize a specific oligomeric state, for tumor necrosis factor (TNF- α), an inflammatory cytokine produced during inflammation binds the intact biologically active trimer resulting in rapid subunit dissociation rendering the enzyme inactive. Other examples include small molecule inhibitors that bind near the oligomeric interface and stabilize a particular conformer such as those that block dissociation or stabilize the association between subunits. The transthyretin (TTR) tetramer is stabilized from dissociation as this is a prerequisite for the formation of insoluble TTR fibrils which has been implicated in several human amyloid diseases. The stabilization of TTR tetramer serves as a medium to restrict TTR-associated amyloid fibril formation.^{253–255} Regulation of oligomerization also occurs by the simultaneous binding of a small-molecule inhibitor to each subunit present in an oligomeric protein.

A well-studied mechanism of oligomeric protein regulation is the allosteric modulation of enzyme activity through the formation of morpheeins.²⁵² Morpheeins are natural homo-oligomeric proteins that can exist as a mixture of dynamic oligomeric assemblies that are physiologically and functionally different. Lower quaternary assemblies of these proteins exist in different conformations (morpheeins) that are in dynamic equilibrium with one

another (**Fig. 1.33**). Regulation occurs through a series of sequential events beginning with dissociation of the oligomer, change in conformation in the dissociated form and reassociation to a functionally and structurally different oligomeric form.²⁵⁶ The basic conformations of the lower oligomeric form of the protein dictate a defined ratio of the

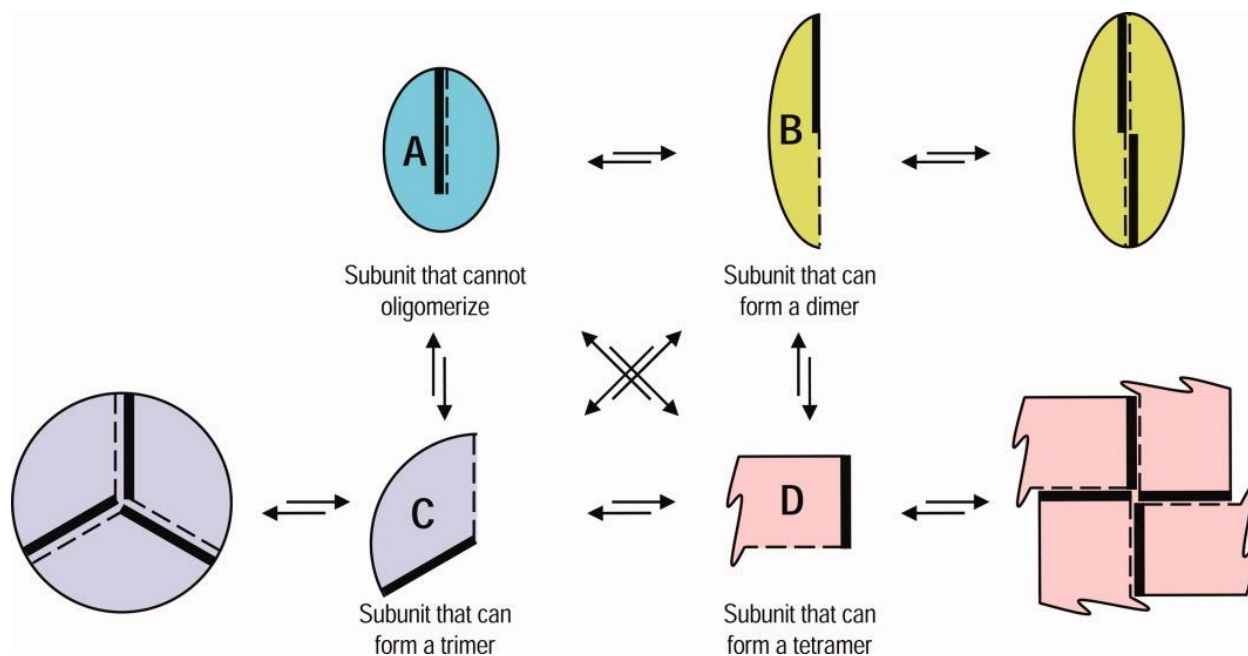


Figure 1.33: Two-dimensional schematic of the morpheein model in an equilibrium of different morpheein forms. Copyright © 2008, International Union of Biochemistry and Molecular Biology, Inc.

higher oligomer form after dissociation. The first enzyme used to study the mechanism of regulation of morpheeins was porphobilinogen synthase (PBGS), an essential enzyme required for the biosynthesis of all tetrapyrroles such as heme, chlorophyll, and vitamin B₁₂. PBGS exists in three different oligomeric states: a high activity octamer, low activity hexamer, and two conformations of a dimer.²⁵⁷ The low activity hexamer dissociates into a dimer, a conformational change generates the alternate dimer, and the reassociation of

the enzyme to the octamer. The different oligomeric assemblies of human PBGS have been observed in solution. The oligomeric equilibrium of PBGS can be changed by altering enzyme concentration, ligand concentration, pH or point mutations.^{257–260} The morpheesins were overlooked for many years because enzymes were thought to exist and function in one fixed quaternary form, however recent studies have demonstrated the utility of the morphein model.

1.5.4 Oligomerization exhibited by Two-Component Systems

Oligomeric changes of FMN reductases of two-component systems have been observed and reported. A rapid monomer-dimer equilibrium was reported for FRP, an NADPH:FMN reductase from *Vibrio harveyi* associated with the bacterial luciferase system. This equilibrium was dependent on the concentration of the enzyme in both its native and apo form, with lower concentrations that was utilized for enzyme assays being predominantly in the monomeric form.²⁶¹ The dimer forms of FerB, an NADPH:FMN reductase from *Paracoccus denitrificans* has been shown to self-associate to a tetrameric form at higher protein concentrations indicating the enzyme is in a dimer-tetramer equilibrium.²⁶² Changes in oligomeric state during catalysis in LuxG, a flavin reductase from *Photobacterium leiognathi* (TH1) could be one of the factors responsible for its half-site reactivity.²⁶³

SsuE was reported as a dimer from initial studies utilizing gel filtration chromatography.⁹⁴ However, SsuE exists as a tetramer in the three-dimensional structure. These alternative results suggests that SsuE may exist in a dynamic tetramer-dimer equilibrium.⁸⁹ Oligomeric changes may play a role in the catalysis of two-component systems by either regulating enzyme activity through substrate binding or

safe-keeping interaction sites required for the handoff of reduced flavin. Protected protein-protein interaction sites in SsuE and SsuD were responsible for effective flavin transfer in the alkanesulfonate monooxygenase system. These sites were shown to be critical for the transfer of reduced flavin from the reductase to the monooxygenase through protein-protein interactions to prevent autooxidation of reduced flavin.^{205,208}

1.6 Protein-Protein Interactions

Proteins work with other proteins in the cell to perform diverse biological functions.^{264,265} These activities are often made possible through protein-protein interactions which are important in different physiological processes such as cell cycle control, signal transduction, DNA replication, transcription, translation, secretion, splicing etc.^{266–268} In the crowded environment of the cell, proteins can bind with other molecules, proteins interact with other proteins through specific intermolecular interactions between their distinct interfaces. These interactions are involved in virtually all biological functions but the principles governing how proteins interact are not fully understood.²⁶⁸

Protein interaction networks have been pertinent to the development of drugs, as the mechanism of many metabolic disease are better targeted by harnessing information from protein homology and protein interaction partners.^{269,270} Experimental and computational methods have been utilized to study protein-protein interactions in cells and organisms because these interaction networks are important in drug discovery and development.^{269,271} The interfaces utilized by proteins for interaction are described as that portion of two or more polypeptide chains that are close and near-by isolated residues that are not covalently linked.²⁷² Across subunit interfaces, two residues are said to be in contact if the distance between the C α atoms of each polypeptide chain is under 6 Å.^{265,273}

These residues are termed “near-by residues” and they are important for the clustering of interfaces.²⁷²

Protein-protein interactions can occur through either of two extreme mediums. The first medium of interaction between two proteins may occur where a small region of one protein fits into the cleft of the other or the two proteins can interact over a large surface area. It has been implied that total surface area buried upon interaction of two proteins is related to the free energy of association and that hydrophobic interactions are the major driving force for the stabilization of protein-protein associations.^{267,274} The minimum amount of surface area buried upon complexation of two proteins is about 600 Å², which correlates with 30 kCal mol⁻¹ of free energy from hydrophobic contributions.^{275–}
²⁷⁸ This suggests from previous investigations that the free energy of association is not evenly distributed across the interface and certain critical residues contribute the bulk of the free binding energy.

Protein-protein complexes could either be homocomplexes (homooligomers) or heterocomplexes which consists of heterooligomers or two different proteins that can exist independently but associate for catalysis. Though these complexes associate through protein-protein interactions, it is important to distinguish between them when exploring their interfaces.²⁷¹ Protein-protein complexes are influenced by the geometric and physicochemical properties of the interfaces of protein subunits. Some of them include a change in accessible surface area (ASA), planarity as the parameter for shape and size, gap volume index to account for complementarity, preference of amino acid residues on the surface as a measure of hydrophobicity and polarity, types of secondary structure present at the interface, and the extent of conformational change of the

protein.^{279,280} Understanding how proteins interact is important in determining the relationship between protein-protein complex formation and their physiological relevance.²⁸¹

1.6.1 Interface Parameters Involved in Determining Protein-Protein Interactions.

1.6.1.1 Hot Spots at Protein-Protein Interfaces

Hot spots at protein interfaces were determined utilizing alanine scanning mutagenesis to probe the energetic contribution of individual amino-acid residues present at protein-protein interfaces.²⁸² Specific key residues contribute most of the free binding energy at protein interfaces and these residues are spread unevenly across the interfaces.²⁸³ These residues are termed “hot spot residues” because the substitution to alanine resulted in a remarkable drop of binding energy ($\Delta\Delta G \geq 2$ kcal).^{283,284} Also, it has been revealed that hot spots residues correlate well with structurally conserved residues. Specific residues at interfaces such as tryptophan and methionine, are often hot spot residues.^{273,285}

The burial of hot spot residues in a hydrophobic environment has been proposed to be the main stabilizing force for protein-protein interactions.^{273,286} An assembly of hot-spot residues are present within tightly packed regions and are non-random at the interface. The clustering of hot spot residues contributes to the stability of the interface. Hot-spot residues are in contact with each other, making a network of interactions termed hot regions. Electrostatic interactions and hydrogen bonds have been shown to play an important role in hot regions.^{283,287} The hot-spot region is tightly packed forming a hydrophobic “O-ring” around the hot spots due to the occlusion of water upon binding,

thereby strengthening the stabilizing effect of charge-charge contributions.²⁶⁵ The formation of the O-ring is also dependent on the surrounding residues that appear to be energetically unimportant but shields hot spot residues from bulk solvent.^{273,283} Tyrosine, tryptophan, and arginine residues appear more frequently as hot spot residues and are found mostly as interface residues compared with the overall protein structure.^{273,288} Other residues frequently located at these hot spot regions include methionine, threonine, valine, and leucine.^{273,288}

1.6.1.2 Residue Interface Propensity

The distribution of certain amino acid residues at the interface of protein complexes gives information about their contribution to the hydrophobicity of the interface.^{280,288,289} The hydrophobicity of the interface is measured by comparing the distribution of residues at protein interfaces with those located on the protein surface.^{240,290} Residue interface propensity for each amino acid at the interface is determined by comparing the fraction which each amino acid contributes to the accessible surface area with its contribution to both the interface and the exterior of the protein.²⁷² Residue propensity > 1 indicates that this residue appears frequently in the protein interface as compared to the protein surface.²⁷⁷ Results reveal that except for methionine, hydrophobic amino acid residues occur more often at homodimer interfaces than at heterocomplexes.²⁴⁰ The decrease in hydrophobic residues in heterocomplexes is balanced by an increase in polar residues.

1.6.1.3 Accessible Surface Area (ASA)

Accessible surface area is a general measure for interacting surfaces as it provides information about the loss of a solvent accessible area of one subunit upon complexation

with another.²⁹¹ The accessible surface area is often determined either on the residue or atomic level. ASA for interface residues with side chains are measured by the decrease of $> 1 \text{ \AA}^2$ upon complexation while at the atomic level the ASAs are defined as those that show a decrease of $> 0.01 \text{ \AA}^2$.^{277,292}

The size and shape of interfaces can be measured from complexation of protein interfaces (ΔASA).²⁹³ ΔASA serves as a measure of binding energy as there is a relationship between the hydrophobic free energy of transfer from a polar environment to a hydrophobic one and the solvent ASA.²⁸⁰ The shape of proteins gives important information about the unique roles they play in biological process and analyzing the shape of proteins interfaces is useful for designing molecular analogues.

1.6.1.4 Secondary Structure Preferences

Previous investigations to determine the different secondary structures present at the interfaces of a subset of oligomers revealed that helix-helix packing, β -sheet packing, loop interactions and extended β -sheet were observed at these interfaces.^{294–296} Another analysis with a wide variety of oligomers showed helices and sheets occurred less frequently while loops and turns occur more.^{240,297} Some interfaces were found to possess only one type of secondary structure while others were mixed.²⁹⁸ For both obligate and non-obligate complexes, interactions between like-like structures such as helix-helix and sheet-sheet packing have been observed.²⁹⁹ It may be that the presence of like-like secondary structure interactions may provide tight packing compared to non-identical interfaces, hence enhancing complementarity.^{240,300}

1.6.1.5 Surface Complementarity

Surface complementarity is a measure of shape complementarity and electrostatic interactions between surfaces, and these have been investigated thoroughly by various groups.^{301,302} Complementarity of protein complexes is determined by the gap index which measures the volume of the gap present between monomers, thus defining the limit of the boundary between them by the amount of maximum allowed space between the interfaces.^{293,302} Gap index is quantified by the following equation (Eq. 2):

$$\text{GAP index } (\text{\AA}) = \text{gap volume between molecules } (\text{\AA}^3) / \text{interface ASA } (\text{\AA}^2) \text{ (per complex)}$$

(Eq.2)

Complementarity is often made possible through tight packing achieved by like-like secondary structures contacts at the interface to create associations that are energetically and functionally favorable.³⁰³

1.6.1.6 Conformational Change

Conformational changes ranging from small changes in amino acid side chains to large chains in domains occur when proteins associate.^{304,305} Some proteins have different alternative conformations that enable them to bind different proteins.^{306,307} Reasons for conformational changes upon association include orientation of specific residues to enhance function, prevention of steric clashes and facilitation of close packing by the formation of electrostatic interactions and hydrogen bonding.^{290,306} Oligomeric proteins with interfaces larger than 1,000 \AA^2 are likely to undergo large scale conformational changes as opposed to interfaces with less interface area.^{241,247} The

largest movements within the interface are not from residues that are functionally relevant such as those that are present in the active site but from surrounding residues.³⁰⁶

1.6.1.7 Binding Affinity

The extent of binding between two proteins is determined by its binding constant.^{305,308} The binding constant is defined as the strength of two proteins that bind reversibly and it can be expressed in several ways from the bimolecular reaction equations (Eq. 3-4):



$$K_d = \frac{[Pf][Lf]}{[PL]} \quad (\text{Eq. 4})$$

From the equations, P represents the bound protein, the bound ligand is L, the protein-ligand complex PL, $[P_f]$ and $[L_f]$ represent the concentration of free (unbound) concentrations of P and L, respectively. The interaction between a protein and ligand is primarily governed by the binding constant K_d . Interaction between protein and ligand can be expressed in two additional ways. Firstly, instead of the binding constant K_d , the affinity constant (K_a) can be used. Here $K_a = 1/K_d$. Lastly, it can be expressed as a ratio of two rate constants, K_a , and K_d . The rate of formation of PL is $K_a [P_f] [L_f]$, where k_a is the association rate constant and the rate of breakdown of PL is k_d is the dissociation constant. The rate of formation of PL equals the rate of breakdown of PL at equilibrium and $K_d = k_d/k_a$.^{309,310}

1.6.2 Role of Protein-Protein Interaction in Enzyme Metabolism

Several studies have revealed that over 80% of proteins do not operate alone but in complexes.³¹¹ Proteins involved in the same pathways have been repeatedly observed to interact with one another.^{312–314} Protein-protein interactions have different properties which includes: modification of the kinetic properties of enzymes, construction of new binding sites for small effector molecules, inactivation and suppression of protein catalysis and as a general mechanism for substrate channeling.³⁰⁹

Substrate channeling or tunneling is the process of transferring the intermediate produced by one enzyme to the next enzyme with the goal of circumventing bulk solvent.³¹⁵ The advantages of substrate channeling over free diffusion include increasing catalysis by escaping unfavorable energetics of desolvating substrates, furnishing new medium of enzyme regulation by modulating enzyme associations and enhancing responsiveness to regulatory signals. Other advantages of substrate channeling include isolating intermediates from competing reactions, protecting labile intermediates, and bypassing unfavorable equilibria and kinetics due to competing metabolites in bulk solvent.^{316,317} Also, substrate channeling shortens the transit time for the transport of reaction products from one active site to another.³¹⁸

Investigating the mechanism of reduced flavin transfer in two-component flavin dependent systems is critical to understanding its role in cellular systems. Free reduced flavin is unstable under aerobic conditions and is prone to unproductive oxidation leading to the release of hydrogen peroxide.^{200,319} The hydrogen peroxide formed undergoes further oxidation to generate oxygen radicals that causes oxidative stress which damages cellular macromolecules.¹⁴⁶ Therefore, a mechanism for reduced flavin transfer which

prevents the formation of reactive oxygen radicals and stabilizes reduced flavin is critical for catalysis. In most flavoproteins, the reductive and oxidative half reactions occur on the same proteins. However, in enzyme systems where two separate proteins catalyze the reductive and oxidative half-reactions, a mechanism for the transfer of reduced flavin that bypasses bulk solvent is required.²⁰⁵ The transfer of reduced flavin from the reductase, SsuE to the monooxygenase, SsuD in the alkanesulfonate monooxygenase system occurs through protein-protein interactions.^{205,208} Prior to the determination of these interaction sites several results pointed to the utilization of a substrate channeling mechanism for the safe transfer of reduced flavin in the two-component alkanesulfonate monooxygenase system. Specific interactions between SsuE and SsuD were determined by affinity chromatography and results from crosslinking experiments further supported the presence of protein interactions between SsuE and SsuD.²⁰⁵ The protein interaction sites identified in SsuD are conserved and variants of these sites resulted in the loss of activity which likely caused the disruption of protein-protein interaction sites.

1.7 Summary

Sulfur is an important element required by bacteria as a constituent of sulfur containing amino acids, cysteine, and methionine.^{9,10} These amino acids have been implicated as precursors for enzymes, cofactors and coenzymes which are vital for various physiological processes.⁶⁷ Inorganic sulfate, the preferred sulfur source for bacteria is limiting in the environment.⁹⁵ Aerobic bacteria have found a mechanism to acquire sulfur under low sulfate conditions from the desulfonation of alternative sulfur sources. Acquisition of sulfur from organosulfonates requires the upregulation of a set of proteins which are termed sulfate starvation-induced (SSI) proteins. SSI proteins

comprise the enzymes utilized for desulfonation, and proteins involved in the uptake of these organosulfonates into the cell.^{30,78} In *E. coli*, the enzymes required for the acquisition of sulfur are expressed from the *tau* and *ssu* operons.^{83,87} The *tau* operon encodes taurine dioxygenase which converts taurine (2-aminoethanesulfonate) to aminoacetaldehyde and sulfite.^{88,147} The *ssu* operon encodes the two-component alkanesulfonate monooxygenase system which catalyzes the generation of sulfite from various alkanesulfonates. Two-component alkanesulfonate monooxygenase systems are comprised of a flavin reductase that catalyzes the reduction and transfer of flavin to a monooxygenase.^{170,172,189} The monooxygenase utilizes reduced flavin to activate dioxygen for desulfonation of organosulfonates. The genes encoding the flavin reductase and monooxygenase are usually located on the same operon.²⁰²

In the two-component flavin-dependent systems, flavin is a substrate and not a cofactor and the reason these systems require two enzymes to catalyze the desulfonation reaction is still being explored. In the alkanesulfonate monooxygenase system, flavin reduction and transfer is catalyzed by the reductase, SsuE and the oxygenolytic cleavage of alkanesulfonates is catalyzed by the monooxygenase, SsuD.^{88,147} These systems work synergistically to carry out the acquisition of sulfur which is made possible by the transfer of reduced flavin from SsuE to SsuD. Several structural features which facilitate the transfer of reduced flavin and desulfonation of organosulfonates have been identified in SsuE and SsuD.^{192,205,232}

SsuE belongs to the NADPH:FMN reductase family based on a flavodoxin fold. Other FMN reductases with a similar structural fold as SsuE include EmoA, MsuE and SfnF.^{89,231} These reductases possess a π -helix secondary structure, which has been

hypothesized to confer an evolutionary functional advantage on these reductases. The π -helix is characterized by the insertion of a single amino acid, Tyr118 into a α 4-helix in SsuE.⁸⁹ The π -helix is located at the tetrameric interface of SsuE where it forms π -stacking interactions. Different oligomeric states have been observed for SsuE utilizing different biophysical techniques.^{89,94} Oligomeric changes have been reported to play different biological and regulatory roles in several enzymes. Some important functions include the creation of new active sites at protein interfaces and regulation of enzyme activity by modulating enzyme concentration or binding of substrates.^{236,252,320} A network of hydrogen bonding contacts between the insertional residue of the π -helix, Tyr118 and the isoalloxazine ring of FMN has been observed across the tetrameric interface of SsuE.²³³ This implies that there may be communication between the tetrameric interface of SsuE, where the π -helix is situated and flavin binding.²³¹

The desulfonation reaction catalyzed by SsuD in the presence of dioxygen occurs through a C4a-(hydro)peroxyflavin intermediate which eventually inserts an oxygen atom into an organic substrate, regenerating oxidized flavin, the corresponding aldehyde and water.⁸⁸ For the desulfonation reaction to occur, SsuD requires reduced flavin from its partner reductase, SsuE. Reduced flavin transfer from SsuE to SsuD has been proposed to occur through protein-protein interactions. Protein-protein interactions are important for the alkanesulfonate monooxygenase system because reduced flavin is highly labile in aerobic conditions and breaks down to form reactive oxygen species. Protein-protein interactions would bring SsuE in proximity to SsuD for efficient transfer of reduced flavin.²⁰⁸

Two-component FMN-dependent systems utilize distinct structural features for sulfur acquisition from organosulfonates. SsuE and MsuE share about 30% amino acid identity and belong to the NADPH:FMN reductase family of enzymes. Previous studies revealed that SsuE exists as either a tetramer or dimer depending on the technique used for investigation.^{89,94} Oligomeric changes have been reported for several FMN reductases but the role of oligomerization in regulating enzyme function has not been fully explored for the reductases, SsuE and MsuE.^{167,231} The first study was performed to determine the oligomeric state of SsuE and MsuE and what factors influence their oligomeric changes. Understanding the role of oligomeric changes of FMN reductases is pivotal for deciphering the evolutionary advantage conferred by the π -helix in these enzymes.^{231–233} Next, we investigated the role the oligomeric changes of SsuE play in protein-protein interactions with SsuD. Protein-protein interaction sites were determined from previous studies to be the mechanism for the transfer of reduced flavin in the alkanesulfonate monooxygenase system (SsuE/SsuD).^{205,208} The interaction sites of SsuE were located at the tetrameric interface involving the π -helix and that for SsuD were close to its active site. SsuE exists in different oligomeric states in the presence of substrates, but it is not known how the presence of SsuD affects its oligomeric state. This study was performed to monitor the formation of the proposed SsuE-SsuD complex and how oligomeric changes of SsuE is affected with SsuD present. Lastly, we investigated structural adaptations that distinguish FMN reductases from canonical flavoproteins. Results from previous studies investigating the role of the π -helix in two-component flavin reductases reveal that the insertional residue cannot be responsible for the disparity in catalysis between canonical flavoproteins and two-component flavin reductases.²³¹ Variants of a

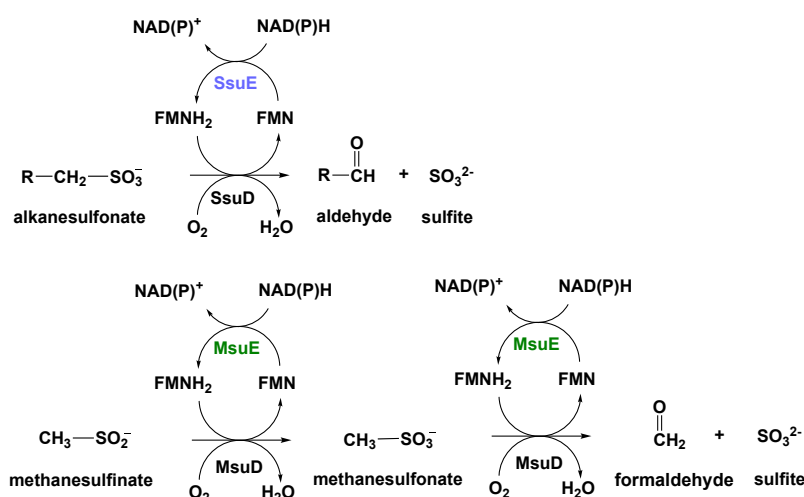
canonical flavoprotein, Chromate reductase (ChrR) which had a Tyr residue at a similar position in SsuE were generated from conserved residues in the π -helix of two-component flavin reductases. Chromate reductase catalyzes the reduction of hexavalent chromium to trivalent chromium without a monooxygenase partner like SsuE.^{321,322} The aim of this study is to convert ChrR to an enzyme that can catalyze the transfer of reduced flavin to a monooxygenase partner. The overall goal of this project is to decipher how the alkanesulfonate monooxygenase system utilizes several distinct structural features for the desulfonation of organosulfonates. Two-component flavin dependent systems are found in a broad range of bacteria which includes pathogenic bacteria that are responsible for several infections that are harmful to infected patients. These systems are unique to bacteria and understanding how these structural features are coordinated for the acquisition of sulfur could lead to the development of drugs that target these fe

CHAPTER TWO

2 Substrate-Induced Oligomeric Changes of Two-Component FMN Reductases Involved in Sulfur Metabolism

2.1 Introduction

Sulfur plays a key role as a component of metabolites needed for the survival of organisms. For bacteria, inorganic sulfate is often limiting in the environment and alternate organosulfur compounds are utilized for sulfur assimilation.^{96,323} Some organosulfur sources that bacteria use under sulfur limiting conditions include alkanesulfonates, aryl sulfonates, aromatic sulfonates, and sulfate esters.³²⁴ The alkanesulfonate monooxygenase system which is ubiquitous in bacteria comprises a NADPH-dependent FMN reductase (SsuE), FMNH₂-dependent alkanesulfonate monooxygenase (SsuD), and alkanesulfonate transport proteins.^{86,110,325} In addition to the alkanesulfonate monooxygenase enzymes, some organisms express the methanesulfinate monooxygenase operon that encodes a flavin-dependent reductase (MsuE) and two structurally distinct monooxygenases (MsuC/MsuD) that together convert methanesulfinate to formaldehyde and sulfite in consecutive reactions.^{99,100,326} In both systems, flavin reduction by the FMN reductase and reduced flavin transfer to the monooxygenase must be coordinated between the enzymes for the desulfonation reaction to be successful (**Scheme 2.1**).



Scheme 2.1: Reactions catalyzed by the alkanesulfonate monooxygenase enzymes.

The two-component flavin reductases involved in sulfur acquisition belong to the NADPH-dependent FMN reductase family. Members of the family have a flavodoxin fold and consist of both canonical flavin reductases with a tightly bound flavin and FMN-dependent reductases with a monooxygenase partner that utilize flavin as a substrate. A distinct structural difference between these two groups within the family is the presence of a π -helix located at the tetramer interface of the FMN-dependent reductases. The π -helix is often contained within a conserved alpha helix and has $i+5$ intrastrand hydrogen bonding resulting in a wide turn and increased flexibility. The altered structure provides a gain of function for enzymes outside of the structural and catalytic properties of the enzyme family. Given the functional difference between the two groups within the NADPH-dependent FMN reductase family, the π -helix has been proposed to play a role in providing a mechanism for flavin release and subsequent transfer to the monooxygenase enzymes. In fact, conversion of the π -helix to the α -helix observed in canonical flavin reductases resulted in the inability of SsuE to transfer flavin. The π -helix

for both SsuE and MsuE is located at the tetramer interface and is stabilized by intersubunit hydrogen bonding. Although SsuE has been shown to exist as a tetramer, altered oligomeric states have been observed depending on the protocol and/or conditions employed to evaluate the structure.^{325,327} However, it has not been established if these different oligomeric states are relevant to catalysis.

Reduced flavin is prone to autooxidation in the presence of oxygen, so a transfer mechanism which prevents the production of reactive oxygen species is favored. In several two-component flavin dependent systems, reduced flavin transfer involves protein-protein interactions between the FMN reductase and monooxygenase.^{204,205,328–331} Flavin transfer in the alkanesulfonate monooxygenase system is dependent on protein-protein interactions and these interaction sites are located at the dimer/dimer interface of the SsuE FMN reductase that includes the π -helix.^{205,330} A switch in oligomeric states promoted by the π -helix would expose the protein-protein interaction sites, and may serve as a regulation mechanism for enzyme activity and/or flavin transfer. The FMN reductases (SsuE and MsuE) in the alkanesulfonate monooxygenase systems have a similar flavodoxin fold and share about 30% amino acid identity.³²⁷ Therefore, these enzymes may utilize a similar mechanism for flavin reduction and transfer. The three-dimensional structure asymmetric unit of apo MsuE (PDB: 4C76) is shown as a dimer, but the interacting subunits are not in a comparable orientation as other enzymes within this family. Therefore, the correct oligomeric state and orientation of apo MsuE remains questionable.

The mechanisms that trigger oligomeric changes in SsuE have not been clearly defined.³²⁷ In addition, there have been no studies to evaluate the oligomeric states of

MsuE common to the methanesulfinate/methanesulfonate system. Because MsuE provides reduced flavin to two different monooxygenase enzymes, oligomeric changes could regulate reduced flavin transfer to each monooxygenase. The studies described herein were carried out to firmly establish the oligomeric state of SsuE and MsuE with and without substrates (FMN, NADPH), and identify if these enzymes share similar oligomeric alterations. This detailed evaluation of oligomeric states is critical to understand if structural changes regulate the catalytic properties of the alkanesulfonate monooxygenase system. The results reported provide the first detailed insights into the mechanisms that facilitate oligomeric changes of the FMN reductases (SsuE/MsuE) in the alkanesulfonate monooxygenase systems.

2.2 Experimental Procedures

2.2.1 Materials

All reagents were purchased from Sigma-Aldrich, Biorad, or Fischer. The *ssuE* and *msuE* genes were cloned separately into RNA polymerase-dependent vector pET21a (Novagen) and expressed in *E. coli* BL21 (DE3) as previously described. The concentrations of SsuE and MsuE in solution at different concentrations were calculated with the molar extinction coefficient of each protein ($20.3 \text{ mM}^{-1} \text{ cm}^{-1}$ and $7.4 \text{ mM}^{-1} \text{ cm}^{-1}$).

2.2.2 Non-Denaturing Polyacrylamide Gel Electrophoresis

Native-PAGE experiments were carried out with SsuE and MsuE in the presence and absence of flavin to perform an initial evaluation of oligomeric states of each enzyme. The gel was composed of a 5% stacking gel, 12% resolving gel without SDS, and Tris-glycine running buffer. Aliquots of the reductases, SsuE and MsuE (20 μM) were separated in the apo form and with substrates. When substrates were included, flavin (100 μM) or

NADPH (500 μ M) was added to 20 μ M SsuE or MsuE and the samples were mixed with native sample buffer to a total volume of 15 μ L. The gels were run at a constant voltage of 120 V for 8 hours at 4 °C. Protein bands were visualized using Coomassie brilliant blue staining and the molecular weight of protein samples were compared to the stokes radius of native gel protein standards. The native gels were imaged under ultraviolet light using a ChemiDoc™ MP imaging system.

2.2.3 Spectrofluorimetric Titrations

All fluorescence spectroscopy measurements were recorded at room temperature using a Shimadzu spectrofluorophotometer RF-6000 (Japan) in a 10 mm quartz cuvette with excitation slit width set at 3 nm and emission slit width set at 5 nm. Aliquots (1 μ L) of FMN (0.04 - 0.4 μ M) or FAD (6 - 120 μ M) was titrated into a 1 mL solution of SsuE (0.4 μ M) in 25 mM potassium phosphate buffer (pH 7.5), 100 mM NaCl. Fluorescent intensity was measured with an emission wavelength of 342 nm and an excitation wavelength of 280 nm. Because of the absence of Trp residues in MsuE, the binding affinity of MsuE for FMN was determined by monitoring the decrease in the relative fluorescence intensity of FMN due to flavin quenching on binding to MsuE. MsuE (0.2 - 4 μ M, 1 μ L aliquots) was titrated into a 1 mL solution of 0.1 μ M FMN or 10 μ M FAD in 25 mM phosphate (pH 7.5), 100 mM NaCl. Emission wavelengths at 525 nm were monitored using an excitation wavelength of 450 nm.

The binding affinity of NADPH to SsuE and MsuE was also investigated through spectrofluorimetric titrations. SsuE (0.4 μ M) in 1 mL 25 mM phosphate (pH 7.5), 100 mM NaCl was titrated with NADPH or NADH (10 - 200 μ M) for a total of 20 additions. The excitation wavelength was set at 340 nm and the emission wavelength was monitored at

450 nm. The binding of NADPH to MsuE was measured by monitoring the increase in fluorescence intensity upon addition of NADPH or NADH (10 - 200 μ M, 1 μ L aliquots) to MsuE (1 μ M) with the excitation wavelength set at 340 nm and emission wavelength 450 nm. All experiments were carried out in triplicates and the fluorescence spectra were measured after a 2 min incubation to reach equilibrium after each addition of titrant. The [ES] bound was calculated as previously described and plotted against the free substrate or enzyme concentration.¹⁷⁰ All plots were fitted with the quadratic equation to obtain the dissociation constant (K_d).

2.2.4 Thermal Melt Circular Dichroism Spectroscopy

CD spectroscopy measurements as a function of both temperature and wavelength was utilized to monitor the thermal stability of SsuE and MsuE using a Chirascan V-100 (Applied Photophysics UK). The temperature was increased at a step interval of 2 $^{\circ}$ C using a peltier-controlled temperature cell holder (Quantum North-West). The thermal melting was measured at a heating rate of 2 $^{\circ}$ C/min. SsuE and MsuE at a concentration of 5 μ M in 10 mM potassium phosphate (pH 7.5), respectively, were placed in sealed quartz cuvette of 0.5 mm pathlength and a temperature probe immersed in the cuvette. The change in absorbance was scanned over a wavelength range of 185-300 nm and a temperature range of 20-94 $^{\circ}$ C. The thermal stability of each protein was also evaluated in the presence of FMN (enzyme (5 μ M): FMN (50 μ M) and NADPH (enzyme (2 μ M): substrate (100 μ M)) for each reductase. All experiments were carried out in triplicate.

The CD thermal melting profiles were analyzed using global thermodynamic analysis. A plot of absorbance against wavelength gives an unfolding curve for each temperature.

Each melting curve is fitted with a sigmoidal function which is derived from the Gibbs-Helmholtz equation:

$$CD(T) = \frac{(m_F T + b_F) - (m_U T + b_U)}{1 + e^{\Delta H_v H / R (1/T_m - 1/T)}} + m_U T + b_U$$

This equation comprises both local and global fitting variables. The thermodynamic parameters, melting temperature T_m and van't Hoff's enthalpy $\Delta H_v H$, are global variables which are consistent for each wavelength. The local fitting parameters, b_F and b_U describe CD signals corresponding to the completely folded and unfolded conformation of the protein at a certain wavelength. The m_F and m_U variables stand for baseline at pre and post transition regions when baseline correction (single-baseline or double-baseline correction) is required. In the equation, T describes the absolute temperature and R is the gas constant (8.314 J/mol/K).

2.2.5 Sedimentation Velocity Analytical Ultracentrifugation

Sedimentation velocity experiments were performed at 20 °C using an Optima XL-A analytical ultracentrifuge (AUC) (Beckman Coulter, Fullerton, CA) equipped with an absorbance detection system and a four-hole AN-60 Ti rotor. The rotor was pre-chilled and equilibrated for an hour prior to the start of the run. All experiments were carried out at a radial step size of 0.003 cm, in continuous mode and no delay between each scan.

Prior to centrifugation, SsuE and MsuE were buffer exchanged into 25 mM phosphate buffer (pH 7.5), 100 mM NaCl using an Amicon Ultra - 4 centrifugal filter with a molecular weight cutoff of 10 kDa from Millipore (Burlington, MA). The AUC experiments were carried out at different rotor speeds based on the mass of the reductases and

substrate. SsuE (12 μ M) and MsuE (20 μ M) were utilized for the initial determination of the sedimentation coefficients in the absence and presence of flavin. Standard epon-double sector centerpieces of 12 mm were loaded with sample in the sample cell and 25 mM phosphate buffer (pH 7.5), 100 mM NaCl in the reference cell. For experiments performed in the presence of flavin, flavin concentration at five times the concentration of the reductases (SsuE and MsuE) was added to 1 mL of the enzymes. The samples were washed three times by 25 mM potassium phosphate (pH 7.5), 100 mM NaCl to a total volume of 4.0 mL. Unbound flavin was removed from the samples by centrifugation at 5,000 rpm for 10 min, utilizing the centrifugal filter so that the free flavin would not contribute to the 280 nm absorbance. The concentrations of SsuE (12 μ M) and MsuE (20 μ M) were determined with flavin spectra at 450 nm absorbance ($12.2 \text{ mM}^{-1}\text{cm}^{-1}$). Radial absorbance scans at 280 nm were collected continuously at 37,000 and 40,000 rpm for SsuE and SsuE/FMN and 40,000 and 37,000 rpm for MsuE and MsuE/FMN, respectively.

Data derived from the scans were evaluated using continuous sedimentation distribution model $c(s)$ with the SEDFIT program using the numerical Lamm equation. Sednterp was used to calculate the fitting parameters for SEDFIT.³³² The partial specific volume of $0.7440 \text{ cm}^3/\text{g}$ for SsuE and $0.7552 \text{ cm}^3/\text{g}$ for MsuE was calculated based on their amino acid composition at 20 °C. A buffer density of 1.00574 g/mL and viscosity of 1.0183 cp was calculated based on the buffer composition of 25 mM phosphate using the same program.

2.2.6 Differential H/D-X Experiments

H/D-X MS experiments. Local amide H/D exchange experiments were carried out using a fully automated system (PAL, LEAP Technologies, Carrboro, NC). Prior to

differential H/D-exchange analysis, SsuE and MsuE apoenzymes were buffer exchanged (25 mM phosphate buffer, pH 7.5, 0.1 M NaCl) using an Amicon Ultra-4 centrifugal filter (10 kDa MWCO, Millipore). H/D-exchange reactions for SsuE and MsuE (20 μ M) apoenzymes were initiated by mixing with a 20-fold (v/v) excess of D₂O-containing exchange buffer (57 μ L, Phosphate buffer, 25 mM, pD 7.5, 0.1 M NaCl). After incubation for 10 sec, 60 sec, 300 sec, 600 sec, 900 sec, or 1800 sec at 20 °C for SsuE or 10 sec, 60 sec, 300 sec, 600 sec and 900 sec for MsuE, unwanted back exchange was minimized with the addition of 1 equivalent (v/v, 60 μ L) of cold quench solution (200 mM phosphate buffer, pH 2.5, 0 °C). For unlabeled reactions (e.g., “0 sec exchange”), apoenzymes were mixed with a 20-fold excess of H₂O-containing buffer (phosphate buffer, 25 mM, pH 7.5, 100 mM NaCl) and quenched as above.

Differential H/D-exchange for substrate bound proteins were measured using freshly buffer-exchanged SsuE and MsuE (20 μ M). Proteins were incubated on ice with a 5-fold molar excess of either FMN (100 μ M) or NADPH (100 μ M) for ~20 min prior to analysis. Exchange reactions were monitored at 0 sec, 10 sec, 60 sec, 300 sec, 600 sec, 900 sec, or 1800 sec for SsuE and 0 sec, 10 sec, 60 sec, 300 sec, 600 sec, 900 sec for MsuE at 20 °C, quenched with quench solution, and digested as above. After quenching, samples (100 μ L) were immediately loaded onto an Enzymate BEH Pepsin Column (2.1 x 30 mm, 5 μ m). Digestion temperature was maintained at 12 °C, a flow rate of 250 μ L/min, and a pressure of ~8000 psi for 4 min. Peptides (10-15 pmol) were subjected to LC/MS-MS analysis immediately following digestion. To help prevent sample carry-over, the inline pepsin column was washed (1.5 M GuHCl, 4% acetonitrile, 0.8% formic acid,

pH 2.5) after each digestion and clean blank injections (0.1% formic acid) were run after every protein injection. H/D exchange reactions were performed in duplicate.

LC/MS-MS. LC-MS/MS analysis was performed using a Synapt XS ion-mobility assisted mass spectrometer in positive mode (Waters, Manchester, UK) coupled to a nano-Acquity UPLC/H/D-X manager system (Waters, Manchester, UK). Post-pepsin digested products were directly loaded onto an Acquity UPLC BEH C18 Vanguard trapping column (1 x 5 mm, 250 μ L/min) and desalted for 4 min. Peptides were separated on a Acquity UPLC BEH C18 1.7 μ m analytical column (1 x 50 mm) using an effective 8-min linear gradient starting at 5% acetonitrile, 0.1% formic acid and increasing over 7 min to 60% acetonitrile, 0.1% formic acid with a flow rate of 150 μ L/min. All chromatographic steps, including trapping and elution, were performed at 2 °C. Ion-mobility assisted DIA HDMS^E data were collected with an ESI capillary voltage of 32 V and the quadrupole used in rf-mode; only ions with m/z >300 was transmitted. For ion-mobility, the T-wave was operated with a wave height of 40 V and wave velocity ramp from 500-800 m/s; collision energy in the trap was continuously alternated between low energy (4 V) and high energy (20-35 V) throughout the run. For all measurements, ToF were acquired in resolution mode with a scan time of 0.4 s. Data were lock-mass corrected post-acquisition using the 1+ charge state of LeuEnk [MH^+ 556.2771], which was infused at a concentration of 200 pg/ μ L at 90° to the analytical sprayer at 10 μ L/min throughout the acquisition.

Peptide identification and data processing. Data were processed using ProteinLynx Global Server (PLGS v 3.03). Data were centroided, de-isotoped, and charge state reduced prior to fragment ion and parent protein assignments based on retention

time alignments. Peak picking thresholds were optimized using PLGS Threshold Inspector: 25 counts and 100 counts were used for all high and low energies. Peak lists were searched against databases containing either the *E. coli* SsuE (Uniprot P80644) or *P. aeruginosa* MsuE (Uniprot ID O31038) and porcine pepsin (Uniprot P00791). Protein identification criteria were set as the detection of at least 3 fragments per protein, 3 fragments per peptide, and 1 peptide per protein. Methionine oxidation was set as a variable modification for all searches. The protein level false discovery rate was set to 4%. PLGS search results and deuterium exchange spectra were imported into DynamX (v 3.0), and peptides were filtered based on the following criteria: 3 fragments per peptide, 2 fragments must be adjacent, have a minimum of 0.1-0.2 products per amino acid residue, and be present in all of the LC/MS-MS injections. Deuterium exchange measurements were analyzed with default settings and data were manually inspected, validated, and curated. In keeping with newly recommended reporting standards for H/DX MS experiments, peptide coverage maps, uptake plots (**Appendix Figs. 3-8**) and H/D-exchange summary data appendices are provided. For all data sets, differences in fractional deuterium uptake over time or between conditions were mapped onto SsuE and an alphafold model of MsuE dimer and tetramer using scripts generated in DynamX and PyMOL.³³³

2.3 Results

2.3.1 Substrate Affinity and Stability

The binding affinity of the alkane FMN reductase enzymes were evaluated to compare the substrate specificity between SsuE and MsuE. Intrinsic Trp fluorescence was utilized to monitor flavin binding to SsuE. Given the lack of Trp residues in MsuE, titrations were

performed monitoring the decrease in flavin fluorescence. SsuE showed a clear flavin preference with an ~40-fold lower K_d value for FMN than FAD (**Fig. 2.1A and B, Table 2.1, Appendix Fig. 1A and B**), but the enzyme showed a similar affinity for NADPH and NADH. NADPH often shows an increase in fluorescence when binding to an enzyme active site.

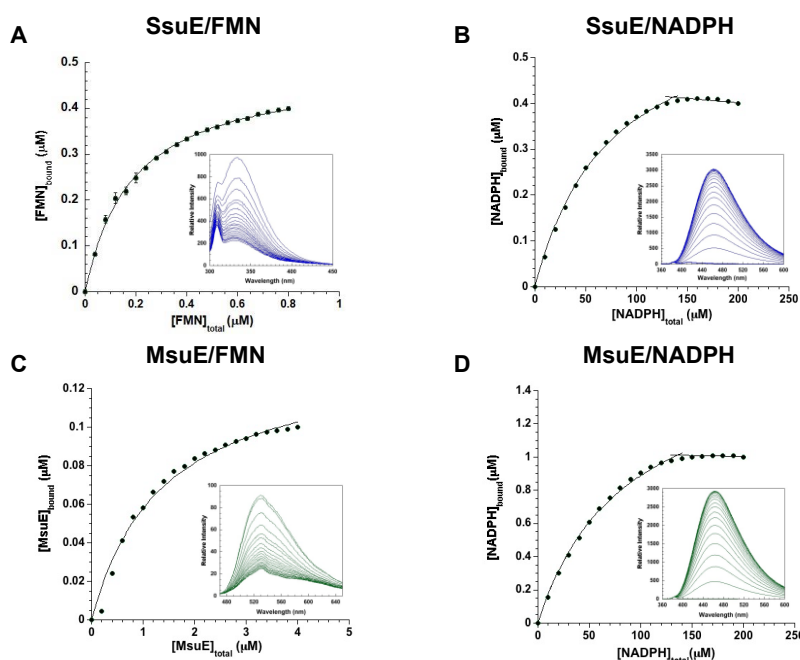


Figure 2.1: Fluorescent titrations of SsuE and MsuE with FMN and NADPH. A) Titration of SsuE (0.04 μM) with FMN (0.04-0.4; λ_{ex} , 280 nm; λ_{em} , 342 nm). B) Titration of SsuE (0.04 μM) with NADPH (10-200 μM ; λ_{ex} , 340 nm; λ_{em} , 450 nm). C) Titration of FMN (0.1 μM) with MsuE (0.2 - 4.0 μM ; λ_{ex} , 450 nm; λ_{em} , 525 nm). D) Titration of MsuE (1 μM) with NADPH (10-200 μM ; λ_{ex} , 340 nm; λ_{em} , 450 nm). All titration experiments were performed in triplicate and fit to a quadratic equation for single site binding.

The fluorescence decrease can occur due to unbound NADPH in solution at increased pyridine nucleotide concentrations.³³⁴ MsuE had a distinct specificity for FMN and NADPH in coupled assays with the MsuD monooxygenase partner, but the specificity of MsuE for each substrate in the absence of MsuD had not been determined.²³¹ MsuE showed a similar affinity for FMN/FAD and NADH/NADPH indicating there was no

apparent preference for a specific substrate under equilibrium conditions (**Fig. 2.1C** and **D**, **Table 2.1**, **Appendix Fig. 1C** and **D**).

Table 2.1. Substrate binding affinity of SsuE and MsuE.

	<i>K</i> FMN (μ M)	<i>K</i> FAD (μ M)	<i>K</i> NADPH (μ M)	<i>K</i> NADH (μ M)
SsuE	0.26 ± 0.03	10.6 ± 0.4	55 ± 5	32 ± 5
MsuE	1.4 ± 0.1	0.83 ± 0.2	69 ± 5	37 ± 4

2.3.2 Oligomeric State of SsuE and MsuE

Alternative oligomeric forms for SsuE have been reported based on the experimental procedure used for analysis. We had previously observed an apparent oligomeric shift from a tetramer to a dimer for SsuE when FMN was included in the sample, but comparable studies have not been performed with NADPH.^{325,327} In addition, there have been no studies to evaluate the oligomeric state of MsuE in the apo form and with the addition of substrates. Molecular weight species of SsuE and MsuE were evaluated by native-PAGE in the apo form and with the addition of substrates. Apo SsuE ran as a higher molecular weight band compared to the SsuE/FMN complex (**Fig. 2.2A**). This shift in molecular weight for the SsuE/FMN complex could correlate with an alternative conformer. A similar gel shift was not observed with SsuE and NADPH (**Fig. 2.2B**). Both the apo MsuE and MsuE/FMN complex separated at a similar molecular weight, suggesting the MsuE/FMN complex did not cause an alteration in the molecular weight as was observed for SsuE (**Fig. 2.2A**). Similar to SsuE, MsuE with the NADPH substrate did not show a band shift for the separated enzyme (**Fig. 2.2B**).

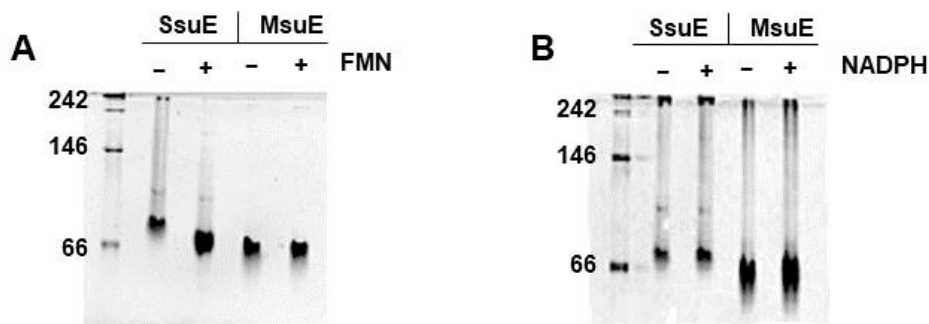


Figure 2.2: Nondenaturing polyacrylamide gel of SsuE and MsuE. A) Separation of apo SsuE or MsuE and the SsuE or MsuE/ FMN complex. B) Separation of apo SsuE or MsuE with NADPH included in the sample. The proteins were separated on 12% native PAGE.

The band shift observed for SsuE on Native-PAGE suggested a structural change may have occurred with the addition of FMN. However, a detailed analysis of which factors trigger these changes in solution had not been performed. Analytical ultracentrifugation (AUC) was performed to identify the oligomeric state(s) of apo SsuE and MsuE in solution. SsuE in the absence of substrate gave a sedimentation value of $s_{20,w}$ of 4.55 ± 0.10 S which corresponded to a molecular mass of 81.5 ± 4.6 kDa (**Fig. 2.3A, Table 2.2**). With a monomeric molecular mass of 21.3 kD for SsuE, the protein existed predominately as a tetramer in the apo form. Given the structural similarity between SsuE and MsuE we expected that MsuE would also exist as a tetramer, but AUC analyses of MsuE gave an $s_{20,w}$ value of 4.14 ± 0.13 S corresponding to a molecular weight of 42.4 ± 1.2 kDa consistent with a dimer (MsuE monomeric molecular weight, ~20.0 kDa) (**Fig. 2.3B, Table 2.2**). Interestingly, for the SsuE/FMN sample there were two species observed ($s_{20,w}$; 4.51 ± 0.04 S and 3.31 ± 0.13 S) corresponding to a tetramer (78.3 ± 1.3 kDa) and dimer (49.3 ± 3.3 kDa) (**Fig. 2.3A, Table 2.2**). Therefore, the addition of FMN to SsuE shifted the quaternary structure of the enzyme from a tetramer to a tetramer/dimer equilibrium. Although the dimer was not identified from a fit

of the sedimentation profiles of apo SsuE, there was some tailing on the right side of the sedimentation distribution plot indicating there may be a small amount of dimer in the absence of substrates. The addition of FMN to SsuE changed the equilibrium leading to an increase in the dimeric species. Contrary to the findings for SsuE/FMN, the addition of FMN to MsuE resulted in a single higher molecular weight species (80.7 ± 0.9 kDa) that corresponded to a tetramer (**Fig. 2.3B, Table 2.2**). Changes to the oligomeric state of

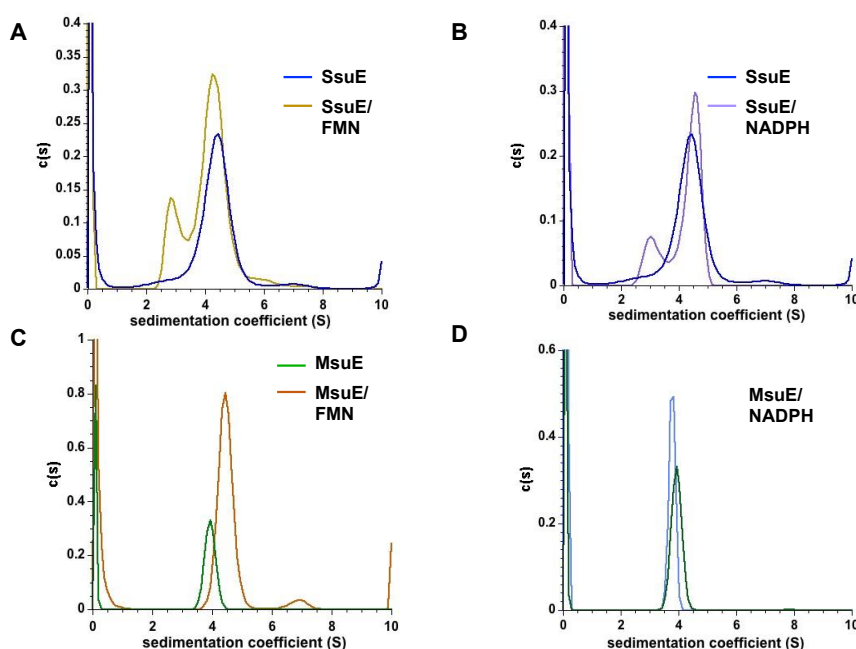


Figure 2.3: Sedimentation distribution plots of SsuE and MsuE. A) SsuE/FMN B) SsuE/NADPH C) MsuE/FMN D) MsuE/NADPH. AUC experiments were performed with SsuE (12 μ M) and MsuE (20 μ M). FMN and NADPH was added at five-fold over the enzyme concentration for both SsuE and MsuE. The reactions were performed in triplicate, but only one fit from each analysis is shown for clarity.

SsuE and MsuE were also evaluated with the addition of NADPH. While the dimer was less pronounced, a similar tetramer to dimer equilibrium shift was also observed with the SsuE/NADPH complex (**Fig. 2.3C, Table 2.2**). However, MsuE with NADPH was

predominantly in the dimeric form and did not shift to a tetramer like the MsuE/FMN complex (**Fig. 2.3B** and **D**, **Table 2.2**).

Table 2.2. Results from AUC analysis of SsuE and MsuE.

	SsuE (kDa)	SsuE +FMN (kDa)		SsuE +NADPH (kDa)	
$s_{20,w}$ (S)	4.55 ± 0.10	4.51 ± 0.04	3.31 ± 0.13	4.70 ± 0.05	3.15 ± 0.15
molecular weight (kDa)	81.5 ± 4.6	78.3 ± 1.3	49.3 ± 3.3	79.3 ± 2.4	43.8 ± 4.1
	MsuE (kDa)	MsuE +FMN (kDa)		MsuE +NADPH (kDa)	
$s_{20,w}$ (S)	4.14 ± 0.13	4.60 ± 0.02		3.96 ± 0.03	
molecular weight (kDa)	42.4 ± 0.3	80.7 ± 0.9		48.5 ± 0.4	

2.3.3 Thermal Stability of SsuE and MsuE

AUC studies demonstrated alterations in the oligomeric state of SsuE and MsuE under specific conditions for each enzyme. Therefore, the binding of substrates and subsequent oligomeric changes may alter the stability of the proteins. The thermal melting temperatures of SsuE and MsuE were evaluated to determine if substrate binding affected the structural stability of the enzymes. The T_m value of apo SsuE was 47.5 ± 0.2 °C using a temperature range from 20-90 °C (**Fig. 2.4A**, **Table 2.3**). Although apo MsuE existed as a dimer, the enzyme had a similar melting temperature in the absence of substrates as SsuE (**Fig. 2.4B**, **Table 2.3**). Interestingly, the T_m value increased for both SsuE and MsuE when FMN was included (**Fig. 2.4C** and **D**, **Table 2.3**). For SsuE, the

change from a tetramer to a tetramer/dimer equilibrium with the addition of FMN led to a sharp increase in the melting temperature ($75.2 \pm 0.1^{\circ}\text{C}$) compared to apo SsuE (**Fig. 2.4C and D, Table 2.3**). However, a similar increase in melting temperature was not observed with NADPH (**Appendix Fig. 2A**). The oligomeric change of MsuE from a dimer to a tetramer in the presence of FMN also resulted in an increase in the melting temperature ($60.8 \pm 0.2^{\circ}\text{C}$) that was not observed with NADPH. (**Appendix Fig. 2B**). The change in melting temperature with the addition of FMN suggested the conformational alteration in the oligomeric state of each enzyme increased enzyme stability. It was curious that even though SsuE and MsuE have different oligomeric states in the presence of FMN, they showed similar increases in the melting temperature and increased stability. For SsuE/FMN, the circular dichroism (CD) spectra for the enzyme complex at 90°C showed a difference in absorbance between 220-240 nm that was not observed in SsuE only. The apo SsuE enzyme still showed some secondary structural features indicative of a random coil compared to the SsuE/FMN complex which showed no secondary structural features.

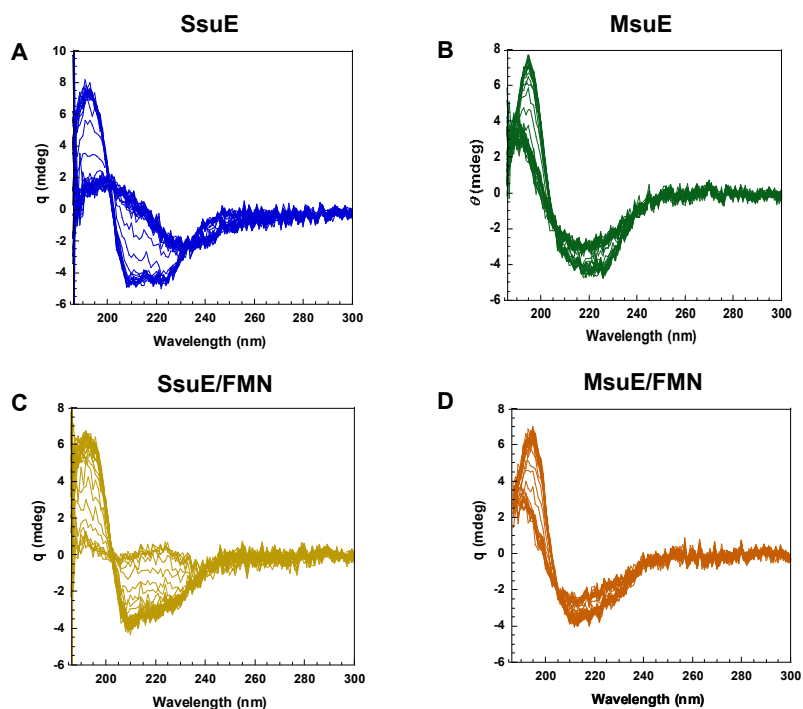


Figure 2.4: Thermal denaturation CD of SsuE and MsuE. A) SsuE B) MsuE C) SsuE/FMN D) MsuE/FMN. SsuE and MsuE (5 μ M) were scanned over a wavelength range of 185-300 nm and a temperature range of 20-94 $^{\circ}$ C. FMN was added in a 1:10 ratio (enzyme: substrate) when included. Each thermal denaturation experiment was performed in triplicate.

Table 2.3. Thermal stability of SsuE and MsuE.

	T_m		
	($^{\circ}$ C)	+FMN ($^{\circ}$ C)	+NADPH ($^{\circ}$ C)
SsuE	47.5 ± 0.2	75.2 ± 0.1	46 ± 1
MsuE	48.5 ± 0.2	60.8 ± 0.2	46 ± 1

2.3.4 H/D-Exchange Mass Spectrometry

H/D-exchange (H/D-X) mass spectrometry (MS) experiments were performed to further probe the solution dynamics of the SsuE and MsuE dimer-tetramer equilibrium in

the absence or presence of FMN and NADPH. H/D-X measures the propensity of main-chain amide protons to exchange with the bulk solvent. Protons that are solvent inaccessible or contained within a strong hydrogen-bonding network will not undergo exchange as readily as those that are exposed to solvent and not extensively involved in hydrogen bonding interactions.³³⁵ Because amide protons in dimer and tetramer interfaces are often protected in H/D-X studies, these experiments afford us the means to compare the ligand-stabilized, higher-order structural rearrangement mechanisms of SsuE and MsuE.^{336,337}

SsuE and MsuE are both highly amenable to interrogation by H/D-X MS. For example, 100% coverage was obtained for SsuE (average peptide lengths of ~13 residues, redundancy of ~3.5-4) in the absence or presence of FMN or NADPH (**Appendix Fig. A3**). Due to the instability of SsuE, exchange reactions were only monitored for 30 min; however, this was ample time to examine the impact of FMN and NADPH on the dimer-tetramer equilibrium. Upon initial inspection, differential H/D-X between SsuE/FMN and apo SsuE indicated FMN reduces deuterium uptake, even at a 10 sec exposure time (**Fig. 2.5A**). Longer exposure times showed greater differences between SsuE/FMN and apo SsuE (**Fig. 2.5B and C**), which was especially apparent at the dimer-tetramer interface (**Fig. 2.5D**). Considering apo SsuE apoenzyme is proposed to exist as a tetramer and the SsuE/FMN complex establishes a dimer-tetramer equilibrium, we expected to see more uptake in the presence of FMN compared to the apoenzyme as the residues contained within the dimer-tetramer interface should be more exposed. Inspection of the isotopic distributions in the mass spectra revealed bimodal distribution patterns for the apoenzyme and SsuE/FMN (**Fig. 2.5E and Appendix Table A1**). Bimodal distribution patterns are

commonly observed when there is a significant heterogeneity in the higher order structures.^{338,339} The SsuE/FMN complex, adopts two different higher ordered structures in the sample, one that protects against deuterium uptake more than the other. The bimodal distributions observed for apo SsuE and SsuE/FMN are most likely due to the presence of dimers (fast-exchanging) and tetramer (slow-exchanging).

The bimodal exchange patterns were largely observed in regions of SsuE near the dimer/tetramer interface and around the π -helix (residues 22-48, 71-84, and 90-138; **Appendix Table A1**). There was little variation in the overall amount of deuterium exchanged over time in the uptake plots of apo SsuE (**Appendix Fig. A4**). The observed bimodal distributions were likely due to the rapid exchange (<10 sec) of solvent for the dimer population at the tetramer interface. In contrast, isotopic distributions of SsuE in the presence of FMN showed both binomial and bimodal exchange patterns at early timepoints, with the tetramer being the predominate species. Longer exposure times consistently showed the appearance of the fast-exchanging dimer, with nearly equal distribution between the dimer and tetramer. While similar bimodal patterns of exchange were observed in the presence of NADPH, the distributions of dimer and tetramer species were consistent with those observed for the apoenzyme, giving rise to nearly identical uptake plots (**Appendix Fig. A5**).

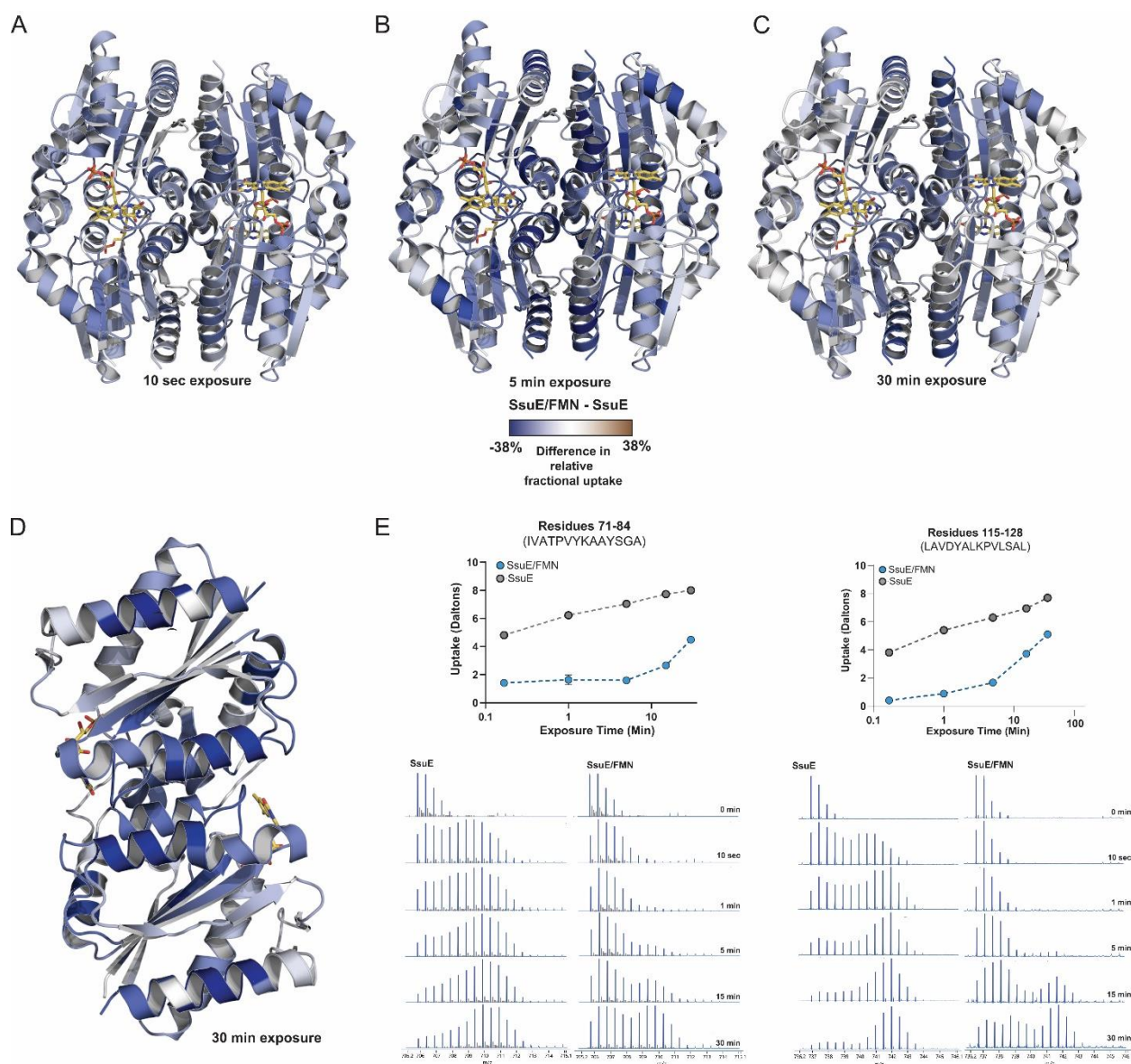


Figure 2.5: Differential H/D-X analysis of SsuE and SsuE/FMN. Differences in relative fractional uptake after (A) 10 sec, (B) 5 min and (C) 30 min D₂O exposure for SsuE/FMN and SsuE mapped onto the SsuE tetramer. Protein regions showing decreased deuterium in the presence of FMN are shown in blue, regions with no difference in exchange are shown in white, and regions where FMN increases deuterium uptake compared to the apoenzyme are shown in brown. D) Differential H/D-X mapped onto the SsuE dimer for 30 min D₂O exposure. Colors as defined in A-C. To highlight the dimer-tetramer interface, (B) is rotated 180° counterclockwise relative to (A). E) Representative deuterium uptake plots and peptide spectra showing bimodal distributions of the isotopic envelope indicating a mixed population of dimer (fast exchanging, higher m/z) and tetramer (slower exchanging, lower m/z) species. Exchange patterns for all peptides identified are summarized in **Appendix Table A1** and all deuterium uptake plots for SsuE/FMN and SsuE/NADPH are provided in **Appendix Fig. A4 and A5**.

Like SsuE, MsuE is equally amenable to interrogation by H/D-X. Peptide coverage was obtained for nearly the entire protein (98.6-99%) with high redundancy (**Appendix Fig. A6**). Unlike SsuE, the MsuE apoenzyme and MsuE/FMN complex displayed binomial isotopic distributions in the mass spectra, suggesting a more homogenous mixture of higher order structures. Differential H/D-X analysis of MsuE/FMN compared to MsuE showed a marked decrease in deuterium uptake in the presence of FMN (**Fig. 2.6A**) which was most apparent at the dimer-tetramer interface (**Fig. 2.6B**) and in regions proposed to stabilize the interface (**Fig. 2.6C**). As seen in the uptake plots (**Appendix Fig. A7**), the decreased deuterium uptake in the presence of FMN was largely due to changes in solvent exposure, or overall deuterium uptake, rather than changes in protein motions of dynamics. Collectively, these data suggest FMN stabilizes MsuE in a single, tetrameric species. In striking contrast, MsuE/NADPH shows no significant difference in deuterium uptake compared to the exchange observed for the apoenzyme. Deuterium uptake plots (**Appendix Fig. A8**) for all peptides analyzed are nearly identical in both exchange rates and relative deuterium incorporation indicating NADPH has little impact on the dimer-tetramer equilibrium of MsuE.

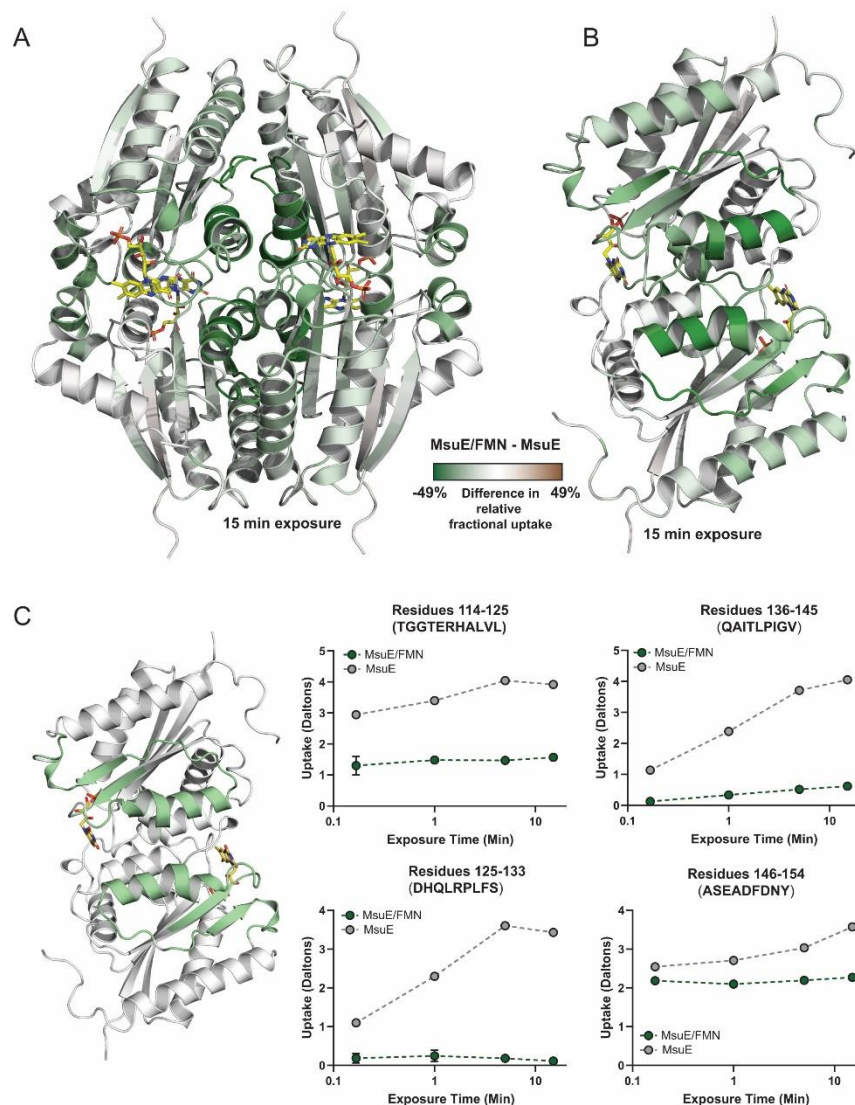


Figure 2.6: Differential H/D-X analysis of MsuE and MsuE/FMN. Differences in relative fractional uptake after 15 min D₂O exposure for MsuE/FMN and MsuE mapped onto the MsuE tetramer (A) and dimer (B). Protein regions showing decreased deuterium in the presence of FMN are shown in green, regions with no difference in exchange are shown in white, and regions where FMN increases deuterium uptake compared to the apoenzyme are shown in brown. To highlight the dimer-tetramer interface, (B) is rotated 180° counterclockwise relative to (A). C) Deuterium uptake plots for the dimer-tetramer interface, including the π -helix. Protein residues captured in these select uptake plots are highlighted on the MsuE/FMN dimer structure (pale green). Deuterium uptake plots for MsuE/FMN and MsuE/NADPH are provided in **Appendix Fig. A7 and A8**.

2.4 Discussion

Oligomeric changes in proteins play diverse roles in enzyme function. Protein oligomers have evolved because of their advantages over their monomers. These advantages include the possibility of allosteric control, higher local concentration of active sites, larger binding surfaces, new active sites at subunit interfaces, and economic ways to produce large protein interaction networks and molecular machines.^{236,237,340} Oligomeric changes have been identified for specific FMN-dependent reductases associated with two-component monooxygenase systems.^{261,327,329,341} Factors that initiate these observed oligomeric changes include interaction with the monooxygenase, fluctuations in cellular concentrations of the enzyme, and substrate binding. The SsuE and MsuE FMN-reductases are part of two-component enzyme systems involved in sulfur acquisition. While SsuE has a single monooxygenase partner, MsuE must be able to transfer flavin to two structurally and functionally different monooxygenase enzymes.^{31,100,326} SsuE and MsuE are classified in the group of NADPH:FMN reductases that are part of the flavodoxin-like superfamily based on their structural similarities.³²⁷ Members of this group include NADPH:FMN reductases with a tightly bound FMN prosthetic group and those enzymes that use FMN as a substrate such as SsuE and MsuE. The principal structural difference between the two groups of enzymes is the presence of a π -helix generated by the insertion of an amino acid in a conserved α -helix.^{231,232,327,342} The presence of a π -helix secondary structure usually leads to a gain of function.^{211–213,229} For SsuE, the insertional residue is a Tyr residue, while MsuE has a His insertional residue. Substitution of the Tyr π -helix insertional residue shifted the tetramer of SsuE to a dimer in the three-dimensional structure, and FMN was tightly

bound to the variant.²³¹ The π -helix is located at the tetramer interface of SsuE and has been proposed to initiate flavin transfer.^{232,342}

The FMN reductases and monooxygenases from two-component systems have a preference for a specific redox form of the flavin. The FMN reductases typically show a higher affinity for oxidized flavin, and their partner monooxygenases prefers reduced flavin.^{189,343} This specificity ensures that the reduced flavin is transferred to the monooxygenase enzyme. Detailed substrate binding analyses of SsuE and MsuE was performed in order to identify the preferred substrate for each enzyme to use in further studies to evaluate oligomeric state changes in the presence of each substrate. SsuE showed a preference for FMN but was able to use either NADH or NADPH for flavin reduction. The MsuE enzyme showed a similar affinity for FMN/FAD and for each pyridine nucleotide. Although MsuE showed no clear preference for a specific pyridine nucleotide in binding studies, FMN and NADPH are the preferred substrates in coupled assays with the monooxygenase enzyme MsuD. It is unclear why NADPH is preferred in coupled assays over NADH. The mechanism of flavin reduction by SsuE was previously shown to utilize a sequential mechanism for binding with the pyridine nucleotide binding first followed by the flavin to form a ternary complex.¹⁷⁰ Following flavin reduction, the reduced flavin is transferred to the monooxygenase and the pyridine nucleotide is released. The preference for NADPH in coupled assays with MsuE/MsuD could be related to the release of the oxidized pyridine product to promote continued flavin reduction by MsuE if a similar binding model as SsuE is used. Moreover, MsuD must be altering the preference of MsuE for NADPH as the specificity is only observed in coupled assays.

The established substrate preference was used to determine if oligomeric changes were initiated by specific substrate binding. SsuE was previously shown to exist as a dimer or tetramer depending on the protocol used to investigate the oligomeric state.^{325,327} Given the structural and functional similarity of MsuE and SsuE with the comparable π -helix providing a gain of function, we anticipated that similar oligomeric changes would be observed between the two enzymes. SsuE existed in different multimeric states in the presence of FMN and NADPH compared to the apo enzyme. With the addition of FMN or NADPH, SsuE shifted from a tetramer to a tetramer/dimer equilibrium. The rapid shift between tetramer and dimer species would lead to the exposed regions of the dimer exchanging over longer exposure times in H/D-X studies, even though the tetramer was the predominant species in solution. This would give inflated deuterium uptake measurements for the apoenzyme at longer (>5 min) time points. In contrast, FMN slows the rapid equilibrium between the dimer and tetramer, which is evident from the slow appearance of the dimer in the mass spectra. The shift from the tetramer to a dimer occurred along the dimer/dimer interface of SsuE. An oligomeric shift at the dimer/dimer interface would disrupt the hydrogen bonding interactions between the insertional tyrosine residue of the π -helices and the amide of the peptide backbone across the dimer interface. The presence of π -helices in proteins often leads to increased flexibility due to the altered intrastrand hydrogen bonding. For soybean lipoxygenase, the π -helix becomes mobile on a nanosecond timescale with the binding of lipid.²²⁶ The substrate binding sites of SsuE are located near the π -helices and the binding of flavin may lead to an initial increase in mobility resulting in the disruption of hydrogen bonding interactions across the dimer/dimer interface. Although SsuE with flavin bound exists as a tetramer in the three-

dimensional structure, preformed crystals of SsuE were soaked with FMN so the tetramer observed may not be an accurate representation of oligomeric states for SsuE.³²⁷

For MsuE, the enzyme shifted from a dimer to a tetramer with the addition of flavin, but there was no change in the oligomeric state with NADPH. The shift to a tetramer was also supported by H/D-X MS studies that demonstrated decreased deuterium uptake at the dimer/dimer interface for the MsuE/FMN complex compared to the apo enzyme. The decreased deuterium uptake for MsuE with FMN was primarily located in the π -helical region. Currently there are no three-dimensional structures of MsuE with FMN bound. The asymmetric unit of the PDB structure (4C76) for MsuE has the π -helices pointing away from the dimer/dimer interaction interface and would not lead to a decrease in deuterium uptake with the conversion of a dimer to a tetramer. In addition, the dimeric structure was not in the commonly observed symmetry for the NADPH:FMN-reductases belonging to the flavodoxin-like superfamily. Therefore, based on these investigations, apo MsuE exists as a dimer and the addition of FMN converts the enzyme to a tetramer with the π -helices located at the dimer/dimer interface.

The changes in the oligomeric state for both SsuE and MsuE with FMN bound likely represents a regulatory control point for reduced flavin transfer. Differences in the observed oligomeric states between SsuE and MsuE were surprising given their structural similarity, and likely is a result of their different physiological roles. Despite these differences, both SsuE and MsuE demonstrated a pronounced increase in enzyme thermal stability. It is not overtly apparent why there was an observed increase in the T_m of the enzyme with FMN bound. There are no major structural changes between the monomeric three-dimensional structure of apo SsuE and the SsuE/FMN complex.

However, a decrease in hydrogen-deuterium exchange was observed in the β -sheets located at the center of SsuE at all time points evaluated by H/D-X MS indicating a more compact or rigid structure that would be more resistant to thermal denaturation. An increase in the stability would also assist in stabilizing the flavin prior to reduction. The tetrameric interface of SsuE forms protein-protein interactions with SsuD, and the tetrameric form of SsuE would have to dissociate along the dimer/dimer interface to interact with SsuD (**Fig. 2.7A**). Therefore, the conversion of SsuE to a tetramer/dimer equilibrium in the presence of substrates would promote these interactions. Binding of dimeric SsuE to SsuD would lead to a tetramer/dimer equilibrium shift to further promote protein-protein interactions. Conversely, MsuE shifted from a dimer to a tetramer with the binding of the FMN substrate only and multiple oligomeric states were not observed (**Fig. 2.7B**). The additional noncovalent interactions to form the tetramer and bind FMN could lead to the observed increase in thermal stability with the MsuE/FMN complex. Based on the location of the flavin at the tetramer interface, it would be difficult to release the flavin unless MsuE was in the dimeric form. MsuE was shown to play a dual role in providing reduced flavin FMN to both MsuC and MsuD.^{100,326} If MsuE forms protein-protein interactions with both MsuC and MsuD, then these interactions and/or FMN reduction may be the catalyst that drive the equilibrium shift from a tetramer to a dimer. Alternatively, flavin transfer in MsuE may occur by a diffusion mechanism and no protein-protein interactions would be necessary. However, it would be difficult to transfer reduced flavin in the tetrameric species of SsuE as the substrate is buried at the dimer/dimer interface. Current studies to evaluate the oligomeric state of SsuE and MsuE in the presence of their partner monooxygenases will provide additional insight into the observed oligomeric

changes between the apo and FMN bound enzyme. Although SsuE and MsuE share ~30% amino acid sequence identity, there is a clear difference in the oligomeric changes that is likely related to differences in their overall functional role.

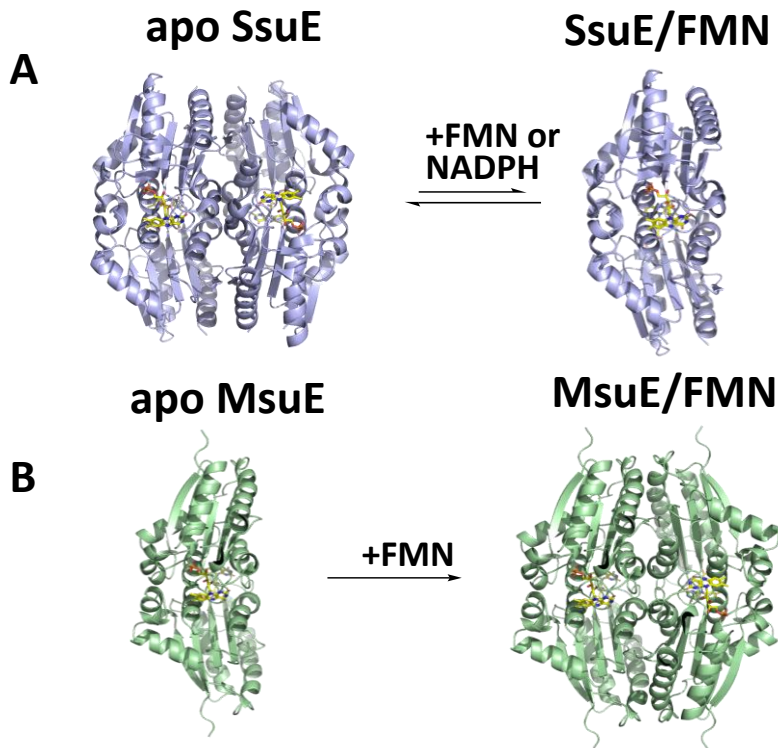


Figure 2.7: Model for SsuE and MsuE oligomeric changes. A. SsuE shifts from a tetramer to a slow tetramer/dimer equilibrium with the addition of FMN or NADPH. B. MsuE shifts from a dimer to a tetramer with the addition of FMN. The oligomeric change was not observed with NADPH. PDB: Pu01 (SsuE), MsuE was generated with AlphaFold.^{327,333}

CHAPTER THREE

3 The Role of Oligomeric Changes of SsuE in Protein-Protein Interactions in the Alkanesulfonate Monooxygenase System

3.1 Introduction

The two-component alkanesulfonate monooxygenase system is utilized by bacteria for furnishing sulfur sources during sulfur limiting conditions.⁷⁸ For sulfite production, the flavin reductase, SsuE transfers reduced flavin to the alkanesulfonate monooxygenase, SsuD for the desulfonation of organosulfonates in the presence of oxygen.^{88,147} This enzyme system utilizes several distinct structural features for the reduction and release of flavin which is pertinent for the desulfonation reaction to occur. In this enzyme system, SsuE utilizes flavin as a substrate not a cofactor as observed for the canonical flavoproteins that belong to the same NADPH:FMN reductase family. Canonical flavoproteins have flavin bound and do not have a monooxygenase partner for flavin transfer. SsuE differs from the other canonical flavoproteins due to a conserved π -helix.⁸⁹ The presence of the π -helix may be responsible for the structural divergence of two-component reductases and canonical flavoproteins.²³¹ The π -helix has been proposed to enhance protein-protein interactions and/or flavin transfer in the alkanesulfonate monooxygenase system.

Before desulfonation occurs, reduced flavin needs to be transferred effectively from the reductase to the monooxygenase. There is no clear consensus about the mechanism of reduced flavin transfer and different mechanisms have been investigated and reported for several two-component systems.¹⁴⁶ Transfer of reduced flavin can occur

through diffusion or a direct transfer mechanism involving protein-protein interactions between the reductase and monooxygenase. Safe transfer of reduced flavin is critical for the desulfonation reaction in the alkanesulfonate monooxygenase system because reduced flavin undergoes autooxidation to generate reactive oxygen species.¹⁴⁶ The direct mechanism of reduced flavin transfer from the reductase to the monooxygenase would be more efficient in a cellular system to prevent autooxidation before catalysis occurs.²⁰⁵

Several investigations have been performed to determine the mechanism of reduced flavin transfer in the alkanesulfonate monooxygenase system. SsuE showed a 1000-fold higher binding affinity for the oxidized form of flavin compared to SsuD, while SsuD had a higher binding affinity of about 10-fold for reduced flavin.^{170,171} The higher affinity of SsuE for oxidized flavin may likely increase the rate of reduced flavin transfer to SsuD.¹⁷⁰ Static protein-protein interactions were observed between SsuE and SsuD in pull-down assays.²⁰⁵ Additionally, results from competitive assays to evaluate the ability of Y118A SsuE (flavin-bound variant) to compete with SsuE for the interaction sites in SsuD revealed a decrease in desulfonation activity, which implies that protein-protein interactions are utilized for reduced flavin transfer from SsuE to SsuD.²³³ Specific protein-protein interaction sites were identified in the alkanesulfonate monooxygenase system and these sites are conserved in both enzymes (**Fig. 3.1**).²⁰⁸ The interaction sites for SsuE were present at the tetramer interface where the π -helix is located. The π -helix is a unique structural feature of SsuE, and it has been hypothesized to play a role in reduced flavin transfer to SsuD. Several unique roles have been observed in different enzymes due to the flexibility and functional advantage conferred by the presence of the π -helix in

these enzymes.^{211,213} Hydrogen bonding interactions have been observed between the π -helix and FMN at the tetrameric interface of SsuE which may affect the oligomeric changes of SsuE upon flavin binding. These observations imply that oligomeric changes of SsuE may be directly linked to protein-protein interactions which are vital for the transfer of flavin to SsuD. The monooxygenase, SsuD belongs to the bacterial luciferase enzyme family and is composed of a TIM-barrel fold with a dynamic loop region in an insertion sequence which deviates from other TIM (β/α)₈ barrel proteins.¹⁸⁶ The active site of SsuD is situated at the C-terminal end of the β -barrel.^{184,185,187} The dynamic loop is flexible, and it undergoes conformational changes upon substrate binding to SsuD. The mobile loop situated over the active site prevents premature release of reactive intermediates and shields the active site from bulk solvent once reduced flavin is bound.¹⁸⁸ The interaction sites in SsuD are located at the active site opening and are connected to each other by a loop.²⁰⁸ Protein-protein interactions may prompt structural changes in the structure of SsuE and SsuD that enhance the desulfonation reaction.

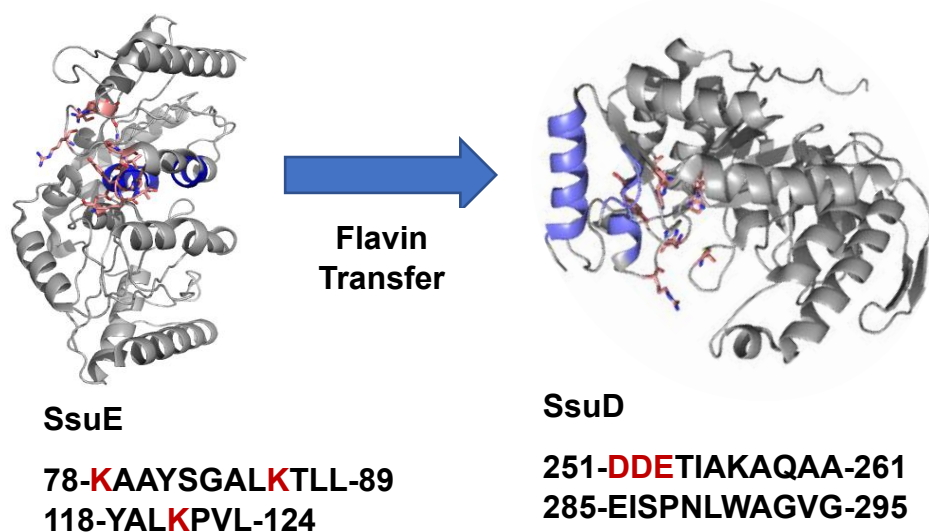


Figure 3.1: Protein-protein interaction sites in SsuE and SsuD were identified. (Adapted from²⁰⁸). Copyright © 2015, American Chemical Society.

SsuE exists in a tetramer-dimer equilibrium with flavin present which may enhance the transfer of reduced flavin to SsuD. However, it is not clear how the oligomeric changes of SsuE are affected by the presence of SsuD. These studies were performed to probe how the oligomeric state of SsuE aids in the flavin transfer process and to determine the molecular weight of the SsuE-SsuD complex formed following protein-protein interactions.

3.2 Materials and Methods

3.2.1 Materials

Expression and purification of wild-type SsuE and SsuD were performed as previously reported.²⁰⁵ All chemicals and reagents were purchased from Sigma-Aldrich, Fisher and Bio Rad. Amicon ultra-4 centrifugal filter with a molecular weight cutoff of 10 kDa were purchased from Millipore (Burlington, MA). All UV-vis spectra were recorded using an Agilent HP 8453 UV-vis spectrophotometer equipped with a peltier-controlled temperature cell holder (Quantum North-West).

3.2.2 Fluorimetric Titrations of SsuE and SsuD

Fluorometric titrations were recorded at room temperature using a Shimadzu spectrofluorophotometer RF-6000 (Japan). Titrations were performed in a 10 mm quartz cuvette with excitation and emission slit widths of 3 nm and 5 nm, respectively. SsuD (0.04 – 0.8 μ M, 1 μ L aliquots) was titrated into a 1 mL solution of equimolar FMN-bound SsuE (0.4 μ M) in 25 mM phosphate (pH 7.5) and 0.1 M NaCl for a total of 20 additions. Binding affinity was measured by monitoring the change in the local flavin environment, the protein sample was excited at 450 nm, and the fluorescence emission was measured at 525 nm. The experiment was performed in triplicate and the fluorescence spectra was

measured after 2 min incubations in order to reach equilibrium after the addition of SsuD. The dissociation constant (K_d) for binding between SsuE and SsuD was obtained using a quadratic equation as previously described.^{205,208}

3.2.3 Analytical Ultracentrifugation of SsuE and SsuD

Oligomeric changes of SsuE in the presence of SsuD were determined in the absence and presence of FMN. The oligomeric changes of the protein samples were monitored by sedimentation velocity on an Optima XL-A analytical ultracentrifuge (AUC) (Beckman Coulter, Fullerton, CA) at 20 °C. The samples were measured in a four-hole AN-60 Ti rotor with standard epon-double centerpieces of 12 mm. The different samples were monitored at a radial step size of 0.003 cm, in continuous mode and with no delay between the 300 scans. The sample cell contained the different protein samples and the reference cells contained 25 mM potassium phosphate (pH 7.5) and 0.1 M NaCl.

Prior to the determination of the oligomeric state of the SsuE-SsuD protein complex, the oligomeric state of SsuD was evaluated at different concentrations (6 μ M and 12 μ M). The SsuD samples were buffer exchanged three times with 25 mM potassium phosphate (pH 7.5) and 0.1 M NaCl in an amicon centrifugal filter. The oligomeric states of the SsuE and SsuD protein complex were monitored utilizing an equimolar concentration of SsuE:SsuD (12 μ M:12 μ M) and a 2:1 combination of SsuE:SsuD (12 μ M:6 μ M). The SsuE and SsuD samples were buffer exchanged separately three times with 25 mM potassium phosphate (pH 7.5) and 0.1 M NaCl to a total volume of 4 mL with each wash. To determine the shift in oligomerization of SsuE with flavin and SsuD present, a 5:1 ratio of FMN to SsuE was utilized for this investigation. The SsuE/FMN was washed three times with 25 mM potassium phosphate (pH 7.5) and

0.1 M NaCl to a total volume of 4 mL with each wash. Unbound flavin was removed by centrifugation at 5000 rpm for 10 min using the amicon centrifuge filter. The concentration of SsuE (12 μ M) after washing was measured at absorbance 450 nm ($12.2 \text{ mM}^{-1} \text{ cm}^{-1}$). SsuD was buffer exchanged and added to FMN-bound SsuE at 6 μ M. For all samples, radial absorbance scans were measured at 280 nm and continuous scans were collected at 37000 rpm.

Sedimentation data from the scans were evaluated using continuous sedimentation distribution model $c(s)$ using the Lamm equation in the SEDFIT program. The partial specific volume for SsuE ($0.7441 \text{ cm}^3/\text{g}$) and SsuD ($0.7359 \text{ cm}^3/\text{g}$) was calculated based on their amino acid composition at 20 °C on Sednterp. The buffer density of 1.00574 g/ml and viscosity of 1.0183 cp was determined based on the buffer composition of 25 mM potassium phosphate (pH 7.5) and 0.1 M NaCl from the Sednterp program. These parameters were used to fit the sedimentation scans on the SEDFIT program. An average of the partial specific volume of SsuE and SsuD were used to fit the scans to determine the sedimentation coefficient of the proposed complex formed between the enzymes.

3.3 Results

3.3.1 Binding of SsuD to FMN-bound SsuE

Fluorescence titrations were performed to evaluate the dissociation constant (K_d) for protein-protein interactions in the two-component alkanesulfonate monooxygenase system. The K_d of SsuD binding to SsuE was evaluated by titrating SsuD into FMN-bound SsuE. For this investigation, the change in fluorescence of the flavin environment of flavin-

bound SsuE with each addition of SsuD was monitored rather than the intrinsic fluorescence of either proteins because it would be difficult to attribute the change in fluorescence intensity to either SsuE or SsuD. Increase in fluorescence binding was monitored at an excitation wavelength of 450 nm emission following each addition of SsuD. The increase in fluorescence following SsuD binding to the SsuE-FMN complex is as a result of protein-protein interactions causing a change in the local flavin environment of SsuE. The concentration of SsuD bound was plotted against total SsuD to obtain a K_d value of $0.26 \pm 0.03 \mu\text{M}$ (**Fig. 3.2**).

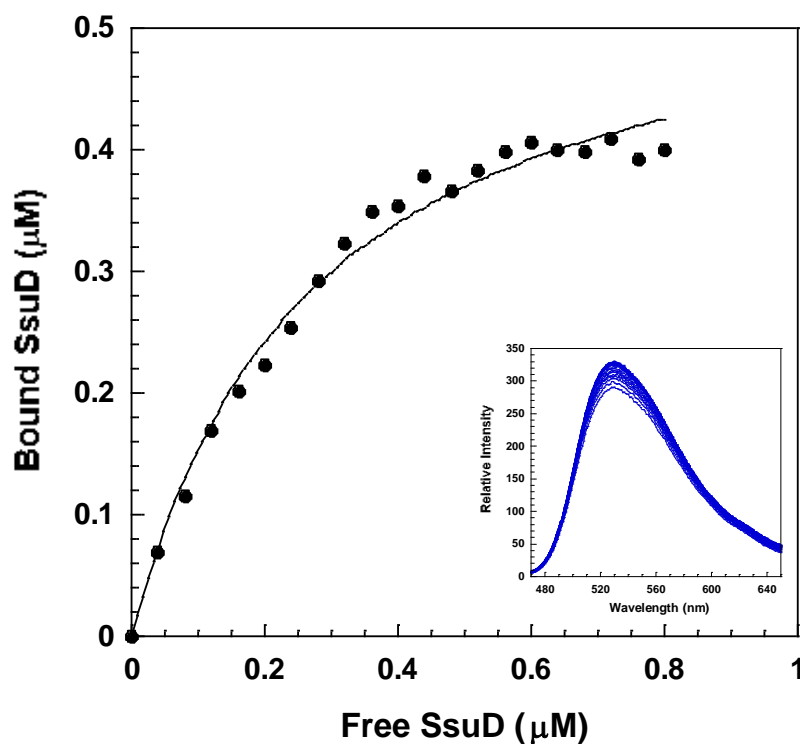


Figure 3.2 Binding affinity of FMN-bound SsuE to SsuD.

3.3.2 Oligomeric State of the SsuE-SsuD Complex Following Protein-Protein Interactions

Analytical ultracentrifugation (AUC) was performed to determine the molecular weight of the complex formed from the protein-protein interactions of SsuE and SsuD. Prior to the determination of the sedimentation value of the SsuE-SsuD complex, the oligomeric state of SsuD was determined before the addition of SsuE. The determination of the sedimentation value for SsuD was performed with two concentrations to account for the different ratios utilized in the presence of SsuE. The sedimentation value of SsuD was 7.75 ± 0.03 S (12 μ M) and 7.84 ± 0.01 S (6 μ M) which corresponded to a tetramer with molecular weights of 154 ± 3 kDa and 154 ± 4 kDa respectively (**Fig. 3.3, Table 3.1**). With the monomeric mass of 41.6 kDa for SsuD, the protein existed as a tetramer.

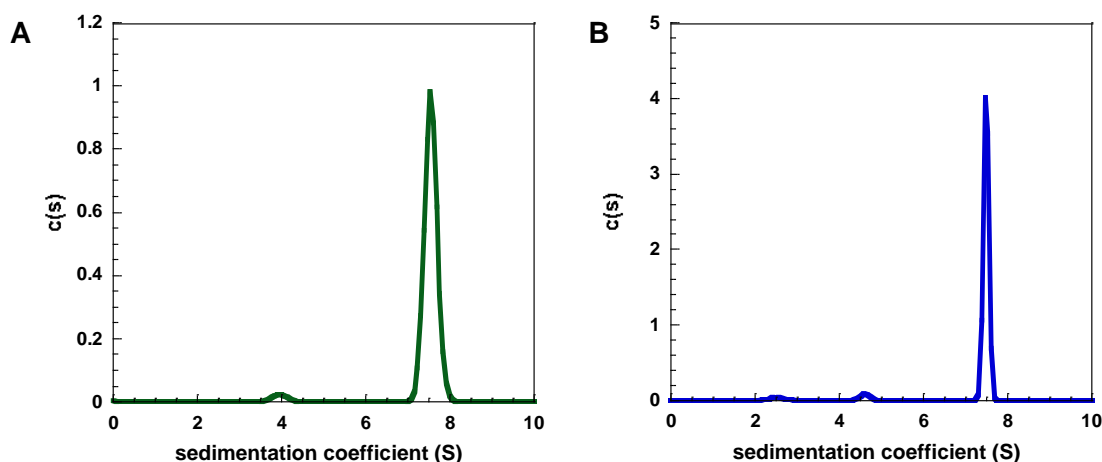


Figure 3.3: Sedimentation distribution plot of SsuD. AUC experiments were performed with SsuD at A) 6 μ M and B) 12 μ M. The reactions were performed in triplicate but only one fit is shown for clarity.

Table 3.1. Results from AUC analysis of SsuD at different concentrations.		
	SsuD (12 μ M)	SsuD (6 μ M)
$s_{20,w}$ (S)	7.75 ± 0.03	7.84 ± 0.01
Experimental MW (kDa)	154 ± 3	154 ± 4
Calculated MW (kDa)	166.6	166.6

Following the determination of the sedimentation value of SsuD, the oligomeric state of the protein complex was determined by utilizing an equimolar concentration of SsuE and SsuD (12 μ M). The four peaks observed gave an $s_{20,w}$ value of 2.9 ± 0.2 S, 4.6 ± 0.1 S, 7.7 ± 0.1 S, 11.2 ± 0.1 S (**Fig. 3.4A, Table 3.2**). The molecular weights were 37.2 ± 2.3 , 74.1 ± 3.5 , 159 ± 7.9 and 278.9 ± 17.2 kDa, respectively. These four peaks corresponded to the dimer of SsuE (peak 1), the tetramer of SsuE (peak 2), the tetramer of SsuD (peak 3) and the proposed SsuE-SsuD protein complex (peak 4). The SsuE-SsuD protein complex was calculated from the experimental molecular weight of SsuE (80.1 kDa) and SsuD (166.6 kDa), which would generate a protein complex of 246 kDa. The oligomeric conformation of the proposed SsuE-SsuD complex would be two dimers of SsuE binding the tetramer of SsuD. Further investigations were carried out similarly with a higher concentration of SsuE to SsuD (12 μ M:6 μ M). Similar results were observed which were comparable to sedimentation coefficients observed with a 1:1 molar ratio of SsuE to SsuD. However, there was more tetramer of SsuE formed at increased concentrations of SsuE compared to the amount of tetramer observed with equimolar concentrations of SsuE and SsuD (**Fig. 3.4B, Table 3.2**).

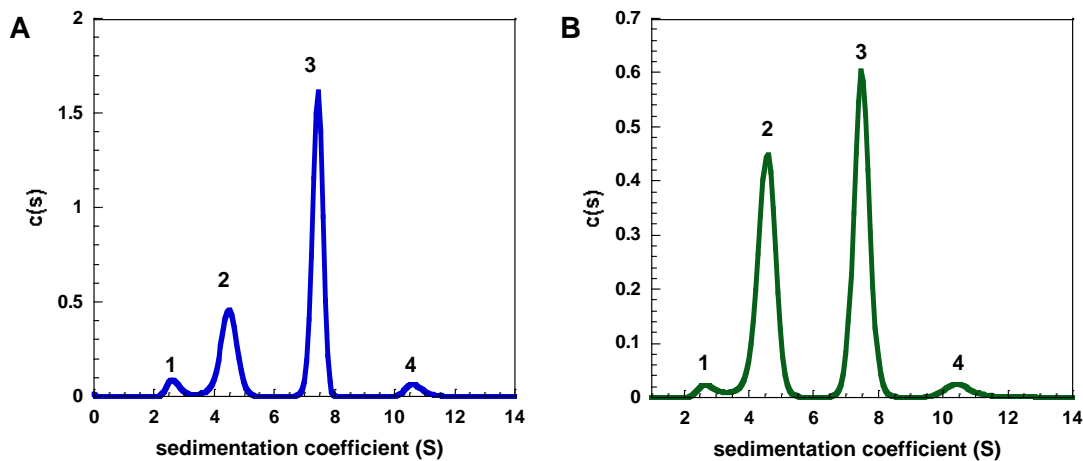


Figure 3.4: Sedimentation distribution plots of the SsuE-SsuD complex. A) SsuE-SsuD (12 μ M:12 μ M) B) SsuE-SsuD (12 μ M:6 μ M). AUC experiments were performed to determine the oligomeric state of the SsuE-SsuD complex at different concentrations of SsuE to SsuD (1:1, 2:1). The reactions were performed in triplicate but only one fit is shown for clarity.

Table 3.2. Results from AUC analysis of SsuE-SsuD complex.

	Peak 1	Peak 2	Peak 3	Peak 4
SsuE:SsuD (1:1) $s_{20,w}$ (S)	2.9 ± 0.2	4.6 ± 0.1	7.7 ± 0.1	11.2 ± 0.1
Molecular weight (kDa)	37.2 ± 2.3	74.1 ± 3.5	159.0 ± 7.9	278.9 ± 17.2
SsuE:SsuD (2:1) $s_{20,w}$ (S)	2.8 ± 0.1	4.7 ± 0.1	7.8 ± 0.1	11.1 ± 0.1
Molecular weight (kDa)	34.8 ± 0.9	74.6 ± 1.5	158.3 ± 2.5	268.9 ± 3.1

Further experiments were performed to monitor the oligomeric changes of SsuE with flavin and SsuD present. For these experiments, flavin addition was performed similarly to the determination of the oligomeric state of SsuE with flavin present. The AUC

analysis of the SsuE/flavin complex with SsuD gave four $s_{20,w}$ values of 3.3 ± 0.4 S, 4.6 ± 0.3 S, 7.77 ± 0.01 S, and 10.9 ± 0.3 S. The molecular weights for the sedimentation coefficients were 46.2 ± 9.2 , 77.2 ± 6.4 , 162.8 ± 7.3 and 269.6 ± 0.1 kDa, respectively. The four sedimentation coefficient peaks observed corresponded to the dimer and tetramer of SsuE (peak 1 and 2), the tetramer of SsuD (peak 3) and the proposed complex of SsuE and SsuD (peak 4) (**Fig. 3.5, Table 3.3**). Interestingly, the addition of flavin with SsuD present shifted the tetramer-dimer equilibrium of SsuE to favor an increase in the dimer species.

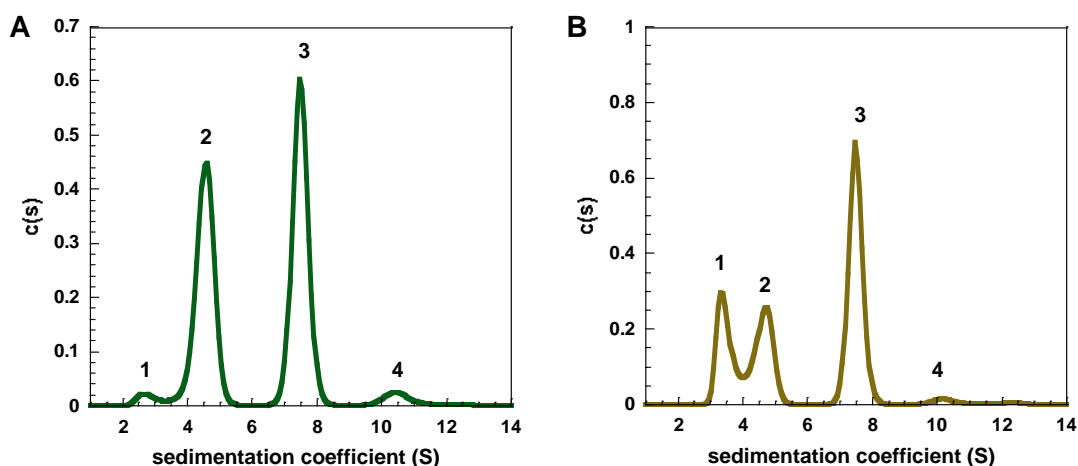


Figure 3.5: Sedimentation distribution plots of SsuE-SsuD complex without and with flavin. A) SsuE-SsuD (12 μ M:6 μ M). B) SsuE(FMN)-SsuD (12 μ M:6 μ M). AUC experiments were performed to determine the oligomeric state of the SsuE-SsuD complex without and with FMN.

Table 3.3. Results from AUC analysis of SsuE-SsuD complex without and with flavin present.

	Peak 1	Peak 2	Peak 3	Peak 4
SsuE:SsuD (2:1)	2.8 ± 0.1	4.7 ± 0.1	7.8 ± 0.1	11.1 ± 0.1
<i>s20,w</i> (S)				
Molecular weight (kDa)	34.8 ± 0.9	74.6 ± 1.5	158.3 ± 2.5	268.9 ± 3.1
SsuE(FMN):SsuD (2:1)	3.3 ± 0.4	4.6 ± 0.3	7.77 ± 0.01	10.9 ± 0.3
<i>s20,w</i> (S)				
Molecular weight (kDa)	46.2 ± 9.2	77.2 ± 6.4	162.8 ± 7.3	269.6 ± 0.1

3.4 Discussion

Reduced flavin is utilized by bacteria for a diverse range of biological processes. Flavoproteins utilize flavin either as a substrate or a cofactor for the reduction of oxidized flavin which serves as the reductive half-reaction. Canonical flavoproteins catalyze both the reductive and oxidative half-reactions with one enzyme active site. However, in two-component flavin-dependent systems, two separate enzymes carry out the reductive and oxidative half-reactions. The two-component alkanesulfonate monooxygenase systems are upregulated for sulfur acquisition when inorganic sulfate is limiting in the environment. The alkanesulfonate monooxygenase system is comprised of the flavin reductase which catalyzes the reduction and transfer of flavin and the monooxygenase which utilizes reduced flavin for the desulfonation of alkanesulfonates. This system utilizes several

unique structural features for the acquisition of sulfur. These different structural features are geared towards the efficient transfer of reduced flavin from the SsuE to SsuD for desulfonation to occur. Results from previous studies have revealed that the medium for reduced flavin transfer from SsuE to SsuD occurs through protein-protein interactions. The interactions sites in SsuE are located on the dimer interface where the π -helix is located while the interaction sites for SsuD are located close to the active site and separated by the dynamic loop. The insertional loop of SsuD has been observed to close over the active site to prevent the loss of reduced flavin to bulk solvent upon transfer from SsuE. Conformational changes have been reported in SsuD upon binding of reduced flavin and oligomeric changes have been observed with SsuE upon binding of oxidized flavin. However, oligomeric changes of SsuE in the presence of SsuD have not been explored and the stoichiometric ratio of the binding of SsuE to SsuD is not known.

The binding of SsuE to SsuD was investigated by fluorescence spectroscopy. There was an observed increase in relative intensity with the titration of FMN-bound SsuE to SsuD which reached saturation. The binding affinity was $0.26 \pm 0.03 \mu\text{M}$, indicating a strong interaction between SsuE and SsuD. The 1:1 stoichiometric ratio for monomeric binding supports a structural model where two dimers of SsuE bind the tetramer of SsuD. However, the effect of the oligomeric changes of SsuE is not yet known for the protein complex formed following reduced flavin transfer.

SsuE was observed to exist in a tetramer-dimer equilibrium in the presence of FMN and NADPH, with the tetramer of SsuE being the predominant form. However, the changes in the oligomeric state of SsuE has not been explored in the presence of SsuD. The oligomeric state of SsuD was determined to be a tetramer from sedimentation

velocity AUC studies. The molecular weight of the complex was determined with both SsuE and SsuD at different concentrations. At equimolar concentrations of SsuE and SsuD, four peaks were observed that corresponded to the tetramer-dimer equilibrium of SsuE, the tetramer of SsuD and the proposed SsuE-SsuD complex. The SsuE-SsuD complex arises because of protein-protein interactions between SsuE and SsuD which are critical for reduced flavin transfer. Similar peaks are observed at higher concentrations of SsuE in complex with SsuD, however more of the SsuE tetramer was formed. The addition of flavin shifted the tetramer-dimer equilibrium in favor of the dimer of SsuE but there was no apparent formation of more SsuE-SsuD protein complex. This may mean that the interaction sites of SsuE at the dimeric interface are made readily available for flavin transfer in the presence of flavin and SsuD.

Protein-protein interactions are utilized for the transfer of reduced flavin from SsuE to SsuD in the alkanesulfonate monooxygenase system. This medium of reduced flavin transfer safeguards reduced flavin from oxidation and ensures that it is deposited at the active site of SsuD for the desulfonation reaction to occur. The oligomeric changes exhibited by SsuE are pertinent for the exposure of protein-protein interaction sites to ensure that after flavin is reduced it is transferred to the monooxygenase. The presence of FMN or SsuD caused SsuE to exist in tetramer-dimer equilibrium, however the tetramer form was more predominant. The dimer-dimer interface of SsuE houses the protein interaction sites utilized for flavin transfer to SsuD and the π -helix. From the analytical ultracentrifugation results, the dimeric species was more predominant than the tetramer species in the presence of FMN and SsuD. The 1:1 stoichiometric ratio for monomeric binding between SsuE and SsuD suggests a structural model involving two dimers of

SsuE bound to a tetramer of SsuD (**Fig. 3.6**). The active site of SsuD is situated on the outside of each monomer which implies that SsuD would not need to undergo oligomeric changes to make this site available for flavin transfer. The dimers of SsuE cannot bind to two active sites of SsuD on the same surface in order not to interfere with the mobile loop that closes over the active site upon the binding of flavin. The results obtained suggest the importance of protein-protein interactions and the role of the oligomeric changes of SsuE in the efficient transfer of reduced flavin to SsuD. Future investigations will focus on increasing the concentration of SsuE to SsuD (4:1) as is implemented in coupled assays to determine the production of sulfite. The coupled assays are performed with a 3-fold SsuE to SsuD ratio to ensure the continued supply of reduced flavin for the desulfonation reaction. Also, the three-dimensional structure of the SsuE-SsuD complex would be determined without and with FMN to study the interactions and structural changes that are influenced by protein-protein interactions.

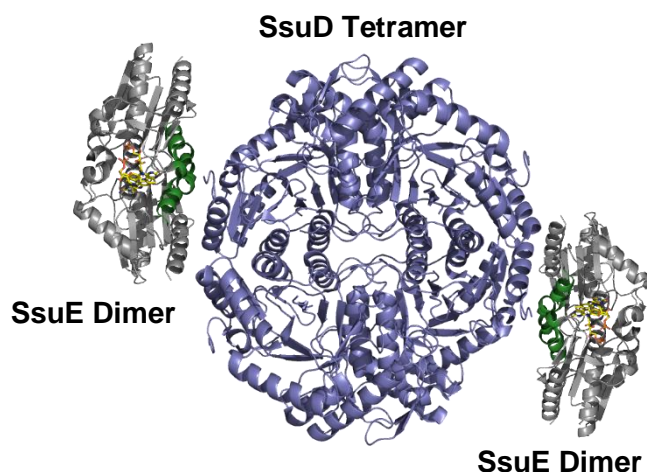


Figure 3.6: Proposed model for the formation of the protein complex between SsuE and SsuD.

CHAPTER FOUR

4 Transformation of a Canonical Flavoprotein to a Flavin-Free NADPH-FMN Reductase Through Mutations of the α -Helix

4.1 Introduction

Sulfur is an essential component of amino acids and cofactors required for the growth and survival of bacteria. However, the scarcity of inorganic sulfur in aerobic soils leads to the synthesis of specific proteins that can utilize organosulfonates to produce sulfite. The alkanesulfonate monooxygenase system is comprised of SsuE and SsuD that are involved in the desulfonation of alkanesulfonates for sulfur acquisition. The FMN reductase, SsuE relies on distinct structural features to catalyze the reduction and transfer of reduced flavin to SsuD.⁸⁸ SsuE belongs to the NADPH:FMN reductase family based on a flavodoxin fold common to these enzymes.⁸⁹ The reductases under this family are further subdivided based on the presence or absence of a π -helix. The π -helix is generated from the insertion of an amino acid into an established α -helix.⁸⁹ It has been found in 15% of proteins and provides functional advantages in different enzymes. Some of these advantages include introduction of catalytic residues or new active site properties that promote metal or cofactor binding.^{211–213}

SsuE utilizes flavin as a substrate and the π -helix has been proposed to contribute to the structural divergence from canonical FMN-bound reductases within the NADPH:FMN reductase family.⁸⁹ The π -helix observed in SsuE was proposed to be formed by the insertion of Tyr residue (Tyr118) into a conserved α -helix of canonical flavoproteins. Hydrogen bonding interactions have been observed between Tyr118 and the isoalloxazine ring of FMN across the tetrameric interface of SsuE. In addition, the

aromatic rings of Tyr118 in the π -helix of each monomer of SsuE forms π -stacking interactions at the tetrameric interface and these interactions stabilize the enzyme.²³³ Several variants of Tyr118 were generated and their three-dimensional structures determined to investigate the structural and functional roles of the π -helix. The Y118A SsuE variant was purified flavin bound and was converted to an α -helix like the FMN-bound members of the NADPH:FMN reductase family. The deletion variant, Δ Y118 SsuE was not purified with flavin bound. Although, the flavin bound to the Y118A SsuE variant was reduced as observed in reductive titrations, it was not oxidized in NADPH oxidase assays. Also, there was no measurable oxidase activity for the deletion variant, Δ Y118 SsuE.²³² Both variants, Y118A and Δ Y118 SsuE formed a dimer unlike wild-type SsuE, which exists as a tetramer. These variants were unable to form the tetramer due to the disruption of hydrophobic packing patterns observed in the wild-type enzyme. MsuE, the FMN reductase in the methanesulfinatase and methanesulfonate monooxygenase system is structurally similar to SsuE, however the insertional residue for the π -helix in MsuE is His126. Exchanging the π -helix insertional residue of both enzymes, SsuE (Y118H) and MsuE (H126Y) did not result in similar kinetic properties with their monooxygenase partners.²³¹ Furthermore, structure-based sequence analysis with other NADPH:FMN reductases showed the presence of a Tyr residue in a similar position in a canonical flavoprotein, chromate reductase (ChrR) as the Tyr118 insertional residue in SsuE. These results obtained from evaluating the structural and functional roles of the π -helix imply that the insertional residue is not solely responsible for the generation of the π -helix and additional structural attributes may be responsible for the gain in function provided by the π -helix in two-component FMN reductases.²³¹

Chromate reductase catalyzes the reduction of hexavalent chromium [Cr(VI)] to trivalent chromium [Cr(III)], and this reaction removes toxic chromium from the environment.³⁴⁴ Chromium exists in nine valence states ranging from -2 to +6.³⁴⁵ Of the different states, Cr (VI) and Cr (III) are the most stable forms in the environment.³⁴⁶ They are found in diverse bodies of water and wastewater. Hexavalent chromium is generated as a by-product of several industrial processes such as welding, chrome-plating, and pigment production.³⁴⁴ It is water soluble, toxic, a major environmental pollutant, and a serious threat to human health. Trivalent chromium is insoluble, less bioavailable, and less toxic compared to hexavalent chromium and it readily forms insoluble oxides/hydroxide above pH 5.5.^{346–348} The reduction from toxic hexavalent chromium to less toxic trivalent chromium by microorganisms serves to neutralize the effect of this form of chromium.³⁴⁹ Like SsuE, ChrR belongs to the NADPH:FMN reductase family but does not require a monooxygenase partner for catalysis.

ChrR and SsuE exist as tetramers and have a characteristic flavodoxin fold common to NADPH:FMN reductases (**Fig. 4.1**).^{89,321,322} However, the α 4-helix for SsuE is the π -helix, while that for ChrR is an α -helix and both enzymes have a tyrosine residue at similar positions but catalyze different reactions.²³¹ Clearly, the insertional residue, Tyr118 in SsuE is not enough to convert ChrR to a two-component reductase that can deliver reduced flavin to a monooxygenase. These studies aim to transform a canonical flavoprotein, ChrR, to a flavin-free reductase that supplies reduced flavin to a monooxygenase in the two-component FMN-dependent system. FMN reductases in two-component systems may have more structural adaptations that accounts for their increased functionality over canonical flavoproteins. Wild-type ChrR was purified, and

several variants were generated to investigate the conserved nature of the substitutions towards understanding the structural differences between ChrR and SsuE.

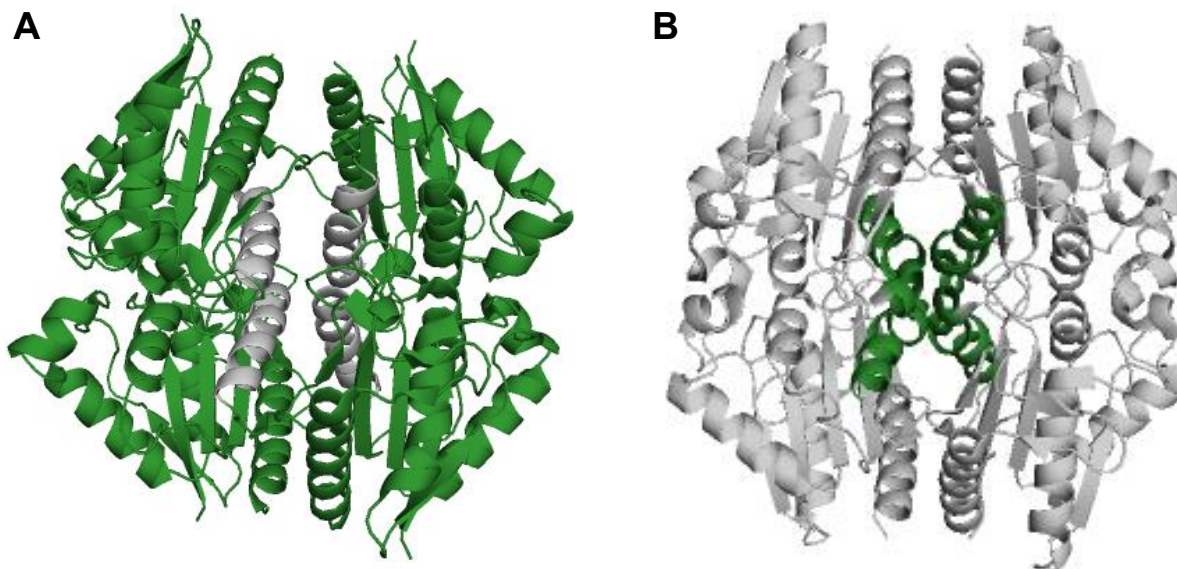


Figure 4.1: Tetramer of ChrR and SsuE. A) The three-dimensional structure of wild-type ChrR, a canonical flavoprotein is a tetramer, with the α -helix (gray) at the tetramer interface. B) The three-dimensional structure of wild-type SsuE, a two-component flavin reductase is a tetramer with the π -helix (green) at the tetramer interface. The structures were rendered with Pymol using Protein Data Bank entries 3SVL (ChrR) and 4PTY (SsuE). (Adapted from^{233,327}).

4.2 Materials and Methods

4.2.1 Materials

All chemicals and reagents were purchased from Sigma-Aldrich, Fischer, or Bio Rad. *Escherichia coli* strain (XL-1 and BL21 (DE3)) was purchased from Stratagene (La Jolla, CA). Plasmid vectors and pET21a were obtained from Novagen (Madison, WI). DNA primers were synthesized by Invitrogen (Carlsbad, CA). Slide-a-lyzer dialysis cassettes were purchased from Thermo Scientific (Rockford, IL). Phenyl Sepharose column matrix was purchased from Amersham Biosciences (Piscataway, NJ). All UV-vis absorbance spectra were recorded utilizing an Agilent Technologies diode-array spectrophotometer (model HP 8453) equipped with a thermostatted water bath.

4.2.2 Construction of ChrR Variants

Variants of ChrR were generated using the pET21a plasmid containing the *chrR* gene from *E. coli*. Primers to construct the Q132P and Q127D ChrR variants were designed as 27-base oligonucleotides substituting the CAG Gln codon for CCG (Pro) and GAT (Asp) codons, respectively. The Qiagen kit plasmid purification protocol was utilized to prepare the ChrR plasmid for site-directed mutagenesis. The double variant, Q132P/127D ChrR was made by using the plasmid containing the Q132P ChrR variant and the primers for Q127D ChrR. The variants were confirmed by DNA sequencing analysis (Eurofins/Genomics, Louisville, KY). Confirmed variants were transformed into *E. coli* BL21 (DE3) and XL-1 competent cells for protein expression and storage at -80 °C.

Chromate reductase, ChrR and the variants were expressed in *E. coli* strain BL21(DE3) following protocols previously described for SsuE.¹⁷⁰ The only exception was the double variant, Q132P/127D ChrR, which was purified with only the macro-prep high Q column and eluted with a 100 – 500 mM NaCl gradient in 25 mM potassium phosphate (pH 7.5). Protein fractions of the ChrR enzymes were selected based on the UV-visible absorbance at 280 nm and purity following analysis on 12% SDS-PAGE. Wild-type and Q132P ChrR were purified flavin bound; however, Q127D and Q132P/127D ChrR were purified flavin free. The concentrations of ChrR enzymes were determined at A280 using a molar extinction coefficient of 11.3 mM⁻¹ cm⁻¹ for ChrR.³²² After purification, the proteins were frozen and stored in -80 °C.

4.2.3 Circular Dichroism Spectroscopy of Wild-Type and the Variants of ChrR

Circular dichroism (CD) spectroscopy was performed with wild-type and variants of ChrR to investigate if the substitutions affected the secondary structure of the enzyme. The spectra were obtained with 5 μM of each protein in 10 mM potassium phosphate buffer (pH 7.5). CD spectra was recorded on a Jasco (Easton, MD) J-810 spectropolarimeter. The experiments were performed at 25 $^{\circ}\text{C}$ using a 0.1 cm path length cuvette. Measurements were performed at 1 nm increments between 300 to 185 nm with a scanning speed of 50 nm/min and a bandwidth of 1 nm. An average of eight scans were performed for each protein sample. Background correction was performed using the default parameters of the Jasco J-720 software.²⁰⁵

4.2.4 Kinetic Properties of Wild-Type and ChrR Variants

NADH oxidase assays for ChrR and MsuE were performed to compare their steady-state kinetic properties. The oxidase activity of flavin-bound ChrR or MsuE (0.1 μM) were obtained with varying concentrations of FMN (0.1 – 1.5 μM) and 200 μM NADH in 25 mM Tris-HCl (pH 7.5) and 0.1 M NaCl at 25 $^{\circ}\text{C}$. Electron transfer to ferricyanide was performed with wild-type and ChrR variants (0.1 μM), varying concentrations of ferricyanide (10 – 400 μM) at fixed concentrations of FMN (10 μM) and NADH (150 μM) in 25 mM Tris-HCl (pH 7.5) and 0.1 M NaCl at 25 $^{\circ}\text{C}$.^{232,233} Initial rates for the NADH oxidase and ferricyanide assay were obtained by monitoring the decrease in absorbance at 340 nm following the oxidation of NADH. Oxidase and ferricyanide assays were performed for Q132P ChrR, Q127D ChrR and Q132P/127D ChrR similar to wild-type ChrR. All assays were performed in triplicate and the steady state kinetic parameters were obtained by fitting the data to the Michaelis-Menten equation.

The steady state coupled assay was performed by monitoring the desulfonation of octanesulfonate as previously described.¹⁸⁹ The reaction was initiated with the addition of 500 μ M NADPH to a reaction mixture containing wild-type SsuE, wild-type ChrR or the ChrR variants (0.6 μ M), SsuD (0.2 μ M), FMN (2 μ M), and varying concentrations of octanesulfonate (10 - 1000 μ M) in 25 mM Tris-HCl (pH 7.5) and 0.1 M NaCl at 25 °C. Coupled assays with SsuE and SsuD were also performed as controls. The reaction was quenched after 3 min with 8 M urea, and the sulfite product was quantified at 412 nm as previously described.¹⁸⁹ All assays were performed in triplicate and steady-state kinetic parameters were evaluated by fitting the data to the Michaelis-Menten equation.

4.2.5 Deflavination of Wild-Type and Q132P ChrR

Deflavination of wild-type and Q132P ChrR was performed with the addition of 25 mM potassium phosphate (pH 7.5), 10% glycerol, and 3 M potassium bromide (500 μ L) to 1 mL of flavin-bound ChrR (245 μ M) or Q132P ChrR (157 μ M) in 25 mM potassium phosphate (pH 7.5), 0.1 M NaCl, and 10% glycerol. While the solution was swirled in an ice bath, 1 mL of precooled acidified ammonium sulfate solution (3 M, pH 1.5) was added to wild-type ChrR or Q132P ChrR solution dropwise for 20 s. After the mixture had been continuously stirred for an additional 40 s, the protein was precipitated with 6 mL of the acidified ammonium sulfate solution (3 M, pH 1.5). The precipitated protein solution was centrifuged at 7800 rpm for 10 min at 4 °C and was redissolved in a 1 mL volume of 25 mM potassium phosphate (pH 7.5), 0.1 M NaCl, and 10% glycerol.³⁵⁰ Deflaminated wild-type and Q132P ChrR (1 mL) was dialyzed against 1 L of 25 mM potassium phosphate (pH 7.5), 0.1 M NaCl, and 10% glycerol for 3 hours followed by a second overnight dialysis using a slide-a-lyzer dialysis cassette (Thermo Scientific). The final concentration of

deflavinated wild-type and Q132P ChrR was 85 μM and 43 μM , resulting in a 35% and 30% yield respectively.

4.2.6 Fluorimetric Titrations of Wild-Type and Variants of ChrR

Fluorometric titrations with FMN were performed to evaluate how the binding affinity of wildtype and the variants of ChrR was affected by the substitutions. Flavin binding to wild-type ChrR and the variants were monitored on a Cary Eclipse Agilent (Santa Clara, CA) fluorescence spectrophotometer with an excitation wavelength at 280 nm and emission wavelength at 344 nm.²⁰⁵ After deflavination, a 1.0 mL solution of wild-type and Q132P ChrR (0.1 μM) in 25 mM potassium phosphate (pH 7.5) and 0.1 M NaCl was titrated with FMN (0.01 - 0.2 μM). Due to the differences in the binding affinity, the concentration of flavin was increased (0.022 - 0.44 μM) for the Q127D ChrR variant. For all fluorometric titrations, the fluorescence spectrum was recorded following a 2 min incubation after each addition of FMN. The K_d value was determined as previously described using the single-site binding equation.^{189,205}

4.2.7 Native PAGE of Wild-Type and Variants of ChrR

Native PAGE experiments were performed with wild-type and the variants of ChrR to determine the oligomeric state of the proteins. The gel was composed of a 5% stacking gel, 12% resolving gel without SDS and Tris-glycine running buffer. Aliquots of the proteins (wild-type ChrR (40 μM), Q132P ChrR (40 μM) and Q127D ChrR (50 μM)) were mixed with native sample buffer to a total volume of 15 μL . The gels were run at 120 V for 4 hours at 4 °C. Protein bands were visualized using Coomassie brilliant blue staining

and the molecular weight of protein samples were compared to stoke radius of protein gel standards.

4.2.8 Proteolytic Susceptibility of Wild-Type and Q127D ChrR

The susceptibility of wild-type and Q127D ChrR to proteolysis was investigated with trypsin at room temperature.^{188,192} Samples of wild-type and Q127D ChrR (24 μ M) were treated with 10 μ g/mL TPCK-treated trypsin in 200 mM ammonium bicarbonate/1 mM calcium chloride reaction buffer (pH 8.4). After the addition of trypsin, 10 μ L aliquots of the reaction mixture was taken at 5, 10, and 15 mins and immediately added to 2 μ L PMSF in isopropanol (6 mg/mL) to quench the reaction. The degree of proteolysis for each sample was analyzed by 12% SDS-PAGE.

4.2.9 Flavin Loading of Wild-Type and Q132P ChrR

Wild-type and the ChrR variants were flavin-loaded because flavin-bound to the enzyme may have been lost during purification. Samples of wild-type and ChrR variants (100 μ M) at 800 μ L were loaded at a flavin concentration (200 μ M) two times the concentration of the protein sample to a total volume of 1 mL. The flavin loaded samples were dialyzed for 3 hours followed by a second dialysis overnight in a slide-a-lyzer dialysis cassette (Thermo Scientific). A Bradford assay was utilized to determine the concentration of wild-type and the ChrR variants and the amount of flavin bound was calculated from the A450 values after dialysis. The standard curve used in the Bradford assay was generated with varying concentrations of SsuE between 0.05 and 0.4 μ M. The percentage flavin bound after dialysis was obtained from the concentration of enzyme at A280 and the concentration of flavin bound after dialysis at A450.

Ferricyanide assays were performed with flavin-loaded wild-type and Q132P ChrR. Electron transfer to ferricyanide was performed with wild-type and Q132P ChrR (0.1 μ M), varying concentrations of ferricyanide (20 – 400 μ M) for wild-type and (10 – 400 μ M) for Q132P ChrR with fixed concentrations of FMN (10 μ M) and NADH (150 μ M) in 25 mM Tris-HCl (pH 7.5) and 0.1 M NaCl at 25 °C. Initial rates for the ferricyanide assay were obtained by monitoring the decrease in absorbance at 340 nm following the oxidation of NADH. All assays were performed in triplicate and the steady state kinetic parameters were obtained by fitting the data to the Michaelis-Menten equation.

4.3 Results

4.3.1 Site-Directed Mutagenesis and Purification of Wild-Type and Variants of ChrR

The π -helix present in SsuE is generated as a result of a Tyr118 insertion in an α -helix resulting in a bulge at the site of insertion.⁸⁹ Previous studies revealed that the insertional residue Tyr118 in SsuE is not fully responsible for the formation of the π -helix.^{231,233} A similar Tyr residue was present in ChrR which is not capable of catalyzing the transfer of reduced flavin to a monooxygenase. These observations imply that additional structural adaptations in the SsuE enzyme could be responsible for the differences between ChrR and SsuE. Utilizing structure-based sequence analysis of FMN reductases and a canonical flavoprotein, variants of the canonical flavoprotein, ChrR, were generated to investigate if certain conserved residues in FMN reductases were responsible for the structural differences between ChrR and SsuE (**Fig. 4.2**). The Q132P ChrR variant was generated because proline residues often signal the end of the π -helix. The Q127D ChrR variant was generated because aspartate residues are conserved in several two-component FMN reductases. The double variant, Q132P/127D ChrR was

generated to determine the effects of both substitutions in the conversion of a canonical flavoprotein to a two-component reductase.

SsuE	104	PLATGGTVAHLLAV	DY	ALK	PVLSALKAQEILH	135
EmoB	107	PLATGGSPAHLVLA	DY	GLR	PVLHSMGVRHVQ	138
MsuE	111	LAATGGTERHALVL	DH	QLR	PLFSFFQAITLPI	142
SfnF	113	LAATGGSERHALMI	DH	QLR	PLFAFFQAHTLPY	144
ChrR	113	IQTSSMGVIGGAR	QY	HLR	QILVFLDAMVMNK	144

Figure 4.2: Structure-based sequence analysis of the $\alpha 4$ helix of NADPH:FMN reductases. SsuE (*E. coli*), EmoB (EDTA-degrading bacterium BNC1), MsuE (*P. aeruginosa*), SfnF (*P. putida*), and a canonical flavoprotein, ChrR (*E. coli*). Copyright © 2018 The Protein Society.

Wild-type and variants of ChrR were expressed and purified in *E. coli* following previously described protocols.¹⁷⁰ Wild-type and Q132P ChrR variant were purified FMN-bound while Q127D ChrR and Q132P/127D ChrR were purified flavin free similar to wild-type SsuE. There was a signature flavin spectrum for the flavin-bound enzymes at A450. CD spectroscopy was utilized to determine if the substitutions in ChrR resulted in a change in the secondary structure of the protein. The CD spectra of Q132P ChrR and Q127D ChrR were similar but different from the wild-type enzyme. The difference could be because of a drop in concentration after purification with the concentration of wild-type ChrR being higher than that of the variants. These differences resulted in more protein being utilized for the CD measurements and more glycerol may have caused the change observed in the CD spectra of Q127D and Q132P ChrR. However, there was a significant change in the spectrum of the double variant, Q132P/127D ChrR indicating that its secondary structure may have been compromised (**Fig. 4.3**).

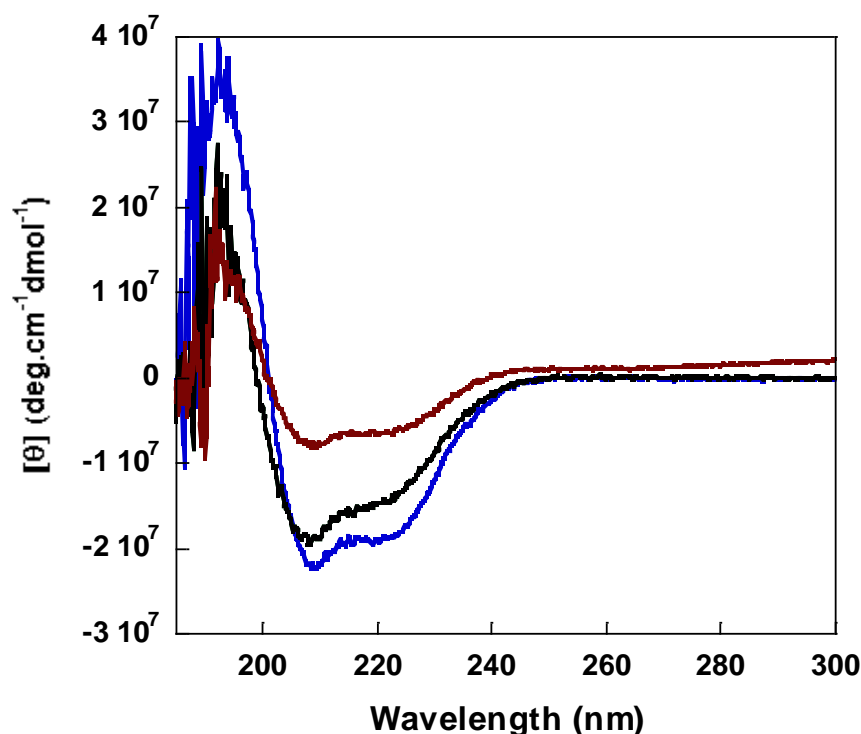


Figure 4.3: The far-UV circular dichroism spectra of wild-type and variants of ChrR. Wild-type ChrR (blue), Q132P ChrR (Green), Q127D ChrR (black), Q132P/127D ChrR (red).

4.3.2 Steady-State Kinetic Properties of Wild-Type and Variants of ChrR

NADPH oxidase assays were performed with wild-type and ChrR variants to determine if the substitutions affected the ability of the enzyme to catalyze the transfer of electrons to oxygen. Neither wild-type nor the ChrR variants showed any measurable oxidase activity. However, in ferricyanide assays, wild-type and Q132P ChrR were capable of transferring electrons to ferricyanide (**Fig. 4.4**). The k_{cat} and K_{m} values for ChrR ($105 \pm 7 \text{ s}^{-1}$, $69 \pm 13 \text{ }\mu\text{M}$) and Q132P ChrR ($11 \pm 1 \text{ s}^{-1}$, $4 \pm 1 \text{ }\mu\text{M}$) were different by about 10-fold. However, they showed comparable $k_{\text{cat}}/K_{\text{m}}$ values (ChrR, $2.8 \pm 0.7 \text{ }\mu\text{M}^{-1} \text{ s}^{-1}$ and

Q132P ChrR, $1.5 \pm 0.3 \mu\text{M}^{-1} \text{s}^{-1}$) (**Table 4.1**). There was no detectable activity in the ferricyanide assays with the Q127D and Q132P/127D ChrR variants. The amount of flavin contained in wild-type and ChrR variants was low, and this could hinder efficient transfer of electrons in the ferricyanide assays. Flavin loading was performed, followed by dialysis and this resulted in an increase in flavin bound (50%) in wild-type ChrR, Q132P ChrR and Q127D ChrR (**Table 4.2**). However, there was no increase in activity for ChrR and Q132P ChrR in ferricyanide assays after flavin loading (**Table 4.3**).

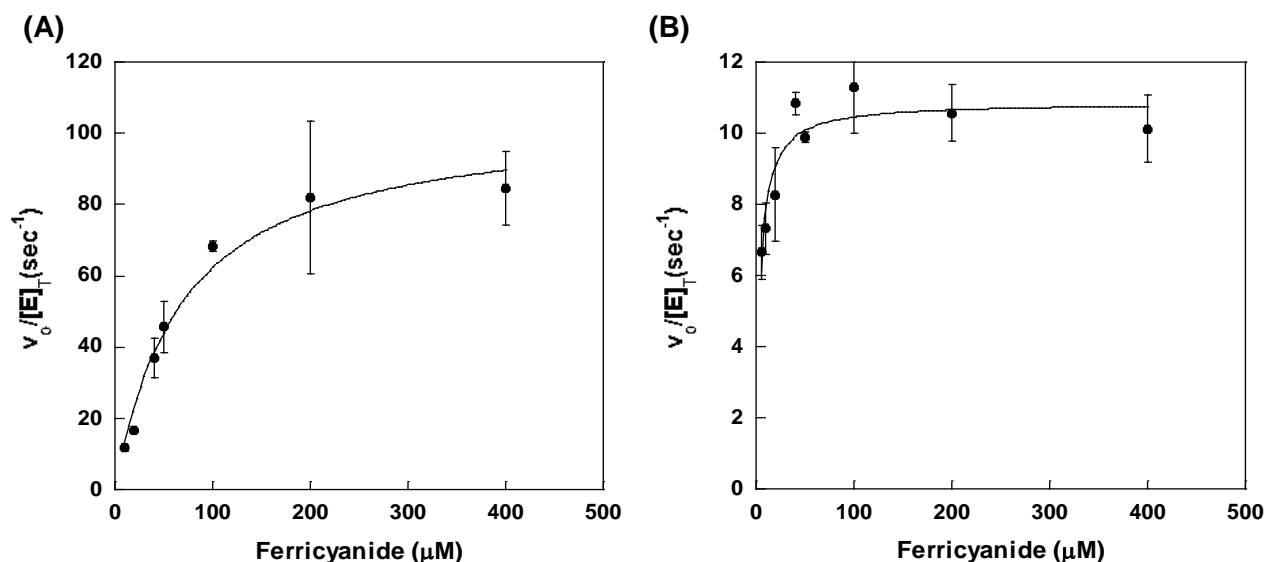


Figure 4.4: Steady-state kinetic plots of wild-type and Q132P ChrR with ferricyanide. a) Kinetic plots of the initial velocities of wild-type ChrR with varying ferricyanide concentrations. b) Kinetic plot of the initial velocities of Q132P ChrR with varying ferricyanide concentrations. The traces are an average of three separate experiments. Steady-state parameters were obtained by fitting the data to the Michaelis-Menten equation.

Table 4.1. Steady-state kinetic parameters for wild-type and variants of ChrR measuring ferricyanide activity.

Flavin Reductase Assay Varying Ferricyanide	k_{cat} (s ⁻¹)	K_m (M, x 10 ⁻⁶)	k_{cat}/K_m (M ⁻¹ s ⁻¹ , x 10 ⁴)	$K_d(FMN)$ (nM)
Wild-type MsuE	19 ± 1	6 ± 2	3.4 ± 1.1	5 ± 2
Wild-type ChrR	105 ± 7	68 ± 13	1.5 ± 0.3	46 ± 7
Q132P ChrR	11 ± 1	4 ± 1	2.8 ± 0.7	69 ± 12
Q127D ChrR ^a	-	-	-	330 ± 63
Q132P/127D ChrR ^a	-	-	-	-

^a Values could not be determined within the experimental conditions.**Table 4.2.** Amount of flavin bound after flavin loading of ChrR and variants.

	Percentage Flavin bound before dialysis	Percentage Flavin bound after dialysis (1:2)
Wild-type ChrR	5%	50%
Q132P ChrR	8%	50%
Q127D ChrR	10%	50%
Q132P/127D ChrR ^a	-	-

^a No observable data under normal conditions**Table 4.3.** Steady-state kinetic parameters for wild-type and variants of ChrR measuring ferricyanide activity after flavin loading.

Flavin Reductase Assay Varying Ferricyanide	k_{cat} (s ⁻¹)	K_m (M, x 10 ⁻⁶)	k_{cat}/K_m (M ⁻¹ s ⁻¹ , x 10 ⁴)
Wild-type ChrR	438 ± 101	331 ± 133	1.3 ± 0.5
Q132P ChrR	160 ± 19	103 ± 30	1.6 ± 0.3

Canonical flavoproteins transformed to two-component FMN reductases should be able to catalyze the transfer of reduced flavin to the monooxygenase for the oxygenolytic cleavage of alkanesulfonates and sulfite production. Coupled assays were performed to evaluate the ability of wild-type ChrR and the variants to catalyze the desulfonation of alkanesulfonates. There was no measurable activity observed with either ChrR or the variants in coupled assays evaluating the production of sulfite with SsuD.

4.3.3 Substrate Binding Studies of Wild-Type and Variants of ChrR

Prior to the determination of the binding affinities of ChrR and the different variants, deflavination of wild-type and Q132P ChrR were performed to remove any flavin bound. (Table 4.1). However, Q127D and Q132P/127D ChrR were purified flavin free. Wild-type and Q132P ChrR showed high binding affinity for oxidized flavin comparable to SsuE; however, Q127D ChrR showed a 10-fold decrease in the binding affinity compared to wild-type ChrR (Fig. 4.5). However, the Q132P/127D ChrR variant had no measurable binding affinity for oxidized flavin.

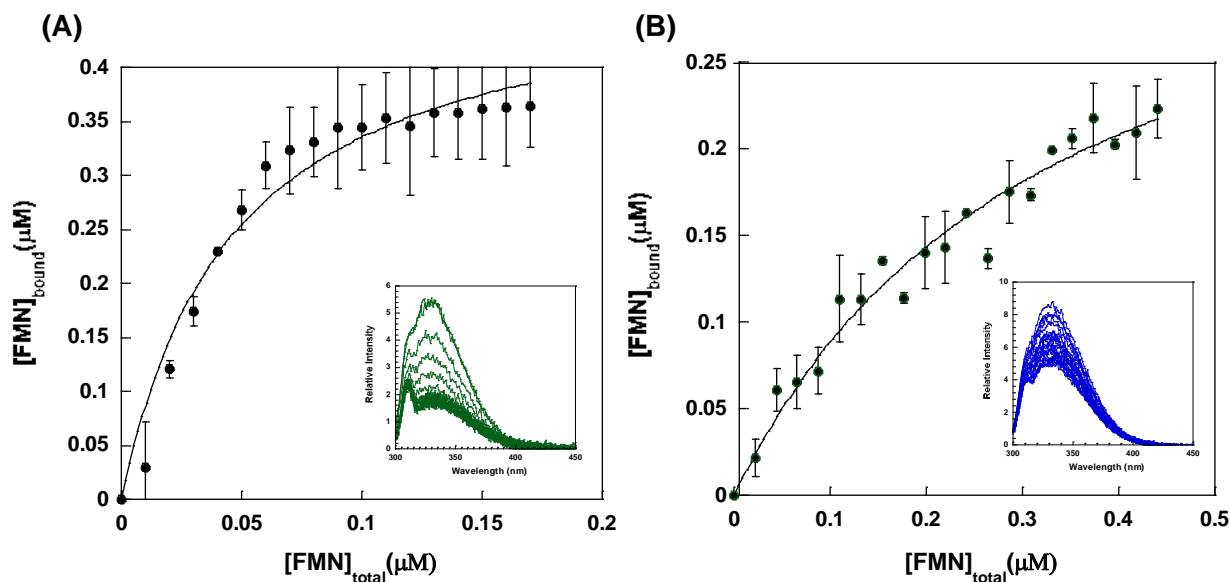


Figure 4.5: Fluorescent titrations of wild-type and Q127D ChrR with FMN. A) Titration of ChrR (0.1 μM) with FMN (0.01 – 0.2 μM; ex, 280 nm; em, 342 nm). B) Titration of Q127D (0.1 μM) with FMN (0.022 – 0.4 μM; ex, 280 nm; em, 342 nm).

4.3.4 Native PAGE Electrophoresis and Proteolytic Susceptibility of Wild-Type and Variants of ChrR

Native PAGE electrophoresis was performed to determine the molecular weight of wild-type and the ChrR variants in their native form. Results from previous studies have established that wild-type ChrR exists as a tetramer similar to most NADPH:FMN reductases. Wild-type ChrR was observed as a high molecular weight protein similar to Q127D ChrR; however, Q132P ChrR had a higher molecular weight when compared to either of the two proteins. This higher molecular weight band was also observed in wild-type and Q127D ChrR variant (**Fig. 4.6**).

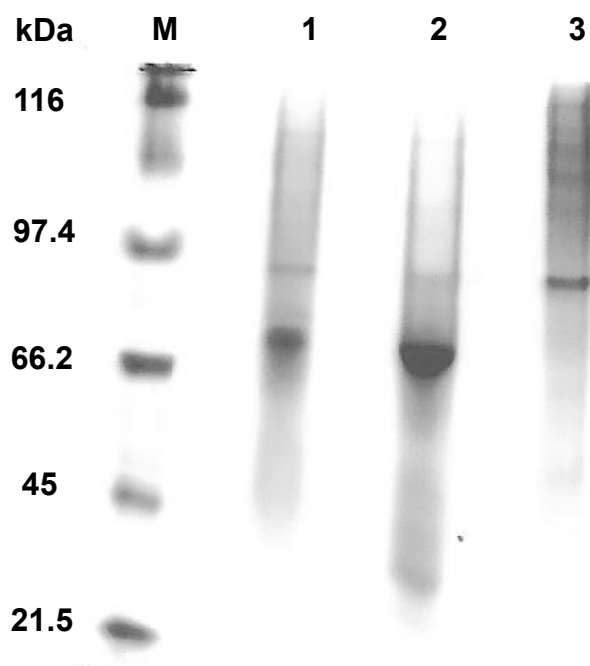


Figure 4.6: Native PAGE analysis of wild-type and variants of ChrR. Gel lanes: molecular weight marker (M), wild-type ChrR (lane 1), Q127D ChrR (lane 2), Q132P ChrR (lane 3). The proteins were separated on 12% native PAGE.

While there was no measurable activity in ferricyanide assays for Q127D ChrR, this variant was able to bind flavin albeit with a lower binding affinity compared to wild-type ChrR. The susceptibility of Q127D ChrR to proteolytic cleavage was assayed and compared to the wild-type enzyme. For analysis, aliquots of the reaction mixtures were withdrawn and quenched with PMSF at specific time points. From PAGE, showing time-dependent proteolysis, Q127D ChrR appeared to be rapidly digested with no protein left at the 5 min mark; however, ChrR was slowly digested over 15 mins (**Fig. 4.7**).

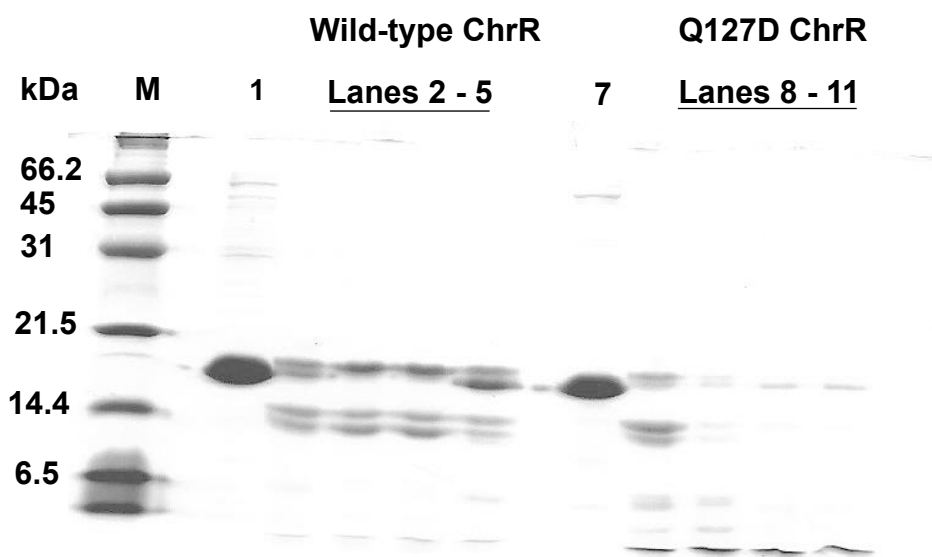


Figure 4.7: Proteolytic susceptibility of wild-type and Q127D ChrR variant. Gel lanes: molecular weight marker (M), wild-type ChrR standard (lane 1), Q127D ChrR standard (lane 7), aliquots were removed and quenched with PMSF after 0 s (lanes 2 and 8), 5 min (lanes 3 and 9), 10 min (lanes 4 and 10), 15 min (lanes 5 and 11).

4.4 Discussion

Two-component FMN-dependent systems are utilized for the acquisition of sulfur when inorganic sulfate is limiting in the environment. Acquisition of sulfur from

organosulfonates is enabled when sulfur starvation proteins are upregulated in response to limiting inorganic sulfur concentrations. Two-component systems under the sulfur starvation response utilize a broad range of substrates for sulfur acquisition. These systems comprise an NADPH:FMN-dependent reductase, that catalyzes the reduction of flavin and a monooxygenase that utilizes reduced flavin for the oxygenolytic cleavage of organosulfonates producing sulfite and the corresponding aldehyde.^{88,147} Two-component NADPH:FMN reductases belong to the flavodoxin-like superfamily based on a flavodoxin fold. They are further classified based on the difference in a conserved α -helix specific for canonical flavoproteins which for two-component reductases is π -helix. Two-component FMN-dependent reductases that possess the π -helix include, SsuE, MsuE and SfnF.²³¹

The π -helix is conserved among NADPH:FMN reductases and is associated with a gain in function and new catalytic roles. It is characterized by an insertional amino acid residue into an α -helix causing a bulge at the site of insertion. The insertional residue in the π -helices of SsuE, MsuE and SfnF are Tyr118, His126 and His128 respectively.²³¹ In SsuE, the π -helix is located at the tetramer interface where it forms aromatic π -stacking interactions.²³³ The π -helix is proposed to be involved in flavin transfer. A network of hydrogen bonds between the insertional residue in the π -helix of SsuE and FMN across the tetrameric interface may play a role in the oligomeric changes exhibited by SsuE.²³³ These oligomeric changes of SsuE facilitate flavin reduction and transfer to SsuD. Results from previous studies investigating the integrity of the π -helix in SsuE showed that Tyr118 cannot be the only structural adaptation responsible for the difference in catalysis between two-component FMN reductases and canonical flavoproteins within the

NADPH:FMN family. Structure-based sequence analysis reveals several conserved residues in the two-component FMN reductases which are not present in canonical flavoproteins such as ChrR.²³¹

Chromate reductase, a quinone reductase in *E. coli* is an FMN reductase with a similar flavodoxin fold as NADPH:FMN reductases and an α 4-helix that is structurally distinct from those present in two-component FMN reductases.²³¹ However, a tyrosine residue in SsuE was found in ChrR at a similar position and ChrR does not require a monooxygenase partner as SsuE to catalyze the reduction of hexavalent chromium to trivalent chromium.³²¹ Substitutions of two glutamine residues near Tyr128 of ChrR were generated in equivalent positions as the proline and aspartic acid residues in the conserved π -helical region of several two-component reductases. The variants, Q132P, Q127D and Q132P/127D ChrR were generated to evaluate their ability to catalyze the transfer of flavin (**Fig. 4.8**). Q132P and Q127D ChrR showed similar CD spectra which overlapped; however, the spectra of these variants were different from that of the wild-type enzyme. This difference may be due to the higher volume of the variants which contained more glycerol utilized for CD spectroscopy as compared to wild-type ChrR. However, there was a significant difference between the spectra of wild-type ChrR and Q132P/127D ChrR, which might explain the loss of activity in every assay utilized to investigate the role of these residues in the conserved nature of the π -helix. The molecular weight of wild-type and Q127D ChrR were comparable; however, a higher molecular weight oligomer was observed with the Q132P ChrR variant. The higher molecular weight conformer in Q132P ChrR is also present in wild-type and Q127D ChrR.

This could mean that Q132P ChrR may be a different oligomer from the dominant species in wild-type ChrR.

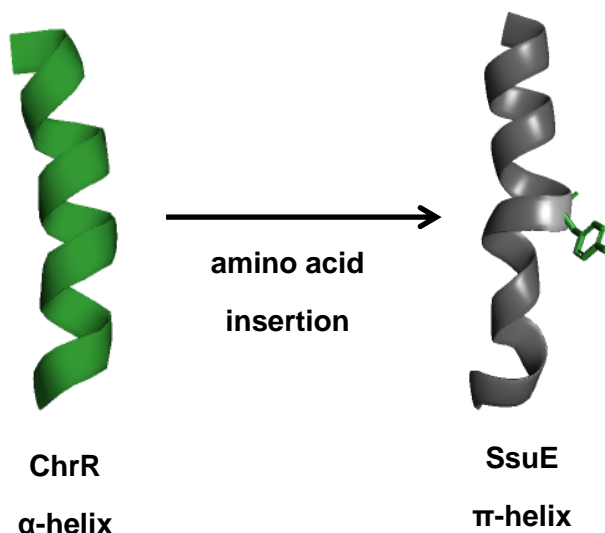


Figure 4.8: Comparison of the α -helix of the canonical flavoprotein, ChrR from *E. coli* to the π -helix in two-component FMN reductase, SsuE from *E. coli*. SsuE belongs to the NADPH:FMN reductase family and has a π -helix that is generated by the insertion of Tyr118 into a α -helix resulting in a bulge. The insertional residue is not present in the α -helix of ChrR. The structures were rendered with Pymol using Protein Data Bank entries 3SVL (ChrR) and 4PTY (SsuE).

Wild-type and Q312P ChrR were purified flavin-bound; however, Q127D and Q132P/127D ChrR were purified flavin free. Two-component FMN-dependent reductases utilize reducing equivalents from NAD(P)H for the reduction of flavin. There was no measurable NADH oxidase activity with wild-type ChrR and any of the variants. NADH oxidase activity is not easily determined for wild-type ChrR because FMN stays reduced and protected from oxidation in the absence of hexavalent chromium. However, the absence of measurable reductase activity for Q132P ChrR could be because it was purified flavin-bound similar to wild-type ChrR. Although the Q127D ChrR variant was purified flavin free, it had no observable oxidase activity. Clearly, changing the glutamine residue to an aspartic acid residue did not cause this variant to act differently from the

wild-type enzyme. If the ChrR variants caused a switch from the α -helix in ChrR to a π -helix, there would be enzymatic activity in NADH oxidase assays as observed for wild-type SsuE. The activity of wild-type ChrR and the variants were measured with ferricyanide assays. Ferricyanide assays were performed because ferricyanide can access the activity site of wild-type ChrR for electron transfer. Wild-type ChrR had comparable ferricyanide activity with the Q132P ChrR variant. However, ferricyanide activity could not be monitored with the Q127D and Q132P/127D ChrR variants. This absence of ferricyanide activity can be attributed to the disruption of the flavin binding site in Q127D ChrR and the loss of secondary structure observed in CD spectroscopy for the double variant.

Changes in secondary structure observed for the double variant, Q132P/127D ChrR may explain its inability to catalyze the transfer of electrons to ferricyanide. The absence of steady-state activity in ferricyanide assay with the Q127D ChrR variant may be due to the differences in polarity with the substitution of a glutamine residue (Q127) with an aspartic acid residue and eventual disruption of the near-by hydrogen bonding interactions of Tyr128 with FMN across the tetrameric interface of ChrR. In the tetramer of ChrR, the dimers interact by a pair of two hydrogen binding networks involving Tyr128 and Glu146 of one dimer and Arg125 and Tyr85 of the other. The hydrogen bonding network of Arg125 and Tyr85 extends to the FMN cofactor and Tyr128 is closer to the FMN of the other dimer (8.4 Å) than the FMN of its own dimer (14.1 Å).³²¹ Similar hydrogen binding interactions are observed between the hydroxyl group of Tyr118 and the carbonyl oxygen of Ala78 across the tetramer interface in SsuE. The amide group of Ala78 forms hydrogen bonding interactions with the C4 carbonyl oxygen of the

isoalloxazine ring of FMN bound to the active site (**Fig. 4.9**).²³³ These interactions are proposed to aid in communication between the π -helix and oligomeric changes of SsuE that occur with the binding of FMN.

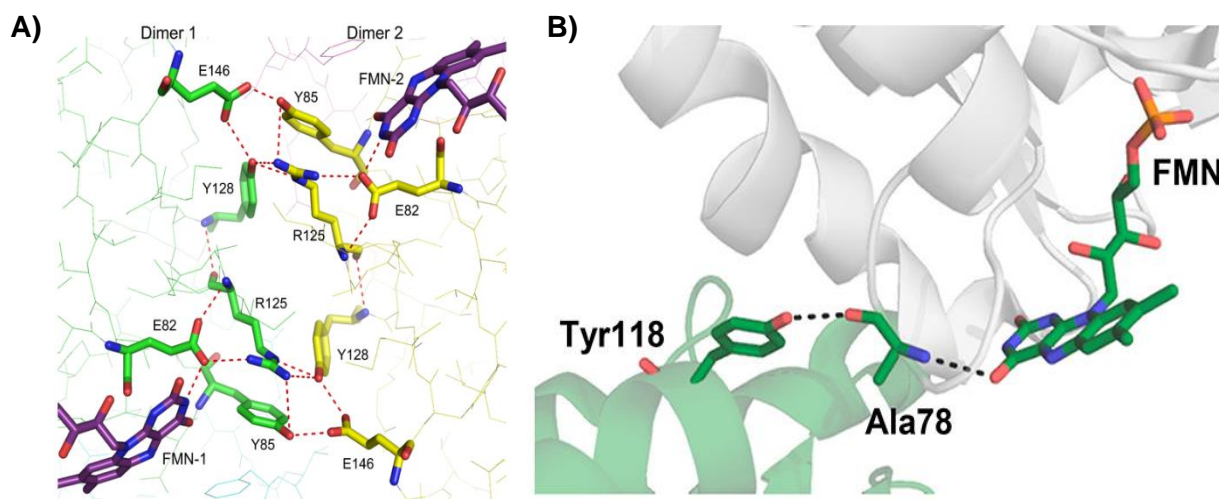


Figure 4.9: Hydrogen bonding interactions in ChrR and SsuE. A) Hydrogen bonding interactions between FMN molecules and two different ChrR dimers. B) Hydrogen bonding interactions between SsuE Tyr118 π -helix and the carbonyl oxygen of Ala78 across the tetramer interface. The amide nitrogen of Ala78 forms hydrogen bonding interactions with the O4 of the isoalloxazine ring of bound FMN. (Adapted from^{233,327}). Copyright © 2018, American Chemical Society.

Fluorometric titrations were utilized to determine if the binding affinity of FMN for wild-type and the ChrR variants was altered due to the conserved substitutions that were generated. Deflavination of wild-type and Q132P ChrR was performed to remove bound flavin to truly evaluate the binding affinity of the variants with flavin. The Q132P ChrR variant had a comparable FMN binding affinity as wild-type ChrR, however Q127D ChrR showed a 10-fold decrease in affinity for FMN. Although, Q127D ChrR could not catalyze the transfer of electrons to ferricyanide, it was not due to flavin not being bound but that the flavin may have been reduced but electrons were not transferred to ferricyanide. Limited trypsin digestion of Q127D ChrR was performed to evaluate how susceptible the variant was to proteolytic cleavage compared to the wild-type enzyme. Q127D ChrR was

more susceptible to digestion with trypsin compared to wild-type ChrR. This susceptibility may be due to the disruption of the pair of hydrogen binding network in the nearby residue Tyr128 with Glu146 that extends to FMN, which may have also caused the decrease in the binding affinity of Q127D ChrR for FMN. Since Q132P ChrR could catalyze the transfer of electrons to ferricyanide, the absence of activity in ferricyanide assays in the double variant, Q132P/127D ChrR may be caused by the disruption of the secondary structure of this variant and the compounded inability of Q127D ChrR to catalyze electron transfer to ferricyanide. This absence of enzyme activity may be linked to the decreased stability of the Q127D variant that led to rapid tryptic digestion compared to the wild-type enzyme. Finally, neither ChrR nor the variants could support sulfite production in the presence of SsuD in desulfonation assays. The absence of activity could be as a result of the flavin being reduced but not released because the oligomeric state of ChrR and its variants did not change to accommodate flavin release. On the other hand, if flavin was reduced and released, the absence of protein-protein interactions observed with SsuE and SsuD, would result in no measurable activity in desulfonation assays.

SsuE belongs to the NADPH:FMN reductase family and reductases belonging to this family have a common flavodoxin fold and they also exist as either dimers or tetramers.⁸⁹ Enzymes in the NADPH:FMN reductase family are further subdivided based on a conserved helix which is a π -helix for two-component FMN reductases but an α -helix for canonical flavoproteins.²³¹ The main structural difference between the π -helix and the α -helix in these reductases has been proposed to be the insertional residue; however, there are more adaptations that influence the different catalytic mechanisms of these reductases. The insertional residue in SsuE is Tyr118, however a similar Tyr128 residue

at an equivalent position is found in the canonical flavoprotein, ChrR.^{89,321} However, SsuE requires a monooxygenase partner to catalyze the desulfonation of organosulfonates, while ChrR does not need a monooxygenase for the reduction of hexavalent chromium. Different variants of ChrR were generated to investigate the additional structural adaptations to the π -helix of SsuE which catalyzes the reduction and transfer of reduced flavin to SsuD. In SsuE, the π -helix and the conserved residues required for protein-protein interactions with the monooxygenase partner are located at the tetramer interface of SsuE. The hydrogen bonding interactions observed with the π -helix and FMN can serve as a medium for communication between the oligomeric changes of SsuE and flavin reduction and transfer. The π -helix is a key structural feature that enhances flexibility in different proteins including SsuE and this advantage is augmented by oligomeric changes and flavin release in the two-component flavin-dependent systems. These studies were performed to investigate the structural adaptations that make FMN-reductases distinct from canonical flavoproteins. Findings from these investigations are important in elucidating how two-component FMN reductases perform their catalytic function and evolved to transfer reduced flavin to their monooxygenase partner for sulfur acquisition. The results obtained here are not conclusive about the exact structural adaptations that distinguish two-component reductases from canonical flavoproteins, and more investigations will need to be performed to ascertain this distinction. Future studies which include generating variants of ChrR by inserting the π -helix residues (110 -127) of SsuE into ChrR would give a more detailed understanding about structural residues that contribute to the divergence of these reductases

CHAPTER 5

Conclusion

Certain two-component flavin-dependent systems are upregulated in bacteria for the generation of sulfur when inorganic sulfate is limiting. These enzymes are utilized for sulfur scavenging from organosulfur compounds.⁸⁰ Sulfur is needed because of its versatility as a component of several critical biomolecules required for diverse biological processes in bacteria.^{16,30} Two-component systems comprise a flavin reductase that supplies reduced flavin to a partner monooxygenase. The monooxygenase catalyzes the cleavage of carbon-sulfur bonds of organosulfonates for sulfite production in the presence of reduced flavin and molecular oxygen.¹⁷⁰ In the alkanesulfonate monooxygenase system, SsuE supplies reduced flavin to SsuD for the desulfonation of linear alkanesulfonates to produce sulfite and the corresponding aldehyde.⁹⁴ *Pseudomonas* sp. has a more complex mechanism for sulfur acquisition. In addition to the alkanesulfonate monooxygenase system, the organism encodes a flavin reductase (MsuE) and two monooxygenases (MsuC/MsuD) in two separate but progressive reactions that converts methanesulfinate to sulfite and formaldehyde.^{167,231}

The flavin reductases, SsuE and MsuE belong to the NAD(P)H:FMN reductase family of the flavodoxin-like superfamily.⁸⁹ The reductases in this family are either purified flavin-free or flavin-bound. SsuE and MsuE are further sub-grouped from the other reductases within the family based on the insertion of an amino acid in a conserved α -helix present in canonical flavoproteins.^{89,231} The insertional residues into the conserved α -helix are aromatic amino acids which form π -helices in two-component FMN reductases. This insertion causes a bulge and a wider turn that deviates from the α -

helix.^{209,211,212} The π -helix has been observed in approximately 15% of proteins and its occurrence has been associated with a distinct functional advantage in several enzymes.²¹³ Most reductases in this family exist as either tetramers or dimers.⁸⁹ The tetrameric interface of SsuE houses the π -helix which engages in aromatic π -stacking interactions and hydrogen bonding interactions at the interface.²³³ This network of hydrogen bonding interactions between the insertional residue, Tyr118 of SsuE and FMN may function in aiding the changes in oligomerization exhibited by SsuE. Results from initial characterization of SsuE revealed that the enzyme exists in different oligomeric states depending on the technique used for investigation.^{89,94} Based on these results, we proposed that SsuE may exist in different oligomeric states that are dependent on the presence of substrates.

SsuE and MsuE have approximately 30% amino acid identity and may utilize similar mechanisms for the reduction and transfer of reduced flavin to their partner monooxygenases. However, MsuE catalyzes the transfer of reduced flavin to two different monooxygenases, MsuE and MsuD.^{100,231} We proposed that MsuE would exhibit similar oligomeric changes which would be dependent on the presence of substrates. First, we evaluated the binding affinity of the reductases for the different flavin substrates, FMN and FAD and pyridine nucleotides, NADH and NADPH. SsuE showed a higher binding affinity for FMN compared to FAD but showed comparable binding affinity for NADH and NADPH. However, MsuE showed comparable binding for FMN and FAD and NADH and NADPH. For the determination of oligomeric state of SsuE and MsuE, FMN and NADPH were utilized because though there were comparable binding affinities for NADH and

NADPH, SsuE and MsuE prefer NADPH in coupled assays with their partner monooxygenases, SsuD and MsuD, respectively.

The oligomeric state of the reductases was determined utilizing sedimentation velocity analytical ultracentrifugation (AUC). Apo SsuE existed as a tetramer which shifted to a tetramer-dimer equilibrium with either FMN or NADPH present. Interestingly, apo MsuE existed as a dimer but shifted to a tetramer in the presence of FMN. However, the oligomeric state of MsuE did not change in the presence of NADPH. The thermal melting temperatures of SsuE and MsuE were determined to investigate if there were changes in the structural stability of the enzymes without and with substrates. SsuE and MsuE portrayed higher melting points with FMN present compared to the melting points in the apo form and in the presence of NADPH. This observed increase in thermal melting temperatures of the reductases suggests that the oligomeric changes of the reductases in the presence of FMN caused increased stability. This increased stability would aid in stabilizing oxidized flavin before it is reduced.

HDX-MS was utilized to probe the conformational fluctuations of SsuE and MsuE without and with substrates. Major differences in deuterium uptake were observed at the dimer-tetramer interface of the apo-form and FMN-bound SsuE. The isotopic distribution of the mass spectra of SsuE with FMN showed a bimodal population representing both dimer (fast-exchanging) and tetramer (slow-exchanging) populations. However, MsuE without and with FMN showed a binomial isotopic distribution and a decrease in deuterium uptake was apparent at the dimer-tetramer interface. The π -helix is located at the tetrameric/dimeric interface of SsuE and MsuE and may be responsible for the flexibility which enables the oligomeric changes exhibited in the presence of substrates.

These studies show that oligomeric changes of the reductases play a role in reduction and transfer of reduced flavin transfer to their partner monooxygenases.

Reduced flavin transfer has been investigated for several two-component systems due to its lability in the presence of oxygen. The mechanism of reduced flavin transfer in the alkanesulfonate monooxygenase system occurred through protein-protein interactions between SsuE and SsuD.²⁰⁵ Complementary protein-protein interaction sites were observed for SsuE and SsuD with HDX-MS experiments. The protein interaction sites in SsuD were conserved and were located adjacent to the active site connected by a loop. The interaction sites in SsuE were observed at the tetrameric interface and one of the sites included the π -helix.²⁰⁸ This suggests that oligomeric changes of SsuE may function in exposing the protein-protein interaction sites to enable efficient handoff of reduced flavin. Studies were performed to evaluate the role of the oligomeric changes of SsuE in the transfer of reduced flavin with SsuD present and this was investigated with sedimentation velocity AUC. SsuD alone existed as a tetramer. Interestingly, with SsuE present, four peaks were observed. The four peaks represented the dimer and tetramer of SsuE, the tetramer of SsuD and the proposed SsuE-SsuD complex formed from protein-protein interactions. In the presence of SsuD and FMN, four similar peaks were observed; however, the dimer of SsuE was more predominant than the tetramer. These results imply that, in the presence of SsuD and FMN, the interaction sites of SsuE would be more exposed in the dimer form which would enhance protein-protein interactions and flavin transfer to SsuD.

The major functional difference between canonical flavoproteins and two-component reductases is the reduced flavin transfer event proposed to occur due to the

presence of the π -helix.⁸⁹ The π -helix is the primary structural difference between two-component reductases and canonical flavoproteins. It has been proposed to function in the transfer of reduced flavin, aiding the flexibility which enhances the oligomeric changes of SsuE that provides protein interactions for efficient flavin transfer to SsuD. The insertional residue in SsuE is not solely responsible for the structural divergence between two-component reductases and canonical flavoproteins. A Tyr residue in SsuE (Tyr118) was found in the canonical flavoprotein, ChrR at a similar position (Tyr126) in the structure-based sequence analysis of these proteins. However, ChrR does not require a monooxygenase for the reduction of hexavalent chromium. We hypothesize that the differences in the mechanisms of catalysis of SsuE and ChrR can be attributed to other structural adaptations in the SsuE enzyme. Further investigations of the π -helical region identified conserved residues in two-component reductases that were not present in ChrR. Variants of conserved proline and aspartic acid residues of two-component reductases (Q132P, Q127D, Q132P/127D ChrR) were generated to investigate if ChrR can be transformed to a two-component reductase capable of transferring flavin to a monooxygenase partner. Q132P ChrR was purified flavin-bound while Q127D ChrR and the double variant, Q132P/127D ChrR were flavin-free. All variants of ChrR were incapable of catalyzing electron transfer to oxygen in NADH oxidase assays. However, wild-type and Q132P ChrR were able to catalyze the transfer of electrons to ferricyanide in ferricyanide assays. The Q127D ChrR and Q132P/127D ChrR variants could not support electron transfer in ferricyanide assays because the flavin binding site may have been disrupted and the double variant showed a loss of secondary structure. Neither ChrR nor any of the variants were able to catalyze the production of sulfite in

desulfonation assays. This absence of measurable activity in desulfonation assays may be due to the lack of protein-protein interactions or oligomeric changes pertinent for the transfer of reduced flavin from the reductase to the partner monooxygenase. Future studies would focus on generating ChrR variants that encompass the length of the π -helix of SsuE (110 -127), this investigation would aid in determining the structural differences between the reductases.

The result from this study provides a basis for understanding how the different structural features of two-component flavin systems catalyze the desulfonation reaction for the acquisition of sulfur. Based on the observations, the presence of the π -helix in SsuE confers flexibility which may be responsible for the oligomeric changes of the enzyme in the presence of FMN and/or SsuD (**Fig. 5.1**). The dimer form of SsuE would provide protein-protein interactions sites in the presence of SsuD ensuring that upon flavin reduction, it is transferred to SsuD to prevent autooxidation. The results observed from investigating the structural differences between canonical flavoproteins and two-component flavin reductases are not conclusive. Additional studies would need to be performed to better investigate the structural adaptations that enable two-component flavin reductases catalyze the transfer of flavin.

Most organisms that utilize two-component flavin-dependent systems for sulfur acquisition are pathogenic and are responsible for several human infections. They are resistant to antibiotics and often lead to the death of infected patients. The two-component flavin-dependent reductases utilize unique structural features for flavin reduction, transfer and desulfonation of organosulfonates. These structural features include oligomeric changes, protein-protein interactions and the π -helix which are synchronized for overall

catalysis in these systems. These systems are unique to bacteria and understanding how these structural features work could serve as targets for drug development.

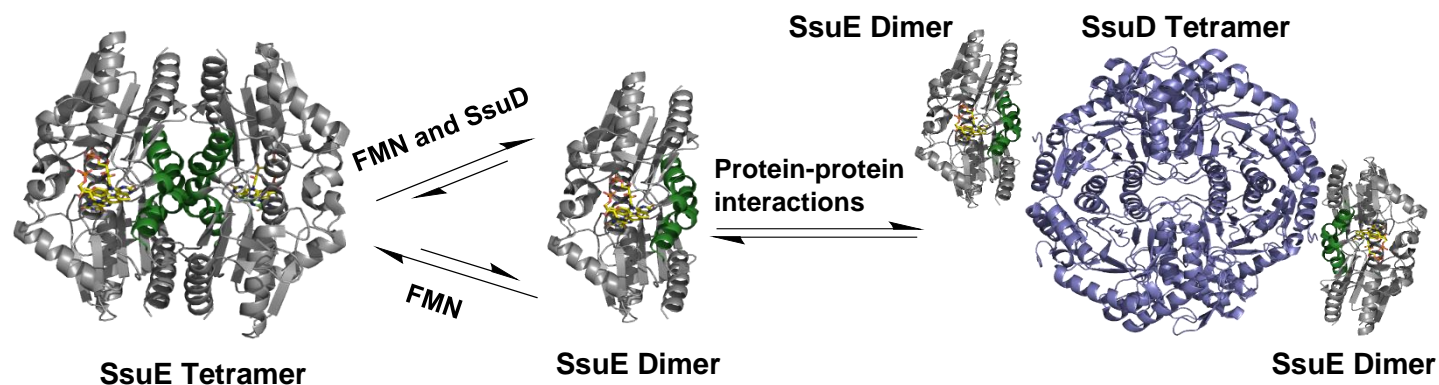


Figure 5.1: Coordination of the structural features of the alkanesulfonate monooxygenase system for catalysis. The π -helix aids the flexibility that promotes oligomeric changes of SsuE and exposes protein-protein interaction sites for reduced flavin transfer and desulfonation of organosulfonates.

REFERENCES

- (1) Mandeville, C. W. Sulfur: A Ubiquitous and Useful Tracer in Earth and Planetary Sciences. *Elements* **2010**, 6 (2), 75–80.
- (2) Lomans, B. P.; van der Drift, C.; Pol, A.; Op den Camp, H. J. M. Microbial Cycling of Volatile Organic Sulfur Compounds. *Cellular and Molecular Life Sciences (CMLS)* **2002**, 59 (4), 575–588.
- (3) Thomas, D.; Surdin-Kerjan, Y. Metabolism of Sulfur Amino Acids in *Saccharomyces Cerevisiae*. *Microbiol Mol Biol Rev* **1997**, 61 (4), 503–532.
- (4) Muyzer, G.; Stams, A. J. M. The Ecology and Biotechnology of Sulphate-Reducing Bacteria. *Nat Rev Microbiol* **2008**, 6 (6), 441–454.
- (5) Fike, D. A.; Bradley, A. S.; Rose, C. V. Rethinking the Ancient Sulfur Cycle. *Annual Review of Earth and Planetary Sciences* **2015**, 43 (1), 593–622.
- (6) Nimni, M. E.; Han, B.; Cordoba, F. Are We Getting Enough Sulfur in Our Diet? *Nutr Metab (Lond)* **2007**, 4, 24.
- (7) Saito, K. Sulfur Assimilatory Metabolism. The Long and Smelling Road. *Plant Physiol* **2004**, 136 (1), 2443–2450.
- (8) Schalinske, K. L. Hepatic Sulfur Amino Acid Metabolism. In *Glutathione and Sulfur Amino Acids in Human Health and Disease*; John Wiley & Sons, Ltd, **2009**; pp 73–90.
- (9) Brosnan, J. T.; Brosnan, M. E. The Sulfur-Containing Amino Acids: An Overview. *The Journal of Nutrition* **2006**, 136 (6), 1636S–1640S.
- (10) Townsend, D. M.; Tew, K. D.; Tapiero, H. Sulfur Containing Amino Acids and Human Disease. *Biomed Pharmacother* **2004**, 58 (1), 47–55.
- (11) Chonoles Imlay, K. R.; Korshunov, S.; Imlay, J. A. Physiological Roles, and Adverse Effects of the Two Cystine Importers of *Escherichia Coli*. *J Bacteriol* **2015**, 197 (23), 3629–3644.
- (12) Tesseraud, S.; Métayer Coustard, S.; Collin, A.; Seiliez, I. Role of Sulfur Amino Acids in Controlling Nutrient Metabolism and Cell Functions: Implications for Nutrition. *Br J Nutr* **2008**, 101 (8), 1132–1139.
- (13) Stipanuk, M. H. Sulfur Amino Acid Metabolism: Pathways for Production and Removal of Homocysteine and Cysteine. *Annu. Rev. Nutr.* **2004**, 24 (1), 539–577.
- (14) Stipanuk, M. H. Metabolism of Sulfur-Containing Amino Acids: How the Body Copes with Excess Methionine, Cysteine, and Sulfide. *The Journal of Nutrition* **2020**, 150, 2494S–2505S.
- (15) Miller, C. G.; Schmidt, E. E. Sulfur Metabolism Under Stress. *Antioxidants & Redox Signaling* **2020**, 33 (16), 1158–1173.
- (16) Johnson, D. C.; Dean, D. R.; Smith, A. D.; Johnson, M. K. Structure, Function, and Formation of Biological Iron-Sulfur Clusters. *Annual Review of Biochemistry* **2005**, 74 (1), 247–281.
- (17) Francioso, A.; Baseggio Conrado, A.; Mosca, L.; Fontana, M. Chemistry and Biochemistry of Sulfur Natural Compounds: Key Intermediates of Metabolism and Redox Biology. *Oxidative Medicine and Cellular Longevity* **2020**, 2020, 1–27.
- (18) Kellogg, W. W.; Cadle, R. D.; Allen, E. R.; Lazrus, A. L.; Martell, E. A. The Sulfur Cycle: Man's Contributions Are Compared to Natural Sources of Sulfur Compounds in the Atmosphere and Oceans. *Science* **1972**, 175 (4022), 587–596.

- (19) Farquhar, J.; Bao, H.; Thiemens, M. Atmospheric Influence of Earth's Earliest Sulfur Cycle. *Science* **2000**, 289 (5480), 756–759.
- (20) Wacey, D.; Kilburn, M. R.; Saunders, M.; Cliff, J.; Brasier, M. D. Microfossils of Sulphur-Metabolizing Cells in 3.4-Billion-Year-Old Rocks of Western Australia. *Nature Geosci* **2011**, 4 (10), 698–702.
- (21) Shen, Y.; Buick, R.; Canfield, D. E. Isotopic Evidence for Microbial Sulphate Reduction in the Early Archaean Era. *Nature* **2001**, 410 (6824), 77–81.
- (22) Philippot, P.; Van Zuilen, M.; Lepot, K.; Thomazo, C.; Farquhar, J.; Van Kranendonk, M. J. Early Archaean Microorganisms Preferred Elemental Sulfur, Not Sulfate. *Science* **2007**, 317 (5844), 1534–1537.
- (23) Muller, É.; Philippot, P.; Rollion-Bard, C.; Cartigny, P. Multiple Sulfur-Isotope Signatures in Archean Sulfates and Their Implications for the Chemistry and Dynamics of the Early Atmosphere. *Proc. Natl. Acad. Sci. U.S.A.* **2016**, 113 (27), 7432–7437.
- (24) Wagner, C. A. Hydrogen Sulfide: A New Gaseous Signal Molecule and Blood Pressure Regulator. *J Nephrol* **2009**, 22 (2), 173–176.
- (25) Shatalin, K.; Shatalina, E.; Mironov, A.; Nudler, E. H₂S: A Universal Defense Against Antibiotics in Bacteria. *Science* **2011**, 334 (6058), 986–990.
- (26) Oguri, T.; Schneider, B.; Reitzer, L. Cysteine Catabolism and Cysteine Desulfhydrase (CdsH/STM0458) in Salmonella Enterica Serovar Typhimurium. *J Bacteriol* **2012**, 194 (16), 4366–4376.
- (27) Liu, H.; Xin, Y.; Xun, L. Distribution, Diversity, and Activities of Sulfur Dioxygenases in Heterotrophic Bacteria. *Appl Environ Microbiol* **2014**, 80 (5), 1799–1806.
- (28) Xin, Y.; Liu, H.; Cui, F.; Liu, H.; Xun, L. Recombinant *Escherichia Coli* with Sulfide:Quinone Oxidoreductase and Persulfide Dioxygenase Rapidly Oxidises Sulfide to Sulfite and Thiosulfate via a New Pathway: Sulfide Oxidation by Recombinant *Escherichia Coli*. *Environmental Microbiology* **2016**, 18 (12), 5123–5136.
- (29) Xia, Y.; Lü, C.; Hou, N.; Xin, Y.; Liu, J.; Liu, H.; Xun, L. Sulfide Production and Oxidation by Heterotrophic Bacteria under Aerobic Conditions. *ISME J* **2017**, 11 (12), 2754–2766.
- (30) Sekowska, A.; Kung, H. F.; Danchin, A. Sulfur Metabolism in *Escherichia Coli* and Related Bacteria: Facts and Fiction. *J Mol Microbiol Biotechnol* **2000**, 2 (2), 145–177.
- (31) Liew, J. J. M.; El Saudi, I. M.; Nguyen, S. V.; Wicht, D. K.; Dowling, D. P. Structures of the Alkanesulfonate Monooxygenase MsuD Provide Insight into C–S Bond Cleavage, Substrate Scope, and an Unexpected Role for the Tetramer. *Journal of Biological Chemistry* **2021**, 297 (1), 100823.
- (32) Cooper, A. J. L. Biochemistry of Sulfur-Containing Amino Acids. *Annual Review of Biochemistry* **1983**, 52 (1), 187–222.
- (33) Mueller, E. G. Trafficking in Persulfides: Delivering Sulfur in Biosynthetic Pathways. *Nat Chem Biol* **2006**, 2 (4), 185–194.
- (34) Williams, S. J.; Senaratne, R. H.; Mougous, J. D.; Riley, L. W.; Bertozzi, C. R. 5'-Adenosinephosphosulfate Lies at a Metabolic Branch Point in Mycobacteria. *Journal of Biological Chemistry* **2002**, 277 (36), 32606–32615.
- (35) Vermeij, P.; Kertesz, M. A. Pathways of Assimilative Sulfur Metabolism in *Pseudomonas Putida*. *J Bacteriol* **1999**, 181 (18), 5833–5837.

- (36) van der Ploeg, J. R.; Weiss, M. A.; Saller, E.; Nashimoto, H.; Saito, N.; Kertesz, M. A.; Leisinger, T. Identification of Sulfate Starvation-Regulated Genes in *Escherichia Coli*: A Gene Cluster Involved in the Utilization of Taurine as a Sulfur Source. *J Bacteriol* **1996**, 178 (18), 5438–5446.
- (37) Bhawe, D. P.; Hong, J. A.; Keller, R. L.; Krebs, C.; Carroll, K. S. Iron–Sulfur Cluster Engineering Provides Insight into the Evolution of Substrate Specificity among Sulfonucleotide Reductases. *ACS Chem. Biol.* **2012**, 7 (2), 306–315.
- (38) Martin, M. N.; Tarczynski, M. C.; Shen, B.; Leustek, T. The Role of 5'-Adenylylsulfate Reductase in Controlling Sulfate Reduction in Plants. *Photosynth Res* **2005**, 86 (3), 309–323.
- (39) Leustek, T.; Martin, M. N.; Bick, J.-A.; Davies, J. P. Pathways And Regulation Of Sulfur Metabolism Revealed Through Molecular And Genetic Studies. *Annu Rev Plant Physiol Plant Mol Biol* **2000**, 51, 141–165.
- (40) Koprivova, A.; Meyer, A. J.; Schween, G.; Herschbach, C.; Reski, R.; Kopriva, S. Functional Knockout of the Adenosine 5'-Phosphosulfate Reductase Gene in *Physcomitrella Patens* Revives an Old Route of Sulfate Assimilation. *Journal of Biological Chemistry* **2002**, 277 (35), 32195–32201.
- (41) Chartron, J.; Shiao, C.; Stout, C. D.; Carroll, K. S. 3'-Phosphoadenosine-5'-Phosphosulfate Reductase in Complex with Thioredoxin: A Structural Snapshot in the Catalytic Cycle. *Biochemistry* **2007**, 46 (13), 3942–3951.
- (42) Shimizu, K. Regulation Systems of Bacteria Such as *Escherichia Coli* in Response to Nutrient Limitation and Environmental Stresses. *Metabolites* **2013**, 4 (1), 1–35.
- (43) Bykowski, T.; Ploeg, J. R. van der; Iwanicka-Nowicka, R.; Hryniewicz, M. M. The Switch from Inorganic to Organic Sulphur Assimilation in *Escherichia Coli*: Adenosine 5'-Phosphosulphate (APS) as a Signalling Molecule for Sulphate Excess: Regulation of Organosulphur Assimilation in *E. Coli*. *Molecular Microbiology* **2002**, 43 (5), 1347–1358.
- (44) Koprivova, A.; Kopriva, S. Role of Plant Sulfur Metabolism in Human Nutrition and Food Security. In *Plant Nutrition and Food Security in the Era of Climate Change*; Elsevier, **2022**; pp 73–95.
- (45) Watanabe, M.; Chiba, Y.; Hirai, M. Y. Metabolism and Regulatory Functions of O-Acetylserine, S-Adenosylmethionine, Homocysteine, and Serine in Plant Development and Environmental Responses. *Frontiers in Plant Science* **2021**, 12.
- (46) Park, C.-M.; Weerasinghe, L.; Day, J. J.; Fukuto, J. M.; Xian, M. Persulfides: Current Knowledge and Challenges in Chemistry and Chemical Biology. *Mol. BioSyst.* **2015**, 11 (7), 1775–1785.
- (47) Ida, T.; Sawa, T.; Ihara, H.; Tsuchiya, Y.; Watanabe, Y.; Kumagai, Y.; Suematsu, M.; Motohashi, H.; Fujii, S.; Matsunaga, T.; Yamamoto, M.; Ono, K.; Devarie-Baez, N. O.; Xian, M.; Fukuto, J. M.; Akaike, T. Reactive Cysteine Persulfides and S-Polythiolation Regulate Oxidative Stress and Redox Signaling. *Proc. Natl. Acad. Sci. U.S.A.* **2014**, 111 (21), 7606–7611.
- (48) Cuevasanta, E.; Möller, M. N.; Alvarez, B. Biological Chemistry of Hydrogen Sulfide and Persulfides. *Archives of Biochemistry and Biophysics* **2017**, 617, 9–25.
- (49) Lec, J.-C.; Boutserin, S.; Mazon, H.; Mulliert, G.; Boschi-Muller, S.; Talfournier, F. Unraveling the Mechanism of Cysteine Persulfide Formation Catalyzed by 3-Mercaptopyruvate Sulfurtransferases. *ACS Catal.* **2018**, 8 (3), 2049–2059.

- (50) Cuevasanta, E.; Reyes, A. M.; Zeida, A.; Mastrogiovanni, M.; De Armas, M. I.; Radi, R.; Alvarez, B.; Trujillo, M. Kinetics of Formation and Reactivity of the Persulfide in the One-Cysteine Peroxiredoxin from Mycobacterium Tuberculosis. *Journal of Biological Chemistry* **2019**, *294* (37), 13593–13605.
- (51) Sawa, T.; Motohashi, H.; Ihara, H.; Akaike, T. Enzymatic Regulation and Biological Functions of Reactive Cysteine Persulfides and Polysulfides. *Biomolecules* **2020**, *10* (9), 1245.
- (52) Cuevasanta, E.; Benchoam, D.; Semelak, J. A.; Möller, M. N.; Zeida, A.; Trujillo, M.; Alvarez, B.; Estrin, D. A. Possible Molecular Basis of the Biochemical Effects of Cysteine-Derived Persulfides. *Front. Mol. Biosci.* **2022**, *9*, 975988.
- (53) Toohey, J. I. Sulphane Sulphur in Biological Systems: A Possible Regulatory Role. *Biochem J* **1989**, *264* (3), 625–632.
- (54) Wang, J.; Guo, X.; Li, H.; Qi, H.; Qian, J.; Yan, S.; Shi, J.; Niu, W. Hydrogen Sulfide From Cysteine Desulfurase, Not 3-Mercaptopyruvate Sulfurtransferase, Contributes to Sustaining Cell Growth and Bioenergetics in E. Coli Under Anaerobic Conditions. *Front. Microbiol.* **2019**, *10*, 2357.
- (55) Dillon, K. M.; Matson, J. B. A Review of Chemical Tools for Studying Small Molecule Persulfides: Detection and Delivery. *ACS Chemical Biology* **2021**, *16* (7), 1128–1141.
- (56) Black, K. A.; Dos Santos, P. C. Shared-Intermediates in the Biosynthesis of Thio-Cofactors: Mechanism and Functions of Cysteine Desulfurases and Sulfur Acceptors. *Biochimica et Biophysica Acta (BBA) - Molecular Cell Research* **2015**, *1853* (6), 1470–1480.
- (57) Mihara, H.; Esaki, N. Bacterial Cysteine Desulfurases: Their Function and Mechanisms. *Appl Microbiol Biotechnol* **2002**, *60* (1–2), 12–23.
- (58) Fontecave, M.; Ollagnier-de-Choudens, S. Iron–Sulfur Cluster Biosynthesis in Bacteria: Mechanisms of Cluster Assembly and Transfer. *Archives of Biochemistry and Biophysics* **2008**, *474* (2), 226–237.
- (59) Giordano, N.; Hastie, J. L.; Smith, A. D.; Foss, E. D.; Gutierrez-Munoz, D. F.; Carlson, P. E. Cysteine Desulfurase IscS2 Plays a Role in Oxygen Resistance in Clostridium Difficile. *Infect Immun* **2018**, *86* (8), e00326–18.
- (60) Fontecave, M. Iron-Sulfur Clusters: Ever-Expanding Roles. *Nat Chem Biol* **2006**, *2* (4), 171–174.
- (61) Py, B.; Barras, F. Building Fe-S Proteins: Bacterial Strategies. *Nat Rev Microbiol* **2010**, *8* (6), 436–446.
- (62) Das, M.; Dewan, A.; Shee, S.; Singh, A. The Multifaceted Bacterial Cysteine Desulfurases: From Metabolism to Pathogenesis. *Antioxidants* **2021**, *10* (7), 997.
- (63) Mishanina, T. V.; Libiad, M.; Banerjee, R. Biogenesis of Reactive Sulfur Species for Signaling by Hydrogen Sulfide Oxidation Pathways. *Nat Chem Biol* **2015**, *11* (7), 457–464.
- (64) *Nutrient Metabolism*; Elsevier, **2003**.
- (65) Colette Daubner, S.; Lanzas, R. O. Pteridines ☆. In *Reference Module in Biomedical Sciences*; Elsevier, **2018**; p B9780128012383662000.
- (66) Hille, R.; Rétey, J.; Bartlewski-Hof, U.; Reichenbecher, W.; Schink, B. Mechanistic Aspects of Molybdenum-Containing Enzymes. *FEMS Microbiol Rev* **1998**, *22* (5), 489–501.

- (67) Kisker, C.; Schindelin, H.; Rees, D. C. Molybdenum-Cofactor-Containing Enzymes: Structure and Mechanism. *Annu. Rev. Biochem.* **1997**, *66* (1), 233–267.
- (68) Zhang, W.; Urban, A.; Mihara, H.; Leimkühler, S.; Kurihara, T.; Esaki, N. IscS Functions as a Primary Sulfur-Donating Enzyme by Interacting Specifically with MoeB and MoaD in the Biosynthesis of Molybdopterin in *Escherichia Coli*. *Journal of Biological Chemistry* **2010**, *285* (4), 2302–2308.
- (69) Kessler, D. Enzymatic Activation of Sulfur for Incorporation into Biomolecules in Prokaryotes. *FEMS Microbiol Rev* **2006**, *30* (6), 825–840.
- (70) Hidese, R.; Mihara, H.; Esaki, N. Bacterial Cysteine Desulfurases: Versatile Key Players in Biosynthetic Pathways of Sulfur-Containing Biofactors. *Appl Microbiol Biotechnol* **2011**, *91* (1), 47–61.
- (71) Lauhon, C. T. Requirement for IscS in Biosynthesis of All Thionucleosides in *Escherichia Coli*. *J Bacteriol* **2002**, *184* (24), 6820–6829.
- (72) van der Ploeg, J. R.; Iwanicka-Nowicka, R.; Kertesz, M. A.; Leisinger, T.; Hryniewicz, M. M. Involvement of CysB and Cbl Regulatory Proteins in Expression of the TauABCD Operon and Other Sulfate Starvation-Inducible Genes in *Escherichia Coli*. *J Bacteriol* **1997**, *179* (24), 7671–7678.
- (73) Kawano, Y.; Suzuki, K.; Ohtsu, I. Current Understanding of Sulfur Assimilation Metabolism to Biosynthesize L-Cysteine and Recent Progress of Its Fermentative Overproduction in Microorganisms. *Appl Microbiol Biotechnol* **2018**, *102* (19), 8203–8211.
- (74) Kertesz, M. A. Riding the Sulfur Cycle – Metabolism of Sulfonates and Sulfate Esters in Gram-Negative Bacteria. *FEMS Microbiology Reviews* **2000**, *24* (2), 135–175.
- (75) Cook, A. M.; Laue, H.; Junker, F. Microbial Desulfonation. *FEMS Microbiol Rev* **1998**, *22* (5), 399–419.
- (76) Kertesz, M. A. Bacterial Transporters for Sulfate and Organosulfur Compounds. *Res Microbiol* **2001**, *152* (3–4), 279–290.
- (77) Reichenbecher, W.; Murrell, J. C. Linear Alkanesulfonates as Carbon and Energy Sources for Gram-Positive and Gram-Negative Bacteria. *Archives of Microbiology* **1999**, *171* (6), 430–438.
- (78) Endoh, T.; Habe, H.; Nojiri, H.; Yamane, H.; Omori, T. The $\Sigma 54$ -Dependent Transcriptional Activator SfnR Regulates the Expression of the *Pseudomonas Putida* SfnFG Operon Responsible for Dimethyl Sulphone Utilization: Regulation of Dimethyl Sulphone Metabolic Genes. *Molecular Microbiology* **2004**, *55* (3), 897–911.
- (79) Uria-Nickelsen, M. R.; Leadbetter, E. R.; Godchaux, W. Sulphonate Utilization by Enteric Bacteria. *Journal of General Microbiology* **1993**, *139* (2), 203–208.
- (80) Endoh, T.; Kasuga, K.; Horinouchi, M.; Yoshida, T.; Habe, H.; Nojiri, H.; Omori, T. Characterization and Identification of Genes Essential for Dimethyl Sulfide Utilization in *Pseudomonas Putida* Strain DS1. *Applied Microbiology and Biotechnology* **2003**, *62* (1), 83–91.
- (81) Kouzuma, A.; Endoh, T.; Omori, T.; Nojiri, H.; Yamane, H.; Habe, H. Transcription Factors CysB and SfnR Constitute the Hierarchical Regulatory System for the Sulfate Starvation Response in *Pseudomonas Putida*. *J Bacteriol* **2008**, *190* (13), 4521–4531.
- (82) Quadroni, M.; Staudenmann, W.; Kertesz, M.; James, P. Analysis of Global Responses by Protein and Peptide Fingerprinting of Proteins Isolated by Two-

- Dimensional Gel Electrophoresis. Application to the Sulfate-Starvation Response of *Escherichia Coli*. *Eur J Biochem* **1996**, 239 (3), 773–781.
- (83) Eichhorn, E.; van der Ploeg, J. R.; Leisinger, T. Deletion Analysis of the *Escherichia Coli* Taurine and Alkanesulfonate Transport Systems. *J Bacteriol* **2000**, 182 (10), 2687–2695.
 - (84) Pereira, C. T.; Moutran, A.; Fessel, M.; Balan, A. The Sulfur/Sulfonates Transport Systems in *Xanthomonas Citri* P. Citri. *BMC Genomics* **2015**, 16 (1), 524.
 - (85) van der Ploeg, J.; Eichhorn, E.; Leisinger, T. Sulfonate-Sulfur Metabolism and Its Regulation in *Escherichia Coli*. *Archives of Microbiology* **2001**, 176 (1–2), 1–8.
 - (86) van der Ploeg, J. R.; Iwanicka-Nowicka, R.; Bykowski, T.; Hryniewicz, M. M.; Leisinger, T. The *Escherichia Coli* SsuEADCB Gene Cluster Is Required for the Utilization of Sulfur from Aliphatic Sulfonates and Is Regulated by the Transcriptional Activator Cbl. *Journal of Biological Chemistry* **1999**, 274 (41), 29358–29365.
 - (87) Eichhorn, E.; van der Ploeg, J. R.; Kertesz, M. A.; Leisinger, T. Characterization of α -Ketoglutarate-Dependent Taurine Dioxygenase from *Escherichia Coli*. *Journal of Biological Chemistry* **1997**, 272 (37), 23031–23036.
 - (88) Ellis, H. R. Mechanism for Sulfur Acquisition by the Alkanesulfonate Monooxygenase System. *Bioorg Chem* **2011**, 39 (5–6), 178–184.
 - (89) Driggers, C. M.; Dayal, P. V.; Ellis, H. R.; Karplus, P. A. Crystal Structure of *Escherichia Coli* SsuE: Defining a General Catalytic Cycle for FMN Reductases of the Flavodoxin-like Superfamily. *Biochemistry* **2014**, 53 (21), 3509–3519.
 - (90) Koch, D. J.; Rückert, C.; Rey, D. A.; Mix, A.; Pühler, A.; Kalinowski, J. Role of the Ssu and Seu Genes of *Corynebacterium Glutamicum* ATCC 13032 in Utilization of Sulfonates and Sulfonate Esters as Sulfur Sources. *Appl Environ Microbiol* **2005**, 71 (10), 6104–6114.
 - (91) van der Ploeg, J. R.; Barone, M.; Leisinger, T. Expression of the *Bacillus Subtilis* Sulphonate-Sulphur Utilization Genes Is Regulated at the Levels of Transcription Initiation and Termination. *Mol Microbiol* **2001**, 39 (5), 1356–1365.
 - (92) Łochowska, A.; Iwanicka-Nowicka, R.; Zielak, A.; Modelewska, A.; Thomas, M. S.; Hryniewicz, M. M. Regulation of Sulfur Assimilation Pathways in *Burkholderia Cenocepacia* through Control of Genes by the SsuR Transcription Factor. *J Bacteriol* **2011**, 193 (8), 1843–1853.
 - (93) Hollenstein, K.; Frei, D. C.; Locher, K. P. Structure of an ABC Transporter in Complex with Its Binding Protein. *Nature* **2007**, 446 (7132), 213–216.
 - (94) Eichhorn, E.; van der Ploeg, J. R.; Leisinger, T. Characterization of a Two-Component Alkanesulfonate Monooxygenase from *Escherichia Coli*. *Journal of Biological Chemistry* **1999**, 274 (38), 26639–26646.
 - (95) Kahnert, A.; Vermeij, P.; Wietek, C.; James, P.; Leisinger, T.; Kertesz, M. A. The Ssu Locus Plays a Key Role in Organosulfur Metabolism in *Pseudomonas Putida* S-313. *J Bacteriol* **2000**, 182 (10), 2869–2878.
 - (96) Kertesz, M. A.; Leisinger, T.; Cook, A. M. Proteins Induced by Sulfate Limitation in *Escherichia Coli*, *Pseudomonas Putida*, or *Staphylococcus Aureus*. *J Bacteriol* **1993**, 175 (4), 1187–1190.
 - (97) Beil, S.; Kertesz, M. A.; Leisinger, T.; Cook, A. M. The Assimilation of Sulfur from Multiple Sources and Its Correlation with Expression of the Sulfate-Starvation-Induced Stimulon in *Pseudomonas Putida* S-313. *Microbiology* **1996**, 142 (8), 1989–1995.

- (98) Endoh, T.; Habe, H.; Yoshida, T.; Nojiri, H.; Omori, T. A CysB-Regulated and Σ 54-Dependent Regulator, SfnR, Is Essential for Dimethyl Sulfone Metabolism of *Pseudomonas Putida* Strain DS1. *Microbiology* **2003**, *149* (4), 991–1000.
- (99) Kertesz, M. A.; Schmidt-Larbig, K.; Wüest, T. A Novel Reduced Flavin Mononucleotide-Dependent Methanesulfonate Sulfonatase Encoded by the Sulfur-Regulated Msu Operon of *Pseudomonas Aeruginosa*. *J Bacteriol* **1999**, *181* (5), 1464–1473.
- (100) Soule, J.; Gnann, A. D.; Gonzalez, R.; Parker, M. J.; McKenna, K. C.; Nguyen, S. V.; Phan, N. T.; Wicht, D. K.; Dowling, D. P. Structure and Function of the Two-Component Flavin-Dependent Methanesulfinate Monooxygenase within Bacterial Sulfur Assimilation. *Biochemical and Biophysical Research Communications* **2020**, *522* (1), 107–112.
- (101) Hryniewicz, M. M.; Kredich, N. M. Hydroxyl Radical Footprints and Half-Site Arrangements of Binding Sites for the CysB Transcriptional Activator of *Salmonella Typhimurium*. *J Bacteriol* **1995**, *177* (9), 2343–2353.
- (102) Kredich, N. M. The Molecular Basis for Positive Regulation of Cys Promoters in *Salmonella Typhimurium* and *Escherichia Coli*. *Mol Microbiol* **1992**, *6* (19), 2747–2753.
- (103) Ostrowski, J.; Kredich, N. M. Molecular Characterization of the CysJIH Promoters of *Salmonella Typhimurium* and *Escherichia Coli*: Regulation by CysB Protein and N-Acetyl-L-Serine. *J Bacteriol* **1989**, *171* (1), 130–140.
- (104) Hryniewicz, M. M.; Kredich, N. M. The CysP Promoter of *Salmonella Typhimurium*: Characterization of Two Binding Sites for CysB Protein, Studies of in Vivo Transcription Initiation, and Demonstration of the Anti-Inducer Effects of Thiosulfate. *J Bacteriol* **1991**, *173* (18), 5876–5886.
- (105) Iwanicka-Nowicka, R.; Hryniewicz, M. M. A New Gene, Cbl, Encoding a Member of the LysR Family of Transcriptional Regulators Belongs to *Escherichia Coli* Cys Regulon. *Gene* **1995**, *166* (1), 11–17.
- (106) Stover, C. K.; Pham, X. Q.; Erwin, A. L.; Mizoguchi, S. D.; Warrenner, P.; Hickey, M. J.; Brinkman, F. S. L.; Hufnagle, W. O.; Kowalik, D. J.; Lagrou, M.; Garber, R. L.; Goltry, L.; Tolentino, E.; Westbrook-Wadman, S.; Yuan, Y.; Brody, L. L.; Coulter, S. N.; Folger, K. R.; Kas, A.; Larbig, K.; Lim, R.; Smith, K.; Spencer, D.; Wong, G. K.-S.; Wu, Z.; Paulsen, I. T.; Reizer, J.; Saier, M. H.; Hancock, R. E. W.; Lory, S.; Olson, M. V. Complete Genome Sequence of *Pseudomonas Aeruginosa* PAO1, an Opportunistic Pathogen. *Nature* **2000**, *406* (6799), 959–964.
- (107) Nelson, K. E.; Weinl, C.; Paulsen, I. T.; Dodson, R. J.; Hilbert, H.; Martins dos Santos, V. A. P.; Fouts, D. E.; Gill, S. R.; Pop, M.; Holmes, M.; Brinkac, L.; Beanan, M.; DeBoy, R. T.; Daugherty, S.; Kolonay, J.; Madupu, R.; Nelson, W.; White, O.; Peterson, J.; Khouri, H.; Hance, I.; Lee, P. C.; Holtzapple, E.; Scanlan, D.; Tran, K.; Moazzez, A.; Utterback, T.; Rizzo, M.; Lee, K.; Kosack, D.; Moestl, D.; Wedler, H.; Lauber, J.; Stjepandic, D.; Hoheisel, J.; Straetz, M.; Heim, S.; Kiewitz, C.; Eisen, J.; Timmis, K. N.; Dusterhoft, A.; Tummeler, B.; Fraser, C. M. Complete Genome Sequence and Comparative Analysis of the Metabolically Versatile *Pseudomonas Putida* KT2440. *Environ Microbiol* **2002**, *4* (12), 799–808.

- (108) Vermeij, P.; Wietek, C.; Kahnert, A.; Wuest, T.; Kertesz, M. A. Genetic Organization of Sulphur-Controlled Aryl Desulphonation in *Pseudomonas Putida* S-313. *Mol Microbiol* **1999**, 32 (5), 913–926.
- (109) Davison, J.; Brunel, F.; Phanopoulos, A.; Prozzi, D.; Terpstra, P. Cloning and Sequencing of *Pseudomonas* Genes Determining Sodium Dodecyl Sulfate Biodegradation. *Gene* **1992**, 114 (1), 19–24.
- (110) Kahnert, A.; Mirleau, P.; Wait, R.; Kertesz, M. A. The LysR-Type Regulator SftR Is Involved in Soil Survival and Sulphate Ester Metabolism in *Pseudomonas Putida*. *Environ Microbiol* **2002**, 4 (4), 225–237.
- (111) Massey, V. The Chemical and Biological Versatility of Riboflavin. *Biochem Soc Trans* **2000**, 28 (4), 283–296.
- (112) Entsch, B.; Ballou, D. P. Flavins. In *Encyclopedia of Biological Chemistry*; Elsevier, **2013**; pp 309–313.
- (113) Revuelta, J. L.; Ledesma-Amaro, R.; Lozano-Martinez, P.; Díaz-Fernández, D.; Buey, R. M.; Jiménez, A. Bioproduction of Riboflavin: A Bright Yellow History. *Journal of Industrial Microbiology and Biotechnology* **2017**, 44 (4–5), 659–665.
- (114) Müller, F. The Flavin Redox-System and Its Biological Function. In *Radicals in Biochemistry*; Boschke, F. L., Dewar, M. J. S., Dunitz, J. D., Hafner, K., Heilbronner, E., Itó, S., Lehn, J.-M., Niedenzu, K., Raymond, K. N., Rees, C. W., Schäfer, K., Vögtle, F., Wittig, G., Series Eds.; Topics in Current Chemistry; Springer Berlin Heidelberg: Berlin, Heidelberg, **1983**; Vol. 108, pp 71–107.
- (115) Miura, R. Versatility and Specificity in Flavoenzymes: Control Mechanisms of Flavin Reactivity. *Chem. Record* **2001**, 1 (3), 183–194.
- (116) Walsh, C. T.; Wencewicz, T. A. Flavoenzymes: Versatile Catalysts in Biosynthetic Pathways. *Nat Prod Rep* **2013**, 30 (1), 175–200.
- (117) Walsh, C. Chemical Approaches to the Study of Enzymes Catalyzing Redox Transformations. *Annu. Rev. Biochem.* **1978**, 47 (1), 881–931.
- (118) Sund, H.; Ullrich, V. *Biological Oxidations*; Springer Berlin Heidelberg: Berlin, Heidelberg, **1983**.
- (119) Lienhart, W.-D.; Gudipati, V.; Macheroux, P. The Human Flavoproteome. *Archives of Biochemistry and Biophysics* **2013**, 535 (2), 150–162.
- (120) Merrill, A. H.; Lambeth, J. D.; Edmondson, D. E.; McCormick, D. B. Formation And Mode Of Action Of Flavoproteins. *Annu. Rev. Nutr.* **1981**, 1 (1), 281–317.
- (121) Averianova, L. A.; Balabanova, L. A.; Son, O. M.; Podvolotskaya, A. B.; Tekutyeva, L. A. Production of Vitamin B2 (Riboflavin) by Microorganisms: An Overview. *Front. Bioeng. Biotechnol.* **2020**, 8, 570828.
- (122) Schwechheimer, S. K.; Park, E. Y.; Revuelta, J. L.; Becker, J.; Wittmann, C. Biotechnology of Riboflavin. *Appl Microbiol Biotechnol* **2016**, 100 (5), 2107–2119.
- (123) Merrill, A. H.; McCormick, D. B. Riboflavin. In *Present Knowledge in Nutrition*; Elsevier, **2020**; pp 189–207.
- (124) Kis, K.; Volk, R.; Bacher, A. Biosynthesis of Riboflavin. Studies on the Reaction Mechanism of 6,7-Dimethyl-8-Ribityllumazine Synthase. *Biochemistry* **1995**, 34 (9), 2883–2892.
- (125) Ghisla, S.; Edmondson, D. E. Flavin Coenzymes. In *eLS*; John Wiley & Sons, Ltd, Ed.; Wiley, **2009**.

- (126) *Flavins and Flavoproteins: Methods and Protocols*; Weber, S., Schleicher, E., Eds.; Methods in molecular biology; Humana Press: New York, **2014**.
- (127) Pimviriyakul, P.; Chaiyen, P. Overview of Flavin-Dependent Enzymes. In *The Enzymes*; Elsevier, **2020**; Vol. 47, pp 1–36.
- (128) Chapman, S. K.; Reid, G. A. *Flavoprotein Protocols*; Humana Press: Totowa, **2002**.
- (129) Ghisla, S.; Massey, V.; Lhoste, J.-M.; Mayhew, S. G. Fluorescence and Optical Characteristics of Reduced Flavines and Flavoproteins. *Biochemistry* **1974**, 13 (3), 589–597.
- (130) Vabulas, R. M. Ferroptosis-Related Flavoproteins: Their Function and Stability. *IJMS* **2021**, 22 (1), 430.
- (131) Ghisla, S.; Massey, V. Mechanisms of Flavoprotein-Catalyzed Reactions. *Eur J Biochem* **1989**, 181 (1), 1–17.
- (132) Chaiyen, P.; Fraaije, M. W.; Mattevi, A. The Enigmatic Reaction of Flavins with Oxygen. *Trends in Biochemical Sciences* **2012**, 37 (9), 373–380.
- (133) Gran-Scheuch, A.; Parra, L.; Fraaije, M. W. Systematic Assessment of Uncoupling in Flavoprotein Oxidases and Monooxygenases. *ACS Sustainable Chem. Eng.* **2023**, 11 (13), 4948–4959.
- (134) Romero, E.; Gómez Castellanos, J. R.; Gadda, G.; Fraaije, M. W.; Mattevi, A. Same Substrate, Many Reactions: Oxygen Activation in Flavoenzymes. *Chem. Rev.* **2018**, 118 (4), 1742–1769.
- (135) Crozier-Reabe, K.; Moran, G. Form Follows Function: Structural and Catalytic Variation in the Class A Flavoprotein Monooxygenases. *IJMS* **2012**, 13 (12), 15601–15639.
- (136) Joosten, V.; van Berkel, W. J. Flavoenzymes. *Current Opinion in Chemical Biology* **2007**, 11 (2), 195–202.
- (137) Dijkman, W. P.; De Gonzalo, G.; Mattevi, A.; Fraaije, M. W. Flavoprotein Oxidases: Classification and Applications. *Appl Microbiol Biotechnol* **2013**, 97 (12), 5177–5188.
- (138) Swoboda, B. E.; Massey, V. Purification And Properties Of The Glucose Oxidase From *Aspergillus Niger*. *J Biol Chem* **1965**, 240, 2209–2215.
- (139) Binda, C.; Mattevi, A.; Edmondson, D. E. Structure-Function Relationships in Flavoenzyme-Dependent Amine Oxidations. *Journal of Biological Chemistry* **2002**, 277 (27), 23973–23976.
- (140) Thorpe, C.; Kim, J. P. Structure and Mechanism of Action of the Acyl-CoA Dehydrogenases ¹. *FASEB j.* **1995**, 9 (9), 718–725.
- (141) Coves, J.; Delon, B.; Climent, I.; Sjöberg, B.-M.; Fontecave, M. Enzymic and Chemical Reduction of the Iron Center of the Escherichia Coli Ribonucleotide Reductase Protein R2. The Role of the C-Terminus. *Eur J Biochem* **1995**, 233 (1), 357–363.
- (142) Fontecave, M.; Eliasson, R.; Reichard, P. NAD(P)H:Flavin Oxidoreductase of Escherichia Coli. A Ferric Iron Reductase Participating in the Generation of the Free Radical of Ribonucleotide Reductase. *J Biol Chem* **1987**, 262 (25), 12325–12331.
- (143) Halle, F.; Meyer, J.-M. Iron Release from Ferrisiderophores. A Multi-Step Mechanism Involving a NADH/FMN Oxidoreductase and a Chemical Reduction by FMNH₂. *Eur J Biochem* **1992**, 209 (2), 621–627.

- (144) Tu, S.-C. Reduced Flavin: Donor and Acceptor Enzymes and Mechanisms of Channeling. *Antioxidants & Redox Signaling* **2001**, 3 (5), 881–897.
- (145) Gibson, Q.; Hastings, J. The Oxidation of Reduced Flavin Mononucleotide by Molecular Oxygen. *Biochemical Journal* **1962**, 83 (2), 368–377.
- (146) Sucharitakul, J.; Tinikul, R.; Chaiyen, P. Mechanisms of Reduced Flavin Transfer in the Two-Component Flavin-Dependent Monooxygenases. *Archives of Biochemistry and Biophysics* **2014**, 555–556, 33–46.
- (147) Ellis, H. R. The FMN-Dependent Two-Component Monooxygenase Systems. *Archives of Biochemistry and Biophysics* **2010**, 497 (1–2), 1–12.
- (148) Gunsalus-Miguel, A.; Meighen, E. A.; Nicoli, M. Z.; Nealson, K. H.; Hastings, J. W. Purification and Properties of Bacterial Luciferases. *Journal of Biological Chemistry* **1972**, 247 (2), 398–404.
- (149) Hastings, J. W. Chemistries and Colors of Bioluminescent Reactions: A Review. *Gene* **1996**, 173 (1), 5–11.
- (150) Nivière, V.; Vanoni, M. A.; Zanetti, G.; Fontecave, M. Reaction of the NAD(P)H:Flavin Oxidoreductase from *Escherichia Coli* with NADPH and Riboflavin: Identification of Intermediates. *Biochemistry* **1998**, 37 (34), 11879–11887.
- (151) Tinikul, R.; Thotsaporn, K.; Thaveekarn, W.; Jitrapakdee, S.; Chaiyen, P. The Fusion *Vibrio Campbellii* Luciferase as a Eukaryotic Gene Reporter. *Journal of Biotechnology* **2012**, 162 (2–3), 346–353.
- (152) Pflieger, K. D. G.; Eidne, K. A. Illuminating Insights into Protein-Protein Interactions Using Bioluminescence Resonance Energy Transfer (BRET). *Nat Methods* **2006**, 3 (3), 165–174.
- (153) De Almeida, P. E.; Van Rappard, J. R. M.; Wu, J. C. In Vivo Bioluminescence for Tracking Cell Fate and Function. *American Journal of Physiology-Heart and Circulatory Physiology* **2011**, 301 (3), H663–H671.
- (154) Knobel, H. R.; Egli, T.; Van Der Meer, J. R. Cloning and Characterization of the Genes Encoding Nitrilotriacetate Monooxygenase of *Chelatobacter Heintzii* ATCC 29600. *J Bacteriol* **1996**, 178 (21), 6123–6132.
- (155) Firestone, M. K.; Tiedje, J. M. Pathway of Degradation of Nitrilotriacetate by a *Pseudomonas* Species. *Appl Environ Microbiol* **1978**, 35 (5), 955–961.
- (156) Bohuslavek, J.; Payne, J. W.; Liu, Y.; Bolton, H.; Xun, L. Cloning, Sequencing, and Characterization of a Gene Cluster Involved in EDTA Degradation from the Bacterium BNC1. *Appl Environ Microbiol* **2001**, 67 (2), 688–695.
- (157) Payne, J. W.; Bolton, H.; Campbell, J. A.; Xun, L. Purification and Characterization of EDTA Monooxygenase from the EDTA-Degrading Bacterium BNC1. *J Bacteriol* **1998**, 180 (15), 3823–3827.
- (158) Filisetti, L.; Fontecave, M.; Nivière, V. Mechanism and Substrate Specificity of the Flavin Reductase ActVB from *Streptomyces Coelicolor*. *Journal of Biological Chemistry* **2003**, 278 (1), 296–303.
- (159) Valton, J.; Filisetti, L.; Fontecave, M.; Nivière, V. A Two-Component Flavin-Dependent Monooxygenase Involved in Actinorhodin Biosynthesis in *Streptomyces Coelicolor*. *Journal of Biological Chemistry* **2004**, 279 (43), 44362–44369.
- (160) Thibaut, D.; Ratet, N.; Bisch, D.; Faucher, D.; Debussche, L.; Blanche, F. Purification of the Two-Enzyme System Catalyzing the Oxidation of the D-Proline

- Residue of Pristinamycin IIB during the Last Step of Pristinamycin IIA Biosynthesis. *J Bacteriol* **1995**, 177 (18), 5199–5205.
- (161) Blanc, V.; Lagneaux, D.; Didier, P.; Gil, P.; Lacroix, P.; Crouzet, J. Cloning and Analysis of Structural Genes from *Streptomyces Pristinaespiralis* Encoding Enzymes Involved in the Conversion of Pristinamycin IIB to Pristinamycin IIA (PIIA): PIIA Synthase and NADH:Riboflavin 5'-Phosphate Oxidoreductase. *J Bacteriol* **1995**, 177 (18), 5206–5214.
- (162) Abin-Fuentes, A.; Mohamed, M. E.-S.; Wang, D. I. C.; Prather, K. L. J. Exploring the Mechanism of Biocatalyst Inhibition in Microbial Desulfurization. *Appl Environ Microbiol* **2013**, 79 (24), 7807–7817.
- (163) Oldfield, C.; Pogrebinsky, O.; Simmonds, J.; Olson, E. S.; Kulpa, C. F. Elucidation of the Metabolic Pathway for Dibenzothiophene Desulphurization by *Rhodococcus* Sp. Strain IGTS8 (ATCC 53968). *Microbiology* **1997**, 143 (9), 2961–2973.
- (164) Gray, K. A.; Pogrebinsky, O. S.; Mrachko, G. T.; Xi, L.; Monticello, D. J.; Squires, C. H. Molecular Mechanisms of Biocatalytic Desulfurization of Fossil Fuels. *Nat Biotechnol* **1996**, 14 (13), 1705–1709.
- (165) Adak, S.; Begley, T. P. Dibenzothiophene Catabolism Proceeds via a Flavin-N5-Oxide Intermediate. *J. Am. Chem. Soc.* **2016**, 138 (20), 6424–6426.
- (166) Adak, S.; Begley, T. P. Flavin-N5-Oxide: A New, Catalytic Motif in Flavoenzymology. *Archives of Biochemistry and Biophysics* **2017**, 632, 4–10.
- (167) Wicht, D. K. The Reduced Flavin-Dependent Monooxygenase SfnG Converts Dimethylsulfone to Methanesulfinic Acid. *Archives of Biochemistry and Biophysics* **2016**, 604, 159–166.
- (168) Jeffers, C. E.; Nichols, J. C.; Tu, S.-C. Complex Formation between *Vibrio Harveyi* Luciferase and Monomeric NADPH:FMN Oxidoreductase. *Biochemistry* **2003**, 42 (2), 529–534.
- (169) Lei, B.; Tu, S.-C. Mechanism of Reduced Flavin Transfer from *Vibrio Harveyi* NADPH-FMN Oxidoreductase to Luciferase. *Biochemistry* **1998**, 37 (41), 14623–14629.
- (170) Gao, B.; Ellis, H. R. Altered Mechanism of the Alkanesulfonate FMN Reductase with the Monooxygenase Enzyme. *Biochem Biophys Res Commun* **2005**, 331 (4), 1137–1145.
- (171) Carpenter, R. A.; Zhan, X.; Ellis, H. R. Catalytic Role of a Conserved Cysteine Residue in the Desulfonation Reaction by the Alkanesulfonate Monooxygenase Enzyme. *Biochimica et Biophysica Acta (BBA) - Proteins and Proteomics* **2010**, 1804 (1), 97–105.
- (172) Gao, B.; Ellis, H. R. Mechanism of Flavin Reduction in the Alkanesulfonate Monooxygenase System. *Biochim Biophys Acta* **2007**, 1774 (3), 359–367.
- (173) Gassner, G.; Wang, L.; Batie, C.; Ballou, D. P. Reaction of Phthalate Dioxygenase Reductase with NADH and NAD: Kinetic and Spectral Characterization of Intermediates. *Biochemistry* **1994**, 33 (40), 12184–12193.
- (174) Gassner, G. T.; Ballou, D. P. Preparation and Characterization of a Truncated Form of Phthalate Dioxygenase Reductase That Lacks an Iron-Sulfur Domain. *Biochemistry* **1995**, 34 (41), 13460–13471.
- (175) Vorontsov, I. I.; Minasov, G.; Brunzelle, J. S.; Shuvalova, L.; Kiryukhina, O.; Collart, F. R.; Anderson, W. F. Crystal Structure of an Apo Form of *Shigella Flexneri* ArSH

- Protein with an NADPH-Dependent FMN Reductase Activity. *Protein Sci.* **2007**, *16* (11), 2483–2490.
- (176) Agarwal, R.; Bonanno, J. B.; Burley, S. K.; Swaminathan, S. Structure Determination of an FMN Reductase from *Pseudomonas Aeruginosa* PA01 Using Sulfur Anomalous Signal. *Acta Crystallogr D Biol Crystallogr* **2006**, *62* (4), 383–391.
- (177) Nissen, M. S.; Youn, B.; Knowles, B. D.; Ballinger, J. W.; Jun, S.-Y.; Belchik, S. M.; Xun, L.; Kang, C. Crystal Structures of NADH:FMN Oxidoreductase (EmoB) at Different Stages of Catalysis. *Journal of Biological Chemistry* **2008**, *283* (42), 28710–28720.
- (178) Teufel, R. Flavin-Catalyzed Redox Tailoring Reactions in Natural Product Biosynthesis. *Archives of Biochemistry and Biophysics* **2017**, *632*, 20–27.
- (179) Adak, S.; Begley, T. P. RutA-Catalyzed Oxidative Cleavage of the Uracil Amide Involves Formation of a Flavin-N5-Oxide. *Biochemistry* **2017**, *56* (29), 3708–3709.
- (180) Adak, S.; Begley, T. P. Hexachlorobenzene Catabolism Involves a Nucleophilic Aromatic Substitution and Flavin-N5-Oxide Formation. *Biochemistry* **2019**, *58* (9), 1181–1183.
- (181) Matthews, A.; Schönfelder, J.; Lagies, S.; Schleicher, E.; Kammerer, B.; Ellis, H. R.; Stull, F.; Teufel, R. Bacterial Flavoprotein Monooxygenase YxeK Salvages Toxic S⁻-(2-succino)-adducts via Oxygenolytic C–S Bond Cleavage. *The FEBS Journal* **2022**, *289* (3), 787–807.
- (182) Matthews, A.; Saleem-Batcha, R.; Sanders, J. N.; Stull, F.; Houk, K. N.; Teufel, R. Aminoperoxide Adducts Expand the Catalytic Repertoire of Flavin Monooxygenases. *Nat Chem Biol* **2020**, *16* (5), 556–563.
- (183) Toplak, M.; Matthews, A.; Teufel, R. The Devil Is in the Details: The Chemical Basis and Mechanistic Versatility of Flavoprotein Monooxygenases. *Archives of Biochemistry and Biophysics* **2021**, *698*, 108732.
- (184) Campbell, Z. T.; Weichsel, A.; Montfort, W. R.; Baldwin, T. O. Crystal Structure of the Bacterial Luciferase/Flavin Complex Provides Insight into the Function of the β Subunit. *Biochemistry* **2009**, *48* (26), 6085–6094.
- (185) Li, L.; Liu, X.; Yang, W.; Xu, F.; Wang, W.; Feng, L.; Bartlam, M.; Wang, L.; Rao, Z. Crystal Structure of Long-Chain Alkane Monooxygenase (LadA) in Complex with Coenzyme FMN: Unveiling the Long-Chain Alkane Hydroxylase. *Journal of Molecular Biology* **2008**, *376* (2), 453–465.
- (186) Eichhorn, E.; Davey, C. A.; Sargent, D. F.; Leisinger, T.; Richmond, T. J. Crystal Structure of Escherichia Coli Alkanesulfonate Monooxygenase SsuD. *Journal of Molecular Biology* **2002**, *324* (3), 457–468.
- (187) Fisher, A. J.; Raushel, F. M.; Baldwin, T. O.; Rayment, I. Three-Dimensional Structure of Bacterial Luciferase from *Vibrio Harveyi* at 2.4 Å Resolution. *Biochemistry* **1995**, *34* (20), 6581–6586.
- (188) Xiong, J.; Ellis, H. R. Deletional Studies to Investigate the Functional Role of a Dynamic Loop Region of Alkanesulfonate Monooxygenase. *Biochim Biophys Acta* **2012**, *1824* (7), 898–906.
- (189) Zhan, X.; Carpenter, R. A.; Ellis, H. R. Catalytic Importance of the Substrate Binding Order for the FMN₂-Dependent Alkanesulfonate Monooxygenase Enzyme. *Biochemistry* **2008**, *47* (7), 2221–2230.

- (190) Farber, G. K.; Petsko, G. A. The Evolution of α/β Barrel Enzymes. *Trends in Biochemical Sciences* **1990**, 15 (6), 228–234.
- (191) Malabanan, M. M.; Amyes, T. L.; Richard, J. P. A Role for Flexible Loops in Enzyme Catalysis. *Curr Opin Struct Biol* **2010**, 20 (6), 702–710.
- (192) Carpenter, R. A.; Xiong, J.; Robbins, J. M.; Ellis, H. R. Functional Role of a Conserved Arginine Residue Located on a Mobile Loop of Alkanesulfonate Monooxygenase. *Biochemistry* **2011**, 50 (29), 6469–6477.
- (193) Wierenga, R. K. The TIM-Barrel Fold: A Versatile Framework for Efficient Enzymes. *FEBS Letters* **2001**, 492 (3), 193–198.
- (194) Armacost, K.; Musila, J.; Gathiaka, S.; Ellis, H. R.; Acevedo, O. Exploring the Catalytic Mechanism of Alkanesulfonate Monooxygenase Using Molecular Dynamics. *Biochemistry* **2014**, 53 (20), 3308–3317.
- (195) Thakur, A.; Somai, S.; Yue, K.; Ippolito, N.; Pagan, D.; Xiong, J.; Ellis, H. R.; Acevedo, O. Substrate-Dependent Mobile Loop Conformational Changes in Alkanesulfonate Monooxygenase from Accelerated Molecular Dynamics. *Biochemistry* **2020**, 59 (38), 3582–3593.
- (196) Fisher, A. J.; Thompson, T. B.; Thoden, J. B.; Baldwin, T. O.; Rayment, I. The 1.5-Å Resolution Crystal Structure of Bacterial Luciferase in Low Salt Conditions. *Journal of Biological Chemistry* **1996**, 271 (36), 21956–21968.
- (197) Robbins, J. M.; Ellis, H. R. Identification of Critical Steps Governing the Two-Component Alkanesulfonate Monooxygenase Catalytic Mechanism. *Biochemistry* **2012**, 51 (32), 6378–6387.
- (198) Huang, S.; Tu, S.-C. Identification and Characterization of a Catalytic Base in Bacterial Luciferase by Chemical Rescue of a Dark Mutant. *Biochemistry* **1997**, 36 (48), 14609–14615.
- (199) Robbins, J. M.; Ellis, H. R. Steady-State Kinetic Isotope Effects Support a Complex Role of Arg226 in the Proposed Desulfonation Mechanism of Alkanesulfonate Monooxygenase. *Biochemistry* **2014**, 53 (1), 161–168.
- (200) Massey, V. Activation of Molecular Oxygen by Flavins and Flavoproteins. *Journal of Biological Chemistry* **1994**, 269 (36), 22459–22462.
- (201) Robbins, J. M.; Ellis, H. R. Investigations of Two-Component Flavin-Dependent Monooxygenase Systems. In *Methods in Enzymology*; Elsevier, **2019**; Vol. 620, pp 399–422.
- (202) Galán, B.; Díaz, E.; Prieto, M. A.; García, J. L. Functional Analysis of the Small Component of the 4-Hydroxyphenylacetate 3-Monooxygenase of *Escherichia Coli* W: A Prototype of a New Flavin:NAD(P)H Reductase Subfamily. *J Bacteriol* **2000**, 182 (3), 627–636.
- (203) Louie, T. M.; Xie, X. S.; Xun, L. Coordinated Production and Utilization of FADH₂ by NAD(P)H-Flavin Oxidoreductase and 4-Hydroxyphenylacetate 3-Monooxygenase. *Biochemistry* **2003**, 42 (24), 7509–7517.
- (204) Jun, S.; Lewis, K. M.; Youn, B.; Xun, L.; Kang, C. Structural and Biochemical Characterization of EDTA Monooxygenase and Its Physical Interaction with a Partner Flavin Reductase. *Molecular Microbiology* **2016**, 100 (6), 989–1003.
- (205) Abdurachim, K.; Ellis, H. R. Detection of Protein-Protein Interactions in the Alkanesulfonate Monooxygenase System from *Escherichia Coli*. *J Bacteriol* **2006**, 188 (23), 8153–8159.

- (206) Morrison, E.; Kantz, A.; Gassner, G. T.; Sazinsky, M. H. Structure and Mechanism of Styrene Monooxygenase Reductase: New Insight into the FAD-Transfer Reaction. *Biochemistry* **2013**, 52 (35), 6063–6075.
- (207) Kantz, A.; Chin, F.; Nallamotheu, N.; Nguyen, T.; Gassner, G. T. Mechanism of Flavin Transfer and Oxygen Activation by the Two-Component Flavoenzyme Styrene Monooxygenase. *Archives of Biochemistry and Biophysics* **2005**, 442 (1), 102–116.
- (208) Dayal, P. V.; Singh, H.; Busenlehner, L. S.; Ellis, H. R. Exposing the Alkanesulfonate Monooxygenase Protein-Protein Interaction Sites. *Biochemistry* **2015**, 54 (51), 7531–7538.
- (209) Chapman, R.; Kulp, III, J. L.; Patgiri, A.; Kallenbach, N. R.; Bracken, C.; Arora, P. S. Trapping a Folding Intermediate of the α -Helix: Stabilization of the π -Helix. *Biochemistry* **2008**, 47 (14), 4189–4195.
- (210) Halling, P. J. *Proteins: Structures and Molecular Properties* (2nd Edition). by Thomas E. Creighton, W. H. Freeman, New York, 1992, Xiii + 512 Pp, Price £22.95. ISBN 0-7167-7030-X. *J. Chem. Technol. Biotechnol.* **1995**, 62 (1), 105–105.
- (211) Weaver, T. M. The Pi-Helix Translates Structure into Function. *Protein Sci* **2000**, 9 (1), 201–206.
- (212) Fodje, M. N.; Al-Karadaghi, S. Occurrence, Conformational Features and Amino Acid Propensities for the π -Helix. *Protein Engineering, Design and Selection* **2002**, 15 (5), 353–358.
- (213) Cooley, R. B.; Arp, D. J.; Karplus, P. A. Evolutionary Origin of a Secondary Structure: π -Helices as Cryptic but Widespread Insertional Variations of α -Helices That Enhance Protein Functionality. *Journal of Molecular Biology* **2010**, 404 (2), 232–246.
- (214) Rohl, C. A.; Doig, A. J. Models for the 3(10)-Helix/Coil, Pi-Helix/Coil, and Alpha-Helix/3(10)-Helix/Coil Transitions in Isolated Peptides. *Protein Sci* **1996**, 5 (8), 1687–1696.
- (215) Armen, R.; Alonso, D. O. V.; Daggett, V. The Role of α -, 3₁₀-, and π -Helix in Helix→coil Transitions. *Protein Sci* **2003**, 12 (6), 1145–1157.
- (216) Mikhonin, A. V.; Asher, S. A. Direct UV Raman Monitoring of 3₁₀-Helix and π -Bulge Premelting during α -Helix Unfolding. *J. Am. Chem. Soc.* **2006**, 128 (42), 13789–13795.
- (217) Mahadevan, J.; Lee, K.-H.; Kuczera, K. Conformational Free Energy Surfaces of Ala₁₀ and Aib₁₀ Peptide Helices in Solution. *J. Phys. Chem. B* **2001**, 105 (9), 1863–1876.
- (218) Lee, K.-H.; Benson, D. R.; Kuczera, K. Transitions from α to π Helix Observed in Molecular Dynamics Simulations of Synthetic Peptides. *Biochemistry* **2000**, 39 (45), 13737–13747.
- (219) Feig, M.; MacKerell, A. D.; Brooks, C. L. Force Field Influence on the Observation of π -Helical Protein Structures in Molecular Dynamics Simulations. *J. Phys. Chem. B* **2003**, 107 (12), 2831–2836.
- (220) Rajashankar, K. R.; Ramakumar, S. π -Turns in Proteins and Peptides: Classification, Conformation, Occurrence, Hydration and Sequence: π -Turns in Proteins and Peptides. *Protein Science* **1996**, 5 (5), 932–946.
- (221) Kumar, P.; Bansal, M. Dissecting π -Helices: Sequence, Structure and Function. *The FEBS Journal* **2015**, 282 (22), 4415–4432.

- (222) Richardson, J. S.; Richardson, D. C. Amino Acid Preferences for Specific Locations at the Ends of α Helices. *Science* **1988**, *240* (4859), 1648–1652.
- (223) Cartailier, J.-P.; Luecke, H. Structural and Functional Characterization of π Bulges and Other Short Intrahelical Deformations. *Structure* **2004**, *12* (1), 133–144.
- (224) Low, B. W.; Grenville-Wells, H. J. Generalized Mathematical Relationships for Polypeptide Chain Helices: The Coordinates of the II Helix. *Proc Natl Acad Sci U S A* **1953**, *39* (8), 785–801.
- (225) Guex, N.; Peitsch, M. C. SWISS-MODEL and the Swiss-Pdb Viewer: An Environment for Comparative Protein Modeling. *Electrophoresis* **1997**, *18* (15), 2714–2723.
- (226) Bradshaw, M. D.; Gaffney, B. J. Fluctuations of an Exposed π -Helix Involved in Lipoygenase Substrate Recognition. *Biochemistry* **2014**, *53* (31), 5102–5110.
- (227) Rennex, D.; Cummings, R. T.; Pickett, M.; Walsh, C. T.; Bradley, M. Role of Tyrosine Residues in Mercury(II) Detoxification by Mercuric Reductase from *Bacillus* Sp. Strain RC607. *Biochemistry* **1993**, *32* (29), 7475–7478.
- (228) Gibson, R. P.; Turkenburg, J. P.; Charnock, S. J.; Lloyd, R.; Davies, G. J. Insights into Trehalose Synthesis Provided by the Structure of the Retaining Glucosyltransferase OtsA. *Chemistry & Biology* **2002**, *9* (12), 1337–1346.
- (229) Sazinsky, M. H.; Lippard, S. J. Product Bound Structures of the Soluble Methane Monooxygenase Hydroxylase from *Methylococcus Capsulatus* (Bath): Protein Motion in the α -Subunit. *J. Am. Chem. Soc.* **2005**, *127* (16), 5814–5825.
- (230) Bailey, L. J.; McCoy, J. G.; Phillips, G. N.; Fox, B. G. Structural Consequences of Effector Protein Complex Formation in a Diiron Hydroxylase. *Proc. Natl. Acad. Sci. U.S.A.* **2008**, *105* (49), 19194–19198.
- (231) McFarlane, J. S.; Hagen, R. A.; Chilton, A. S.; Forbes, D. L.; Lamb, A. L.; Ellis, H. R. Not as Easy as π : An Insertional Residue Does Not Explain the Π -helix Gain-of-function in Two-component FMN Reductases. *Protein Science* **2019**, *28* (1), 123–134.
- (232) Musila, J. M.; Ellis, H. R. Transformation of a Flavin-Free FMN Reductase to a Canonical Flavoprotein through Modification of the π -Helix. *Biochemistry* **2016**, *55* (46), 6389–6394.
- (233) Musila, J. M.; L. Forbes, D.; Ellis, H. R. Functional Evaluation of the π -Helix in the NAD(P)H:FMN Reductase of the Alkanesulfonate Monooxygenase System. *Biochemistry* **2018**, *57* (30), 4469–4477.
- (234) Gotte, G.; Libonati, M. Protein Oligomerization. In *Oligomerization of Chemical and Biological Compounds*; Lesieur, C., Ed.; InTech, 2014. <https://doi.org/10.5772/57489>.
- (235) Anfinsen, C. B. Principles That Govern the Folding of Protein Chains. *Science* **1973**, *181* (4096), 223–230.
- (236) Frieden, C. Protein Oligomerization as a Metabolic Control Mechanism: Application to ApoE. *Protein Sci* **2019**, *28* (4), 837–842.
- (237) Levy, E. D.; Teichmann, S. A. Structural, Evolutionary, and Assembly Principles of Protein Oligomerization. In *Progress in Molecular Biology and Translational Science*; Elsevier, **2013**; Vol. 117, pp 25–51.
- (238) Griffin, M. D. W.; Gerrard, J. A. The Relationship between Oligomeric State and Protein Function. In *Protein Dimerization and Oligomerization in Biology*; Matthews, J. M., Ed.; Advances in Experimental Medicine and Biology; Springer New York: New York, NY, **2012**; Vol. 747, pp 74–90.

- (239) Monod, J.; Wyman, J.; Changeux, J.-P. On the Nature of Allosteric Transitions: A Plausible Model. *Journal of Molecular Biology* **1965**, *12* (1), 88–118.
- (240) *Protein Dimerization and Oligomerization in Biology*; Matthews, J. M., Ed.; Advances in Experimental Medicine and Biology; Springer: New York, NY, **2012**; Vol. 747.
- (241) Nooren, I. M. A.; Thornton, J. M. Diversity of Protein-Protein Interactions. *EMBO J* **2003**, *22* (14), 3486–3492.
- (242) Jones, S.; Thornton, J. M. Analysis of Protein-Protein Interaction Sites Using Surface Patches 1 Edited by G.Von Heijne. *Journal of Molecular Biology* **1997**, *272* (1), 121–132.
- (243) Teyra, J.; Pisabarro, M. T. Characterization of Interfacial Solvent in Protein Complexes and Contribution of Wet Spots to the Interface Description. *Proteins* **2007**, *67* (4), 1087–1095.
- (244) Acuner Ozbabacan, S. E.; Engin, H. B.; Gursoy, A.; Keskin, O. Transient Protein-Protein Interactions. *Protein Eng Des Sel* **2011**, *24* (9), 635–648. <https://doi.org/10.1093/protein/gzr025>.
- (245) McCafferty, C. L.; Marcotte, E. M.; Taylor, D. W. Simplified Geometric Representations of Protein Structures Identify Complementary Interaction Interfaces. *Proteins* **2021**, *89* (3), 348–360.
- (246) Schreiber, G.; Haran, G.; Zhou, H.-X. Fundamental Aspects of Protein-Protein Association Kinetics. *Chem. Rev.* **2009**, *109* (3), 839–860.
- (247) Nooren, I. M. A.; Thornton, J. M. Structural Characterisation and Functional Significance of Transient Protein-Protein Interactions. *J Mol Biol* **2003**, *325* (5), 991–1018.
- (248) Dehner, C. Why Do Proteins Have Quaternary Structure: Non-Allosteric Proteins. In *Molecular Life Sciences: An Encyclopedic Reference*; Wells, R. D., Bond, J. S., Klinman, J., Masters, B. S. S., Bell, E., Eds.; Springer: New York, NY, **2014**; pp 1–7.
- (249) Berg, J. M.; Tymoczko, J. L.; Stryer, L. *Biochemistry: This Edition Is for Use Outside the USA and Canada*, 7. ed., international ed., [Nachdr.]; Freeman, Palgrave Macmillan: New York, NY, **2012**.
- (250) Miles, E. W. Tryptophan Synthase: A Multienzyme Complex with an Intramolecular Tunnel. *Chem. Record* **2001**, *1* (2), 140–151.
- (251) Hilario, E.; Caulkins, B. G.; Huang, Y.-M. M.; You, W.; Chang, C.-E. A.; Mueller, L. J.; Dunn, M. F.; Fan, L. Visualizing the Tunnel in Tryptophan Synthase with Crystallography: Insights into a Selective Filter for Accommodating Indole and Rejecting Water. *Biochimica et Biophysica Acta (BBA) - Proteins and Proteomics* **2016**, *1864* (3), 268–279.
- (252) Gabizon, R.; Friedler, A. Allosteric Modulation of Protein Oligomerization: An Emerging Approach to Drug Design. *Front. Chem.* **2014**, *2*:9.
- (253) He, M. M.; Smith, A. S.; Oslob, J. D.; Flanagan, W. M.; Braisted, A. C.; Whitty, A.; Cancilla, M. T.; Wang, J.; Lugovskoy, A. A.; Yoburn, J. C.; Fung, A. D.; Farrington, G.; Eldredge, J. K.; Day, E. S.; Cruz, L. A.; Cachero, T. G.; Miller, S. K.; Friedman, J. E.; Choong, I. C.; Cunningham, B. C. Small-Molecule Inhibition of TNF- α . *Science* **2005**, *310* (5750), 1022–1025.
- (254) Dömling, A.; Li, X. TNF- α : The Shape of Small Molecules to Come? *Drug Discovery Today* **2022**, *27* (1), 3–7.

- (255) O'Connell, J.; Porter, J.; Kroeplien, B.; Norman, T.; Rapecki, S.; Davis, R.; McMillan, D.; Arakaki, T.; Burgin, A.; Fox III, D.; Ceska, T.; Lecomte, F.; Maloney, A.; Vugler, A.; Carrington, B.; Cossins, B. P.; Bourne, T.; Lawson, A. Small Molecules That Inhibit TNF Signalling by Stabilising an Asymmetric Form of the Trimer. *Nat Commun* **2019**, *10* (1), 5795.
- (256) Lawrence, S. H.; Jaffe, E. K. Expanding the Concepts in Protein Structure-Function Relationships and Enzyme Kinetics: Teaching Using Morpheesins. *Biochem. Mol. Biol. Educ.* **2008**, *36* (4), 274–283.
- (257) Breinig, S.; Kervinen, J.; Stith, L.; Wasson, A. S.; Fairman, R.; Wlodawer, A.; Zdanov, A.; Jaffe, E. K. Control of Tetrapyrrole Biosynthesis by Alternate Quaternary Forms of Porphobilinogen Synthase. *Nat Struct Mol Biol* **2003**, *10* (9), 757–763.
- (258) Jaffe, E. K. Morpheesins – a New Structural Paradigm for Allosteric Regulation. *Trends in Biochemical Sciences* **2005**, *30* (9), 490–497.
- (259) Selwood, T.; Tang, L.; Lawrence, S. H.; Anokhina, Y.; Jaffe, E. K. Kinetics and Thermodynamics of the Interchange of the Morpheein Forms of Human Porphobilinogen Synthase. *Biochemistry* **2008**, *47* (10), 3245–3257.
- (260) Tang, L.; Breinig, S.; Stith, L.; Mischel, A.; Tannir, J.; Kokona, B.; Fairman, R.; Jaffe, E. K. Single Amino Acid Mutations Alter the Distribution of Human Porphobilinogen Synthase Quaternary Structure Isoforms (Morpheesins). *Journal of Biological Chemistry* **2006**, *281* (10), 6682–6690.
- (261) Liu, M.; Lei, B.; Ding, Q.; Lee, J. C.; Tu, S.-C. Vibrio Harveyi NADPH:FMN Oxidoreductase: Preparation and Characterization of the Apoenzyme and Monomer–Dimer Equilibrium. *Archives of Biochemistry and Biophysics* **1997**, *337* (1), 89–95.
- (262) Sedláček, V.; Klumpler, T.; Marek, J.; Kučera, I. The Structural and Functional Basis of Catalysis Mediated by NAD(P)H:Acceptor Oxidoreductase (FerB) of Paracoccus Denitrificans. *PLoS ONE* **2014**, *9* (5), e96262.
- (263) Nijvipakul, S.; Ballou, D. P.; Chaiyen, P. Reduction Kinetics of a Flavin Oxidoreductase LuxG from Photobacterium Leiognathi (TH1): Half-Sites Reactivity. *Biochemistry* **2010**, *49* (43), 9241–9248.
- (264) *Protein-Protein Recognition*; Kleanthous, C., Ed.; Frontiers in molecular biology; Oxford University Press: Oxford ; New York, **2000**.
- (265) Keskin, O.; Ma, B.; Nussinov, R. Hot Regions in Protein–Protein Interactions: The Organization and Contribution of Structurally Conserved Hot Spot Residues. *Journal of Molecular Biology* **2005**, *345* (5), 1281–1294.
- (266) *Molecular Biology of the Cell*, 4th ed.; Alberts, B., Ed.; Garland Science: New York, **2002**.
- (267) Sukhwal, A.; Sowdhamini, R. Oligomerisation Status and Evolutionary Conservation of Interfaces of Protein Structural Domain Superfamilies. *Mol Biosyst* **2013**, *9* (7), 1652–1661.
- (268) Wang, J.; Zhang, L.; Jia, L.; Ren, Y.; Yu, G. Protein-Protein Interactions Prediction Using a Novel Local Conjoint Triad Descriptor of Amino Acid Sequences. *IJMS* **2017**, *18* (11), 2373.
- (269) Shen, J.; Zhang, J.; Luo, X.; Zhu, W.; Yu, K.; Chen, K.; Li, Y.; Jiang, H. Predicting Protein–Protein Interactions Based Only on Sequences Information. *Proc. Natl. Acad. Sci. U.S.A.* **2007**, *104* (11), 4337–4341.

- (270) Robinson, C. V.; Sali, A.; Baumeister, W. The Molecular Sociology of the Cell. *Nature* **2007**, *450* (7172), 973–982.
- (271) Janin, J.; Bahadur, R. P.; Chakrabarti, P. Protein-Protein Interaction and Quaternary Structure. *Q Rev Biophys* **2008**, *41* (2), 133–180.
- (272) Keskin, O.; Tsai, C.-J.; Wolfson, H.; Nussinov, R. A New, Structurally Nonredundant, Diverse Data Set of Protein-Protein Interfaces and Its Implications. *Protein Sci.* **2004**, *13* (4), 1043–1055.
- (273) Bogan, A. A.; Thorn, K. S. Anatomy of Hot Spots in Protein Interfaces. *J Mol Biol* **1998**, *280* (1), 1–9.
- (274) Chakrabarti, P.; Janin, J. Dissecting Protein-Protein Recognition Sites. *Proteins* **2002**, *47* (3), 334–343.
- (275) Chothia, C.; Janin, J. Principles of Protein–Protein Recognition. *Nature* **1975**, *256* (5520), 705–708.
- (276) Horton, N.; Lewis, M. Calculation of the Free Energy of Association for Protein Complexes. *Protein Sci* **1992**, *1* (1), 169–181.
- (277) Jones, S.; Thornton, J. M. Principles of Protein-Protein Interactions. *Proc Natl Acad Sci U S A* **1996**, *93* (1), 13–20.
- (278) Privalov, P. L. Stability of Proteins Small Globular Proteins. In *Advances in Protein Chemistry*; Elsevier, **1979**; Vol. 33, pp 167–241.
- (279) Jones, S.; Thornton, J. M. Prediction of Protein-Protein Interaction Sites Using Patch Analysis. *J Mol Biol* **1997**, *272* (1), 133–143.
- (280) Jones, S.; Marin, A.; Thornton, J. Protein Domain Interfaces: Characterization and Comparison with Oligomeric Protein Interfaces. *Protein Engineering, Design and Selection* **2000**, *13* (2), 77–82.
- (281) Tsai, C.-J.; Lin, S. L.; Wolfson, H. J.; Nussinov, R. A Dataset of Protein–Protein Interfaces Generated with a Sequence-Order-Independent Comparison Technique. *Journal of Molecular Biology* **1996**, *260* (4), 604–620.
- (282) Thorn, K. S.; Bogan, A. A. ASEdb: A Database of Alanine Mutations and Their Effects on the Free Energy of Binding in Protein Interactions. *Bioinformatics* **2001**, *17* (3), 284–285.
- (283) Res, I.; Lichtarge, O. Character and Evolution of Protein-Protein Interfaces. *Phys Biol* **2005**, *2* (2), S36–43.
- (284) Wells, J. A. [18] Systematic Mutational Analyses of Protein-Protein Interfaces. In *Methods in Enzymology*; Elsevier, **1991**; Vol. 202, pp 390–411.
- (285) Clackson, T.; Wells, J. A. A Hot Spot of Binding Energy in a Hormone-Receptor Interface. *Science* **1995**, *267* (5196), 383–386.
- (286) Keskin, O.; Tuncbag, N.; Gursoy, A. Predicting Protein–Protein Interactions from the Molecular to the Proteome Level. *Chem. Rev.* **2016**, *116* (8), 4884–4909.
- (287) Sheinerman, F. B.; Honig, B. On the Role of Electrostatic Interactions in the Design of Protein–Protein Interfaces. *Journal of Molecular Biology* **2002**, *318* (1), 161–177.
- (288) Tsai, C. J.; Lin, S. L.; Wolfson, H. J.; Nussinov, R. Studies of Protein-Protein Interfaces: A Statistical Analysis of the Hydrophobic Effect. *Protein Sci* **1997**, *6* (1), 53–64.
- (289) Rodier, F.; Bahadur, R. P.; Chakrabarti, P.; Janin, J. Hydration of Protein-Protein Interfaces. *Proteins* **2005**, *60* (1), 36–45.

- (290) Veselovsky, A. V.; Ivanov, Y. D.; Ivanov, A. S.; Archakov, A. I.; Lewi, P.; Janssen, P. Protein-Protein Interactions: Mechanisms and Modification by Drugs. *J Mol Recognit* **2002**, 15 (6), 405–422.
- (291) Janin, J.; Miller, S.; Chothia, C. Surface, Subunit Interfaces and Interior of Oligomeric Proteins. *Journal of Molecular Biology* **1988**, 204 (1), 155–164.
- (292) Lee, B.; Richards, F. M. The Interpretation of Protein Structures: Estimation of Static Accessibility. *Journal of Molecular Biology* **1971**, 55 (3), 379–IN4.
- (293) Lawrence, M. C.; Colman, P. M. Shape Complementarity at Protein/Protein Interfaces. *Journal of Molecular Biology* **1993**, 234 (4), 946–950.
- (294) Guharoy, M.; Chakrabarti, P. Secondary Structure Based Analysis and Classification of Biological Interfaces: Identification of Binding Motifs in Protein–Protein Interactions. *Bioinformatics* **2007**, 23 (15), 1909–1918.
- (295) Argos, P. An Investigation of Protein Subunit and Domain Interfaces. *Protein Eng Des Sel* **1988**, 2 (2), 101–113.
- (296) Dou, Y.; Baisnée, P.-F.; Pollastri, G.; Pécout, Y.; Nowick, J.; Baldi, P. ICBS: A Database of Interactions between Protein Chains Mediated by β -Sheet Formation. *Bioinformatics* **2004**, 20 (16), 2767–2777.
- (297) Ansari, S.; Helms, V. Statistical Analysis of Predominantly Transient Protein-Protein Interfaces. *Proteins* **2005**, 61 (2), 344–355.
- (298) Luo, J.; Liu, Z.; Guo, Y.; Li, M. A Structural Dissection of Large Protein-Protein Crystal Packing Contacts. *Sci Rep* **2015**, 5 (1), 14214.
- (299) Miller, S. The Structure of Interfaces between Subunits of Dimeric and Tetrameric Proteins. *Protein Eng Des Sel* **1989**, 3 (2), 77–83.
- (300) Hoskins, J.; Lovell, S.; Blundell, T. L. An Algorithm for Predicting Protein-Protein Interaction Sites: Abnormally Exposed Amino Acid Residues and Secondary Structure Elements. *Protein Sci.* **2006**, 15 (5), 1017–1029.
- (301) Prasad Bahadur, R.; Chakrabarti, P.; Rodier, F.; Janin, J. A Dissection of Specific and Non-Specific Protein–Protein Interfaces. *Journal of Molecular Biology* **2004**, 336 (4), 943–955.
- (302) Kuroda, D.; Gray, J. J. Shape Complementarity and Hydrogen Bond Preferences in Protein-Protein Interfaces: Implications for Antibody Modeling and Protein-Protein Docking. *Bioinformatics* **2016**, 32 (16), 2451–2456.
- (303) Jiang, S.; Tovchigrechko, A.; Vakser, I. A. The Role of Geometric Complementarity in Secondary Structure Packing: A Systematic Docking Study. *Protein Sci.* **2003**, 12 (8), 1646–1651.
- (304) Guo, F.; Li, S. C.; Ma, W.; Wang, L. Detecting Protein Conformational Changes in Interactions via Scaling Known Structures. *Journal of Computational Biology* **2013**, 20 (10), 765–779.
- (305) Perkins, J. R.; Diboun, I.; Dessailly, B. H.; Lees, J. G.; Orengo, C. Transient Protein-Protein Interactions: Structural, Functional, and Network Properties. *Structure* **2010**, 18 (10), 1233–1243.
- (306) Betts, M. J.; Sternberg, M. J. E. An Analysis of Conformational Changes on Protein–Protein Association: Implications for Predictive Docking. *Protein Engineering, Design and Selection* **1999**, 12 (4), 271–283.
- (307) Janin, J.; Chothia, C. The Structure of Protein-Protein Recognition Sites. *J Biol Chem* **1990**, 265 (27), 16027–16030.

- (308) Erijman, A.; Rosenthal, E.; Shifman, J. M. How Structure Defines Affinity in Protein-Protein Interactions. *PLoS ONE* **2014**, 9 (10), e110085.
- (309) Phizicky, E. M.; Fields, S. Protein-Protein Interactions: Methods for Detection and Analysis. *Microbiol Rev* **1995**, 59 (1), 94–123. <https://doi.org/10.1128/mr.59.1.94-123.1995>.
- (310) Kastritis, P. L.; Bonvin, A. M. J. J. On the Binding Affinity of Macromolecular Interactions: Daring to Ask Why Proteins Interact. *J. R. Soc. Interface*. **2013**, 10 (79), 20120835.
- (311) Rao, V. S.; Srinivas, K.; Sujini, G. N.; Kumar, G. N. S. Protein-Protein Interaction Detection: Methods and Analysis. *International Journal of Proteomics* **2014**, 2014, e147648.
- (312) Yanagida, M. Functional Proteomics; Current Achievements. *Journal of Chromatography B* **2002**, 771 (1–2), 89–106.
- (313) Berggård, T.; Linse, S.; James, P. Methods for the Detection and Analysis of Protein–Protein Interactions. *Proteomics* **2007**, 7 (16), 2833–2842.
- (314) Von Mering, C.; Krause, R.; Snel, B.; Cornell, M.; Oliver, S. G.; Fields, S.; Bork, P. Comparative Assessment of Large-Scale Data Sets of Protein–Protein Interactions. *Nature* **2002**, 417 (6887), 399–403.
- (315) Srere, P. A. Complexes Of Sequential Metabolic Enzymes. *Annu. Rev. Biochem.* **1987**, 56 (1), 89–124.
- (316) Rudolph, J.; Stubbe, J. Investigation of the Mechanism of Phosphoribosylamine Transfer from Glutamine Phosphoribosylpyrophosphate Amidotransferase to Glycinamide Ribonucleotide Synthetase. *Biochemistry* **1995**, 34 (7), 2241–2250.
- (317) Spivey, H. O.; Ovádi, J. Substrate Channeling. *Methods* **1999**, 19 (2), 306–321.
- (318) Easterby, J. S. A Generalized Theory of the Transition Time for Sequential Enzyme Reactions. *Biochemical Journal* **1981**, 199 (1), 155–161.
- (319) Imlay, J. A. Pathways of Oxidative Damage. *Annu. Rev. Microbiol.* **2003**, 57 (1), 395–418.
- (320) Ali, M. H.; Imperiali, B. Protein Oligomerization: How and Why. *Bioorg Med Chem* **2005**, 13 (17), 5013–5020.
- (321) Eswaramoorthy, S.; Poulain, S.; Hienerwadel, R.; Bremond, N.; Sylvester, M. D.; Zhang, Y.-B.; Berthomieu, C.; Van Der Lelie, D.; Matin, A. Crystal Structure of ChrR—A Quinone Reductase with the Capacity to Reduce Chromate. *PLoS ONE* **2012**, 7 (4), e36017.
- (322) Jin, H.; Zhang, Y.; Buchko, G. W.; Varnum, S. M.; Robinson, H.; Squier, T. C.; Long, P. E. Structure Determination and Functional Analysis of a Chromate Reductase from *Gluconacetobacter Hansenii*. *PLoS ONE* **2012**, 7 (8), e42432. h
- (323) M., K.; C., W. Desulfurization and Desulfonation: Applications of Sulfur-Controlled Gene Expression in Bacteria. *Applied Microbiology and Biotechnology* **2001**, 57 (4), 460–466.
- (324) Kertesz, M. A. Riding the Sulfur Cycle – Metabolism of Sulfonates and Sulfate Esters in Gram-Negative Bacteria. *FEMS Microbiol Rev* **2000**, 24 (2), 135–175.
- (325) Eichhorn, E.; Van Der Ploeg, J. R.; Leisinger, T. Characterization of a Two-Component Alkanesulfonate Monooxygenase from *Escherichia Coli*. *Journal of Biological Chemistry* **1999**, 274 (38), 26639–26646.

- (326) Wicht, D. K. The Reduced Flavin-Dependent Monooxygenase SfnG Converts Dimethylsulfone to Methanesulfinat. *Archives of Biochemistry and Biophysics* **2016**, *604*, 159–166.
- (327) Driggers, C. M.; Dayal, P. V.; Ellis, H. R.; Karplus, P. A. Crystal Structure of *Escherichia Coli* SsuE: Defining a General Catalytic Cycle for FMN Reductases of the Flavodoxin-like Superfamily. *Biochemistry* **2014**, *53* (21), 3509–3519.
- (328) Tu, S.-C.; Lei, B.; Liu, M.; Tang, C.-K.; Jeffers, C. Probing the Mechanisms of the Biological Intermolecular Transfer of Reduced Flavin. *The Journal of Nutrition* **2000**, *130* (2), 331S–332S.
- (329) Jeffers, C. E.; Nichols, J. C.; Tu, S.-C. Complex Formation between *Vibrio Harveyi* Luciferase and Monomeric NADPH:FMN Oxidoreductase. *Biochemistry* **2003**, *42* (2), 529–534.
- (330) Dayal, P. V.; Singh, H.; Busenlehner, L. S.; Ellis, H. R. Exposing the Alkanesulfonate Monooxygenase Protein–Protein Interaction Sites. *Biochemistry* **2015**, *54* (51), 7531–7538.
- (331) Li, H.; Forson, B.; Eckshtain-Levi, M.; Valentino, H.; Martín Del Campo, J. S.; Tanner, J. J.; Sobrado, P. Biochemical Characterization of the Two-Component Flavin-Dependent Monooxygenase Involved in Valanimycin Biosynthesis. *Biochemistry* **2021**, *60* (1), 31–40.
- (332) Schuck, P. Size-Distribution Analysis of Macromolecules by Sedimentation Velocity Ultracentrifugation and Lamm Equation Modeling. *Biophysical Journal* **2000**, *78* (3), 1606–1619.
- (333) Jumper, J.; Evans, R.; Pritzel, A.; Green, T.; Figurnov, M.; Ronneberger, O.; Tunyasuvunakool, K.; Bates, R.; Žídek, A.; Potapenko, A.; Bridgland, A.; Meyer, C.; Kohl, S. A. A.; Ballard, A. J.; Cowie, A.; Romera-Paredes, B.; Nikolov, S.; Jain, R.; Adler, J.; Back, T.; Petersen, S.; Reiman, D.; Clancy, E.; Zielinski, M.; Steinegger, M.; Pacholska, M.; Berghammer, T.; Bodenstein, S.; Silver, D.; Vinyals, O.; Senior, A. W.; Kavukcuoglu, K.; Kohli, P.; Hassabis, D. Highly Accurate Protein Structure Prediction with AlphaFold. *Nature* **2021**, *596* (7873), 583–589.
- (334) Li, B.; Lin, S.-X. Fluorescence-Energy Transfer in Human Estradiol 17 β -Dehydrogenase-NADPH Complex and Studies on the Coenzyme Binding. *Eur J Biochem* **1996**, *235* (1–2), 180–186.
- (335) James, E. I.; Murphree, T. A.; Vorauer, C.; Engen, J. R.; Guttman, M. Advances in Hydrogen/Deuterium Exchange Mass Spectrometry and the Pursuit of Challenging Biological Systems. *Chem. Rev.* **2022**, *122* (8), 7562–7623.
- (336) Sitkiewicz, E.; Tarnowski, K.; Poznański, J.; Kulma, M.; Dadlez, M. Oligomerization Interface of RAGE Receptor Revealed by MS-Monitored Hydrogen Deuterium Exchange. *PLoS ONE* **2013**, *8* (10), e76353.
- (337) Dautant, A.; Meyer, P.; Georgescauld, F. Hydrogen/Deuterium Exchange Mass Spectrometry Reveals Mechanistic Details of Activation of Nucleoside Diphosphate Kinases by Oligomerization. *Biochemistry* **2017**, *56* (23), 2886–2896.
- (338) Illes-Toth, E.; Meisl, G.; Rempel, D. L.; Knowles, T. P. J.; Gross, M. L. Pulsed Hydrogen–Deuterium Exchange Reveals Altered Structures and Mechanisms in the Aggregation of Familial Alzheimer’s Disease Mutants. *ACS Chem. Neurosci.* **2021**, *12* (11), 1972–1982.

- (339) Polakowska, M.; Steczkiewicz, K.; Szczepanowski, R. H.; Wyslouch-Cieszyńska, A. Toward an Understanding of the Conformational Plasticity of S100A8 and S100A9 Ca²⁺-Binding Proteins. *Journal of Biological Chemistry* **2023**, 299 (4), 102952. <https://doi.org/10.1016/j.jbc.2023.102952>.
- (340) Marsh, J. A.; Teichmann, S. A. Structure, Dynamics, Assembly, and Evolution of Protein Complexes. *Annu. Rev. Biochem.* **2015**, 84 (1), 551–575.
- (341) Kendrew, S. G.; Harding, S. E.; Hopwood, D. A.; Marsh, E. N. G. Identification of a Flavin:NADH Oxidoreductase Involved in the Biosynthesis of Actinorhodin. *Journal of Biological Chemistry* **1995**, 270 (29), 17339–17343.
- (342) Musila, J. M.; L. Forbes, D.; Ellis, H. R. Functional Evaluation of the π -Helix in the NAD(P)H:FMN Reductase of the Alkanesulfonate Monooxygenase System. *Biochemistry* **2018**, 57 (30), 4469–4477.
- (343) Sucharitakul, J.; Phongsak, T.; Entsch, B.; Svasti, J.; Chaiyen, P.; Ballou, D. P. Kinetics of a Two-Component *p*-Hydroxyphenylacetate Hydroxylase Explain How Reduced Flavin Is Transferred from the Reductase to the Oxygenase. *Biochemistry* **2007**, 46 (29), 8611–8623.
- (344) Ackerley, D. F.; Gonzalez, C. F.; Keyhan, M.; Blake, R.; Matin, A. Mechanism of Chromate Reduction by the Escherichia Coli Protein, NfsA, and the Role of Different Chromate Reductases in Minimizing Oxidative Stress during Chromate Reduction. *Environ Microbiol* **2004**, 6 (8), 851–860.
- (345) Arévalo-Rangel, D. L.; Cárdenas-González, J. F.; Martínez-Juárez, V. M.; Acosta-Rodríguez, I. Hexavalent Chromate Reductase Activity in Cell Free Extracts of *Penicillium* Sp. *Bioinorganic Chemistry and Applications* **2013**, 2013, 1–6.
- (346) Viti, C.; Marchi, E.; Decorosi, F.; Giovannetti, L. Molecular Mechanisms of Cr(VI) Resistance in Bacteria and Fungi. *FEMS Microbiol Rev* **2014**, 38 (4), 633–659. 6976.12051.
- (347) Thatoi, H.; Das, S.; Mishra, J.; Rath, B. P.; Das, N. Bacterial Chromate Reductase, a Potential Enzyme for Bioremediation of Hexavalent Chromium: A Review. *Journal of Environmental Management* **2014**, 146, 383–399.
- (348) Myers, C. R.; Carstens, B. P.; Antholine, W. E.; Myers, J. M. Chromium(VI) Reductase Activity Is Associated with the Cytoplasmic Membrane of Anaerobically Grown *Shewanella Putrefaciens* MR-1: C.R. MYERS ET AL. *Journal of Applied Microbiology* **2001**, 88 (1), 98–106.
- (349) Morais, P. V.; Branco, R.; Francisco, R. Chromium Resistance Strategies and Toxicity: What Makes *Ochrobactrum Tritici* 5bvl1 a Strain Highly Resistant. *Biometals* **2011**, 24 (3), 401–410.
- (350) Strittmatter, P. The Nature of the Flavin Binding in Microsomal Cytochrome B5 Reductase. *Journal of Biological Chemistry* **1961**, 236 (8), 2329–2335.

APPENDICES

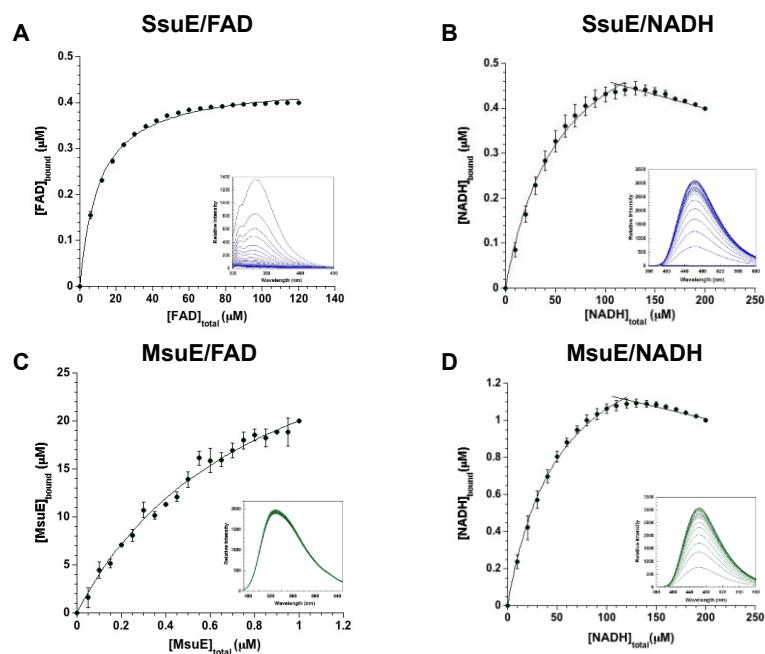


Figure 1: Fluorescent titrations of SsuE and MsuE with FAD and NADH. A. Titration of SsuE (0.4 μM) with FAD (6-120 μM ; λ_{ex} , 280 nm; λ_{em} , 342 nm). B. Titration of SsuE (0.4 μM) with NADH (10-200 μM ; λ_{ex} , 340 nm; λ_{em} , 450 nm). C. Titration of FAD (20 μM) with MsuE (0.05 - 1.0 μM ; λ_{ex} , 450 nm; λ_{em} , 525 nm). D. Titration of MsuE (1 μM) with NADH (10-200 μM ; λ_{ex} , 340 nm; λ_{em} , 450 nm). The titrations were performed in triplicate and fit to a quadratic equation for single site binding.

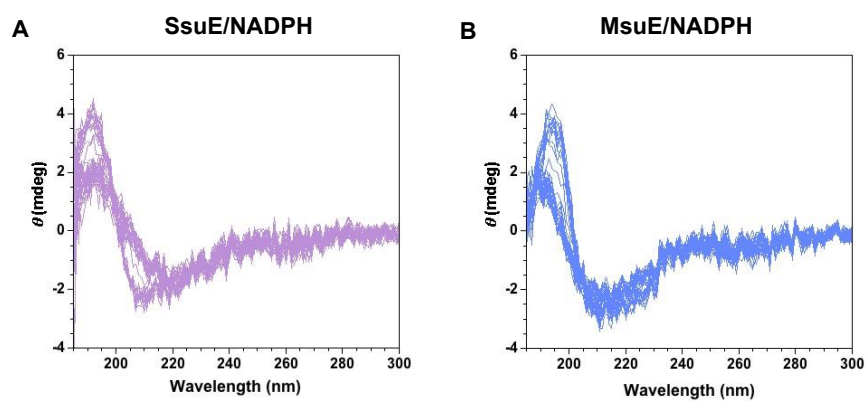
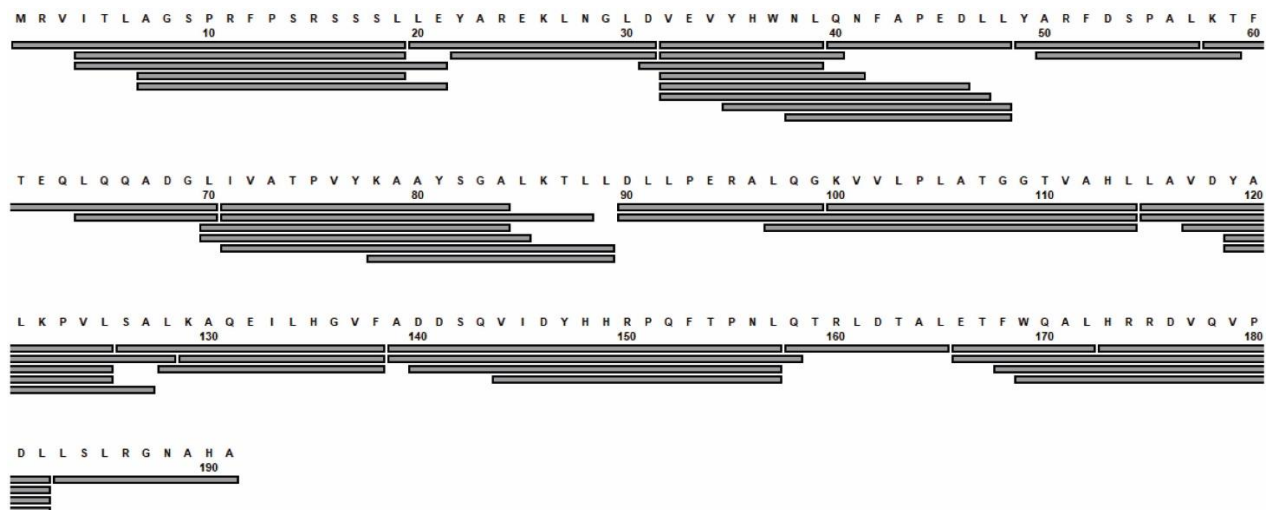


Figure 2: Thermal denaturation CD of SsuE and MsuE. (A) SsuE/NADPH (B) MsuE/NADPH. SsuE and MsuE (5 μ M) were scanned over a wavelength range of 185-300 nm and a temperature range of 20-94 $^{\circ}$ C. NADPH was added in a 1:10 ratio (enzyme: substrate) when included. Each thermal denaturation experiment was performed in triplicate.

Figure A3: Coverage map for SsuE with (A) FMN and (B) NADPH

(A) 49 peptides, 3.35 redundancy, 100% coverage



(B) 58 peptides, 3.91 redundancy, 100% coverage

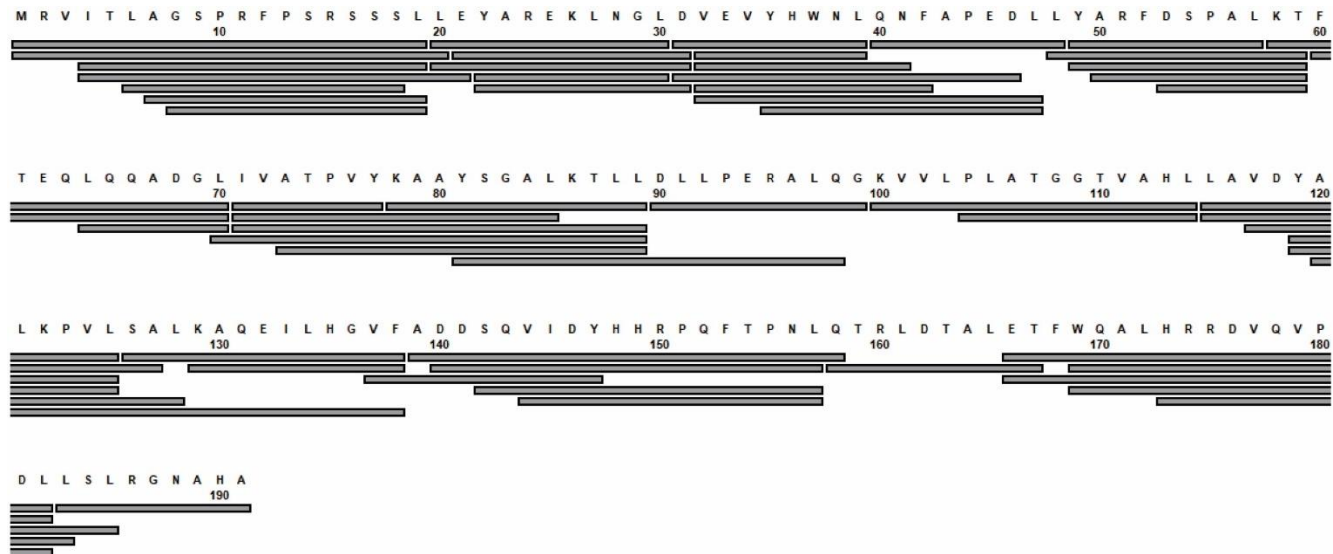
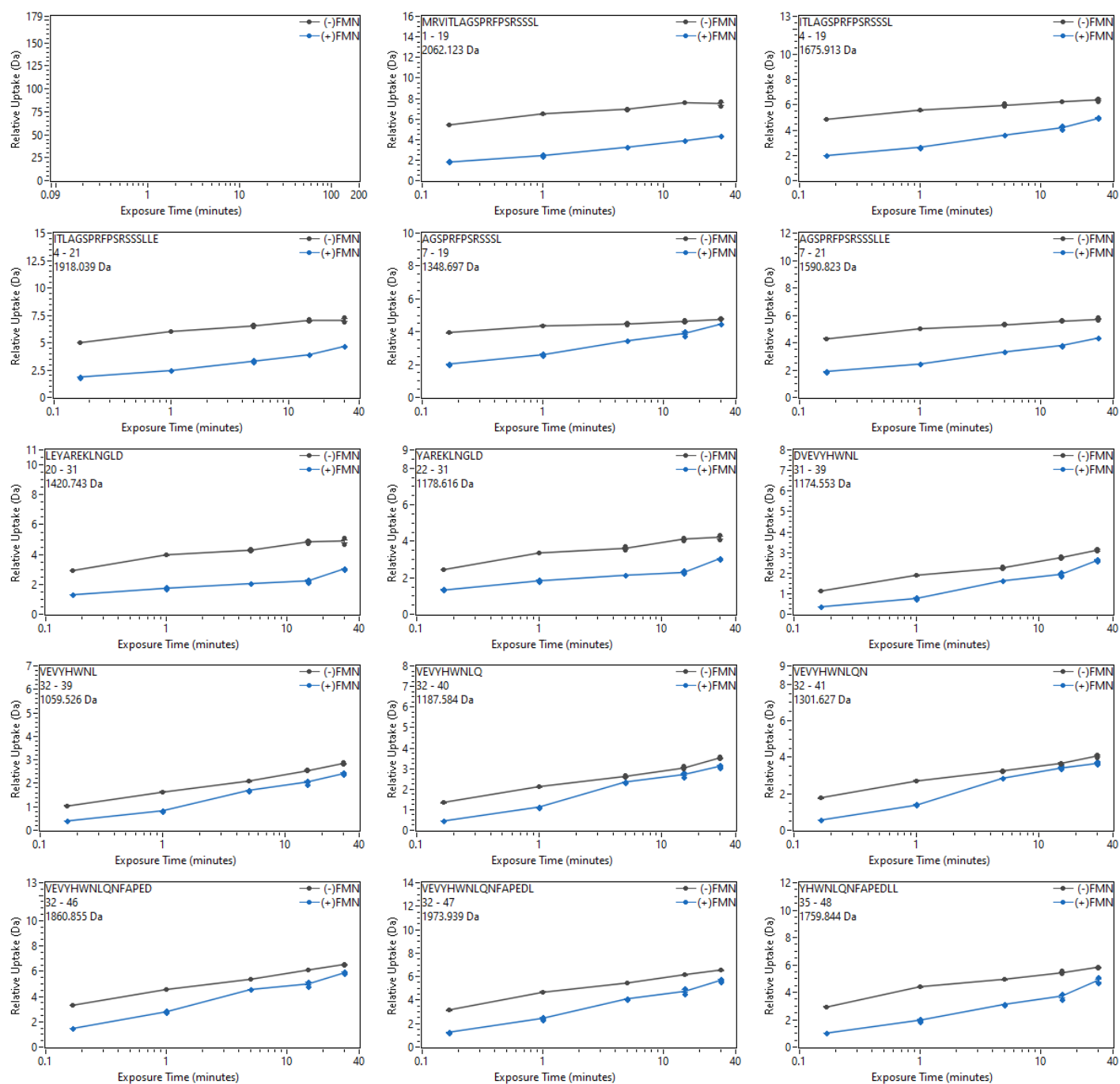
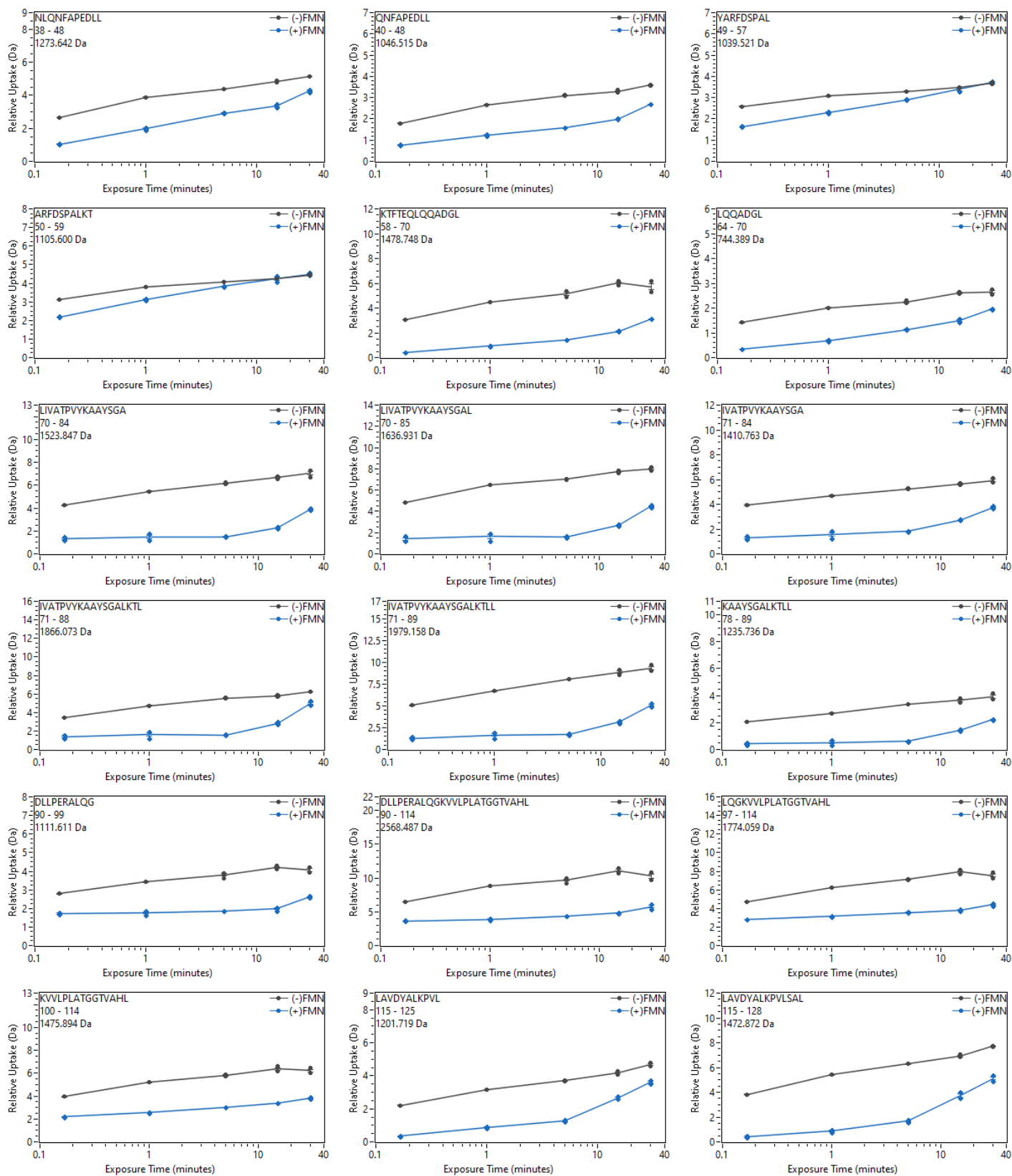


Figure A4: Uptake plots for differential H/D-X analysis of the SsuE apoenzyme (grey) and SsuE incubated with FMN (blue).





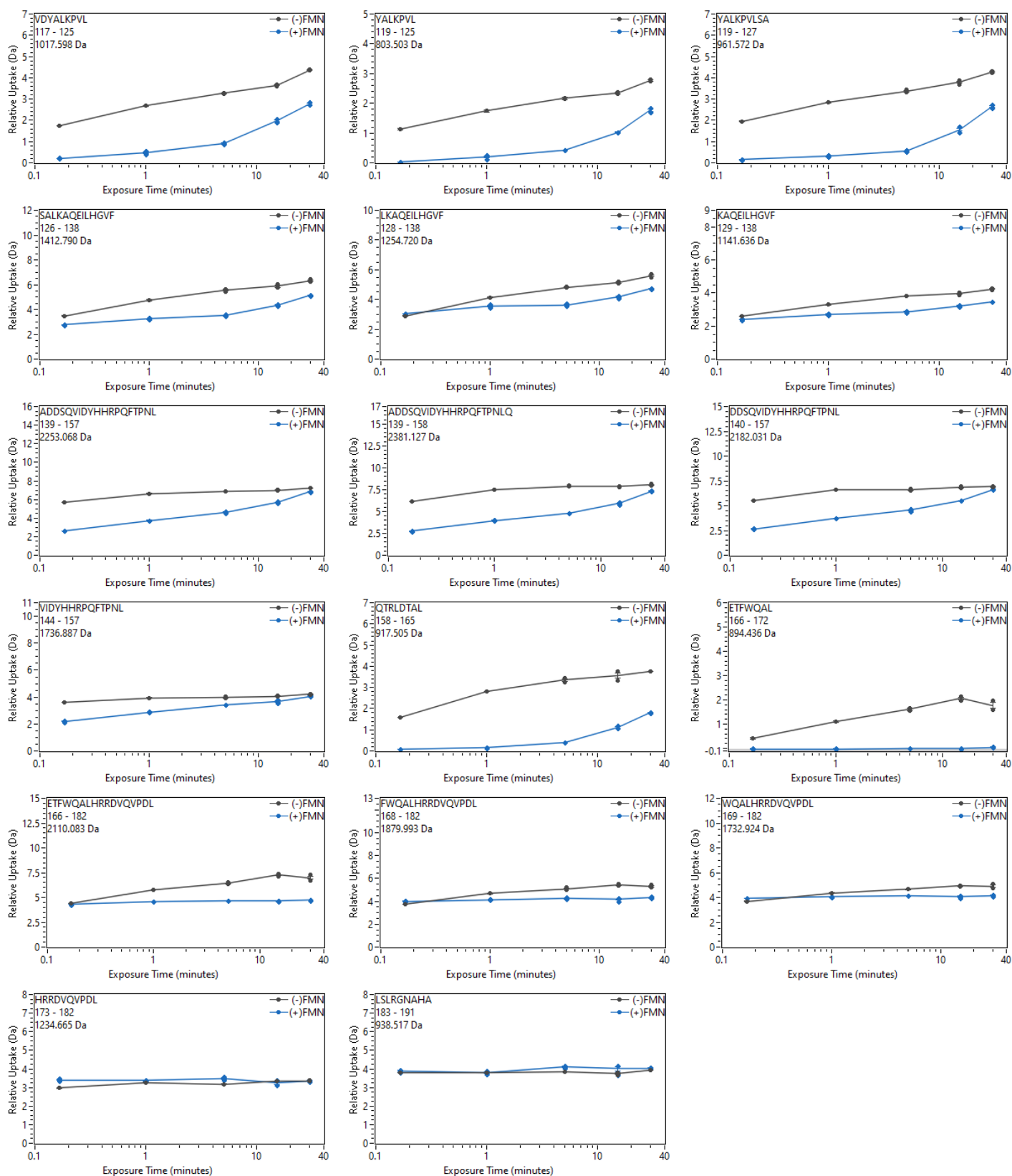
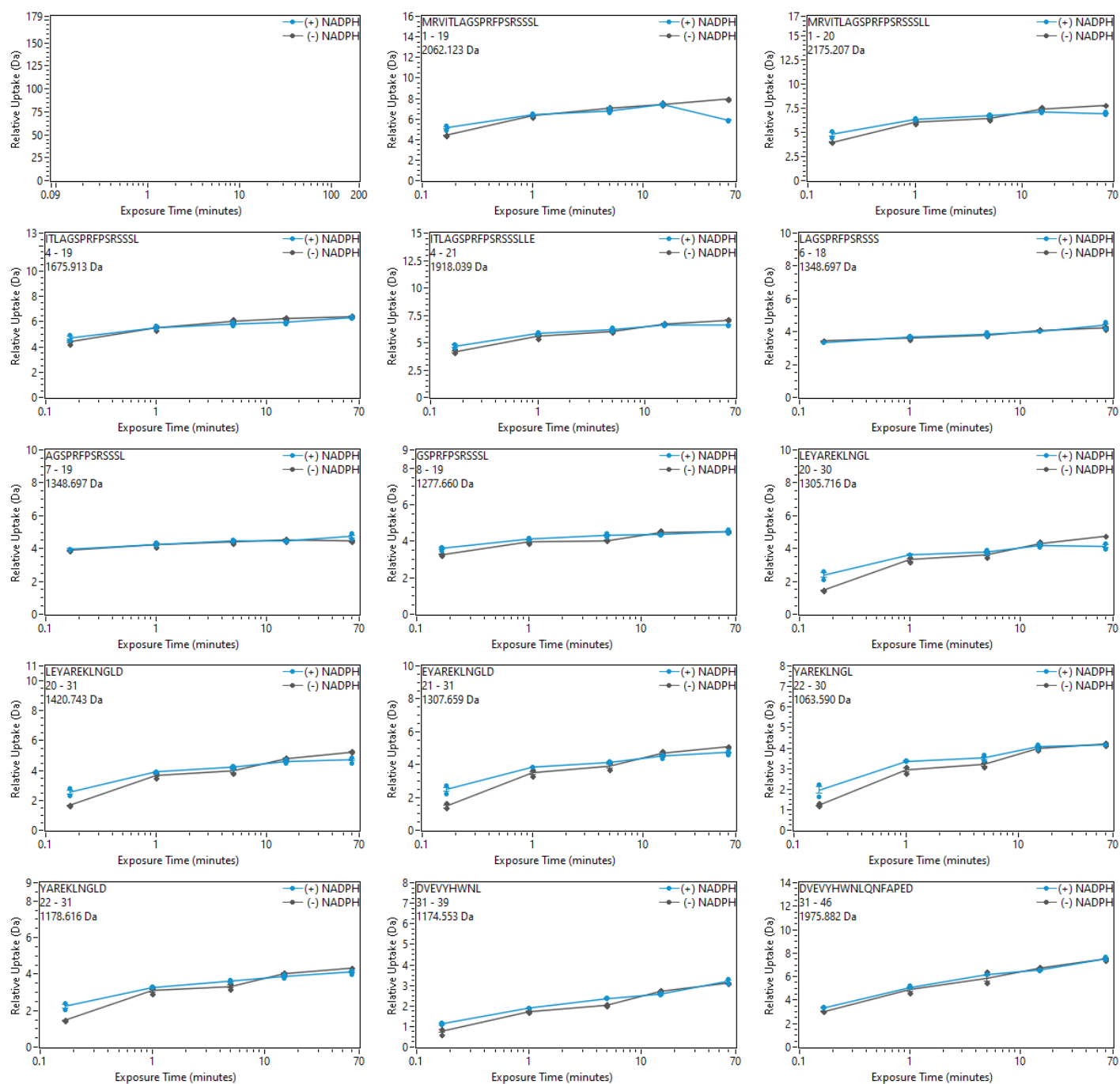
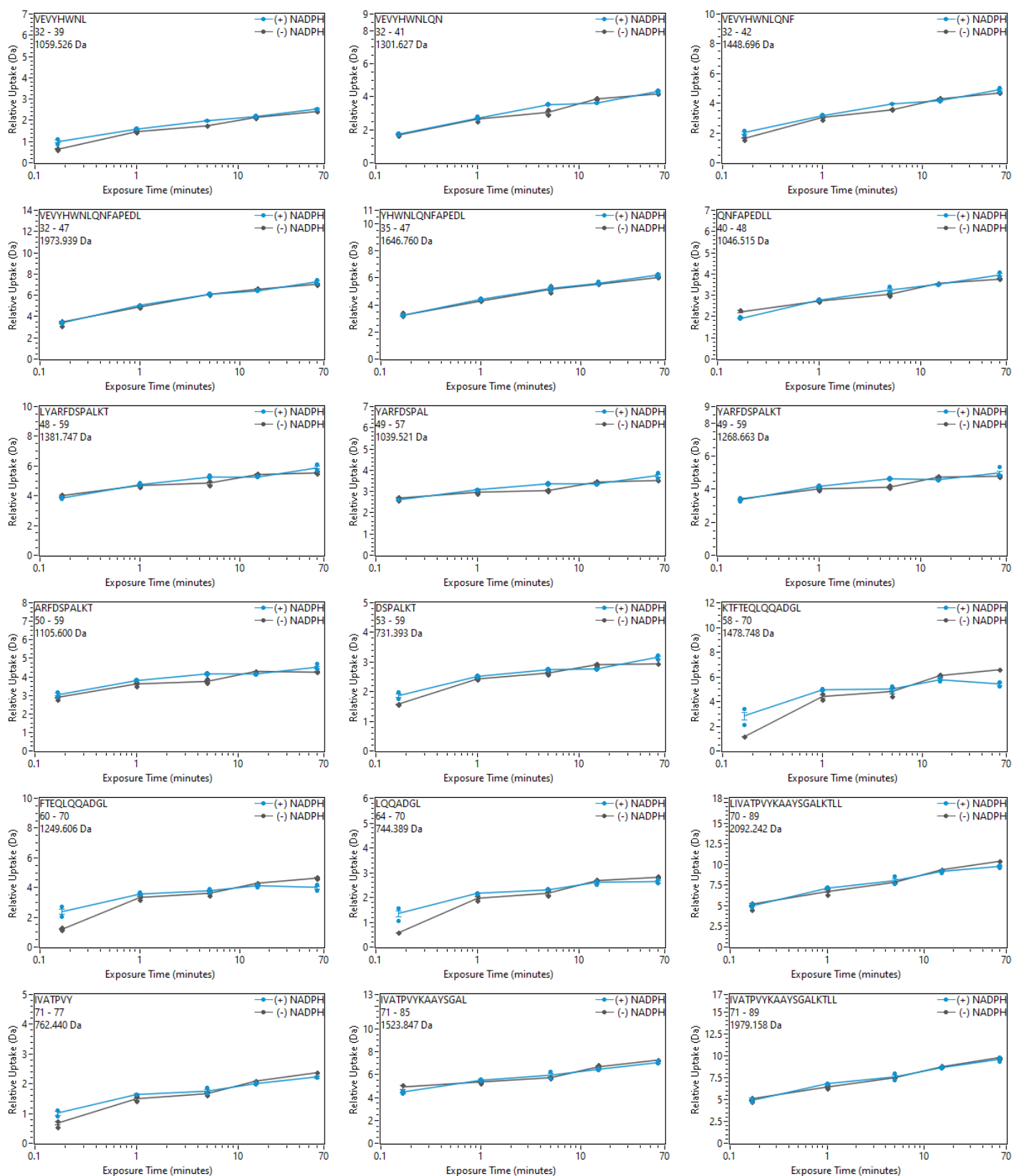
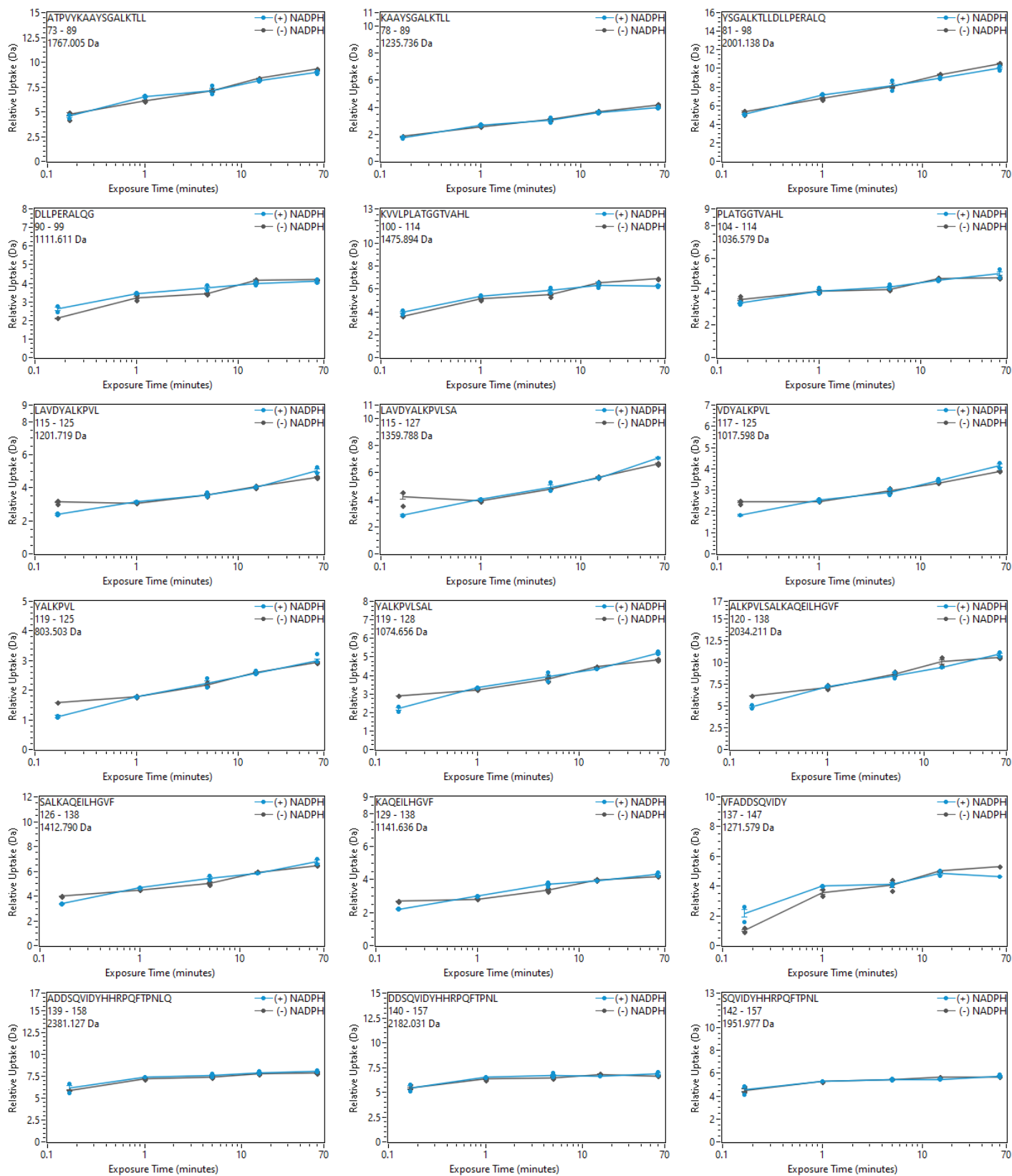


Figure A5: Uptake plots for differential H/D-X analysis of the SsuE apoenzyme (grey) and SsuE incubated with NADPH (blue).







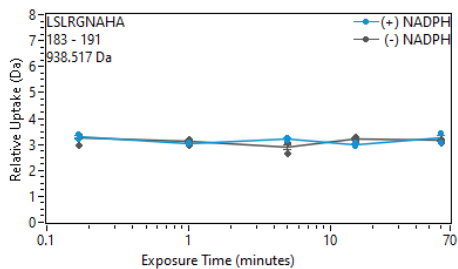
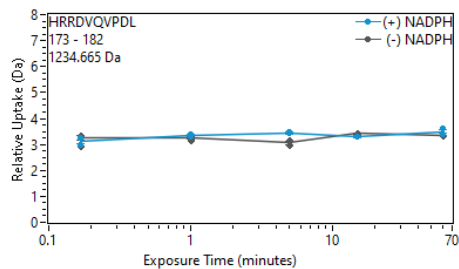
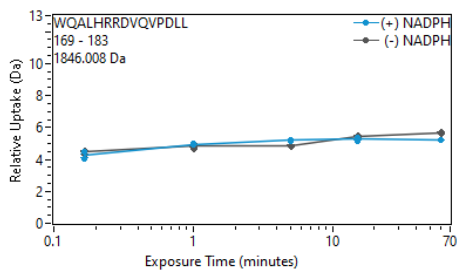
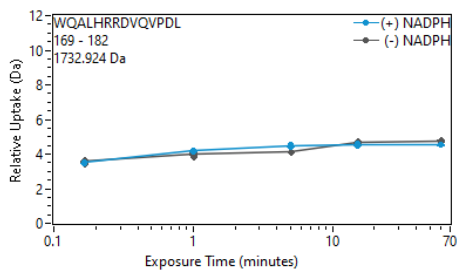
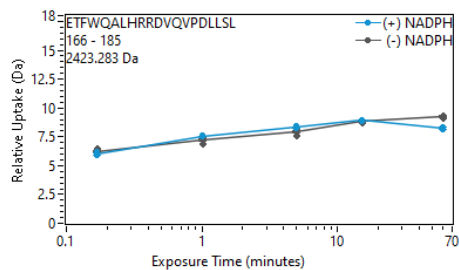
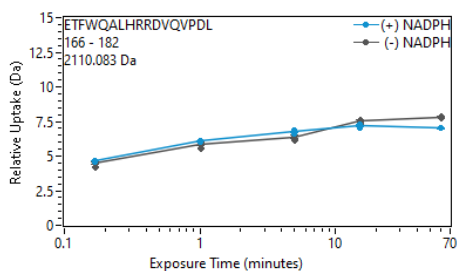
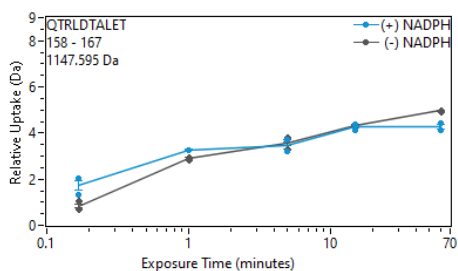
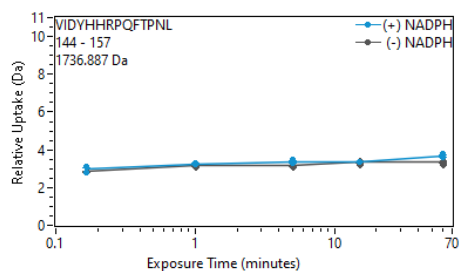


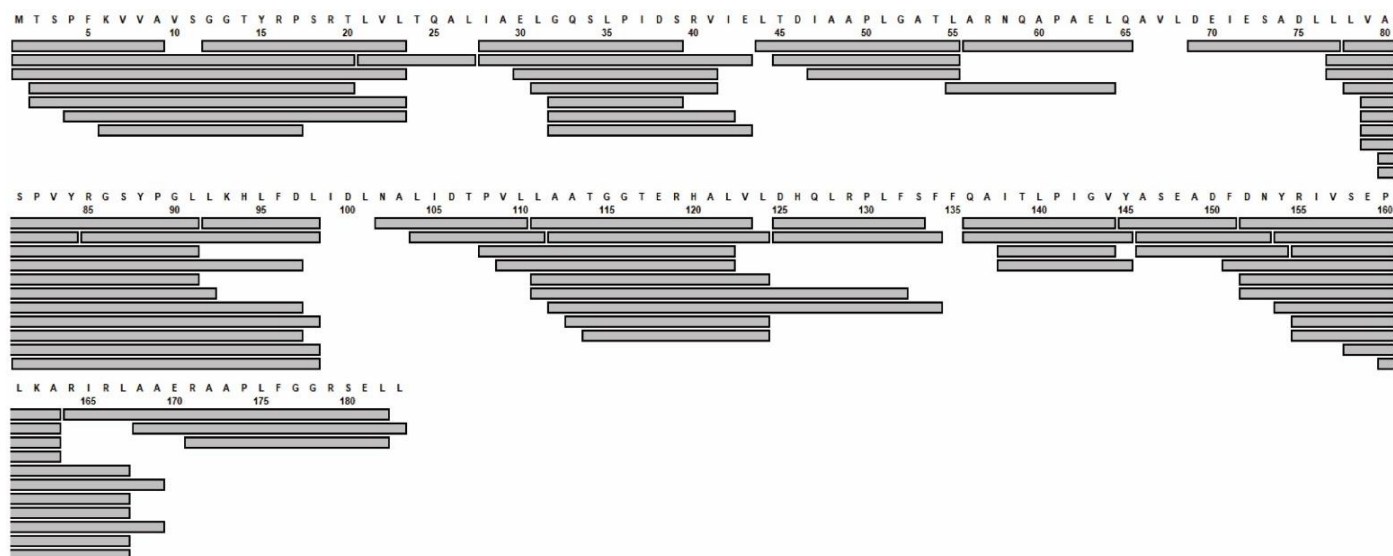
Table A1. Table of H/D-X patterns for SsuE peptides determined for the apoenzyme and in the presence of FMN and NADPH. Regions highlighted in blue indicate exchange patterns that are different with FMN or NADPH present compared to the apoenzyme.

Start	End	Sequence	Apoenzyme	(+) FMN	(+) NADPH
1	19	MRVITLAGSPRFPSRSSSL	EX1	bimodal	bimodal, crossover
1	20	MRVITLAGSPRFPSRSSLL	bimodal		bimodal, crossover
4	19	ITLAGSPRFPSRSSSL	bimodal	bimodal	no EX
4	21	ITLAGSPRFPSRSSLLE	bimodal	bimodal	no EX
6	18	LAGSPRFPSRSSS	no EX		no EX
7	19	AGSPRFPSRSSSL	no EX	bimodal	no EX
7	21	AGSPRFPSRSSLLE	no EX	bimodal	
8	19	GSPRFPSRSSSL	no EX		no EX
20	30	LEYAREKLNGL	bimodal, early		bimodal, crossover
20	31	LEYAREKLNLGD	bimodal, early	no EX	bimodal, crossover
21	31	EYAREKLNLGD	bimodal, early		bimodal, crossover
22	30	YAREKLNGL	bimodal, early		bimodal
22	31	YAREKLNLGD	bimodal	no EX	no EX
31	39	DVEVYHWNL	bimodal	bimodal	bimodal
31	46	DVEVYHWNLQNFAPED	bimodal		bimodal
32	39	VEVYHWNL	bimodal	bimodal	bimodal
32	40	VEVYHWNLQ	bimodal	bimodal	
32	41	VEVYHWNLQN	bimodal	bimodal	
32	42	VEVYHWNLQNF	bimodal		bimodal
32	46	VEVYHWNLQNFAPED	bimodal	bimodal	
32	47	VEVYHWNLQNFAPEDL	bimodal	bimodal	bimodal
35	47	YHWNLQNFAPEDL	bimodal		bimodal
35	48	YHWNLQNFAPEDLL	bimodal	bimodal	
38	48	NLQNFAPEDLL	bimodal	bimodal	
40	48	QNFAPEDLL	bimodal	bimodal	bimodal
48	59	LYARFDSPALKT	no EX		no EX
49	57	YARFDSPAL	no EX	no EX	no EX
49	59	YARFDSPALKT	no EX		no EX
50	59	ARFDSPALKT	no EX		no EX
53	59	DSPALKT	bimodal		bimodal
58	70	KTFTEQLQQADGL	bimodal		bimodal
60	70	FTEQLQQADGL	bimodal all		bimodal all
64	70	LQQADGL	no EX	bimodal	bimodal late
70	84	LIVATPVYKAAYSGA	bimodal early	bimodal late	
70	85	LIVATPVYKAAYSGAL	bimodal early	bimodal late	
70	89	LIVATPVYKAAYSGALKTLL	bimodal early, exchange		bimodal early, exchange

71	77	IVATPVY	bimodal early, exchange		bimodal early, exchange
71	84	IVATPVYKAAYSGA	bimodal early	bimodal late	
71	85	IVATPVYKAAYS GAL	bimodal early, exchange		bimodal early, exchange
71	88	IVATPVYKAAYS GALKTL	bimodal early	bimodal late	
71	89	IVATPVYKAAYS GALKTLL	bimodal early	bimodal late	bimodal early, exchange
73	89	ATPVYKAAYS GALKTLL	bimodal early, exchange	bimodal early, exchange	bimodal early, exchange
78	89	KAAYS GALKTLL	no EX	no EX, bimodal late	no EX
81	98	YSGALKTLLDLLPERALQ	bimodal early, exchange		bimodal early, exchange
90	99	DLLPERALQG	no EX	no EX, bimodal late	no EX
90	114	DLLPERALQGVVLPATGGTVAHL	bimodal, exchange	no EX, bimodal late	
97	114	LQGVVLPATGGTVAHL	bimodal, exchange	no EX, bimodal late	
100	114	KVVLPATGGTVAHL	bimodal, exchange	no EX, bimodal late	bimodal, EX
104	114	PLATGGTVAHL	no EX		no EX
115	125	LAVDYALKPVL	bimodal, pop change	bimodal, pop change	bimodal, pop change
115	127	LAVDYALKPVL SA	bimodal early, pop change		bimodal, pop change
115	128	LAVDYALKPVL SAL	bimodal early, pop change	bimodal, late pop change	
117	125	VDYALKPVL	bimodal early, pop change	bimodal, late pop change	bimodal early, pop change
119	125	YALKPVL	bimodal early, pop change	no EX, bimodal late	bimodal early, pop change
119	127	YALKPVL SA	bimodal early, pop change	no EX, bimodal late	
119	128	YALKPVL SAL	bimodal early		bimodal early, pop change
120	138	ALKPVL SALKAQEILHG VF	bimodal early		bimodal early, pop change
126	138	SALKAQEILHG VF	bimodal all	bimodal early	bimodal early
128	138	LKAQEILHG VF	bimodal short	bimodal	
129	138	KAQEILHG V	bimodal	bimodal	bimodal early
137	147	VFADDSQVIDY	bimodal early		bimodal early
139	157	ADDSQVIDYHHRPQFTP NL	no EX	bimodal	
139	158	ADDSQVIDYHHRPQFTP NLQ	no EX	bimodal	no EX
140	157	DDSQVIDYHHRPQFTP NL	no EX	bimodal	no EX
142	157	SQVIDYHHRPQFTP NL	no EX		no EX
144	157	VIDYHHRPQFTP NL	no EX	bimodal	no EX
158	165	QTRLDTAL	no EX	no EX	
166	172	ETFWQAL	no EX, no Exposure	no EX, no Exposure	
166	182	ETFWQALHRRDVQVP DL	no EX, no Exposure	no EX, no Exposure	no EX, no Exposure
166	185	ETFWQALHRRDVQVP DLLSL	no EX, no Exposure	no EX, no Exposure	no EX, no Exposure
168	182	FWQALHRRDVQVP DL	no EX	no EX	
169	182	WQALHRRDVQVP DL	no EX	no EX	no EX
169	183	WQALHRRDVQVP DLL	no EX		
173	182	HRRDVQVP DL	no EX	no EX	no EX
183	191	LSLRGNAHA	no EX	no EX	no EX

Figure A6: Coverage map for MsuE with (A) FMN and (B) NADPH

(A) 69 peptides, 5.20 redundancy, 96.2% coverage



(B) 92 peptides, 6.70 redundancy, 98.9% coverage

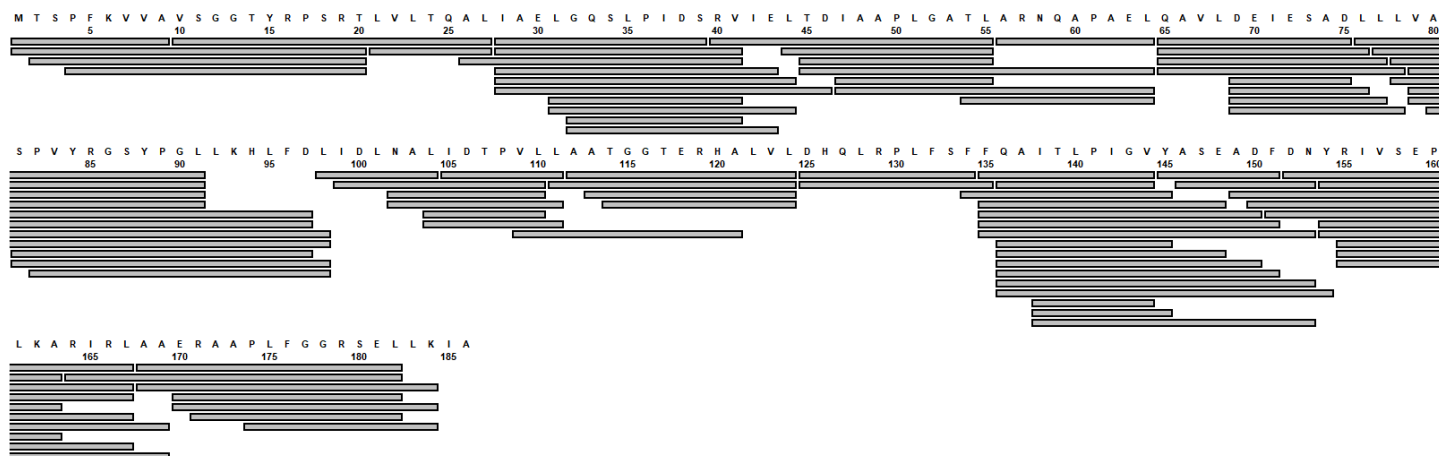
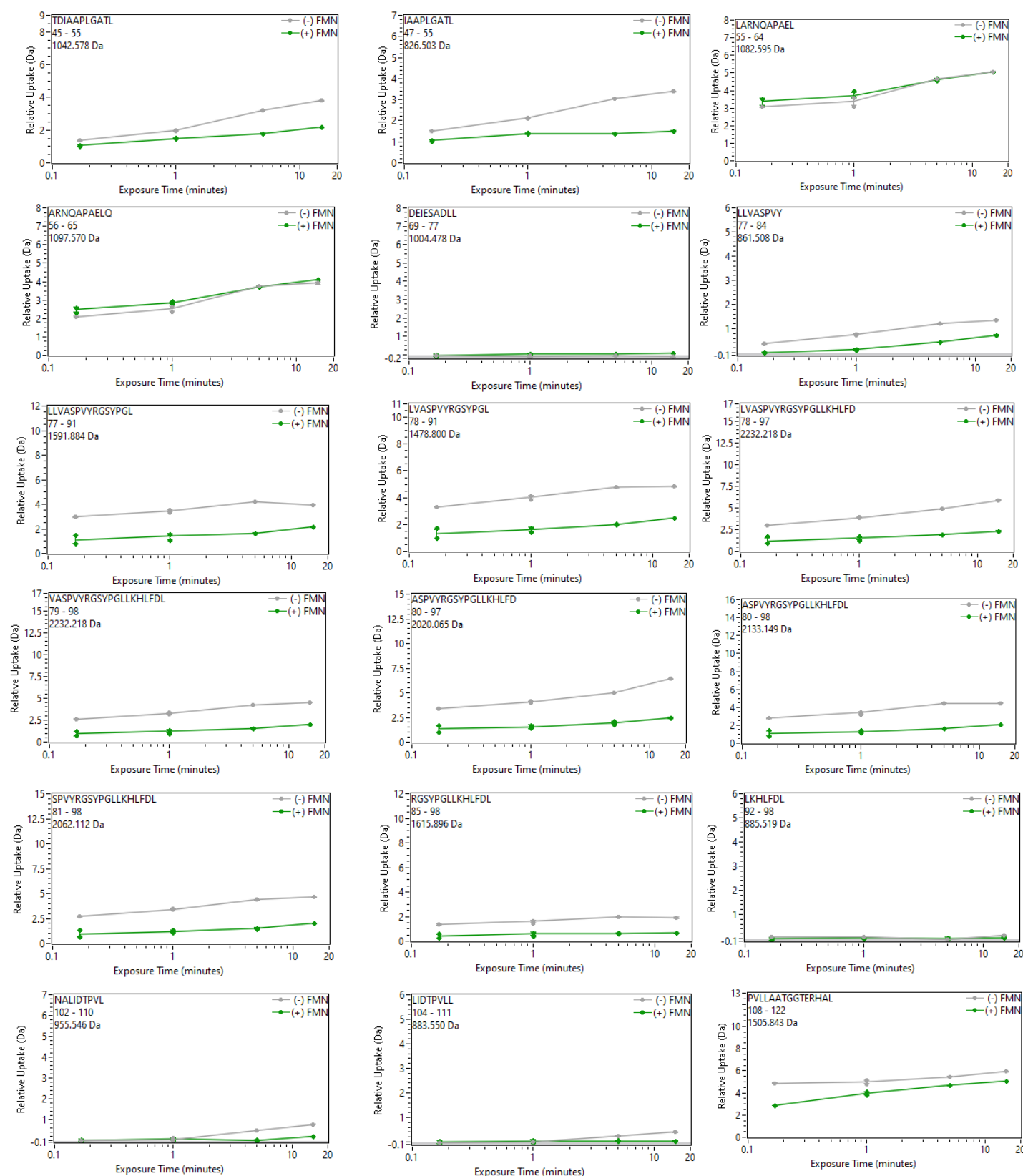
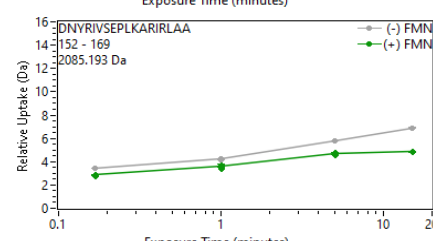
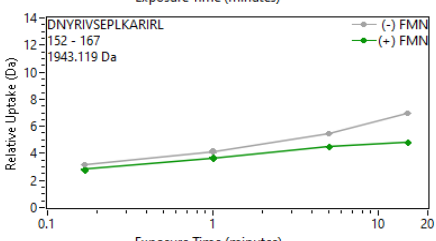
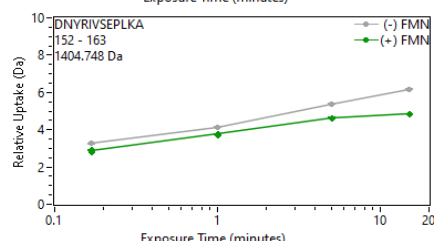
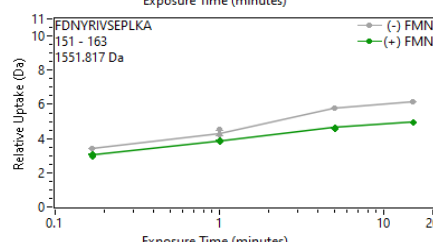
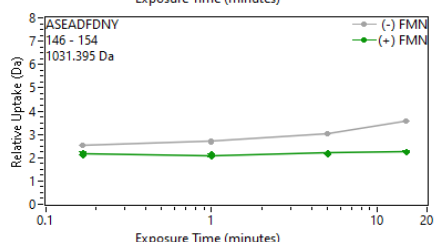
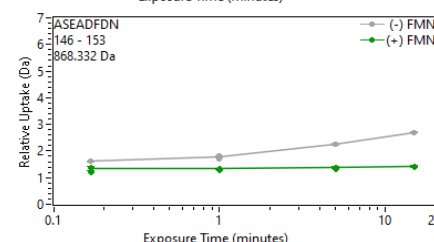
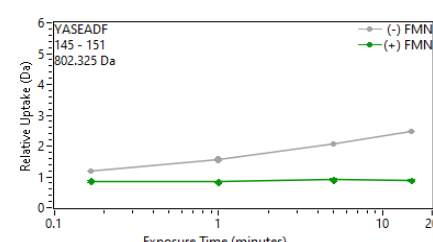
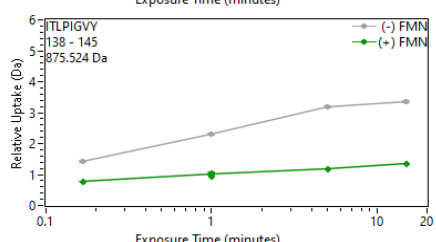
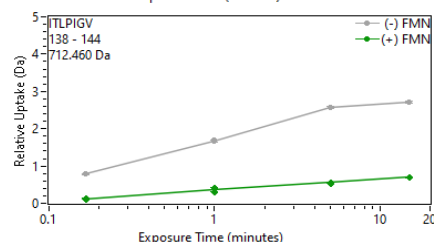
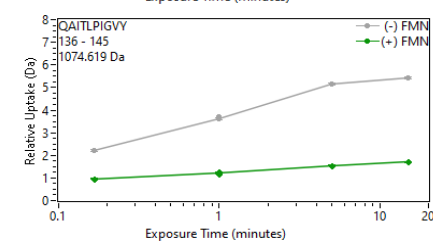
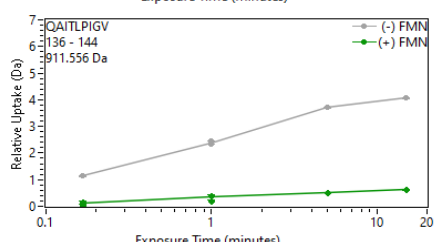
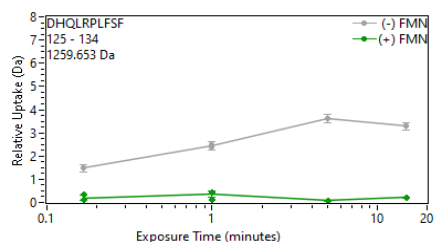
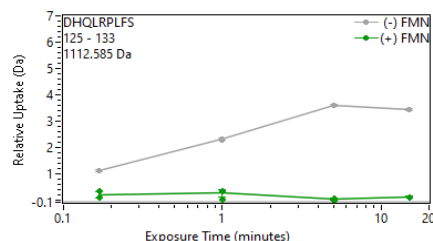
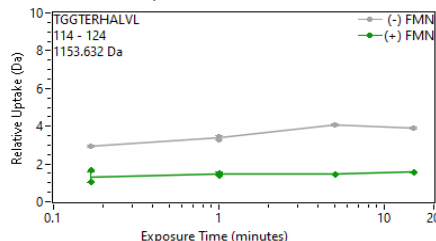
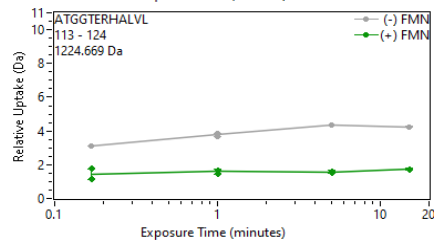
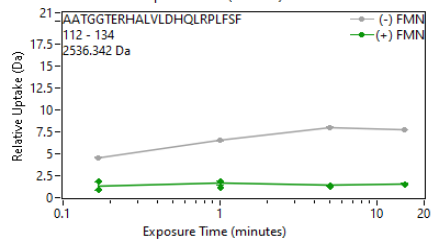
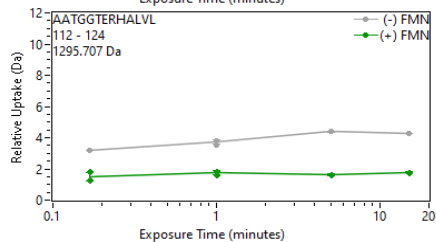
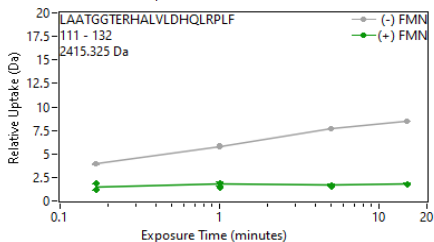
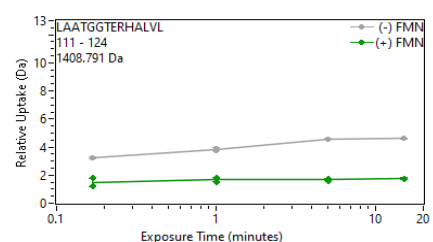
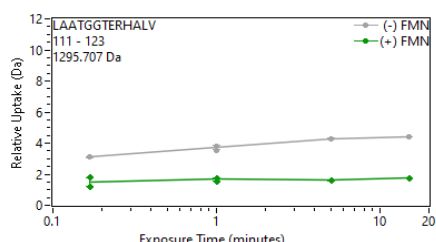
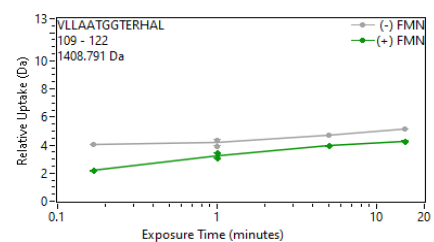


Figure A7: Uptake plots for differential H/D-X analysis of the MsuE apoenzyme (grey) and MsuE incubated with FMN (green)





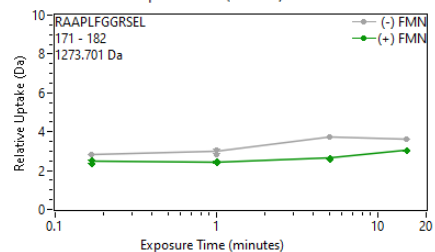
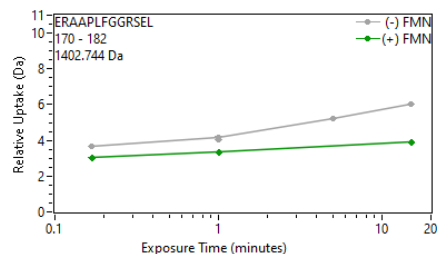
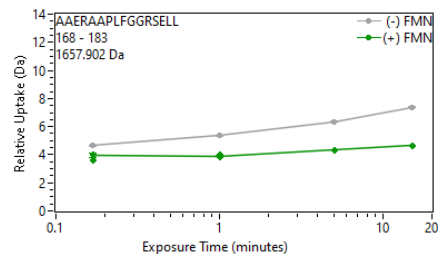
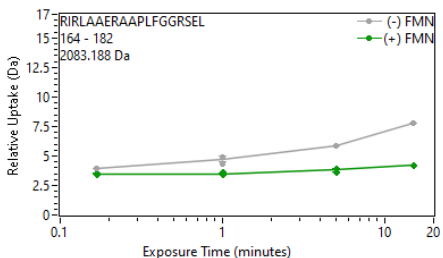
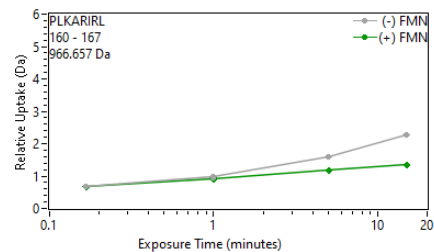
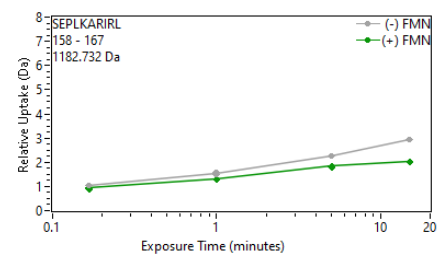
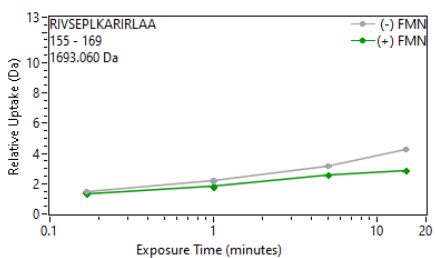
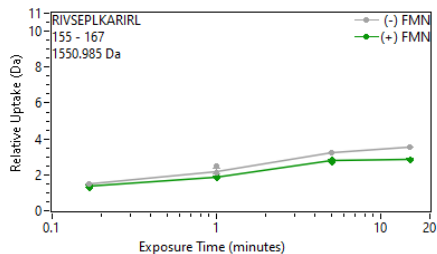
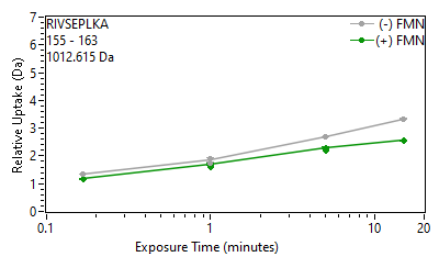
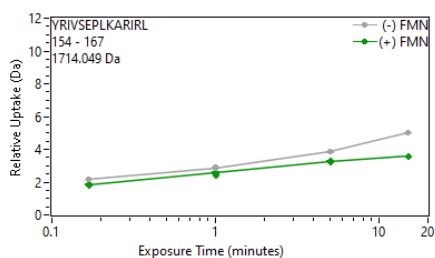
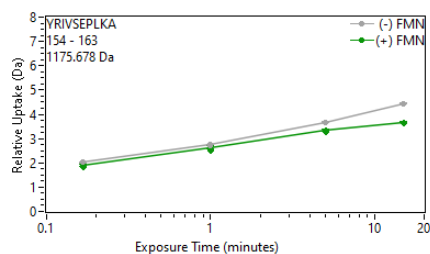


Figure A8: Uptake plots for differential H/D-X analysis of the MsuE apoenzyme (grey) and MsuE incubated with NADPH (green)

